2008

The Interactive Toxicity of Benzo(a)Pyrene and Ultraviolet Radiation - an In Vitro Investigation

Lyle, Zoe Jean

The Interactive Toxicity of Benzo(a)Pyrene and Ultraviolet Radiation – an *In Vitro* Investigation.

by

Zöe Jean Lyle

A thesis submitted to the University of Plymouth

in partial fulfilment for the degree of

DOCTOR OF PHILOSOPHY

School of Biological Sciences

Faculty of Science

University of Plymouth

January 2008

ABSTRACT

The Interactive Toxicity of Benzo(a)Pyrene and Ultraviolet Radiation – an *In Vitro* Investigation.

The work presented here adopted an *in vitro* approach with cell types from different species (fish: Epithelioma Papillosum Cyprini (EPCA1), Rainbow Trout Gonad (RTG-2); mammals: Chinese Hamster Ovary (CHO-K1), primary human fibroblast cells (84BR)) to elucidate the potential genotoxic effects of the interaction of the polycyclic aromatic hydrocarbon (PAH), benzo(a)pyrene (B(a)P) (0.0, 0.1, 1.0 and 3.2 μg ml^{-1}) with ultraviolet radiation (UVA/UVB) (typically 25, 50, 100, 200, 500, 1000, 2000, 4000, 6000, 8000 J m^{-2}). Initially the experimental techniques and conditions were optimised and validated in the CHO-K1, EPCA1 and RTG-2 cell lines. It was shown that mammalian (CHO-K1) and fish cells (EPCA1 and RTG-2) exhibited similar sensitivities to chemicals with different modes of action i.e. clastogenic ethyl methansulphonate (EMS) (0.0, 0.8, 1.6 and 3.2 mM) and aneugenic colchicine (COL) (0.0, 0.1, 1.0 and 1.8 μg ml^{-1}) following cytotoxicity experiments with neutral red retention (NRR). Similarly, using the micronucleus assay (Mn) all the cell lines tested showed a similar response to EMS and COL and the use of the anti-kinetochore stain provided a useful approach with which to distinguish between clastogenic and aneugenic effects in the cell. Following comet assay experiments the importance of optimising and validating variables was demonstrated. The optimal variables chosen for the comet assay were 20 minutes unwinding for fish cells (EPCA1 and RTG-2) and 40 minutes unwinding time for mammalian cells (CHO-K1 and 84BR) with 20 minutes electrophoresis for all cell types. Following these

validation studies, the cytotoxic and genotoxic effects produced in cells of aquatic (EPCA1, RTG-2) and mammalian (CHO-K1, 84BR) origin following treatment with B(a)P and UVR was investigated. The incubation of all cells (EPCA1, RTG-2, CHO-K1) with B(a)P alone caused limited cytotoxicity (NRR), increased DNA damage (comet assay) and altered cellular functions that were from aneugenic and clastogenic mechanisms (Mn assay). EPCA1, RTG-2 and CHO-K1 cells irradiated with UVB displayed a significant increase in cytotoxicity (NRR) and DNA damage (comet assay). Cells irradiated with UVA (RTG-2, CHO-K1, 84BR) showed no significant increases in cytotoxicity and only CHO-K1 showed increased DNA damage (comet assay). There were significant increases in cellular alterations (Mn assay) following UVA irradiation. All cells (RTG-2, CHO-K1, 84BR) incubated with B(a)P followed by irradiation with UVA showed a synergistically increased cytotoxicity (NRR) and DNA damage (comet assay) from a 1.2-fold increase up to a 4-fold increase in DNA damage. There were also altered cellular mechanisms that may be due to both aneugenic and clastogenic mechanisms (Mn assay). Oxidative stress as a product of the formation of the hydroxyl radical was shown to be a key element in these processes (Electron Spin Resonance (ESR)). It is therefore concluded that the genotoxic effects of the PAH B(a)P and UVA irradiation are synergistically increased when both insults are experienced in combination. This worrying result was observed within both fish and mammalian cell types and appeared to be mediated via an oxidative stress mechanism which included the formation of the hydroxyl radical.

Table of Contents

Page

CHAPTER II – MATERIALS AND METHODS

CHAPTER III – OPTIMISATION AND VALIDATION

List of Tables

Table 3.3 Effect of various concentrations of EMS on the mean number of micronuclei produced in the CHO-K1, EPCA1 or RTG-2 cell lines using the anti-kinetochore stain (n=26,349). Significant differences are indicated (*) between the tested dose and the control (Mann Whitney U-test, $p<0.05$).

Table 3.4 Effect of various concentrations of COL on the mean number of micronuclei produced in the CHO-K1, EPCA1 and RTG-2 cell lines (n=56,592) using the anti-kinetochore stain. Significant differences from the control are indicated (*) (Mann Whitney U-test, $p<0.05$).

Table 3.5 Summary of the advantages and disadvantages of the cell lines CHO-K1, EPCA1 and RTG-2 in ecotoxicological testing for the purposes of this work.

Table 4.1 Effect of various doses of B(a)P on the mean generation of micronuclei (±SE) in the EPCA1 cell line using Giemsa or anti-kinetochore stain (n=27,383). No nucleoplasmic bridges, incidences of 2, 3 or 4+ nuclei or multinucleated cells were observed. Significant differences (Mann Whitney U-test $p<0.05$) for each cellular response from the control are indicated (*).

Table 4.2 Effect of various doses of B(a)P on the mean generation (±SE) of micronuclei in the RTG-2 cell line using Giemsa or anti-kinetochore stain (n=30,849). There were no incidences of nucleoplasmic bridges, K- mononucleated cells or 2, 3 or 4+ nuclei observed. Significant increases (Mann-Whitney U-test $p<0.05$) in cellular responses from the control are indicated (*).

Table 4.3 Effect of various doses of UVA on the mean generation (±SE) of micronuclei in the RTG-2 cell line (n=23,506) using Giemsa or anti-kinetochore stain. There were no multinucleate cells observed. Significant increases (Mann-Whitney U-test $p<0.05$) in the cellular responses from the control are indicated (*).

Table 4.4 Effect of interactive toxicity following pre-incubation with 0.05 μg ml^{-1} B(a)P with various doses of UVA on the mean generation (±SE) of micronucleus in RTG-2 cells (n=17,445) using Giemsa or anti-kinetochore stain. There were no multinucleate cells observed. Significant differences (Mann-Whitney U-test $p<0.05$) from the control are indicated (*).

Table 5.1 Effect of various concentrations of B(a)P (0.00, 0.05, 0.10, 1.00 and 3.20 μg ml^{-1}) on the mean generation (±SE) of micronuclei in the CHO-K1 cell line (n=32,064) using Giemsa or anti-kinetochore stain. There were no nucleoplasmic bridges or incidences of 2 or 4+ nuclei. Significant differences (Mann-Whitney U-test $p<0.05$) from the control are indicated (*).

Table 5.2 Effect of B(a)P (0.00 and 0.05 μg ml^{-1}) on the generation of micronuclei in 84BR cells (n=13,730) using Giemsa or anti-kinetochore stain. There were no nucleoplasmic bridges, incidences of 2 or 3 nuclei, multinucleate cells or micronuclei in mononucleate cells detected using anti-kinetochore stain.

Table 5.3 Effect of various doses of UVA on the mean generation (±SE) of micronuclei in the CHO-K1 cell line (n=28,444) using Giemsa or anti-kinetochore stain. There were no multinucleate cells observed. Significant differences

List of Figures

Figure 3.3 The effect of unwinding times (10, 20, 30 and 40 minutes) with 40 (Figure 3.3 a,b), 30 (Figure 3.3 c,d), 20 (Figure 3.3 e,f) or 10 (Figure 3.3 g,h) minutes electrophoresis time on DNA damage (Tail DNA (%)) to EPCA1 cells following negative control (left plots) or exposure to 20 minutes H_2O_2 (100 µM) (right plots). Significant differences (Mann-Whitney U test, $p<0.05$) between the H_2O_2 positive controls and the corresponding negative controls are indicated (*). There were no significant differences between the unwinding times for different electrophoresis times or between the electrophoresis times for different unwinding times ($p>0.05$). Each box represents 200 cells (total n=800).

Figure 3.4 The effect of unwinding times (10, 20, 30 and 40 minutes) with 40 (Figure 3.4 a,b), 30 (Figure 3.4 c,d), 20 (Figure 3.4 e,f) or 10 (Figure 3.4 g,h) minutes electrophoresis time on median DNA damage to RTG-2 cells following negative control (left plots) or exposure to 20 minutes H_2O_2 (100 µM) (right plots). Significant differences (Mann-Whitney U test, $p<0.05$) between the H_2O_2 positive controls and the corresponding negative controls are indicated (*). There were no significant differences between the unwinding times for different electrophoresis times or between the electrophoresis times for different unwinding times ($p>0.05$). Each box represents 200 cells (total n=800).

Figure 3.5 Median DNA damage observed in CHO-K1 cells following 6 hour exposure to EMS at various concentrations (0.0, 0.8, 1.6 and 3.2 mM). DNA damage is assessed by the % Tail DNA. All EMS concentrations are significantly different from the control ($p < 0.001$).

Figure 3.6 Median DNA damage observed in EPCA1 cells following 6 hour exposure to EMS at various concentrations (0.0, 0.8, 1.6 and 3.2 mM). DNA damage is assessed by % Tail DNA. All EMS concentrations are significantly different from the control ($p < 0.001$).

Figure 3.7 Median DNA damage observed in RTG-2 cells following 6 hour exposure to EMS at various concentrations (0.0, 0.8, 1.6 and 3.2 mM). DNA damage is assessed by % Tail DNA. The observed damages at all the EMS concentrations are significantly different from the control ($p < 0.001$).

Figure 3.8 DNA damage to 84BR cells following exposure to 20 minutes H_2O_2 at various concentrations (0, 10, 50 and 100 μM). DNA damage is assessed by the % Tail DNA. The DNA damage produced by all the H_2O_2 concentrations were significantly different from that of the control ($p < 0.0001$).

Figure 3.9 Spectral distribution in the UV cabinet and produced by the free-standing UVB lamp indicating the wavelengths and wavelength intensities produced by each.

Figure 3.10 Spectral distribution of the free-standing UVA lamp indicating the wavelength and wavelength intensity emitted.

Figure 4.1 Cell viability assessed through the uptake of neutral red dye by EPCA1 (Figure 4.1a) and RTG-2 cells (Figure 4.1b) following exposure of cells to 24 hour B(a)P at various concentrations (0.0, 0.1, 1.0 and 3.2 μg ml^{-1}). Cell viability is expressed as a percentage of the control (% control), with the control value being 100 %. Asterisk (*) indicates a significant difference from the control in RTG-2 cells ($p < 0.05$).

Figure 4.2 DNA damage to EPCA1 cells following exposure to 6 hour B(a)P at various concentrations (0.0, 0.1, 1.0 and 3.2 μg ml^{-1}) without (Figure 4.2a) exogenous metabolic activation (S9), with S9 (Figure 4.2b) or following exposure to 24 hour B(a)P (0.0, 0.1, 1.0 and 3.2 μg ml^{-1}) without S9 (Figure 4.2c). DNA damage is assessed by the % Tail DNA. (Data marked with * (all concentrations) are significantly different to the control at $p < 0.0001$).

Figure 4.3 DNA damage to EPCA1 cells following exposure to 6 hour B(a)P at various concentrations (0.0, 0.1, 1.0 and 3.2 μg ml^{-1}) without (Figure 4.3a) exogenous metabolic activation (S9), with S9 (Figure 4.3b) or following exposure to 24 hour B(a)P (0.0, 0.1, 1.0 and 3.2 μg ml^{-1}) without S9 (Figure 4.3c). DNA damage is assessed by the % Tail DNA. (Data marked with *(all concentrations) are significantly different to the control at $p < 0.0001$).

Figure 4.4 Cell viability assessed through (a) trypan blue, (b) dual stain fluorescence or (c) NRR in EPCA1 and RTG-2 cells following exposure to UVB (0*, 200, 500, 625, 750, 875, 1000 J m^{-2}). Cell viability is expressed as percentage viability (%) (trypan blue and dual stain fluorescence) or as a percentage of the control absorbance (NRR) (control values are 100 %). Significant difference (Mann-Whitney U-test) from the control indicated by * ($p < 0.05$) or @ ($p < 0.001$). Results are from replicate studies.

Figure 4.5 Pilot study time course of UVB (50 J m^{-2} UVB). (a) 2 hours post irradiation (b) 4 hours post irradiation and (c) 6 hours post irradiation with Annexin V using RTG-2 cells to identify apoptosis or necrosis.

Figure 4.6 Cell viability assessed by the uptake of neutral red dye by RTG-2 cells following their exposure to various doses of UVA (0*, 500, 2000 and 4000 J m^{-2}). Cell viability is expressed as a percentage of the control (% control), with the control value being 100 %. Significant difference (Mann-Whitney U-test) from the control indicated by (*) in RTG-2 cells ($p < 0.05$).

Figure 4.7 DNA damage to EPCA1 cells (n=1600) following exposure to various doses of UVB (0*, 200, 350 and 500 J m^{-2}). DNA damage was assessed by the % Tail DNA. All UVB doses were significantly different (*) to the control (Mann-Whitney U-test $p < 0.0001$). N.B. control (0.0*) was sham irradiated for the same time period as 500 J m^{-2}.

Figure 4.8 DNA damage to RTG-2 cells following exposure to various doses of UVB (0*, 200, 350 and 500 J m^{-2}) (Figure 4.8a) or (0*, 25, 50, 75, 100 and 200 J m^{-2}) (Figure 4.8b). DNA damage was assessed by the % Tail DNA. All UVB doses tested were significantly different (*) to the control (Mann-Whitney U-test, $p < 0.0001$). N.B. control (0*) was sham irradiated for the same time period as 500 J m^{-2} (Figure 4.8a) or 200 J m^{-2} (Figure 4.8b).

Figure 4.9 DNA damage to RTG-2 cells following exposure to various doses of UVA (500, 1000, 2000, 4000, 6000 and 8000 J m^{-2}). DNA damage was assessed by the % Tail DNA. No UVA doses gave % Tail DNA results which were significantly different from the control (Mann-Whitney U-test, $p > 0.05$). N.B. control (0*) was sham irradiated for the same time period as 8000 J m^{-2}.

Figure 4.10 Cell viability assessed through the uptake of neutral red dye by RTG-2 cells following pre-treatment with B(a)P for

24 hours at various concentrations (0.0, 0.1, 1.0 and 3.2 μg ml^{-1}) and then exposure to various doses UVB (0*, 100 and 200 J m^{-2}) (Figure 4.10a) or UVA (0*, 500, 2000 and 4000 J m^{-2}) (Figure 4.10b). Cell viability was expressed as a percentage of the control absorbance, with the control value being 100 %. Significant effects are indicated (*) (NB control (0*) for each experiment was sham irradiated for the same time as either 100 or 200 J m^{-2} UVB or 500, 2000 or 4000 J m^{-2} UVA).

Figure 4.11 Median DNA damage to RTG-2 cells following pre-incubation for 24 hours with B(a)P (0.0, 0.1, 1.0 and 3.2 μg ml^{-1}) and exposure to UVB (0*, 25, 50, 75, 100 and 200 J m^{-2}) (Figure 4.11a) or UVA (0*, 500, 1000, 2000, 4000, 6000 and 8000 J m^{-2}) (Figure 4.11b). DNA damage was assessed by the % Tail DNA (0* is the sham irradiated control for each experiment, and controls were sham irradiated for the same time as each UVB or UVA dose). Significant differences (Mann-Whitney-U test, $p<0.001$) from the additive B(a)P and UVB/UVA irradiated response are indicated (*).

Figure 4.12 Cell viability assessed through the uptake of neutral red dye by RTG-2 cells following pre-treatment with B(a)P at various doses (0.1, 1.0 and 3.2 μg ml^{-1}) and then exposure to UVA (500 (Figure 4.12a), 2000 (Figure 4.12b), or 4000 J m^{-2} (Figure 4.12c). Cells were then incubated for various times (0, 1, 6, 24 hours) in GM. Significant differences (Mann-Whitney-U test, $p < 0.05$) from the control are indicated (*).

Figure 4.13 The effect of UVA irradiation on RTG-2 cells (Figure 4.13a). Figure 4.13b shows the clear DMPO-OH signal after UVA irradiation (500 J m^{-2}) of the B(a)P treated (3.2 μg ml^{-1}) RTG-2 cells.

Figure 4.14 Treatment of RTG-2 cells with 3.2 μg ml^{-1} B(a)P (24 hours) followed by UVA (500 J m^{-2}) with the addition of DETAPAC (Figure 4.14a), mannitol (which greatly decreased the yield of DMPO-OH) (Figure 4.14b). Addition of SOD had little effect (Figure 4.14c). Addition of catalase also had a small effect (Figure 4.14d). This indicated that the major radical product is ·OH.

Figure 5.1 Cell viability assessed through the uptake of neutral red dye by CHO-K1 cells following exposure of cells to 24 hour B(a)P at various concentrations (0.0, 0.1, 1.0 and 3.2 μg ml^{-1}). Cell viability is expressed as a percentage of the control (% control) with the control value being 100 %. Asterisks (*) indicate a significant difference from the control (Mann-Whitney-U test, $p < 0.05$).

Figure 5.2 Median DNA damage to CHO-K1 cells following exposure to 6 hour B(a)P at various concentrations (0.0, 0.1, 1.0 and 3.2 μg ml^{-1}) without (Figure 5.2a) exogenous metabolic activation (S9), with S9 (Figure 5.2b) or following exposure to 24 hour B(a)P (0.0, 0.1, 1.0 and 3.2 μg ml^{-1}) without S9 (Figure 5.2c). DNA damage is assessed by the % Tail DNA. Data marked with @ are significantly different to the control (Mann-Whitney-U test, $p < 0.05$) or with * are significantly different to the control (Mann-Whitney-U test, $p < 0.0001$).

Figure 5.3 Median DNA damage to 84BR cells following exposure to 24 hour B(a)P at various concentrations (0.00, 0.05, 0.10, 0.32, 1.00 and 3.20 μg ml^{-1}). DNA damage is assessed by the % Tail DNA. Data marked with @ are significantly different to the control (Mann-Whitney-U test, $p < 0.01$) or with * are significantly different to the control (Mann-Whitney-U test, $p < 0.001$).

Figure 5.4 Cell viability in CHO-K1 cells assessed through trypan blue and dual stain fluorescence technique (Figure 5.4a) or neutral red retention (NRR) assay (Figure 5.4b) following exposure to various doses of UVB (0*, 200, 500, 625, 750, 875 and 1000 J m^{-2}). Cell viability is expressed as percentage viability (%) for trypan blue and dual stain fluorescence assays or as a percentage of the control (%) for the NRR assay where control values are 100 %. 0* value is sham irradiated (Data marked with * are significantly different to the control, Mann-Whitney-U test, $p < 0.01$).

Figure 5.5. Cytotoxicity in CHO-K1 and 84BR cells following exposure to various doses of UVA (0*, 500, 2000 and 4000 J m^{-2}). 0* value is sham irradiated. Cytotoxicity is assessed through NRR assay and values are presented as a percentage of the control value. Data marked with * (CHO-K1) are significantly different to the control (Mann-Whitney-U test, $p < 0.05$).

Figure 5.6 DNA damage to CHO-K1 cells following exposure to various doses of UVB (0*, 200, 350 and 500 J m^{-2}) (Figure 5.6a) or UVA (0*, 500, 2000 and 4000 J m^{-2}) (Figure 5.6b). DNA damage is assessed by the % Tail DNA. All UVB doses tested are significantly different (*) (Mann-Whitney-U test, $p < 0.0001$) from the sham irradiated control (0*) but not significantly different from each other (Mann-Whitney-U test, $p > 0.05$). UVA doses which are significantly different (Mann-Whitney-U test, $p < 0.01$) from the sham irradiated control (@) are indicated and all doses are significantly different from each other (Mann-Whitney-U test, $p < 0.0001$).

Figure 5.7 DNA damage to 84BR cells following exposure to various doses of UVA (0*, 500, 1000 and 2000 J m^{-2}). DNA damage is assessed by the % Tail DNA. There was no significant difference (Mann-Whitney-U test, $p > 0.05$) between the sham irradiated control (0*) or any of the UVA doses tested.

Figure 5.8 Cytotoxicity in CHO-K1 (Figure 5.8a) and 84BR (Figure 5.8b) cells following 24 hours pre-incubation with B(a)P (0.0, 0.1, 1.0 and 3.2 µg ml^{-1}) and exposure to various doses of UVA (0*, 500, 2000 and 4000 J m^{-2}). 0* value is sham irradiated for the same time as 4000 J m^{-2} UVA. Cytotoxicity is assessed through NRR assay and values are presented as a percentage of the control value. All CHO-K1 data are significantly different (*) to the control (Mann-Whitney-U test, $p < 0.05$) with the exception of 0.1 µg ml^{-1} interacting with 500 J m^{-2} (Mann-Whitney-U test, $p > 0.05$) whilst all 84BR data are significantly different (*) to the control (Mann-Whitney-U test, $p < 0.05$) with the exception of 0.1 µg ml^{-1} B(a)P interacting with 4000 J m^{-2} (Mann-Whitney-U test, $p > 0.05$).

Figure 5.9 DNA damage to CHO-K1 cells following pre-incubation for 24 hours with B(a)P (0.0, 0.1, 1.0 and 3.2 µg ml^{-1}) and exposure to various doses of UVA (0*, 500, 1000 and 2000 J m^{-2}). DNA damage is assessed by the % Tail DNA. Significant differences (Mann-Whitney-U test, $p<0.0001$) from the combined B(a)P and UVA irradiated response are indicated (*). Plots for B(a)P alone are significantly different to the control (Mann-Whitney-U test, $p < 0.0001$) at all concentrations.

Figure 5.10 DNA damage to 84BR cells following pre-incubation for 24 hours with B(a)P (0.00, 0.05, 0.10, 0.32, 1.00 and 3.20 µg ml^{-1}) and exposure to various doses of UVA (0*, 500, 1000 and 2000 J m^{-2}). DNA damage is assessed by the % Tail DNA.

Significant differences (Mann-Whitney-U test, $p<0.001$) from the combined B(a)P and UVA irradiated response are indicated (*).

Figure 5.11 The effect of UVA (500 J m^{-2}) (no B(a)P) (Figure 5.11a), 24 hours treatment with B(a)P (3.2 µg ml^{-1}) without UVA treatment (500 J m^{-2}) (Figure 5.11b). Figure 5.11c shows B(a)P treated (24 hours) CHO-K1 cells after UVA irradiation (500 J m^{-2}).

Figure 5.12 The effect of UVA irradiated (500 J m^{-2}) DMPO control (Figure 5.12a) on 84BR cells. Figure 5.12b shows the effects of treatment (24 hours) with B(a)P (3.2 µg ml^{-1}) with UVA (500 J m^{-2}) on free radical formation in 84BR cells.

Figure 5.13 The effect of mannitol (Figure 5.13b), catalase (Figure 5.13c) and superoxide dismutase (Figure 5.13d) on cells treated with B(a)P (3.2 µg ml^{-1}) followed by UVA (500 J m^{-2}) (Figure 5.13a) on free radical formation.

Figure 6.1 Simple diagram to illustrate the possible mechanisms of DNA damage following exposure to PAH and UV in the cell.

ABBREVIATIONS

AhR	Aryl hydrocarbon receptor
B(a)P	Benzo(a)pyrene
BCC	Basal cell carcinoma
BPDE	Benzo(a)pyrene 7,8-diol-9,10-epoxide
BN	Binucleate cell
84BR	Primary human fibroblast cells
Calcein AM	Acetomethoxy derivate of calcein
CHO-K1	Chinese hamster ovary cell line
CO_2	Carbon dioxide
COL	Colchicine
CPD	Cyclobutane pyrimidine dimer
Cyto B	Cytochalasin B
DAPI	4'6-diamidino-2-phenylindole
DETAPAC	Diethylenetriaminetetraacetic acid
DMPO	5,5-dimethyl-1-pyrroline-N-oxide
DMSO	Dimethylsulphoxide
DNA	Deoxyribosenucleic acid
DSB	Double strand breaks
EC_{50}	Half maximal effective concentration
EMEM	Eagles minimum essential medium
EMS	Ethyl methanesulphonate
EPCA1	Epithelioma papillosum cyprini cell line
ESR	Electron spin resonance
EthD III	Ethidium homodimer III

FBS	Fetal bovine serum
GM	Growth medium
Ham F12	Ham F12 nutrient mixture
H_2O_2	Hydrogen peroxide
K-	Kinetochore negative
K+	Kinetochore positive
KCl	Potassium chloride
K_{OW}	Octanol water partition coefficient
L-GLUT	L-glutamine
LMP	Low melting point agarose
MEM	Minimum essential medium
Mn	Micronucleus
Mono	Mononucleate cell
NEAA	Non-essential amino acids
NMP	Normal melting point agarose
NRR	Neutral red retention assay
NPB	Nucleoplasmic bridges
$^{\cdot}OH$	Hydroxyl radical
$O_2^{\cdot -}$	Superoxide radical
8-oHdG	8-oxo-7,8-dihydro-2'-deoxyguanosine
PBS	Phosphate buffered saline
(6-4) P-P	(6-4) photoproduct
PM_{10}	Particulate matter <10 μm in diameter
RTG-2	Rainbow trout gonad cells
ROS	Reactive oxygen species
SCC	Squamous cell carcinoma

SCGE	Single cell gel electrophoresis ('comet assay')
SSB	Single strand breaks
TRITC	Tetramethyl rhodamine iso-thiocyanate
UVR	Ultraviolet radiation
0*	Sham irradiated control

ACKNOWLEDGEMENTS

Thanks go out to my supervisory team for their diligent and attentive help, support, endless patience and encouragement. My memories go to the late Dr David Gould. Also grateful thanks to Dr Nick Dodd for his wealth of knowledge and skill with the practical aspects of ESR and all his advice. Thanks also to Peninsula Medical School and the Duchy Health Charity for funding. A huge thankyou to Lynne Cooper who taught me about patience and timings!

Thanks also to the huge support network of friends, workmates and housemates who have been there through it all – risotto obsessions, red trainers, wine moments, dancing, tears and laughter – usually involving a hoover – cheers guys...!

My love to mum for being really mean when it was needed; to dad for looking totally baffled and having much better suggestions and my sis, and of course to Molly and Dylan who love us whatever happens, qualified or not!

Of course thanks to the Trades for buying me some time, kicking in and getting me back.

Big cuddles go to Musha for driving me crazy and keeping me sane all at once, and to Angus for making me laugh and keeping Musha out of trouble! Finally, my love to Mawgs – I couldn't have done it without you! Thanks Darling.

AUTHOR'S DECLARATION

At no time during the registration for the degree of Doctor of Philosophy has the author been registered for any other University award without prior agreement of the Graduate Committee.

This study was financed with the aid of a dual studentship from Peninsula Medical School and The Duchy Health Charity and carried out in the School of Biological Sciences, The University of Plymouth.

A programme of advanced study was undertaken, which included a course on the safe handling of cryogenic liquids and ethical use of fish in laboratory research.

Relevant scientific seminars and conferences were regularly attended at which work was often presented; external institutions were visited for consultation purposes (Covance Laboratory, Harrogate, UK) and two papers are being prepared for publication.

Conferences Attended:

Lyle, Z., Salter, L., Jha, A. and Curnow, A. 2004. Presentation: Optimisation and validation of techniques to detect genetic damage: an *in vitro* study using established cell lines. Peninsula Medical School Annual Research Event, Torquay, UK, February, 2004.

Lyle, Z., Salter, L., Jha, A. and Curnow, A. 2004. Presentation: Optimisation and validation of techniques to assess DNA damage: an *in vitro* investigation using permanent cell lines. University of Plymouth, Plymouth, UK. March 2004.

Lyle, Z., Salter, L., Jha, A. and Curnow, A. 2005. Presentation - Relative genotoxic sensitivity of fish and mammalian cells to environmental agents: an *in vitro* study

using established cell lines. Peninsula Medical School Annual Research Event, Torquay UK, March 2005.

Lyle, Z., Curnow, A., Salter, L. and Jha, A. 2005. Poster Presentations and Abstract submitted: Do fish cells exhibit differential sensitivity for genotoxic but not for cytotoxic effects of chemicals? Annual Meeting of the European Environmental Mutagen Society (EEMS): Kos, Greece. 3–4 July 2005. pp147.

Lyle, Z., King, C. and Jha, A. 2005. Presentations and Abstract submitted: *In vitro* evaluation of potential genotoxic effects of Bisphenol A in fish cells. Annual Meeting of the European Environmental Mutagen Society (EEMS): Kos, Greece. 3–4 July 2005. pp146.

Lyle, Z., Curnow, A., Jha, A., Salter, L. and Dodd, N. 2007. Poster Presentation: Interactive toxicity of B(a)P and UVA radiation. 5th International Conference on Marine Pollution and Ecotoxicology, Hong Kong, 3–6 June 2007.

Word count of main body of thesis: 59, 620

Signed:  .

Date: 25th March 2009.

CHAPTER I - INTRODUCTION

1.1 Environmental Pollution

Human activities have led to increases in environmental pollutants that pose both constant and increasing threats to all organisms (Lehto *et al.*, 2003; Matsuzawa *et al.*, 2001). Aquatic and terrestrial (including atmospheric) environments form complex and dynamic ecosystems, and whilst the aquatic environment provides a sink for many natural and anthropogenically derived chemicals (Arfsten *et al.*, 1996; Barron *et al.*, 2000; Law *et al.*, 1997), the terrestrial environment contains many pollutants in solid, liquid and gaseous form (Danaee *et al.*, 2004; Durant *et al.*, 1996; Onuska, 1989). Environmental pollutants may contain mutagens which are physical or chemical agents that change the genetic information and they can be lethal (Kawanishi *et al.*, 2001; Durant *et al.*, 1996). Some mutations may lead to detrimental effects at the population level, such as a loss of genetic diversity, and this could lead to serious implications for species survival and ecosystem functioning (Anderson *et al.*, 1994; Bickham *et al.*, 2000; Dixon *et al.*, 2002; Würgler & Kramers, 1992) and have far reaching consequences for organism health, food resources and commercial interest. Polycyclic aromatic hydrocarbons (PAHs - sometimes polynuclear aromatic hydrocarbons) are a major class of organic contaminants in both aquatic and terrestrial environments (Arfsten *et al.*, 1996; Choi & Oris, 2000a) and the work reported in this thesis deals with aspects of the toxic effects of the commonly found PAH Benzo(a)Pyrene (B(a)P) particularly when in the presence of ultraviolet light (UVA and UVB).

1.2 Polycyclic Aromatic Hydrocarbons (PAHs)

PAHs are a group of organic molecules made up usually of hydrogen and carbon comprising two or more fused benzene rings with cyclopentene inclusions or alkyl side-chain substitutions (Neff, 1979). PAHs are found throughout the environment (Table 1.1) for example, measured concentrations in topsoil have been shown to range from 8.6 to 3881 μg kg^{-1} (with an average of 397 μg kg^{-1}) in China (Ping *et al.,* 2007) or 59 to 1350 ng g^{-1} in Europe (Wilcke *et al.,* 2005). PAHs have also been detected in water (Poma *et al.,* 2002) and whilst levels in uncontaminated groundwater may range between 0 to 5 ng l^{-1} concentrations in contaminated groundwater may exceed 10 mg l^{-1} (WHO, 2003). More typical concentration ranges for PAHs in drinking water are from 1 ng l^{-1} to 11 mg l^{-1} (WHO, 2003). In sea water samples PAH concentrations have been measured from 0.28 to 39.57 μg l^{-1} (Said & El Agroudy, 2006). PAHs can be found in the atmosphere (for example, 456 ng m^{-3} has been measured in Turkey (Tasdemir & Esena, 2007)) attached to dust particles and deposited via atmospheric processes (Pekey *et al.,* 2007; Tsapakis *et al.,* 2006). The main natural inputs occur as releases from volcanoes and forest fires. For example, it was shown that there was a daily downward flux of PAHs (7.29 μg m^{-2} per day) from the eruption of Mount Etna in Southern Italy (Stracquadanio *et al.,* 2003). Anthropogenic sources include cigarette smoke, vehicle exhaust (Kuljukka-Rabb *et al.,* 2001), incomplete combustion of coal (Binkova *et al.,* 1995), coal tar (Carlsten *et al.,* 2005; Karlehagen *et al.,* 1992), wood and agricultural burning, waste incineration (Lee *et al.,* 2002), discharges from industrial plants, waste water treatment plants and natural gas for industrial and domestic purposes (Binkova & Sram, 2004; Cizmas *et al.,* 2004; Walker, 2001). PAHs are also used in medicines and in dyes, plastics and pesticides, whilst others occur in asphalt for road constructions. Aquatic contamination by PAHs is largely caused through human activities such as petroleum spills, discharges and seepages, industrial and municipal wastewater, urban runoff (for example, concentrations of individual PAHs have been measured as

300-10,000 ng l^{-1}, with the concentrations of most PAHs above 1,000 ng l^{-1} (Cole *et al.,* 1984)) and atmospheric deposition (Albers, 1995; ATSDR, 2004; Sargaonkar, 2006). PAHs are especially present in large amounts around industrialised areas (Bojes & Pope, 2007) and the offshore oil industry and oil tanker wreckages may contribute to localised inputs of PAHs to the aquatic environment (Ho *et al.,* 1999).

PAHs are persistent in the environment and it has been demonstrated that they may travel long distances through the atmosphere or by water currents before falling to the earth through precipitation or settling as particles to sediment (Chen *et al.,* 2006a; Chen *et al.,* 2006b; Luo *et al.,* 2006). The transformation and degradation of PAHs in sediments is under the control of complex biological and environmental factors. PAH concentrations will vary spatially; surface waters may contain quantifiable amounts, whilst direct land surface runoff and sediments will contain much higher accumulated levels (Kilemade *et al.,* 2004a; Kilemade *et al.,* 2004b; Van Dolah *et al.,* 2005). For example sediment samples from Casco Bay in Maine contained total PAH concentrations ranging from 16 to 20,800 µg kg^{-1} dry weight (Kennicutt *et al.,* 1994). In oxidized surface sediments, salinity, season, temperature, and ambient PAH concentration play a major role in the rates of PAH transformation (Shiaris, 1989). There is therefore the potential for these settled PAHs to become liberated back into the atmosphere, or if contained within terrestrial sediments, to leach into the groundwater (ATSDR, 1995).

PAHs have been identified as one of the major hazards to the marine and aquatic environment, and can pose a threat to a variety of organisms (Nigro *et al.,* 2002). Most of the PAH in surface waters are believed to result from atmospheric deposition (Santodonato *et al.,* 1981) but it is estimated that PAH inputs to water may be more than 80,000 t yr^{-1} (NRCC, 1983). Aromatics with 1- and 2-rings generally do not persist in the natural environment, but the larger 3- , 4- , 5-

ring aromatics can (Barron & Ka'aihue, 2001; Pelletier *et al.,* 1997) as the larger compounds are not volatile, have low water solubility and are much more difficult to degrade. Higher concentrations of PAHs are often found in coastal and estuarine samples and can range from 0-10.7 μg l^{-1} (Law *et al.,* 1997). For larger PAHs, toxicity operates intracellularly, with effects directed to DNA or to proteins. The aromatic content of petroleum, in particular PAHs, has generally been assumed to be the principal determinant of the toxicity of oil to aquatic organisms (Pelletier *et al.,* 1997). However, parent PAHs have no functional groups and are chemically quite unreactive, even though they can be oxidised in both the natural environment and biochemically. For example, chemical dispersants (surfactants) have been widely used as a tool for reducing the impact of oil spills on the shoreline and subsequently to marine life and because of oxidative processes this may increase the bioaccessible fraction and result in enhanced bioaccumulation and/or changes in the metabolism of the compound leading to indirect or direct toxicity through the food chain (Lemiere *et al.,* 2004; Wolfe *et al.*, 2000). Short-term LC_{50} values are generally in excess of 0.1 mg l^{-1} (NRCC, 1983) and chronic no-observed-effect-concentrations (NOEC) for fish and crustaceans exposed to PAH exceed 1 μg l^{-1} (Call *et al.,* 1986; OSPARCOM, 1994).

For humans in proximity to sources of fossil fuel combustion (for example, industrial or motor vehicle emissions) the possibility of direct inhalation and absorption through the skin of free and particle bound PAH presents a serious health hazard and exposure to these potentially mutagenic agents can occur both indoors and outdoors; usually as a combined exposure to a complex mixture of mutagenic substances (for example, cigarette smoke or the emissions from diesel exhausts (Vainio *et al.,* 1990)) that could be a major contributing factor in air pollution-related diseases (Weglarz & Skrok, 2000). Studies have also shown that people living in urban environments that are polluted by heavy traffic emissions exhibit high

levels of oxidative DNA damage (Avogbe *et al.,* 2005) and increased susceptibility to disease (Becker *et al.,* 2002; Binkova *et al.,* 1995; Lee *et al.,* 2002). For instance, exposure to air pollution is linked with reduced birth weights, increases in premature births and reduced semen quality (Sram *et al.,* 1996). What is certain is that there are demonstrable relationships between increases in urban air pollution from traffic emissions and the incident of asthma, especially in children (Petroeschevsky *et al.,* 2001; Thompson *et al.,* 2001). Evidence also suggests that exposure of the foetus to air pollutants in pregnancy may increase susceptibility to developing asthma (Hamada *et al.,* 2007) and in one study, the incidence of asthma was positively linked to the levels of benzene (Thompson *et al.,* 2001). Other allergic respiratory diseases may be exacerbated by exposure to environmental air pollution, such as allergic rhinitis (Vimercati *et al.,* 2006) but exposure to air pollution is also linked to more serious diseases such as lung cancer (Peluso *et al.,* 2005; Vineis *et al.,* 2007). PAHs are also directly ingested by humans through contaminated water, and foodstuffs containing quantities of PAH such as barbequed, charcoal-broiled, or smoked products and PAHs may circulate systemically as measured through blood and urinary samples (Hara *et al.,* 1997; Perico *et al.,* 2001; Ruchirawat *et al.,* 2006). PAH exposure risks for humans are estimated to be around 10^4 - 10^7 mg/kg/day for cancer risk (ATSDR, 1995). There is no information available regarding lethal exposures to total PAH in humans however, a dose-related decrease in survival was noted in hamsters after 60 weeks of inhalation exposure to 46.5 mg m^{-3} benzo(a)pyrene for 109 weeks (Thyssen *et al.,* 1981). Exposure to indoor pollutants (for example from cigarette smoke or coal fires (Merlo *et al.,* 1998; Qian *et al.,* 2007; Salo *et al.,* 2004)) may predispose people to more serious conditions such as asthma, chronic obstructive pulmonary disease (COPD), chronic lung diseases and even cardiovascular diseases of the arteries and vasculature when combined with non-specific inflammatory agents. For example, air pollutants often

contain PM_{10} particles (particulate matter < 10 μm in diameter) that may cause acute respiratory effects such as asthma, and elevated rates of asthma have been suggested to be due to interactions between PM_{10} and nitrogen dioxide (NO_2) and elevated levels of ozone (O_3) (Delfino *et al.*, 2002).

Table 1.1. Examples of PAH and B(a)P detected globally in air, water and sediments.

Sample Type and Location	**Total PAH or B(a)P concentrations detected**	**Reference**
Freshwater - Europe	Total PAH – 23-1285 μg kg^{-1}	Aouadene *et al.*, 2008
Sediment - UK	B(a)P – 3600 μg kg^{-1}	Clemons *et al.*, 1999
Sediment - Africa	Total PAH - 78-25,000 ng g^{-1}	Gaspare *et al.*, 2009
Sediment - USA	Total PAH–1500-3000 μg g^{-1}	Ingersoll *et al.*, 2002
Air - Europe	B(a)P – 2.1 ng m^{-3}	Jedrychowski *et al.*, 2007
Seawater - UK	Total PAH – 0-10.7 μg l^{-1}	Law *et al.*, 1997
Freshwater - China	Total PAH – 107-707 ng g^{-1}	Liu *et al.*, 2008
Sediment - China	Total PAH – 189-637 ng g^{-1}	Luo *et al.*, 2006
Air - Europe	B(a)P – 1.1 ng m^{-3}	Menichini *et al.*, 2007
Air - USA	Total PAH - 4.2-160 ng m^{-3}	Naumova *et al.*, 2002
Sea water - UK	Total PAH - <1-50 ng l^{-1}	Readman *et al.*, 1982

It has been widely demonstrated that once ingested certain PAHs can be metabolised to much more carcinogenic compounds within the body. Benzo(a)pyrene (B(a)P) ($C_{20}H_{12}$, CAS Registry: 50-32-8) exemplifies this. It is an archetypal PAH and toxicologically one of the best studied and therefore was the PAH of choice for this

investigation. It is also a ubiquitous environmental contaminant produced by various combustion processes and occurs in cigarette smoke, charbroiled foodstuffs and is often a component of PAH based air pollution (Boelsterli, 2003). It has been estimated that the total amount of B(a)P produced in the United States is between 300 and 1,300 metric tons annually (NRC, 1983). Direct inhalation of cigarette smoke can contain levels of 0.5-7.8 µg B(a)P per 100 cigarettes and cigarette smoke environments may contain between 0.4-760 µg m^3 B(a)P (Guerin *et al.,* 1992). B(a)P enters the body through direct inhalation (affecting the respiratory tract), through ingestion (affecting the gastrointestinal tract) and topically via the skin. For example, human respiratory exposure to 0.0001 mg m^3 B(a)P over 6 months to more than 6 year periods caused serious effects such as reduced lung functions and throat and chest irritations (Gupta *et al.,* 1993). Placental exposure to B(a)P (50 µmol) has been shown to stimulate human gonadotropin release by first trimester human placental explants *in vitro* (Barnes & Shurtz-Swirski, 1992) suggesting that B(a)P can alter human placental endocrine function early in pregnancy. Concentrations of B(a)P in air are estimated to be 0.095-0.0435 µg per day, in drinking water as 0.0011 µg per day and in food incidental ingestion is estimated at 0.16-1.6 µg per day (Santodonato *et al.,* 1981). B(a)P levels have been estimated from several countries in different foodstuffs, for example; margarine (0.2-6.8 ppb), smoked fish (trace-6.6 ppb), smoked or broiled meats (trace-105 ppb), grains and cereals (not detected-60 ppb) and vegetables and fruits (from not detected to 24.3 ppb and 29.7 ppb) (Santodonato *et al.,* 1981). B(a)P as with all PAH may accumulate in the body in the lipids due to the lipophilic properties. B(a)P has low water solubility, low vapour pressure and high (6.06) octanol-water partition coefficient (K_{ow}) (Mabey *et al.,* 1982) resulting in its partitioning mainly between soil (82 %) and sediment (17 %), with approximately 1 % partitioning into water and < 1 % into air, suspended sediment and biota (Hattemer-Frey & Travis, 1991). This

means that as with other 5- ring PAHs, they are found predominantly in the particle phase (Zhou *et al.,* 2005). However, it has been estimated that 1-2 tons of B(a)P were released from municipal sewage effluents and 0.1-0.4 tons of B(a)P were released from petroleum refinery waste waters in the United States in a year (Brown & Weiss, 1978).

It has been shown that B(a)P is noncovalently associated with lipoproteins but not acidic compartments or mitochondria. B(a)P enters into cells from plasma lipoproteins (Plant *et al.,* 1985) and biodistribution studies have shown different localisation of B(a)P in rat organs and tissues depending on lipoprotein classes. The liver and adrenals showed the highest levels of B(a)P when all classes of lipoproteins were used, but especially with high-density lipoproteins (Panin *et al.,* 1991; Polyakov *et al.,* 1996). B(a)P can exert multiple effects in the cell and trigger multiple pathways including covalent binding with DNA, activation of the aryl hydrocarbon receptor (AhR) and activation of oxidative stress pathways.

B(a)P biotransformation leads to reactive electrophilic metabolites which are able to bind covalently to DNA to form DNA adducts (Abe *et al.,* 1983; Diamond *et al.,* 1980; Durant *et al.,* 1996; Ortiz-Delgado *et al.,* 2007). The enzymatic oxidation and hydrolysis of B(a)P to a more water soluble polar form occurs in a multi-step process (Figure 1.1). B(a)P is firstly oxidised to a 7,8-epoxide and then hydrolysis transforms this to trans-7,8-diol-epoxide catalysed by epoxide hydrolase. Oxidation forms the 9,10-epoxide that contains an active centre which is the carbon atom at the C-10 position. The final electrophilic intermediate following this sequence of metabolic activation steps is the "ultimate metabolite and carcinogen" B(a)P 7,8-diol-9,10-epoxide (BPDE). From this point the carcinogenicity of B(a)P becomes more apparent as this compound can circulate systemically and intercalate and react with DNA at guanine-cytidine

(G-C) base pairs creating DNA adducts and causing the modification of guanine. The normal base-pairing is G-C (with three hydrogen bonds), however the presence of a B(a)P adduct at the N-2 amine position of guanine precludes binding via these three hydrogen bonds and instead the guanine adduct will pair with adenine, causing a base transversion i.e. the major adduct on DNA is B(a)P-N_2-dG (Kushman *et al.,* 2007) and this N_2 amine position where the B(a)P adduct is covalently bonded interferes with one of the hydrogen bonds, so this adduct will only pair with adenine. Therefore, in the next cell cycle the adenine (wrong base) will pair with thymine (T) which results in a base pair transversion. If this mismatch escapes the cell's repair mechanisms then the change becomes permanent and a point mutation will arise. This lesion i.e. point mutation may cause DNA strand breaks, both single strand and double strand (Mouron *et al.,* 2006; Nwagbara *et al.,* 2007). These effects may be irreparable and lead to permanent mutations in the cell that will continue to be reproduced when the cells replicate (Mouron *et al.,* 2006). Mutation through B(a)P adducts may have dangerous repercussions possibly leading to abnormal growth of the cells and cancer (Mahadevan *et al.,* 2005). However mutation induction is not necessarily deleterious for an organism as mutations that occur in inactive regions of the genome may have little downstream biological effects but if mutations hit a proto-oncogene (abnormal activation or overexpression) or a tumour suppressor gene (inactivation) then the alteration is potentially carcinogenic (Li *et al.,* 2004). As B(a)P metabolites can induce G-T transversions (Dong *et al.,* 2004) in specific codons (the 12^{th}) of the *ras* family of proto-oncogenes then the gene may possibly be converted into an active oncogene and is therefore potentially carcinogenic. Figure 1.1 illustrates the bioactivation of B(a)P to the ultimate metabolite and carcinogen, 7,8-diol-9,10-epoxide (Routledge *et al.,* 2001). The excreted metabolites in bile have been shown to be mutagenic (Chipman *et al.,* 1983) and

in the long term may interfere with normal organ functions (Mann *et al.*, 1999; Savabieasfahani *et al.*, 1999; Smith *et al.*, 2007).

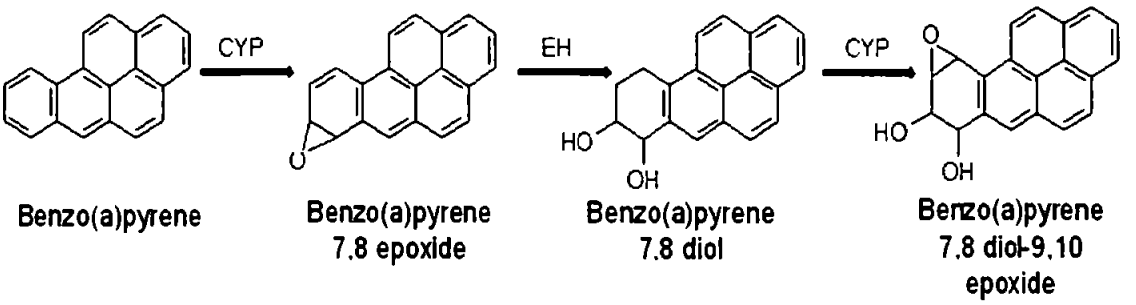

Figure 1.1 Bioactivation of B(a)P to the ultimate metabolite and carcinogen, 7,8-diol-9,10-epoxide (Adapted from Boelsterli, 2003).

The activation of the AhR is considered an important determinant of mutagenic potency of chemicals (Cheung *et al.*, 1993) including PAHs (Machala *et al.*, 2001). For example, the AhR is normally in the cytoplasm as a protein complex including heat shock protein 90 (Hsp90), an immunophilin like molecule known as AhR associated protein 9 (ARA9) and chaperone p23 which prevent the AhR from binding with DNA and allow ligand binding of the AhR with a xenobiotic such as B(a)P (Chen & Perdew, 1994; Kaslauskas *et al.*, 1999; Perdew, 1988; Yu *et al.*, 2008). Once B(a)P has bound to the AhR it translocates into the nucleus where a heterodimer is formed with the AhR nuclear translocator. This heterodimer binds to xenobiotic responsive enhancers that are located proximally to the promoter region of specific genes including CYP1A1, CYP1A2 and CYP1B1 (Chen *et al.*, 2003; Elbekai *et al.*, 2004; Hooven *et al.*, 2005) which are enzymes for metabolic activation of B(a)P. B(a)P is also subject to redox cycling following metabolic activation which can generate reactive oxygen species that may be involved in stress responses. For example, one of the major metabolites is B(a)P-1,6-hydroquinone which can be autoxidised to B(a)P-1,6-semiquinone and finally to B(a)P-1,6-quinone (Bolton *et al.*, 2000). The electophilic metabolites produced from B(a)P can modify and activate

a protein complex in the cell which can activate the antioxidant response element (ARE)/ electrophilic response element (EpRE)-binding protein. The ARE/EpRE-binding protein translocates into the nucleus and binds to the ARE/EpRE located in the promoter region of critical genes concerned with antioxidant and stress responses including GST, NQO, ALDH and the heme oxygenase-1 (HO-1) gene (Bolton *et al.,* 2000). Reactive oxygen species have been shown to induce oxidative stress (for example, lipid peroxidation) based on *in vitro* studies using fish liver microsomes and a fish cell line (Choi & Oris, 2000a; 2000b). It has also been hypothesised that B(a)P acts as a photosensitiser when exposed to UVR (Strniste *et al.,* 1980) and the metabolites from B(a)P, in particular BPDE, may also interact with UVR to increase the mutation frequencies in the *supF* gene (Routledge *et al.,* 2001).

1.3 Ultraviolet Radiation (UVR)

Solar UVR (100-400 nm) is a ubiquitous environmental agent and induces acute and chronic reactions in both human and animal skin (Ichihashi *et al.,* 2003). Solar radiation is also a major factor in the development of certain types of skin cancer, with the carcinogenic properties being linked to the UVR region (200-400 nm) (IARC, 1992; Ting *et al.,* 2003). The nature of carcinogenesis is dependent upon a contingency of factors: namely the UV exposure time, wavelength, frequency and the UV dose received (De Gruijl & Forbes, 1995). UVR consists of highly energetic photons that have the potential to damage many biological molecules, including DNA. The actual absorption of UVR by different biological molecules is highly dependent upon wavelength; therefore emphasis is generally given to the wavelength dependence of the detrimental effects of UVR. UVR wavelengths range between 100 nm and 400 nm and together comprise the most energetic region of the optical radiation spectrum (Cridland & Saunders, 1994). This range is outside that of visible

light (400-700 nm). UVR is conventionally classified into three wavelength categories: UVC (<280 nm), UVB (280-315 nm) and UVA (315-400 nm) (Figure 1.2).

Short wavelength UVC is energetically most active and damaging to living tissues, but is completely blocked in the upper atmosphere by ozone; however, studies have demonstrated its direct mutagenic effect on DNA (McLuckie *et al.,* 2004). UVB has received the greatest attention as the major risk factor in skin carcinogenesis (Thomas-Ahner *et al.,* 2007). Although UVB is partially blocked by ozone it is known to induce genotoxicity through DNA damage (Ikehata *et al.,* 2003; Mitchell *et al.,* 1999; Morales *et al.,* 2003; Tsilimigaki *et al.,* 2003), in particular the formation of cyclobutane pyrimidine dimers (CPDs) and (6-4) photoproducts (Figure 1.2) which induce mutations in epidermal cells, potentially leading to uncontrolled cellular proliferation. The acute effects of UVB on the skin are mainly adverse, such as erythema, which if severe enough can cause blistering and destruction of the skin layers (including necrosis and apoptosis), and immune suppression (Young, 1987; Brash *et al.,* 1996; Nghiem *et al.,* 2001; Norval *et al.,* 2007).

UVR reaching the earth's surface can range widely due to altitude and seasonality. For example in Europe measurements were made between 7.39-36.50 M J m^{-2} day^{-t} at 3576 m above sea level and 5.09-29.45 M J m^{-2} day^{-t} at 577 m above sea level between winter and summer seasons respectively in each location (Blumthaler *et al.,* 1997). Ozone plays a critical role in absorbing solar UV radiation in the upper atmosphere and therefore protecting life on Earth. However, stratospheric ozone levels have declined, and evidence has long suggested that a loss of ozone would affect the flux of UVB levels at the Earth's surface (Calkins & Thordardottir, 1980; Karentz & Lutze, 1990; Madronich *et al.,* 1995; Malloy *et al.,* 1997; Taalas *et al.,* 1997). Therefore, a reduction in ozone would lead to an increase

in UVB levels. This increase would not only detrimentally affect man, but also agricultural systems, plant and animal ecosystems, and the marine environment (Bentham, 1993; de Gruijl *et al.,* 2003; Manning & Van Tiedemann, 1995; Mayer, 1992). For example, in the aquatic environment, many studies have recognised UVR as an environmental stressor (e.g. along with water quality or pH (Hatch & Blaustein, 2000)) that can penetrate through the water column (Hader *et al.,* 1995; Kuhn *et al.,* 1999; Wulff *et al.,* 1999). Biologically significant levels of UVR are known to penetrate tens of metres in clear freshwater lakes and marine waters which are relatively low in productivity (Kuhn *et al.,* 1999) and shallow water sediments (Garcia-Pichel & Bebout, 1996). For wild populations in clear water high-altitude lakes there may be considerably higher mortalities in fish from exposure to increased UVB (Battini *et al.,* 2000). Variability in cloud cover, water quality, and vertical distribution and displacement within mixed layers also affects the flux of UVB radiation penetrating the water column (Karentze & Lutze, 1990). For instance, in less transparent environments, the damaging effects of UVR may be attenuated within the first 30-40 cm (Battini *et al.,* 2000) and whilst it has been demonstrated that dissolved organic matter (DOM) is one of the most important factors affecting the attenuation of UVR in water (Bracchini *et al.,* 2004), quantification of surviving cells at 30 metres has indicated biological responses even at these depths (Karentze & Lutze, 1990). Surface solar spectral irradiance has shown daily fluctuations intertidally to maximal levels of 670 μW cm^{-2} for UVA and 26 μW cm^{-2} for UVB whilst measurements were 3000 μW cm^{-2} for UVA and 160 μW cm^{-2} for UVB in an estuarine location (Barron *et al.,* 2000). Total intensities of visible light at the surface of the ocean were > 3000 μW cm^{-2}, 4500 μW cm^{-2} (UVA) and 225 μW cm^{-2} (UVB) (Barron *et al.,* 2000).

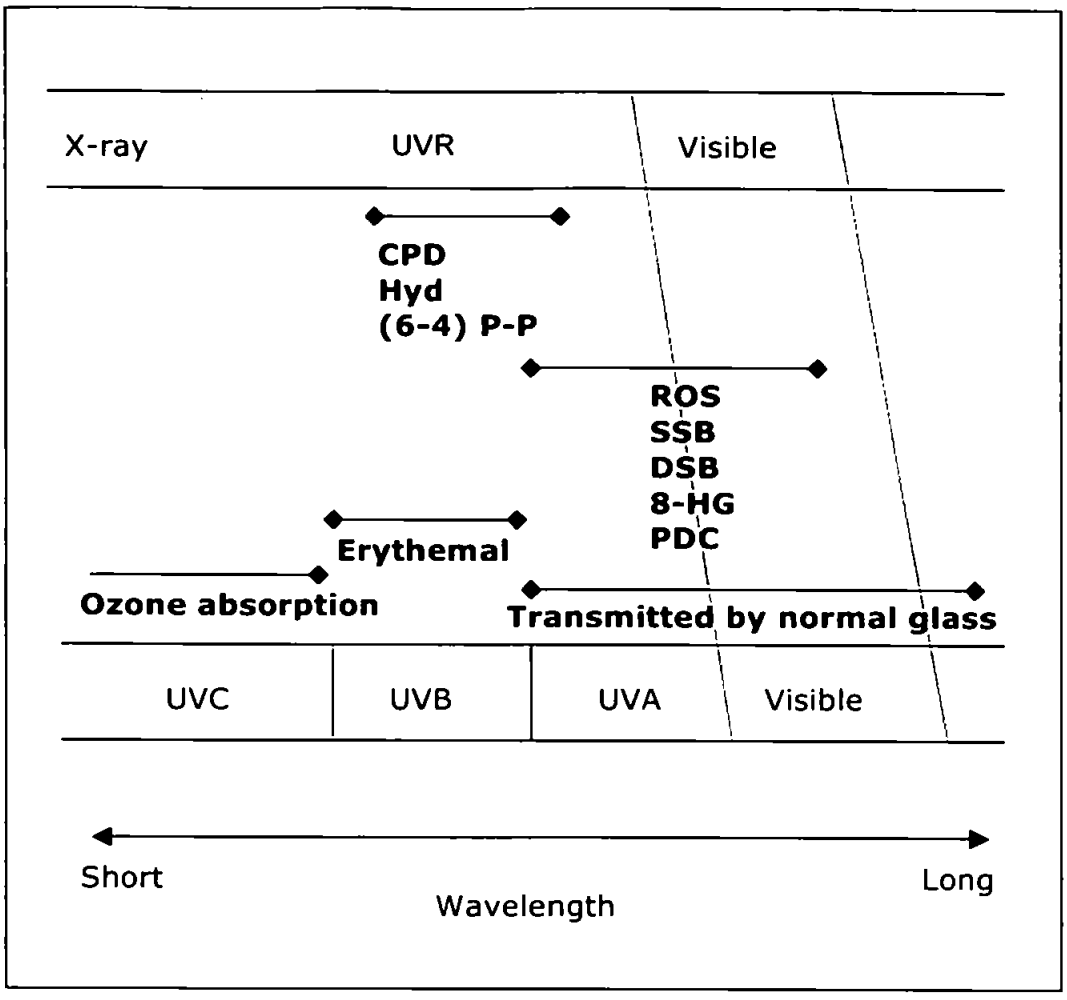

Figure 1.2 The UVR spectrum showing some of the effects of each wavelength and a summary of the principle pathways of UVR–induced DNA damage. Pathways that produce the most common photoproducts at each wavelength are shown. Abbreviations: (6-4)pp, (6-4) photoproducts; Hyd, pyrimidine hydrates; CPD, cyclobutane pyrimidine dimers; SSB, single strand breaks; DSB, double strand breaks; PDC, protein-DNA crosslinks; 8-HG, 8-hydroxyguanine; ROS, reactive oxygen species (adapted from Cridland & Saunders, 1994).

UVR levels reaching the Earth's surface are monitored by various laboratories (Roy *et al.,* 1995) and although there has been some detection and quantification of UVA levels, monitoring has mainly focused on fluctuating UVB levels (McKenzie *et al.,* 2007) because it is considered to be the most important (and most damaging) wavelength as terrestrial UVA levels show little flux (Ilyas *et al.,* 1988). Conversely, the overall contribution of the more abundant UVA wavelengths (320-400 nm) to the skin is poorly understood. UVA radiation comprises the majority of the UVR reaching the Earth's surface and moderate exposure to UVA has been linked to the induction of oxidising reactions in the body and leads to melanogenesis (Yanase *et al.,* 2001), skin inflammation, especially when skin has been exposed to photo-sensitising chemicals that may lead to photo-toxicity and photo-allergy (Albès *et al.,* 2004; Burren *et al.,* 1998; Danaee *et al.,* 2004) and direct mutations in the DNA including single strand breaks (Cayrol *et al.,* 1999), C-T transitions, (found at dipyrimidine sites), and CC-TT random substitutions. UVA wavelengths are not directly absorbed by DNA however it is now known that UVA penetrates into the deeper dermal cells causing ROS production (Agar *et al.,* 2004). Interestingly, recent research has shown that CPDs, more typically associated with UVB, were produced in significant yield in whole human skin exposed to UVA and furthermore, CPD production was greater than production of the oxidative lesion, 8-oxo-7,8-dihydro-2'-deoxyguanosine (Mouret *et al.,* 2006).

Skin is an incredibly complex organ, and differs between organisms. Human skin can be split into 3 regions, at the bottom there is the subcutaneous layer, followed by the dermis, and finally the epidermis on the surface. The subcutaneous layer consists of a layer of adipose tissue that insulates the body and provides mechanical protection against physical shock. This subcutaneous fatty layer is fed by blood vessels and nerves that carry nutrients and essential components to

the skin. The dermis is the major component of the skin and is typically several millimetres thick and is composed of a network of connective tissue containing structures such as blood and lymphatic vessels, nerve endings, pilosebaceous units (hair follicles and sebaceous glands), and sweat glands. This extensive vasculature is essential for regulation of body temperature whilst also delivering oxygen and nutrients to the tissue and removing toxins and waste products. The epidermis is highly complex and is normally described as containing four histologically distinct layers which are the stratum germinativum on the inner section, the stratum spinosum, stratum granulosum and the stratum corneum on the surface.

Evidence, both experimental and epidemiological, has implicated UVR in the induction of both basal cell (BCC) and squamous cell carcinomas (SCC) the most common and generally the most easily treated forms of cancer (Urbach, 1997). In recent years there has been an increase in personal leisure time which has led to an increase in outdoor pursuits and holiday time to tropical destinations and with this an increase in skin cancer incidence as epidemiological studies have shown that tumour incidence correlates positively with circumstances that elevate cumulative skin exposure to UV radiation (Fears *et al.,* 2002; Tsilimigaki *et al.,* 2003; Whiteman *et al.,* 2001). However, even at home or in an office environment there is a risk of exposure to UVR which may be emitted by fluorescent and tungsten-halogen lighting, its effects however are thought to be minimal (Swerdlow *et al.,* 1988). Furthermore, tumours are predominantly seen in individuals and ethnic groups with weakly pigmented skin (Chuang *et al.*, 1990; Czarnecki & Meehan, 2000). Tumour incidence tends to be associated with body surfaces that receive the greatest UVR exposure, such as the head and neck (Haenszel, 1963; McCord *et al.,* 2000).

Malignant melanoma is a highly aggressive cutaneous cancer of melanocytes and is of growing concern since it is increasingly affecting young adults and is often lethal (Fears *et al.,* 2002; Ichihashi *et al.,* 2003; Phillipson *et al.,* 2002; Vitaliano, 1978; Whiteman & Green, 1999). Its incidence is increasing faster than any non-cutaneous cancer and primarily occurs in pale skinned populations (Armstrong & Kricker, 1994; Diepgen & Mahler, 2002), as with other types of skin cancers (Armstrong *et al.,* 1997). Melanoma incidence is associated with skin exposure to UVR (IARC, 1992) and suggestions have been made that melanoma risk is related to childhood exposure and intermittent UVR exposure as adults (Armstrong *et al.,* 1997; Garland *et al.,* 1990; Lee & Strickland, 1980; Whiteman *et al.,* 2001). This relationship is more complicated than with other skin cancers since it seems to involve intense but intermittent exposures to sun which may be related to increased global travel to tropical destinations by a larger proportion of the population (Agredano *et al.,* 2006; Rafnsson *et al.,* 2000). Melanoma incidence in individuals with outdoor occupations is actually lower than for those receiving intermittent exposures (Gallagher *et al.,* 1996; Lee & Strickland, 1980; Linet *et al.,* 1995) and melanoma incidence is related to latitude (Armstrong, 1984; Whiteman & Green, 1999). Other factors for melanoma risk include the extent of intermittent exposure to the sun, skin type and the numbers of dysplastic nevi, which are possible precursors to melanoma (Tucker *et al.,* 1997).

Fish skin differs most notably from terrestrial vertebrate skin mainly where the epidermal layers are in contact with the environment (Frenkel *et al.,* 2000; Hawkes, 1974; Sadovy *et al.,* 2005; Whitear *et al.,* 1980). The skin of fish shows greater susceptibility to sunburn damage than human skin when exposed to UVB because fish skin lacks a keratinised outer layer, has dividing cells in all layers of the epidermis, and is often lacking in protective epidermal melanin-

containing cells (Bullock *et al.,* 1978; Bullock, 1982). Fish are covered in scales which are blanketed with epidermal cells and interspersed with mucosal cells, an essential part of the fish epidermis, providing an immune defence and considerable protection against both photoproduct formation and sunburn (Fabacher & Little, 1985; Meador *et al.,* 2000). However, the scales can become damaged; particularly when fish are under stress conditions (e.g. in high population density loads in aquaculture conditions) and stress may alter the skin and immune functions (Iger *et al.,* 1992) leading to secondary infections and increased susceptibility to sunburn (Fabacher *et al.* 1994; Little and Fabacher, 1994). A study conducted in a high altitude farm was able to demonstrate physical damage to fish such as focal thickening of the dorsal fin, which progressed to fin erosion culminating in necrosis and sloughing of the entire fin (Bullock & Coutts, 1985) and photodermal necrosis has been reported in simulated and aquaculture conditions (Little & Fabacher, 1994; Roberts & Bullock, 1981). Sunburn has been shown in many fish species including salmonid fishes such as Rainbow trout (*Onchorynchus mykiss*), Apache trout (*Onchorynchus apache*) and Lahontan cutthroat trout (*Onchorynchus clarki henshawi*) within 2 days of exposure, (Little & Fabacher, 1994). UVB may degrade the epidermal layer of fish skin, causing the appearance of sunburn cells, epidermal hyperplasia, and reducing mucus secretion, sloughing the mucus layer (Little & Fabacher, 1994; Sharma *et al.,* 2005). *In vivo*, Kaweewat & Hofer (1997) showed that UVB significantly reduced the number of goblet cells in the dorsal epidermis in both cyprinid fish and salmonids which may have consequence for non-specific defence in immune function (Kaweewat & Hofer, 1997).

UVR-induced stress can reduce immune system functioning, both local and systemic, and immune modulation is induced by both UVA and UVB radiation (Jokinen *et al.,* 2000; Salo *et al.,* 2000). UVB exposure has lead to altered respiratory burst in blood leucocytes and

changes in major lymphatic organs (Jokinen *et al.,* 2000). Additionally should radiation levels compromise the integrity of the epidermis, then invasion by a variety of opportunistic pathogens, such as *Vibrio* spp., mycobacterial infections and fungal pathogens (*Saprolegnia*) (Little & Fabacher, 1994), combined with physical damage can cause inevitable risk of transmission throughout the stock. For example, UVB induced epidermal damage can be exacerbated by parasitic invasion due to the epidermis already being compromised (Bullock, 1985). In contrast, UVA has produced only minor effects in immune function. These data suggest that UVB induced a strong stress response (such as the increase in granulocytes, decrease in lymphocytes and elevated plasma cortisol levels) and that UVB may be a modulator of immune parameters (Jokinen *et al.,* 2000). These deleterious effects may certainly have serious implications for the host fish, for the economics of commercial fish farms, and for the surrounding environment.

1.4 Photo-Enhanced Toxicity of PAHs

Photo-enhanced toxicity investigates the effects of the environmental variable UVR on environmental contaminants such as PAHs (McClosky & Oris, 1993; Tilgman Hall & Oris, 1991). For example, a well documented case is the interaction of arsenite and UVR, which is known to cause impairment of DNA repair enzymes, which in turn may lead to enhanced UV mutagenesis (Bau *et al.,* 2001; Danaee *et al.,* 2004). Often even low levels of solar irradiance are adequate to induce photo-enhanced toxicity, suggesting that this may be a concern even in habitats with low-UV transparency (Barron *et al.,* 2000; Pelletier *et al.,* 1997). A summary of some studies that have investigated the interactive toxicity of PAH and UVR is presented in Table 1.2. The data presented in this table indicate that PAH and UVR can interact to increase toxicity but the genotoxicity or mechanisms underlying any damage have not been elucidated

makeing this subject worthy of further study using *in vitro* models to begin to untangle the effects of this interaction. Most PAHs show little toxicity below their water solubility concentration (Yamada *et al.*, 2003), but even at such low concentrations they may become highly toxic through photo-enhanced toxicity (Barron *et al.*, 2003; Pelletier *et al.*, 1997; Schirmer *et al.*, 1997). Photo-enhanced toxicity can occur through two mechanisms: photo-modification and photo-sensitisation (Mallakin *et al.*, 1999). Photo-modification is the mechanism by which UVR causes a structural change to the chemical which may be to a more toxic form (Huang *et al.*, 1993). Photo-modification may also occur through the process of photo-degradation, whereby UVR and microbial action work to degrade the PAHs. Guieysse and co-workers (2004) showed that UV treatment along with microbial action acts preferentially to degrade larger 4- and 5-ring PAHs but does not work so well on degrading the smaller PAHs, further, they were not able to characterise the photoproducts formed.

Table 1.2 Summary of some recent studies investigating the interactive toxicity of PAH and UVR.

Model	**Exposure concentrations**	**Response**	**Reference**
Pacific herring (*Clupea pallasi*) eggs and larvae	Weathered Alaska oil (total PAH content: 8 μg l^{-1}), sunlight (4 h, 1,350 μW cm^{-2} UVA, 14 μW cm^{-2} UVB, 14,900 μW cm^{-2} visible)	Toxicity of weathered oil increased with sunlight: 1.5-48-fold over control. Photoenhanced toxicity occurred when oil present in larval tissue.	Barron *et al.* 2003
Bluegill sunfish (*Lepomis macrochirus*) liver microsomes	Anthracene (0.77, 1.54, 7.7 μg ml^{-1}) & solar ultraviolet radiation (SUVR) (UVA: 83.72± 2.2 μW cm^{-2} UVB: 7.0 ± 0.35 μW cm^{-2})	Photoinduced toxicity of anthracene manifested in part through lipid peroxidation. High levels of reactive oxygen species (ROS) produced.	Choi & Oris, 2000a
Topminnow (*Poeciliopsis lucida*) hepatoma cell line (PLHC-1)	Anthracene: (2.16, 4.33, 8.65, 21.6, and 43.3 μM) & solar ultraviolet radiation (SUVR): (UVA: 159.55 ± 5.69 μW cm^{-2} UVB: 3.83 ± 0.28 μW cm^{-2})	Pre-exposure of anthracene/cell culture media to SUVR caused photo-modification and reduced the phototoxicity of parent anthracene compound to PLHC-1	Choi & Oris, 2003
Northern pike (*Esox lucius* L.)	UVB (1.0, 1.8 or 2.7 kJ m^{-2} per day) & retene (3, 9, 30 & 82 μg l^{-1})	Retene (9–82 μg l^{-1}) induced CYP1A with & without UVB. Severe skin damage in co-exposed larvae. UVB alone significant mortality.	Hakkinen *et al.*, 2004
Rainbow trout (*Oncorhynchus mykiss*) lenses	Fluoranthene (4900 nm), B(a)P (265 nm), creosote (70 μg ml^{-1}), fluorene (128 μM) & UVR (UVA 9.27 μmol m^{-2} s^{-1} for 12 hours.	Photomodification of PAH not cataractogenic, simultaneous exposure to UV and PAH - increased mean focal length variability (FLV).	Laycock *et al.*, 2000
In vivo exposure to mouse skin	UVA (40/50/100 kJ m^{-2}) & B(a)P (20/200/400 nmol/mouse)	Synergistic increase in genetic damage & carcinogenic processes	Saladi *et al.*, 2003
Rainbow trout (*Oncorhynchus mykiss*) primary gill cells (RTgill-W1)	Liquid creosote (1 g ml^{-1}) UV (UVB: 53 μW cm^{-2})	UV enhanced the toxicity of creosote.	Schirmer *et al.*, 1999

Photo-sensitisation is the postulated mechanism by which UV energy is absorbed by the chemical within the organism causing subsequent tissue injury; the photo-sensitised chemical (PAH) is excited by light energy to a triplet energy state. The energy associated with these excited state PAH molecules is released by non-radiative pathways and can indirectly generate singlet oxygen (Zhang *et al.,* 2004) and other ROS, such as superoxide and hydroxyl, that may cause tissue damage (Choi & Oris, 2000a). The toxicity of PAHs has been shown to increase to greater than 1000 times in the presence of UVR in numerous laboratory studies (Arfsten *et al.,* 1996). The combined effect of UVR and other environmental factors may result in synergistic effects (McLuckie *et al.,* 2004), leading to increased DNA damage. Whilst links have been shown between levels of arsenic ingested into the body and seemingly coincidental increases in skin cancer, there are suggestions that rates of air pollution increases over the recent years are paralleled by increased rates of skin cancer over this period (Goldsmith, 1996; Saladi *et al.,* 2003). The current concerns over climate change are also beginning to be reflected by increasing research into the effects of UVR on human health and the effects of increasing air pollution (Avogbe *et al.,* 2005; Sorensen *et al.,* 2003) causing diseases such as asthma, allergic disorders and deaths due to the effects of air pollution as well as the impacts on biodiversity and environment. Many studies have concentrated on the toxicology of the PAH compounds and UVR (Boese *et al.,* 1997; Huang *et al.,* 1993; Holst & Giesy, 1989; Okay & Karacik, 2007), but have looked only at the toxicity and not investigated the genetic impact of the interactions. Other studies have concentrated on the impacts of PAH and UVC (McLuckie *et al.,* 2004) (in the natural environment UVC is mainly blocked by ozone) or PAH and UVB (Lean, 1998). These studies have generally not taken into account UVA, a major part of the UVR spectrum and evidence suggests that UVA may have an important function in the toxicology of PAHs (Weinstein & Diamond, 2006) and that targeted research needs to address this.

1.5 The Use of *In Vitro* Model Systems in Environmental Toxicology

There is greater complexity and variability in trying to accurately interpret the results of studies at high levels of organisation due to the difficulties in determining cause and effect relationships between contaminant changes and varying ecosystem endpoints (Clements & Kiffney, 1994). There is an ever increasing load of chemicals being released into the aquatic and terrestrial environment (Chen *et al.,* 2006b; Wang *et al.,* 2006) and most chemicals lack adequate toxicological data, in most cases causal links between the observed abnormalities and the chemical exposure are not established (Lacour *et al.,* 2006). Therefore, the use of a more reductionist and mechanistic approach to predict or establish safety factors is essential in order to predict effects at higher levels of biological organisation (Reichert *et al.,* 1998). The use of *in vitro* cell culture conditions provides good experimental models to investigate the toxic potentials of PAHs and UV under controlled laboratory conditions (Crews *et al.*, 1995; Schirmer *et al.,* 2000; Taylor & Harrison, 1999).

There is currently tremendous growth in molecular and cellular toxicological approaches, mainly attributed to the rapid development of quick tests that incorporate the use of *in vitro* activation systems (Landolt & Kocan, 1983; Segner, 1998). The uses of cultured cells for toxicological research and screening have been recognised for many years in the field of biomedical research (Allen-Hoffman & Rheinwald, 1984; Butterworth *et al.,* 1989; Garcon *et al.,* 2006) but it has only been in the last few years that *in vitro* cell culture work is starting to find favour in aquatic and environmental toxicology (Castano *et al.,* 2003). However, although the use of *in vitro* systems as a replacement for *in vivo* studies is often criticised for lacking specificity for the particular system under investigation, the application of *in vitro* cell culture methodologies for toxicity testing

offers a number of scientific, technical and ethical advantages (Segner, 1998).

In vitro methodologies link with the tier-structure approach of establishing causative relationships between toxicants and biological effects before progressing to *in vivo* studies. Whilst *in vitro* studies provide information about the 'intrinsic' toxic effects of chemicals, the *in vivo* studies provide the 'expressed' toxic effects, taking into account the uptake, metabolism and repair capacity of the organism in question. The *in vitro* approach of using cultured fish cells is suitable for the tiered approach of testing aquatic contaminants for genotoxicity and cytotoxicity assays (Babich & Borenfreund, 1987; Dixon *et al.,* 2002). Although the information obtained from *in vitro* tests is not enough to make predictions at the ecosystem level, cellular effect studies are important because the primary interactions between chemicals and biota occurs at the surface of, or within cells therefore cellular effects provide an excellent system for establishing intrinsic toxic mechanisms and the underlying controls which regulate complex systems at the scale of the whole organism (Fent, 2001). *In vitro* tests are often commended for being more sensitive than using whole animal systems and they have the advantage of being less time-consuming and less expensive. Technically, *in vitro* tests enable rapid screening of large numbers of samples with economy of both space and resources. This makes them particularly valuable as a means of assessing the effects on living systems of the ever-increasing loading of man-made chemicals in the environment. There is also a good ethical rationale for the use of cultured cells because their use significantly reduces the number of animals that are sacrificed through *in vivo* experimentation (Segner, 1998). *In vitro* models, such as the use of cell lines are useful for establishing baseline data on potentially toxic agents, and can provide essential insight into ecotoxicological processes and play a key role in elucidating modes of action (Fent, 2001). When conducting clinical

research with carcinogens, it would be unethical to administer carcinogenic compounds in clinical trials (Weindling, 2001) as procedures must be approved by ethical review, and carried out in an approved manner that minimises long term health risks to the subject. However, even with approval by an ethics committee, clinical trials may go wrong and pose serious risks to the volunteers (ASCO, 2003).

However, the drawbacks to *in vitro* testing are numerous. For instance, *in vitro* systems lack the complete defence mechanisms of entire organisms and are often chosen on the basis of their convenience and availability rather than their relevance to the ecosystem under investigation (Landolt & Kocan, 1983). The types of *in vitro* models routinely used are organ perfusion, organ/tissue slices, tissue explants, primary cell homogenates and established cell lines. In biomedical research, the use of *in vitro* cell culture systems has been utilised effectively for many years (Abe *et al.,* 1983; Butterworth *et al.,* 1989), but within environmental toxicological research, *in vitro* systems incorporating cell lines have only been recognised as important tools for the last decade (Castano *et al.,* 2003; Parry, 2002). Cell lines from aquatic organisms such as amphibians and reptiles have been established but have found little application in toxicology; however, the use of *in vitro* systems incorporating fish cell lines is of growing importance as a tool in aquatic toxicology (Villena, 2003; Fent, 2001; Segner, 1998).

1.6 The Use of Cell Cultures for *In Vitro* Studies

In human skin cancer studies, human keratinocytes are often used to investigate the effects of UV radiation on the skin (Marrot *et al.,* 2004; Seo *et al.,* 2002). The epidermis is mainly constituted of keratinocytes. Differentiation of keratinocytes defines the organisation and distinction between the different layers of the epidermis; keratinocytes migrate from the basal layer (*stratum*

germinatum) to the superficial layer (*stratum corneum*), where they differentiate into corneocytes (Baudouin *et al.*, 2002). Table 1.3 illustrates a few examples of *in vitro* techniques and assays used in established cell lines from both mammalian and aquatic species.

In vitro, many cells are anchorage-dependent and require a suitable substrate to which they can attach and grow to form a 2-dimensional confluent monolayer over the surface. Once seeded, cells undergo a series of distinct phases. First, the lag phase, where the cell glycocalyx attaches to the substrate; second, the log phase, in which there is exponential cellular division and third, the plateau or stationary phase, where a confluent monolayer is formed. The formation of a confluent monolayer causes 'contact inhibition', as the density of the cells reduces cell proliferation. This stage is more representative of an *in vivo* tissue as the cell-cell contact may allow expression of specific cell functions. Sub-confluency is therefore essential prior to experimentation (Segner, 1998) however, in the case of keratinocytes, confluence greater than 70 % may permanently alter the cells due to contact inhibition. Table 1.4 illustrates a variety of experiments using established cell lines following exposure to B(a)P and has direct relevance to the work reported here. However, the choice of cell line for toxicity testing is a factor that can modify the outcome of studies, as certain cell types may exhibit specific sensitivities.

Table 1.3 Examples of cell culture techniques and assays used to investigate the effects of the *in vitro* exposure to environmental contaminants in established cell lines.

Cell Line	Origin	Toxicant Tested	Endpoint	Reference
RTL-W1	Rainbow trout (*Oncorhynchus mykiss*) liver	Nine PAHs	Induction of cytochrome P4501A	Behrens *et al.*, 2001
RTG-2	Rainbow trout (*Oncorhynchus mykiss)*	Industrial effluents	ATP, NRR, TP, CTI	Castano *et al.*, 1994
AS52	Chinese hamster	UVA	8-oxo-G, *gpt*, endonuclease sensitive sites	Dahle *et al.*, 2008
HaCaT	Human	UVA	ERK	He *et al.*, 2004
RTG-2	Rainbow trout (*Oncorhynchus mykiss*)	EMS	Mn, NRR	Kolpoth *et al.*, 1999
MCF-7	Human	PAH complex mixture	^{33}P-postlabelling, HPLC, western blot	Mahadevan *et al.*, 2005
MRC5 84BR NHEK	Human	UVA	SCGE	Morley *et al.*, 2005
CHO-K1	Chinese hamster	Arsenite	SCGE, CBMN	Raissuddin & Jha, 2004

Abbreviations: intracellular ATP content (ATP), 4-chlorophenol (4-CP), Cytokinesis-block micronucleus assay (CBMN), 2,4-dinitrophenol (2,-DNP), ethyl methane sulphonate (EMS), extracellular signal regulated kinase (ERK), guanine phosphoribosyl transferase gene (*gpt*), human keratinocytes (HaCaT), hydrogen peroxide (H_2O_2), FRAME kenacid blue protein (KBP), human mammary carcinoma derived (MCF-7), normal fetal lung fibroblasts (MRC5), N-methyl-N'-nitro-N-nitrosoguanidine (MNNG), nitroquinoline-l-oxide (4NQO), normal human epidermal keratinocytes (NHEK), neutral red retention (NRR), 7,8-dihydro-8-oxoguanine (8-oxoG), proteins (TP), rainbow trout liver cells (RTL-W1), single cell gel electrophoresis (SCGE), cytotoxicity index value (CTI)

Table 1.4 Examples of different endpoints used to detect cytotoxicity and genotoxicity in established cell lines following exposure to B(a)P.

Cell line	Concentration of B(a)P	Endpoint	Reference
XEM2	0, 50, 100, 200, 400 and 700 nM (DMSO added at control of 140 µl) (3 h)	^{32}P post-labelled DNA adducts	Helleberg *et al.*, 2001
RTG-2	0.0, 5, 10, 15, 20 and 25 µM in DMSO (DMSO < 1 % (v/v))	Mn NRR	Kolpoth *et al.*, 1999
MCF-7	313, 1563, 3125, 3750, 4500, 5625, 6250 and 7500 ng (Exposed 24 h)	^{32}P post-labelled DNA adducts	Kuljukka-Rabb *et al.*, 2001
MCF-7	1 µM	Synchronous fluorescence spectrophotometry, p53 protein by immunoblotting, thin layer chromatography (TLC), MTT assay, ATP quantitation	Myllynen *et al.*, 2007
RTG-2 RTL-W1	0.94 – 50 µM L^{-1}, LOEC = 3.74 µM L^{-1} (RTG-2), LOEC = 1.20 µM L^{-1} (RTL-W1) (2 h)	SCGE	Nehls & Segner, 2001
RTG-2	0.05, 0.1, 0.5, 1 µg ml^{-1} (DMSO 0.01 %) (8, 24, 48 and 72 h)	Mn	Sanchez *et al.*, 2000
RTgill-W1	Not specified – B(a)P not directly cytotoxic – low water solubility	Alamar blue CFDA-AM NRR	Schirmer *et al.*, 1998
BF-2	0.5 µg ml^{-1} (acetone 0.1 %)	Hydrocarbon – deoxyribonucleoside adducts, B(a)P metabolites	Smolarek *et al.*, 1988
A549 MCF-7	1, 2.5, 5, 10, 20 or 40 µM (24, 48, 72 or 96 h)	Caspase-3-like protease activity, internucleosomal DNA fragmentation	Tampio *et al.*, 2008
HepG2	150 µM (DMSO 1%) (24 h)	SCGE	Uhl *et al.*, 1999
HELF	2 µmol l^{-1} or 100 µmol l^{-1}	Western blot, flow cytometry	Ye *et al.*, 2008

Abbreviations: human lung carcinoma cells (A549), bluegill fry cells (BF-2), 5-carboxyfluorescein diacetate acetoxymethyl ester (CFDA-AM), genetically engineered V79 Chinese hamster fibroblasts (XEM-2), human breast adenocarcinoma cells (MCF-7), Human embryo lung fibroblasts (HELF), human hepatocellular carcinoma cells (HepG2), lowest observed effect concentration/level (LOEC), lung fibroblast cells (V79), micronucleus (Mn), 3-(4,5-dimethylthiazol-2-yl)-2,5-diphenyl tetrazolium bromide (MTT), neutral red retention (NRR), rainbow trout gill cell line (RTgill-W1), rainbow trout gonad cell (RTG-2), rainbow trout liver cells (RTL-W1), sister chromatid exchange (SCEs), single cell gel electrophoresis (SCGE)

Cell culture concerns the growth of cells under controlled conditions, in order to limit variability and to investigate specific effects. Cells that are cultured directly from an animal or person are known as primary cells but most primary cell cultures have limited lifespan (with the exception of some cells derived from tumours). Primary cells will only undergo a certain number of population doublings before they begin the process of senescence and stop dividing although they will generally retain viability (Freshney, 2000). In most cell culture studies, an established cell line will be used that has acquired the ability to grow indefinitely either through a random mutation or by genetic modification. There are numerous well established cell lines that are representative of particular cell types. However, many established cell lines have lost their original function (such as metabolic capability) and therefore need to be supplemented. All cells in culture need supplementation with nutrients and substances such as serum, amino acids or glutamine and need to be maintained at temperatures appropriate to each cell type (Freshney, 2000). For this project, three established cell lines were initially selected to optimise and validate the first stage of the project: a Chinese Hamster Ovary (CHO-K1) cell line, an Epithelioma Papillosum Cyprini (EPCA1) cell line, and finally a Rainbow Trout Gonad (RTG-2) cell line. For later inclusion into the project, a primary cell type human skin fibroblasts (84BR) was incorporated to compare with the established cell lines. These cells and the reasons for choosing them are discussed below.

1.6.1 Chinese Hamster Ovary (CHO-K1) Cell Line

The CHO-K1 cell line is a fibroblastic-like subclone from a parental CHO cell line that was initiated from an ovary biopsy of an adult chinese hamster. It is well characterised and is commonly used in genotoxicity studies (Huynh-Delerme *et al.*, 2003; Raisuddin & Jha,

2004), hence its inclusion in this study. However, this cell line does not contain appreciable levels of cytochrome P-450-dependent monooxygenase activity, thus an exogenous activation system must be introduced when using these cells with chemicals that have indirect action (i.e. they require metabolism to express their toxicity) (Ellard *et al.*, 1991; Ellard & Parry, 1993).

1.6.2 Epithelioma Papillosum Cyprini (EPCA1) Cell Line

Epithelial cells form a barrier between an organism and its environment and they are a primary target for environmental contaminant related carcinogenesis (Iger *et al.*, 1992). The EPCA1 cell line was introduced into this study to investigate the effects of PAH on an epithelial system and because it has been previously documented for use in environmental toxicology studies (Kammann *et al.*, 2001; Ruiz-Leal & George, 2004). The EPCA1 cell line is an established cell line and is reported to have retained normal levels of the ROS-scavenging intracellular thiols, glutathione and metallothionein (George *et al.*, 2000; Wright *et al.*, 2000), some enzymatic activation (Kammann *et al.*, 2001) and it has been used with hepatic microsomal enzymes to activate B(a)P in sediment extracts (Kammann *et al.*, 2001).

1.6.3 Rainbow Trout Gonad (RTG-2) Cell Line

The RTG-2 cell line is a fibroblastic-like cell line originating from the gonads of rainbow trout juveniles. It was originally developed for the study of fish viruses (Wolf & Quimby, 1962) but is commonly used to investigate a variety of endpoints (Braunbeck & Neumuller, 1996; Nicholson, 1971; Tarazona *et al.*, 1993; Walton *et al.*, 1987). The RTG-2 cell line is generally maintained at 21 °C, however, the cell line

can grow at temperatures between 5 and 26 °C (Mosser *et al.*, 1986). The RTG-2 cell line is able to retain at least rudimentary cytochrome P-450-dependent monooxygenase activity and is able to metabolise compounds (Castano *et al.*, 1996; Fent, 2001; Segner, 1998).

1.6.4 Human Skin Fibroblasts (84BR)

In order to begin investigating the relevance of the interactive toxicity of PAH and UV to humans, it was necessary and interesting to introduce a primary cell type into the project. For this reason, the primary cells 84BR were obtained (Chapter 2, Section 2.2). These cells are fibroblastic-like and originate from human epidermal tissue and are well characterised in toxicology studies (Alsbeih *et al.*, 1996; van den Brule *et al.*, 2003). 84BR are primary skin cells and only remain viable at low passage number for a short time, hence their inclusion at a more critical and later stage of the project, following baseline optimisation and validation of techniques with the more robust mammalian cells (CHO-K1).

1.7 Toxic Effects at the Cellular Level: Cytotoxicity

A number of bioassays have been developed for the assessment of potentially hazardous chemicals, effluents or sediments to marine and freshwater biota (Canty *et al.*, 2007; Li & Zhang, 2002), and to assess the effects of airborne pollutants on humans (Butterworth *et al.*, 1989). It is usual to select a tier-structured approach, with relatively simple bioassays for initial (tier I) screening of the relative toxicity of chemicals, followed by more extensive toxicity characterisation on the basis of (sub) chronic and reproduction tests (tier II) (Fent, 2001). This tiered approach is important for both genotoxic and cytotoxic studies. *In vitro* cytotoxicity bioassays utilising cell lines have therefore been suggested as an alternative for toxicity ranking of chemicals (Castano *et al.*, 1996).

The toxic action of chemicals on cells can be assessed by a variety of endpoints, including measures of cell death, viability and functionality, morphology, energy metabolism and cell proliferation (Walum *et al.,* 1990). *In vitro* research methods to investigate the cytotoxicity of chemicals and measures of cell death and cell viability that can be easily quantified in 96-well plates via a plate reader have found widespread acceptance. Cell death is mediated through apoptosis or necrosis and can be estimated by determining the decrease in total protein per well using dye-binding assays (for example, kenacid blue or crystal violet protein stain). Cell viabilities can be colorimetrically or fluorometrically determined by the abilities of cells to metabolise dyes (such as neutral red, tetrazolium salts or fluorescein diacetate) (Segner, 1998). The analysis of acute cytotoxicity in fish and mammalian cell lines is often assessed through neutral red, MTT tetrazolium tests and protein stains (Crallan *et al.,* 2005; Segner, 1998).

Cytotoxicity and genotoxicity investigations are equally important and they are interrelated; toxicity of chemicals is known to be one of the major confounding factors in the interpretation of the results from genotoxicity testing (Mendelshon *et al.,* 1992). Elucidation of any associated cytotoxicity of the test chemicals used is therefore necessary for validation of the genotoxic studies used in this study. In addition to standard cytotoxicity testing, which mainly investigates acute toxicity, investigations into apoptosis may give interesting insight into mechanisms of action and effects of chemical and UVR interactions (Valencia & Kochevar, 2006). Apoptosis is a normal physiological process that occurs from embryogenesis through to normal tissue maintenance and is characterised by specific morphological features, such as the loss of plasma membrane integrity, condensation of the cytoplasm and nucleus and the appearance of 'blebbing' within the cell. Knowledge of the mechanisms of apoptosis progression or inhibition may lead to

greater knowledge regarding chemical modes of action, cell repair or death; for example, failed apoptosis may indicate the potential for tumour development and carcinogenesis. There are many methods available to detect apoptosis, and one of the most commonly used methods (Annexin V) is explained here.

1.7.1 Annexin V-FITC Apoptosis Detection

The loss of plasma membrane integrity is one of the earliest features observed during apoptosis. In apoptotic cells, phosphstidylserine (PS) is translocated from the inner to the outer membrane, which exposes PS to the external environment where it can be detected. Annexin-V is a Ca^{2+} dependent phospholipid-binding protein that has high affinity for PS, and therefore binds to it. Annexin-V can be conjugated with propidium iodide (PI) to simultaneously detect early and late onset of apoptosis, which can be measured over time. PI is excluded from the intact membrane of viable cells, but membrane compromised apoptotic or necrotic cells will stain positive, therefore, detection of the red fluorescing PI will indicate late apoptosis/necrosis.

1.8 Toxic Effects at the Genetic Level: Genotoxicity

Genetic toxicology identifies and analyses the action of agents that have toxicity specifically directed toward the hereditary components of living organisms (Landolt & Kocan, 1983). Genotoxic agents can affect the integrity of DNA. The universality of the DNA molecule means that an agent, which is genotoxic for one group of organisms, is typically genotoxic for others (Landolt & Kocan, 1983). At the ecological scale, both chemical and physical agents can produce heritable genetic alterations at subtoxic concentrations, therefore resulting in altered hereditary characteristics (Landolt & Kocan, 1983). This may result in a loss in total genetic diversity at the population

level, with potentially damaging implications for the long-term survival of the exposed population (Jha, 1998).

The detection of genotoxicity can occur in two ways; first, at the biochemical or molecular level (for example, gene mutations, DNA adducts or DNA strand breaks) and second, at a cytogenetical level (including structural and numerical chromosomal aberrations (CAbs), sister chromatid exchanges (SCE), or the detection of a micronucleus). Ultimately, all these assays are investigating whether a chemical or its metabolites induces damage to DNA (Dixon *et al.*, 2002). DNA strand breakage is a sensitive indicator of genotoxicity and correlates with mutagenic and carcinogenic properties of environmental pollutants (Mitchelmore & Chipman, 1998). In this study, assays representing both biochemical and molecular genotoxicity were chosen to investigate the potential genotoxicity of PAH. The detection of strand breaks can be elucidated through alkaline single cell gel electrophoresis (SCGE) (also known as the comet assay) whilst genetic changes can be produced by mutations to the gene, structural chromosomal changes and numerical chromosome changes (aneuploidy) and can be detected through the micronucleus (Mn) assay. Table 1.3 gives examples of a variety of cell lines and their different applications (e.g. comet assay, Mn assay etc.) in toxicology.

1.8.1 Single Cell Gel Electrophoresis (SCGE)

Single cell gel electrophoresis (SCGE) is a rapid, highly sensitive and relatively inexpensive method used to determine DNA damage. DNA damage is manifested in the form of single strand breaks (SSBs), double strand breaks (DSBs) and alkaline-labile sites (ALS) in individual cells (all of which can be induced by alkylating agents, intercalating agents and oxidative damage). The comet assay is able

to detect DNA damage in all these forms. Östling and Johanson (1984) first introduced the microelectrophoretic technique for detecting and directly visualising DNA damage in cells. The method was originally applied to irradiated mammalian cells and has undergone several technical modifications, the most significant being the introduction of alkaline conditions to investigate the occurrence of DNA SSBs (Singh *et al.*, 1988). The technique is sensitive enough to measure low levels of DNA damage in a fairly short time and requires only a relatively small number of cells. The principle of the assay is particularly simple and is usually performed according to the protocol of Singh *et al.* (1988) and also described by Tice *et al.* (2000). For example, individual cell nuclei that have been previously exposed to a potentially genotoxic agent are firstly treated chemically (by pH or alkaline unwinding) so that the nuclear material relaxes and unwinds. The cells are then microelectrophoresed and stained with a fluorescent stain. DNA is negatively charged, therefore during electrophoresis the presence of strand breaks allows fragments and loops of DNA to migrate towards the anode (Singh *et al.*, 1988). Analysis is conducted with a fluorescence microscope connected to image analysis software to standardise the procedure. Many different calculated parameters are used to assess the DNA damage: for example, the 'percentage tail DNA', or the 'olive tail moment'. The percentage tail DNA is a commonly used parameter and is based on the fluorescence intensity (Møller, 2006; Olive *et al.*, 1990). The 'percentage tail DNA' has certain advantages over the 'olive tail moment' in the sense that it represents absolute values and could help in inter-laboratory comparison (Kumaravel & Jha, 2006). This parameter is also being recommended for regulatory use (Burlinson *et al.*, 2007). It is recommended that between 50 and 100 cells are analysed per experimental condition in duplicate (Wiklund & Agurell, 2003; Cotelle & Férard, 1999). The disadvantages of the comet assay are related to small cell samples (hence it is important to analyse a wide range of cells), the time demands of scoring single cell

data, and the sensitivity of the assay due to technical variability. All of these may lead to misinterpretation of the data.

The technique can be used for cells cultured *in vitro*, as well as for isolated cells taken directly from an organism after *in vivo* exposures (Tice *et al.*, 2000). However, adaptations for optimising different cell lines *in vitro* (or for *ex vivo* studies) are necessary for each new experiment (Cotelle & Férard, 1999; Tice *et al.*, 2000) as variation occurs between different cell types. Conditions should be optimised to show some migration from control cells in order to provide information suitable to evaluate intra-laboratory variation (Tice *et al.*, 2000). Hydrogen peroxide (H_2O_2) may be used to optimise the comet assay because it is rapid and generates strand breaks through oxidative damage (Raisuddin & Jha, 2004). For experiments with the comet assay involving indirectly acting genotoxins, the use of an exogenous source of metabolism is desirable. The most commonly used system is a co-factor-supplemented postmitochondrial fraction (S9) prepared from the livers of fish or rodents treated with enzyme-inducing agents such as Aroclor 1254 (Johnson *et al.*, 1996; Walton *et al.*, 1988; Walton *et al.*, 1987) or a combination of phenobarbitone and β-naphthoflavone (Johnson *et al.*, 1996). Studies have demonstrated that S9 can be used to activate PAH across cell lines of different phylogenetic origin (Walton *et al.*, 1987) and therefore this is the method employed here. The postmitochondrial fraction is usually used at concentration ranges from 1-10% (v/v) in the final test medium. S9 was not used for periods greater than 6 hours due to its cytotoxic potential and its consequent ability to produce false-positive results due to cytotoxicity.

1.8.2 Micronucleus (Mn) Assay

The binucleate (BN) micronucleus (Mn) assay is a well validated method for the detection of micronuclei as a measure of chromosomal damage (Fenech & Morley, 1986; Parry *et al.,* 2002) to investigate any potential genomic instability. Micronuclei are small, extranuclear bodies formed during mitosis and occur when chromosomal fragments or whole chromosomes fail to segregate and become separated from the daughter nuclei. They may be caused through exposure to environmental pollutants such as cigarette smoke (DeMarini, 2004). Micronuclei are used for the quantification of the exposure of cells to chemicals and can be observed in almost any cell type; therefore many variations of the assay exist (Tucker & Preston, 1996). The Mn assay provides many advantages over other cytogenetic assays, such as chromosomal aberrations (CAbs), in the speed and ease of analysis, and the non-requirement for cells to be in metaphase (Tucker & Preston, 1996). The Mn assay can be suitably employed in studies with humans, laboratory animals or cells following *in vivo* or *in vitro* exposures.

The Mn assay is assessed through the quantification of the number of micronuclei formed in exposed cells (compared to the reference or control cells) to investigate the level of damage that has become incorporated into the cell cycle. In order to count micronuclei, it is necessary to identify cells that have divided once. The cytokinesis-block technique is the most frequently applied methodology, which limits cell scoring to cells that have divided once since chemical stimulation (Parry *et al.,* 2002). Cytochalasin B (Cyto B) is an actin polymerisation inhibitor, which acts by disrupting the contractile filaments. This therefore inhibits cell division thereby giving rise to binucleate cells (which indicates the primary dividing cells) easing identification of the micronucleus (Surrallés *et al.,* 1994). Binucleate cells can be identified by the presence of two nuclei of the same size

within the cytoplasm. Cell strains and types may vary in their sensitivity to Cyto B but the concentration used is usually reported to be between 3 and 6 μg ml^{-1}, although an appropriate concentration for the cell type in question should be used (Parry *et al.*, 2002).

The two mechanistic factors responsible for the formation of micronuclei include clastogenic (chromosomal breakage) and aneugenic (spindle disruption) agents (Albertini *et al.*, 2000; Tucker & Preston, 1996). Aneuploidy is associated with both carcinogenesis and reproductive failure in humans, and can be detected through the presence of micronuclei (Parry *et al.*, 2002). Until recently there was considerable debate concerning the size of the micronuclei and the mechanisms that were causing their formation. The basic premise assumed that larger micronuclei were formed through spindle disruption and would contain whole chromosomes, whilst smaller micronuclei would consist of one or more chromosome fragments (Tucker & Preston, 1996). Although there may be a relationship between the size of a micronucleus and the mechanism of origin, without having some way to semi-quantitatively analyse the micronuclei it is impossible to know for certain the mechanisms of formation. In order to identify the links between the mechanisms of micronuclei formation and how they appear under the microscope, two general methods have arisen. The first, identifies either an aneugenic and/or clastogenic mechanism for the induction of Mn by the absence or presence of kinetochore protein within the Mn (Kirsch – Volders *et al.*, 1997). This technique is based on the association of kinetochores with the centromeres and is based on the theory that a centric chromosome or centric chromosome fragment in a Mn has arisen through an aneugenic mechanism. Anti-kinetochore antibody staining is used to identify kinetochore proteins that are associated with the centromeres of the chromosomes, or to indicate their absence from acentric chromosome fragments (Brinkley *et al.*, 1985). Secondary antibodies can then be used to amplify the signal of the

first bound antibody, and a fluorescent stain, such as DAPI can be used to counterstain the background chromosomes for contrast (Parry *et al.*, 2002). The cells are then examined and scored under a fluorescence microscope. Hence the second technique uses fluorescently labelled centromeric DNA probes to identify centromeres because kinetochore damage may be a potential aneugenic mechanism (Marshall *et al.*, 1996; Parry *et al.*, 2002). The anti-kinetochore antibody staining technique was used in this study due to its relative ease of use and its ability to distinguish between clastogenic and aneugenic agents. Ethyl methanesulphonate (EMS) was used as a positive control for clastogenic activity, whilst colchicine (COL) is a classical aneugen, and was used in this study as a positive control for aneugenic activity.

1.9 Chemical Effects: Oxidative Stress

Cellular processes leading to both cytotoxic and genotoxic effects can be mediated by reactive oxygen species (ROS). Although oxygen is essential for life, it can also diminish the normal function of a cell and/or contribute to its destruction. It is hypothesised that UVA induced skin damage is mediated via ROS (Bossi *et al.*, 2008; Valencia & Kochevar, 2006), such as singlet oxygen, the superoxide anion, hydrogen peroxide and others. UVA is absorbed by chromophores in cells, but other molecules in cells (both endogenous compounds (such as haem, cytochromes or porphyrins) or exogenous compounds (such as B(a)P or arsenicals)) may also form ROS following UVA exposure (McMillan *et al.*, 2008; Yin *et al.*, 2008). These ROS contribute to 'oxidative stress' a term used to describe an excessive amount of ROS in and around the cell, which can cause deleterious effects to it (McMillan *et al.*, 2008; Poulos & Raag, 1992; Schlezinger *et al.* 1999; Shyong *et al.*, 2003). ROS-induced DNA damage can include effects such as base modifications, strand

breakage and chromosomal rearrangements. ROS and their products can be investigated using electron spin resonance (ESR). This is a spectroscopic technique that allows for the detection of free radicals and which can also give structural and lifetime information about them (free radicals are defined as molecules or atoms possessing one or more unpaired electrons (Buettner & Mason, 2003)). ESR depends on the fact that every electron has a magnetic moment. The energy levels of the magnetic system are influenced by the surrounding atoms and by external magnetic fields. Changes amongst these levels can be detected by monitoring the power absorbed from an alternating magnetic field and comparing these observed transitions with model calculations that enable deduction of the features of the environment around the moment (Buettner, 1987). For example, in the presence of an external magnetic field the electron's magnetic moment aligns itself either parallel or anti-parallel to the field, each alignment having a specific energy. ESR absorption occurs when the irradiation frequency "matches" the energy level separation created by the magnetic field. ESR is applied to biological systems because although radicals are highly reactive and do not normally occur in high concentrations in biology, it is possible to spin-label radicals of interest so their lifetime increases and a strong signal is produced which can be detected using ESR (Buettner & Mason, 2003). Specially-designed non-reactive radical molecules can attach to radicals in a biological cell, and EPR spectra can then give information on the environment of the spin-trapped radical. Spin trapping involves the addition of a diamagnetic radical scavenger (the spin trap) to a reaction mixture containing radicals of interest. Reactive free radicals add to the scavenger, forming a long-lived paramagnetic adduct that is detected through ESR. The presence of an unpaired electron means that the radical is considerably more reactive than the other chemical species; radicals derived from oxygen have highest reactivity. Molecular oxygen (O_2) is effectively a radical that reacts with other radical molecules to create a triplet state. Thermodynamic

parameters dictate that the diatomic oxygen species will be reduced. The four single-electron steps from molecular oxygen to water are summarised below in Figure 1.3. ESR enables the identification and quantification of these radical species and is routinely used to measure radicals such as superoxide, hydroxyl and nitric oxide.

$$O_2 \xrightarrow{e^-} O_2^{\cdot -} \xrightarrow{e^-.2H^+} H_2O_2 \xrightarrow{e^-.\cdot OH^-} \cdot OH \xrightarrow{e^-.H^+} H_2O$$

Molecular Oxygen - Superoxide - Hydrogen Peroxide - Hydroxyl - Water

Figure 1.3 Summary of the four electron steps involved in the breakdown of molecular oxygen.

1.10 Aims and Objectives of the Work Reported Here

The hypothesis of this project was that the interactive toxicity of the PAH B(a)P with UVR would cause both a cytotoxic and genotoxic response in cells from aquatic and mammalian origins. The combined effects of B(a)P and UVB/UVA may cause cytotoxicity through reductions in cell viability. Genotoxicity from B(a)P and UVB/UVA may occur by increases in DNA damage (strand breakage) and cytogenetic effects such as increases in chromosomal damage and effects on the cell cycle. It is also hypothesised that B(a)P and UVA will cause oxidative damage in the cell. These effects could well be involved in carcinogenesis. The potential effects on the cell from the combined insult of B(a)P and UVB/UVA are summarized in Figure 1.4.

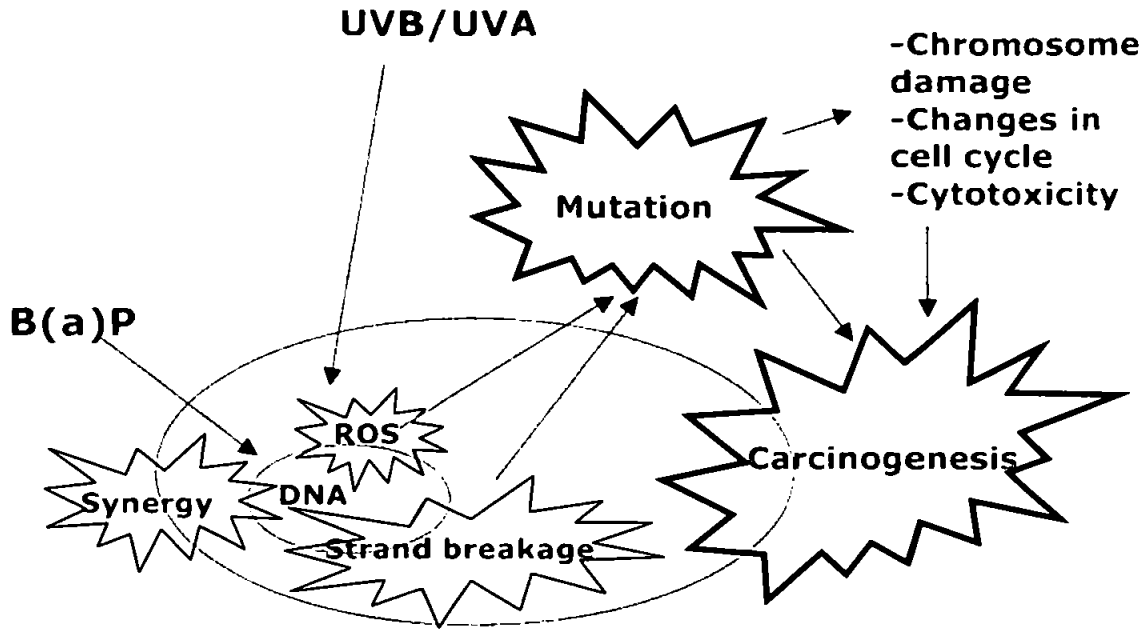

Figure 1.4 Diagram of the potential cytotoxic and genotoxic responses in the cell following exposure to B(a)P and UVR

The aim of this project was to elucidate the potential cytotoxic and genotoxic effects of B(a)P with UVB/UVA using *in vitro* techniques including cell culture, and a suite of cytotoxicity and genotoxicity assays. The specific objectives were twofold:

1. To optimise and validate the experimental techniques and conditions to be used throughout the investigation.

   a) To investigate the relative cytotoxic sensitivities of the cell types used and to optimise and validate the comet assay (DNA damage including DNA strand breakage) and the micronucleus assay (chromosome damage and cell cycle changes). This data would ensure further experiments were reliable and reproducible.

2. To investigate the interactions of B(a)P and UVR and the cytotoxic and genotoxic effects produced in cells derived from aquatic or mammalian organisms:

a) To study the potential cytotoxicity and genotoxicity of B(a)P, UVB or UVA separately and to explore the possible interactions between cells treated with B(a)P and UVB or UVA radiation using cytotoxic and genotoxic assays to determine DNA damage, chromosome changes or alterations in the cell cycle.
b) To examine potential oxidative stress from these interactions.

Hence, ultimately, this project aims to elucidate the effects on the chosen cell types of co-exposure to B(a)P and UV radiation. It also aims to advance the standardisation of techniques for use in environmental testing and to also introduce some novel techniques to complement the research.

CHAPTER II – MATERIALS AND METHODS

2.1 Sources of Chemicals and Cell Culture Materials

A list of all cell culture materials and chemicals used (including all abbreviations), and their sources is detailed in Appendix 1.1.

2.2 Sources of Cells

The School of Biological Sciences, University of Plymouth, supplied the Chinese Hamster Ovary (CHO-K1), Epithelioma Papillosum Cyprini (EPCA1) and Rainbow Trout Gonad (RTG-2) cell lines which were originally procured from the European Collection of Cell Culture, Wiltshire, UK. These cell lines are well characterised and readily available (Van den Brule *et al.,* 2003; Walton *et al.,* 1988; Wolf & Mann, 1980). The primary human fibroblast cells, 84BR were a gift from Cornwall Dermatology Research (CDR), Peninsula Medical School, Truro, UK and were originally procured from the European Collection of Cell Culture, Wiltshire, UK.

2.3 Routine Cell Culture

Confluent cells were subcultured as described by Freshney (2000). Cells were maintained in 25 cm^2 and 75 cm^2 flasks for routine cell culture at pH 7.2-7.4. Growth medium (GM) for routine cell culture was MEM supplemented with 1 % NEAA and 10 % FBS for the RTG-2 (Bols & Lee, 1994; Lannan, 1994; Segner, 1998; Wolf & Ahne, 1982) and EPCA1 cell lines, HAM-F12 supplemented with 10 % FBS for the CHO-K1 cell line (Toyooka *et al.,* 2006), and EMEM supplemented with 1 % NEAA, 2 mM L-GLUT and 15 % FBS for the 84BR cells. All procedures were carried out under strict aseptic conditions using a

laminar flow cabinet (Lamin Air, Model 1.2, Heto-Holten Ltd, Surrey, UK). The spent medium was discarded and approximately 5 ml of PBS prewash was added to 25 cm^2 flasks. The cell monolayer was washed with PBS by rotating the flasks, the excess discarded and the step repeated to remove traces of serum that would inhibit the enzymatic action of the trypsin (or trypsin-versene). One ml of trypsin (0.25 %) was added (CHO-K1 cells) or 1 ml of trypsin (0.25 %) was combined with 4 ml of versene (0.05 %) (RTG-2, EPCA1 and 84BR cells). The flask was then rotated so the trypsin (or trypsin-versene) completely covered the monolayer and the excess was immediately discarded. Disaggregation was observed under an inverted stereomicroscope. Fresh medium was added to stop the action of the trypsin and the cells resuspended by gently pipetting up and down, to create a homogenous suspension. Cell suspensions from several flasks were combined and the suspension mixed by gentle pipetting. Cells were counted with a haemocytometer. For initial subculture of CHO-K1 cells, a split ratio of 1:2 was employed: a 25 cm^2 flask was typically seeded with approximately 5 x 10^4 cells ml^{-1}, with cells becoming confluent in approximately 4 days. For routine subculture, a split ratio of up to 1:12 was employed. Cells were incubated at a temperature of 37 ± 1 °C. For routine subculture of RTG-2 or EPCA1 cells, a split ratio of 1:3 was employed: a 25 cm^2 flask was typically set at approximately 5 x 10^4 cells ml^{-1} for the RTG-2 cell line and a minimum of 1.25 x 10^4 cells ml^{-1} for the EPCA1 cell line, with cells becoming confluent in approximately 10 days. Cells were incubated at a temperature of 21 ± 1 °C in a 5 % CO_2 atmosphere. For routine subculture of 84BR cells, a split ratio of 1:4 was employed: a 75 cm^2 flask was typically set at approximately 1 x 10^6 cells ml^{-1} with cells becoming confluent in about 10-14 days. Cells were incubated at a temperature of 37 ± 1 °C in a 5 % CO_2 atmosphere. Trypan blue was used to determine cell viability (Section 2.4.1). Only cell suspensions that had a viability of >90 % were used in experiments.

2.4 Cell Viability Studies

Cell viability was assessed by various assays in order to determine cytotoxic events occurring in the cells. Cytotoxicity that does not affect particular cell properties may not be accurately represented or assessed using some methods; therefore a suite of assays is necessary to give a wider insight.

2.4.1 Trypan Blue

Standard methodology was followed for using the trypan blue exclusion dye, which relies on membrane integrity to distinguish between viable or non-viable cells: viable cells can exclude the dye, which is able to permeate viable and non-viable cells (this leaves non-viable cells stained blue). The advantages of this method are that it is a quick and easy technique that gives a rapid result. The disadvantage of this method is that the dye does not indicate the way that the cells die, for example by either apoptosis or necrosis. Briefly, 0.5 ml of cell suspension was mixed with 0.5 ml of 0.4 M trypan blue solution (Sigma, UK) and incubated at room temperature for 10 minutes. The visibility of viable (non-stained) and non-viable (stained) cells was observed under light microscope and the cells counted with a haemocytometer to determine the cell number. Percentage viability was calculated as the number of non-stained cells divided by the total number of cells.

2.4.2 Dual-Staining

Dual staining was conducted with a commercially available kit (Viability/Cytotoxicity Assay Kit for Animal Live & Dead Cells, Biotium Inc, USA, Cat. No. 30002, Appendix 1.1) which uses a fluorescence dual stain, Calcein AM (acetomethoxy derivate of calcein)/EthD III (ethidium homodimer III) that assesses intracellular esterase activity

and plasma membrane integrity (Papadopoulos *et al.,* 1994; Wang *et al.,* 1993). Live cells are identified through the presence of ubiquitous intracellular esterase activity, determined by the enzymatic conversion of the virtually non-fluorescent cell-permeant calcein AM to the intensely fluorescent polyanionic dye calcein, which is retained within live cells, producing green fluorescence in live cells (excitation approximately 495 nm, emission approximately 515 nm). EthD-III is excluded by the intact plasma membrane of live cells but can enter cells and bind to nucleic acids, which produces a red fluorescence in dead cells (excitation approximately 530 nm, emission approximately 635 nm). This assay has the advantage of being relatively quick to carry out, and provides a more robust method for detecting viability as it is more sensitive than traditional methods such as trypan blue because it detects two parameters of cell viability: plasma membrane activity and intracellular esterase activity. The disadvantage of this method is the inability of the assay to distinguish between non-viable cells by apoptotic or necrotic mechanisms. Also, the determination of cell viability depends on the physical and biochemical properties of plasma membrane stability and intracellular esterase activity so cytotoxic events that do not affect these cell properties may not be accurately reflected through this assay. Cells were treated with the test compounds and/or UV light for the appropriate time (according to each compound) or to achieve the correct dose (for UV) and the assay prepared according to supplied protocol. Briefly, a 2 mM EthD-III stock solution (20 µl) is mixed with 10 ml of PBS, to give a 4 µM EthD-III solution. This is combined with 5 µl of the supplied 4 mM calcein AM stock solution. Cells are washed with PBS and Calcein AM/EthD-III solution added and the cells incubated for 30–45 minutes at room temperature; following which the cells are viewed under the fluorescence microscope. Cells were counted with a haemocytometer to determine the cell number. Percentage viability was calculated as the number of viable cells (green fluorescence) divided by the total number of cells.

2.4.3 Annexin V-FITC Apoptosis Detection

A useful apoptotic marker is the translocation of phosphatidylserine (PS) – one of the first events in apoptosis. PS translocation from the inner to the outer face of the lipid bilayer membrane relies on cell's loss of membrane asymmetry in the early stages of apoptosis. The advantages of this assay are the ability to differentiate between apoptosis and necrosis as well as to distinguish between early apoptosis and late apoptosis (Wilkins *et al.,* 2002). PS translocation was measured using a commercial kit (Annexin V: FITC Apoptosis Detection Kit I, BD Biosciences, UK, Cat. No. 556547, Appendix 1.1) containing fluorescein-conjugated Annexin-V in conjunction with PI. Cells were plated in two-chamber precoated slides (Barloworld Scientific Ltd, UK) and incubated for 24 hours in normal growth medium under normal growth conditions. Cells were incubated with B(a)P for 24 hours, washed twice with PBS prior to irradiation conducted in PBS. Following irradiation, cells were incubated in buffer containing Annexin V (10 µl) and PI (10 µl) for 15 minutes. Fluorescence was observed by confocal microscope (Zeiss, UK) using 488 nm excitation and 530 nm emission for Annexin V-FITC and 580 nm excitation and 610 nm emission for PI, under 40x oil immersion objective.

2.4.4 Neutral Red Retention (NRR) Assay

The NRR assay is based on the retention of neutral red in the lysosomes of viable cells. Neutral Red (2-amino-3-methyl-7-dimethyl-amino-phenazoniumchloride) is a weakly cationic supravital dye, which can diffuse across the phospholipid membrane and bind to anionic sites in the lysosome (Lowe *et al.,* 1992). Lysosomes are recognised target sites for most environmental contaminants, which can cause destabilisation of the lysosomal membrane. The NRR

assay evaluates the lysosomal membrane integrity, which can be used as an indicator of exposure to xenobiotics (Babich *et al.,* 1992; Babin & Tarazona, 2005; Nigro *et al.,* 2006; Speilmann *et al.,* 1998). The assay is intended to yield a reasonable indication of the acute toxicity of chemical exposure to the cellular system under investigation and therefore give an indication of cytotoxicity. The NRR assay is a relatively rapid and cost effective procedure, which is reliable, sensitive and quantitative. The assay allows for the determination of cell viability in monolayer cultures when exposed to cytotoxic agents. Only viable cells are able to retain the dye, thus chemicals causing membrane damage inhibit the retention of this dye, due to destabilisation of the lysosomal membrane (Babich & Borenfreund, 1992). It is therefore possible to assess the degree of cell viability through measurement of spectrophotometric absorbency of the neutral red dye.

The method used in this study adapts the protocol of Mori and Wakabayashi (2000). Modifications to this assay are detailed in the relevant chapters. Briefly, confluent cell monolayers were trypsinised and resuspended to give a count of 5 x 10^4 cells per well (2.5 x 10^5 cells ml^{-1} in fresh medium containing 10 % FBS). Aliquots of 0.2 ml cell suspension were added to each of a 96-well cell culture cluster plate (Corning, USA). The outermost wells contained medium only. Each experiment contained 6 replicates for each variable and experiments were conducted at least twice. Culture plates were incubated at 37 ± 1 °C without 5 % CO_2 (CHO-K1) or with 5 % CO_2 (84BR), or 20 ± 1 °C in 5 % CO_2 (EPCA1 and RTG-2) for 24 hours. Control wells contained medium supplemented with 1 % FBS only. Cells were exposed for 24 hours to the test compounds, unless stated otherwise. Following this period, the medium was withdrawn and discarded, the monolayer was washed twice with PBS and the medium replaced with 100 µl of medium containing 40 µg ml^{-1} (0.02 g of neutral red dissolved in 5 ml PBS, 500 µl aliquot of this solution

diluted again in 49.5 ml of MEM) of neutral red. The plate was incubated for 3 hours at 37 ± 1 °C to allow for uptake of the neutral red stain. Excess neutral red dye was removed and the cells fixed with 1 % formal saline containing 1 % $CaCl_2$ to enhance cell attachment to the substrate. Cells were washed twice with PBS to remove any traces of unbound neutral red. Extraction of the neutral red dye was carried out by adding 200 µl of 1 % acetic acid in 50 % ethanol to each well. The plate was left to stand for 15 minutes at room temperature, shaken for two seconds and read at 540 nm absorbance on a spectrophotometric microplate reader (Optimax, Sunnyvale, USA.). Results were expressed as a percentage of the control (Babich *et al.,* 1988).

2.5 Single Cell Gel Electrophoresis (comet assay)

The comet assay was developed to detect DNA damage in individual cells. Cells are embedded in agarose on microscope slides and the cell membranes lysed followed by electrophoresis of the DNA and subsequent analysis of the damage produced through image analysis software. All steps associated with the comet assay are necessarily important in order to obtain reliable and reproducible effects. This assay was used to detect DNA damage following treatment of the cells with test compounds or UVR. The advantages of this assay are the relative speed at which the assay can be performed and the rapid determination of DNA damage that can be obtained. However, it is a non-specific biomarker of genotoxic damage and care needs to be taken with the many steps associated with the assay to reduce variability in the method. All experiments were carried out at least twice giving a minimum of quadruplicate data (each sample slide contained duplicate samples and 50 comets were scored in each sample area). Buffers and reagents for the comet assay are detailed in Appendices 1.1 and 1.2. For comet assay experiments cells were

seeded at a density of approximately 4 x 10^5 per 25 cm^2 culture flask for CHO-K1, RTG-2 and 84BR and 1 x 10^6 per 25 cm^2 culture flask for EPCA1 in 8 ml fresh medium to obtain optimal growth conditions for each cell type and incubated to obtain 60-80% confluence so that cells would not display restricted growth due to contact inhibition. Cells were treated with test compounds or UVR as specified in the text and then treated as follows.

2.5.1 Slide Preparation and Lysis

Frosted ended slides were prepared by coating with molten normal melting point (NMP) agarose (1% in PBS) and allowed to set at 30 °C for a minimum of 10 minutes. For some experiments, pre-coated CometSlides™ (Trevigen, USA) were used. These slides are specially treated to promote adherence of low melting point (LMP) agarose and are more reliable and easier to use than the time consuming traditional slide preparation method of preparing slides with NMP agarose base layers. However these CometSlides™ are expensive so their use was limited to the later stages of the thesis. The cell monolayer was washed twice with PBS, trypsinised and resuspended in growth medium, cells were counted and the concentration adjusted in medium to ensure approximately 2 x 10^4 cells per slide (170 µl). Aliquots of 500 µl adjusted cell suspension were transferred to centrifuge tubes. Cell suspensions were centrifuged for 3 minutes at 2000 rpm and the supernatant discarded. Cells were resuspended in 170 µl LMP agarose and added to the prepared slides to give two replicates of 85 µl LMP at either end of the slide. Coverslips were added to each replicate and the slides placed at 4 ± 1 °C in the dark to set for approximately 5-10 minutes. Coverslips were carefully removed from the slides, ensuring no disruption to the agarose, and the slides transferred to coplin jars containing chilled lysing solution (Appendix 1.2) for 1 hour in the dark at 4 ± 1 °C. Following lysis, which removes the cellular membranes leaving only the embedded

DNA, the slides were rinsed dropwise for 5 minutes with distilled water. This step was repeated twice more.

2.5.2 Alkali (pH>13) Unwinding

Slides were transferred to lie horizontally in the electrophoresis chamber (Pharmacia Biotech GNA 200). Freshly prepared alkaline (pH > 13) electrophoresis buffer (2 l buffer stabilised to 4 ± 1 °C) (for buffer see Appendix 1.2) was then added. DNA was left to unwind in the electrophoresis chamber (Pharmacia Biotech GNA200) at 4 ± 1 °C in freshly prepared electrophoresis buffer (pH >13) stabilised to 4 ± 1 °C, in the dark. The alkali treatment unwinds and denatures the DNA and hydrolyses sites of damage. Alkaline electrophoresis can detect single strand DNA breaks (SSBs), double stranded DNA breaks (DSBs), apurinic sites, apyrimidinic sites and alkali labile DNA adducts.

2.5.3 Electrophoresis

Electrophoresis was conducted with the same alkaline (pH >13) buffer used during alkaline unwinding (Appendix 1.2). The electrophoretic conditions of 25 V and 300 mA (BioRad PowerPac 300, USA) as developed by Singh *et al.* (1988) were employed. DNA is negatively charged, therefore during electrophoresis the presence of strand breaks allows fragments of DNA to migrate towards the anode (Singh *et al.*, 1988) resulting in the comet formation observed in the next step (Section 2.5.4).

2.5.4 Neutralisation, Staining, Comet Visualisation and Scoring

Embedded cells were washed 3 times dropwise with neutralisation buffer (Appendix 1.2) for approximately 5 minutes each to neutralise the alkaline buffer solution used previously. Slides were then allowed

to air dry for approximately 5 minutes and immediately exposed to cold methanol (100 %) for 3 minutes to dehydrate and improve staining and visualisation. Slides were stored at this stage for later reference, or immediately scored. Slides were stained with 40 µl ml^{-1} ethidium bromide (in a fume cupboard with gloves because this compound is carcinogenic) which is a fluorescent DNA intercalating dye, and coverslips added. Excess stain was blotted away from the edges of the slide. For visualisation of DNA damage, a fluorescence microscope (Leica, UK) using x20 objective was employed, linked to a camera to assess the extent of DNA damage in the cells by measuring the percentage of migrated tail DNA (% Tail DNA). This measurement includes tail length, width and DNA content and is based on the fluorescence intensity. DNA damage was analysed using the Komet 5 (Kinetic Imaging Ltd., Merseyside, UK) image analysis software, which calculates the % Tail DNA. Fifty randomly selected cells were analysed per replicate, giving a total of 200 scored cells per treatment group. All slides including positive and negative controls were independently coded before microscopic analysis and scored without knowledge of the code to help prevent observer bias in scoring.

2.5.5 Comet Assay with Benzo(a)Pyrene

Cells at 70-80 % confluency were exposed to various concentrations of benzo(a)pyrene (B(a)P) in medium to ensure that the cells were still provided with the correct nutrients for growth and uptake of the compound. The concentrations of B(a)P were based on those used by other workers (Sanchez *et al.*, 2000) and were set at 0.1, 1.0 and 3.2 µg ml^{-1}. A 1 mg ml^{-1} stock solution of B(a)P was prepared in DMSO and then dilutions made in medium containing 1 % FBS, before adding to the cell monolayer. The cells were incubated for 6 hours at 37 ± 1 °C for the mammalian cells and 21 ± 1 °C for the fish cells according to the recommendations set out by Tice *et al.* (2000).

Replicate slides were made for each treatment condition, and the protocol as outlined in Sections 2.5.1 to 2.5.4 was followed. The results are presented in Sections 5.3.1.2 and 4.3.1.2.

2.5.6 Metabolic Activation

Due to the indirect action of B(a)P, this test substance was added to the cells both in the presence and absence of an appropriate metabolic activation system (S9). Briefly, cells at 70-80 % confluency were exposed to various concentrations of B(a)P in medium containing S9 - an exogenous metabolic source. It was not possible to obtain fish-derived S9 from commercial sources. Aroclor 1254 induced rat liver homogenate (S9) was obtained from Moltox (Moltox Toxicology, Inc, Boone, USA). Ten ml S9 mix contained 0.15 ml of S-9 homogenate, 0.60 ml of 'core' mixture (Appendix 1.2) and 9.25 ml medium with 1 % FBS. This S9 mixture was then immediately dispensed into each flask with 0.1, 1.0 or 3.2 µg ml^{-1} B(a)P. Cells in flasks (containing B(a)P and S9) were then incubated for 6 hours at 37 ± 1 °C for the CHO-K1 cell line and 21 ± 1 °C for the fish cells according to the recommendations set out by Tice *et al.* (2000). Replicate slides were made for each treatment condition, and the protocol as outlined in Sections 2.5.1 to 2.5.4 was followed. The results are presented in Sections 5.3.1.2.1 and 4.3.2.1.

2.6 Micronucleus (Mn) Assay

The micronucleus assay is used to detect chromosomal damage and is presented here with two staining techniques, Giemsa and anti-kinetochore antibody staining. The first technique detects crude damage but does not differentiate between clastogenic or aneugenic mechanisms, whilst the second technique can differentiate between

the two types of damage. All experiments were carried out at least twice and each experiment contained duplicate flasks for each treatment, ensuring quadruplicate data for each treatment group.

Briefly, confluent cells were trypsinised and seeded into new flasks in 8 ml growth medium (HAM-F12 for CHO-K1, MEM for EPCA1 and RTG-2, EMEM for 84BR) containing 10 % FBS. Cell cultures were incubated for 24-48 hours and then treated with test chemicals for approximately one cell cycle (24 hours for CHO-K1 and 48 hours for EPCA1, RTG-2 and 84BR cells) in 1 % FBS, unless stated otherwise. Following this incubation period, cell cultures were washed twice with PBS and 8 ml fresh medium added containing Cytochalasin B (Cyto B) to inhibit cytokinesis in 10 % FBS and incubated at their optimal growth conditions for one cell cycle. Following this second incubation period, the cell cultures were washed with PBS, trypsinised and resuspended in medium containing 10 % FBS and treated as either Section 2.6.1 or 2.6.2 below.

2.6.1 Giemsa Staining

The resuspended cells were then centrifuged at 800 rpm for 10 minutes, the supernatant removed, and approximately 5 ml of cold KCl (0.56 %) added using a vortex mixer to cause the cells to swell slightly. Cells were left for 10-20 minutes before being centrifuged at 800 rpm for 10 minutes. Following this, the supernatant was removed, and the cells were resuspended. Five ml of acetic acid (100 %): methanol (100 %) (1:3) was added at room temperature to fix the cells and the cells centrifuged at 800 rpm for 10 minutes. Five ml of acetic acid (100 %): methanol (100 %) (1:3) was added at room temperature, and the cells left for a minimum of 30 minutes. Following this second fixation step, the cells were centrifuged at 800 rpm for 10 minutes. The supernatant was removed leaving approximately 1 ml and the cells were resuspended in this. An

aliquot of approximately 20–40 µl was applied carefully to a slide and left to air-dry. Slides were stained with 10 % Giemsa stain (to distinguish between cytoplasm and nuclear material) for 10 minutes in coplin jars, followed by a two-rinse step in distilled water. The slides were left to air dry and mounted with DPX Mountant for examination under a light microscope to determine the presence of micronuclei.

2.6.2 Antikinetochore Staining

A cell count was performed on the resuspended cells to adjust the cell concentration to 3×10^4 cells ml^{-1} which produces a suitable number of cells for visualisation under the microscope. An aliquot of cell suspension (0.4 ml for a single cytofunnel, or 0.25 ml for each part of a double cytofunnel) was added to each tube of the cytofunnel, placed in the cytocentrifuge (Cytospin; Shandon Southern, Ltd) to flatten the cells onto clean slides and spun down onto clean slides at 900 rpm for 5 min (Ding *et al.*, 2003). The preparations were then fixed in ice cold methanol for 10 minutes. The slides were then dried in the dark for approximately 1 hour to remove traces of methanol. The fixed slides were stored at -20 °C in airtight moisture proof packaging and scored within 7-10 days using fluorescence microscopy as detailed below to detect the presence of kinetochore positive or negative micronuclei (Section 2.6.3).

2.6.3 Immunofluorescence Staining

Primary antibody (human anti-nuclear antibody, centromere specific) was diluted 1:2 in 5 % FBS in PBS, which was kept on ice until use. Prepared slides (Section 2.6.2) were washed 3 times, for 5 minutes each in PBS. Excess PBS was removed and approximately 100 µl of diluted primary antibody pipetted over the cells to localise the centromeres present and covered with a glass coverslip. The slides

were incubated in a humidified box at 37 °C for approximately 45-60 minutes. Secondary antibody (anti-human IgG (Fc specific) Cy3 conjugate) was diluted 1:100 in 5 % FBS in PBS and kept on ice until use. Coverslips were removed and slides washed with PBS: 5 minutes (x3) in glass coplin jars. Excess PBS was removed and approximately 100 µl of diluted secondary antibody pipetted over the cells and covered with a coverslip. The slides were incubated in a humidified box at 37 °C for approximately 45-60 minutes. Coverslips were removed and slides washed with PBS: 5 minutes (x3) in glass coplin jars, and then air dried in the dark. Slides were stored at 1-10 °C in a dark box until scoring. Slides were scored blind with DAPI (4',6-Diamidino-2-Phenylindole) antifade (0.1 µg ml^{-1} DAPI in antifade) using a fluorescence microscope fitted with DAPI and TRITC (Tetramethyl Rhodamine Iso-Thiocyanate) filters. Micronuclei were identified according to Section 2.6.2. A micronucleus was classified as either kinetochore-negative or kinetochore-positive by the absence or presence of a kinetochore signal within micronuclei, respectively.

2.6.4 Scoring of Micronuclei

Micronuclei are identifiable by the following criteria (adapted from Albertini *et al.*, 2000):

i) Micronuclei present within the cytoplasm
ii) Micronuclei diameter less than a third the size of the nucleus
iii) Micronuclei with identical morphology to nucleus
iv) Micronuclei should not be linked to main nuclei by bridge
v) Micronuclei may overlap boundaries with the main nuclei

Micronuclei were scored from a minimum of 1000 cells per slide (Section 2.6.1), and only micronuclei contained within binucleate cells were scored where possible, according to the requirements of all the

above criteria and employing a balanced scoring system, as recommended by Albertini *et al.* (2000) unless stated otherwise. Micronuclei linked to the main nucleus ('nucleoplasmic bridges' (NPB)) were also noted, for their possible importance in this type of study as recommendations for this assay change and criteria becomes more unanimously agreed throughout all laboratories (Fenech *et al.*, 2003a). The micronuclei scoring procedure was adapted throughout this period of study and the method as a whole is likely to be adapted over the course of the thesis to include more features such as apoptosis, necrosis and multinucleated cells in line with recent recommendations (Fenech *et al.*, 2003b).

2.7 UVR

Measurements of UVB (Phillips, UK) and UVA (XX-40 FB, Spectroline, USA) lamps were made using a spectroradiometer (Model SR 9910-V7, Macam Photometrics Ltd., UK) provided by the University of Plymouth. UVR doses were calculated from the spectral outputs received from the spectroradiometer, and dosage times adjusted accordingly. UVR doses were based on existing literature and adjusted for each experiment as appropriate. Cell exposure to UVR was conducted in PBS in all cases to prevent possible confounding effects from constituents in the media and cellular exposure was conducted as stated for each assay. Cellular exposure to UV was conducted in PBS following incubation with either medium alone, or B(a)P.

2.8 Electron Spin Resonance (ESR)

Spin trapping was mostly carried out using the trap 5,5-dimethyl-1-pyrroline-N-oxide (DMPO) which mainly detects superoxide and hydroxyl radicals (giving DMPO-OOH or DMPO-OH adducts, respectively). However, in preliminary experiments the spin traps α-(4-pyridyl-1-oxide)-N-*tert*-butylnitrone (POBN, l-hydroxyethyl radical), the small nitroxide probe 2,2,6,6-tetramethyl-4-piperidinol (TMPol, singlet oxygen) and 4,5-dihydroxy-m-benzenedisulphonic acid disodium salt (Tiron, singlet oxygen) were also used. All chemicals were obtained from Sigma-Aldrich UK.

2.8.1 ESR Measurements

ESR measurements were made using a Bruker ECS 106 X-band spectrometer. Spectra were recorded at room temperature with a modulation frequency of 100 kHz and amplitude of 0.1 mT, microwave frequency of 9.425 GHz and power level 10 mW, magnetic field 335.9 ± 5.0 mT, time constant 0.3 seconds and scan time 168 seconds. Cells were microcentrifuged to a pellet in medium, the medium removed and cells resuspended in ice cold PBS. These samples were then contained in 40 mm lengths of 0.8 mm o.d. gas-permeable teflon tubing (Zeus Industrial Products, USA), which were folded in half and held in open ended 4 mm o.d. quartz tubing, and were then irradiated on the bench under a UVA lamp (500 J m^{-2}). The samples were then placed in the microwave cavity of the spectrometer and acquisition of spectra started within 1 minute of the end of irradiation (UVA: (XX-40 FB, Spectroline, USA)). When cells were examined with ESR, the trypsinised cells were washed 3 times with PBS to remove serum and free B(a)P. The cell suspension from each 25 ml culture flask was divided into two and the cell pellet from each half was resuspended in 50 µl of 250 mM DMPO in PBS prior to

irradiation. For preliminary experiments, the spin traps TMPol and POBN were both used at a concentration of 50 mM.

2.9 Statistics

For comet assay, data were collected from Excel and transferred into MINITAB for statistical analysis. The data is non-parametric, therefore, the median value was applied to the Mann-Whitney *U*-test to investigate the level of significant difference between the medians ($p < 0.05$) (Morley *et al.*, 2005). In some cases the data were then transferred into SigmaPlot to illustrate as box and whisker plots which show the spread of the data. For micronucleus experiments, data was presented in tables to show the various examined parameters, and the statistical level of significance tested between mean micronuclei frequencies with Mann-Whitney *U*-tests. For NRR assay results, the results were tested for significance using Mann-Whitney *U*-tests.

CHAPTER III - OPTIMISATION AND VALIDATION

3.1 Introduction

An important aspect of toxicological investigations is the optimisation and validation of techniques in order to elucidate the observed effects. Assay development is necessary to correctly produce and interpret results, and it is necessary to ensure that variability is kept to a minimum. The relative sensitivities of various cell types are important in the development of suitable assays, particularly in relation to biomarkers, to sensitively detect the effects of environmental pollution. Hence, their use to determine acceptable levels of environmental contamination is contingent on knowledge of their sensitivities. Cell lines from different tissues and from different species of varying origin have been widely used in toxicology studies. Because of variations in sensitivity, the choice of cell line can drastically affect the observed outcomes, therefore it is vital to fully optimise and validate experiments prior to investigating a test substance. In this study, an *in vitro* approach has been adapted with a variety of established cell types from different origins (fish: RTG-2, EPCA1; mammals: CHO-K1, 84BR). This, amongst other things, enables comparisons to be made of the different sensitivities between these cell types. However, cell types are not the only variable to be taken into account in an *in vitro* study. The assay process may alter the outcome and needs to be optimised and validated.

In the work presented here, comet assay parameters of unwinding times and electrophoresis times were initially optimised and validated using hydrogen peroxide (H_2O_2) as a reference chemical to find the optimal conditions with which to investigate test chemicals with each type of cell. H_2O_2 was used due to its rapid oxidising activity. The clastogenic alkylating agent, ethyl methanesulphonate (EMS) acts directly on the cell, via DNA adduct formation and hence EMS was

used as a positive control not requiring metabolic activation prior to induction of DNA damage in accordance with guidelines described by Tice *et al.* (2000). EMS is a monofunctional ethylating agent that has been found to be mutagenic in a number of systems from viruses to mammals and it can react via a mixed SN_1/SN_2 - type mechanism which causes ethylation of cellular, nucleophilic sites in DNA (Sega, 1984). EMS is not primarily a DNA strand - breaking agent, as it does not induce direct scission of the DNA backbone (Singer & Grűnberger, 1983).

Other positive controls can be used depending on their function. For example, in the cell, microtubules are highly labile structures that are sensitive to specific anti-mitotic drugs. Colchicine (COL) is a mitotic spindle poison that inhibits the polymerisation of tubulin, therefore preventing spindle formation and blocking mitosis. Unlike EMS, the target molecule of COL is protein (whereas EMS targets the DNA as an alkylating agent). COL has aneugenic properties but only when used at low concentrations (high concentrations freeze the cells at mitosis) making this a suitable positive control for use in the micronucleus assay.

Both EMS and COL are considered suitable positive controls for use in the micronucleus assay (Surrales *et al.,* 1994). The cytokinesis block micronucleus assay (CBMN) (see Section 1.9.2) is considered to be more sensitive and precise than the conventional micronucleus assay or classical metaphase analysis (Fenech & Morley, 1986) and is often used with the actin polymerisation inhibitor Cytochalasin B (Cyto B). Cyto B is considered an important baseline variable in determining micronuclei frequencies with clastogens (such as EMS) and aneugens (such as COL) (Surrales *et al.,* 1994). Therefore the concentration of Cyto B selected is important; if it is too low, it can lead to false positive results from multiple cell divisions (Surrales *et al.,* 1994). If

it is too high it may act cytotoxically and cause a reduction in cell viability (Champion *et al.*, 1995).

3.1.2 Aims and Objectives

The aims of the work reported in this chapter were to provide a baseline set of data which allowed the optimisation and validation of the experimental techniques used subsequently and it was also necessary to establish the appropriate conditions to be employed for the *in vitro* investigations using cells from different species. More specifically the objectives were:

a) To investigate the relative sensitivities of the cell types by means of the NRR assay.
b) To optimise the comet assay for use with the CHO-K1, EPCA1 and RTG-2 cell lines using different unwinding and electrophoresis times and using hydrogen peroxide as a reference chemical. This process was not conducted in the 84BR cells as optimisation data already established in these cells was used from Cornwall Dermatology Research (CDR).
c) To validate the comet assay in the CHO-K1, EPCA1 and RTG-2 cell lines using EMS as a reference genotoxin and to validate the comet assay in 84BR cells using hydrogen peroxide as a reference genotoxin. After investigation with these two compounds it was found that hydrogen peroxide was just as effective at generating a positive response, hence EMS was not used in the 84BR cells.
d) To optimise the Mn assay for the induction of micronuclei and the generation of binucleate cells in the CHO-K1, EPCA1 and RTG-2 cell lines using different concentrations of Cyto B. After investigations with the above cell types a standard concentration of Cyto B for mammalian cells (84BR) as

recommended in current literature (Antoccia *et al.*, 1993; Ellard *et al.*, 1991) was used.

e) To validate the Mn assay for the CHO-K1, EPCA1 and RTG-2 cell lines using a reference clastogenic genotoxin (EMS) and then to further validate the assay with the known aneugen, colchicine (COL), using antikinetochore stain. EMS and COL were used with the 84BR cells as positive controls following results from CHO-K1 cells (Sections 3.3.5.2.1 and 3.3.5.3.1 respectively).

3.2 Materials and Methods

3.2.1 Source of Chemicals, Cell Culture Materials and Cell Culture Technique

A list of all cell culture materials and chemicals used (including all abbreviations), and their sources is detailed in Appendix 1.1. All cell culture techniques were detailed in Chapter 2, Sections 2.3.1 and 2.3.2.

3.2.2 Cell Viability and Cytotoxicity

Details of trypan blue, dual-staining and NRR assays were detailed in Chapter 2, Sections 2.4.1, 2.4.2 and 2.4.4. The NRR assay was validated with EMS. The concentrations of EMS were based on an earlier study by Horvàthovà *et al.* (1998) which employed hamster V79 cells, and were set at 0.8, 1.6 and 3.2 mM for the purposes of this investigation. A 1 M stock solution of EMS was prepared in serum free medium (Busch *et al.,* 2001) and then serial dilutions to 0.1 mM made in medium containing 1 % FBS, before adding to the cell monolayer. Cells were treated for 24 hours with various concentrations of EMS (0.0, 0.8, 1.6 and 3.2 mM) in 96-well plates. Wells contained a total of 0.2 ml and 6 replicate wells were used per treatment. The NRR assay was conducted as in Chapter 2, Section 2.4.4.

3.2.3 Single Cell Gel Electrophoresis (comet assay)

The comet assay steps were conducted as detailed in Chapter 2, Sections 2.5.1 through to 2.5.4. The following modifications were made. Alkali (pH > 13) unwinding of DNA was optimised by investigating various times - 10, 20, 30 or 40 minutes. Additionally electrophoresis of DNA was optimised by investigating various times -

10, 20, 30 or 40 minutes as detailed below. This process was necessary to ensure that the responses of the different cell types were consistent and to provide the optimal conditions for investigating and scoring DNA damage in each cell type. Comet visualisation and scoring was conducted as detailed in Chapter 2, Section 2.5.4.

3.2.3.1 Comet Assay Optimisation with Hydrogen Peroxide (H_2O_2)

Hydrogen Peroxide (H_2O_2) was used as a reference chemical to investigate the effects of different unwinding times and electrophoresis times to find the optimal conditions (it is necessary to show that DNA damage can be produced and detected by a reference compound during validation studies) with which to investigate the effects of the test chemicals on each type of cell. CHO-K1, EPCA1 and RTG-2 cells at 70-80 % confluency were prepared onto slides as detailed in Chapter 2, Section 2.5.1. Aliquots of 500 µl cell suspension were made in centrifuge tubes. Cell suspensions were exposed to 100 µM H_2O_2 prepared in PBS for 20 minutes at room temperature. Cell suspensions were then centrifuged for 3 minutes at 2000 rpm and the pellet mixed with 170 µl LMP agarose. This agar mix was then added to the slides and left to set at 4 °C for a minimum of 10 minutes. Cells were lysed as in Chapter 2, Section 2.5.1 and transferred to alkali electrophoresis buffer to unwind for 10, 20 30 or 40 minutes in electrophoresis buffer (Chapter 2, Section 2.5.2) in the dark at 4 °C. Following this step, cells were subject to electrophoresis at 10, 20, 30 or 40 minutes in alkali electrophoresis buffer in the dark at 4 °C (Chapter 2, Section 2.5.3). The protocol as outlined in Chapter 2, Section 2.5.4 was then followed.

3.2.3.2 Validation of the Comet Assay with Ethyl Methanesulphonate (EMS)

CHO-K1, EPCA1 and RTG-2 cells at 70-80 % confluence were exposed to various concentrations (0.0, 0.8, 1.6 and 3.2 mM) of EMS (prepared as detailed in Section 3.2.2) in medium to ensure that the cells were still provided with the correct nutrients for growth and uptake of the compound. EPCA1 and RTG-2 cells were incubated for 6 hours at 21 ± 1 °C in 5 % CO_2 whilst the CHO-K1 cells were incubated at 37 ± 1 °C according to the recommendations set out by Tice *et al.* (2000). Following treatment with EMS, cells were prepared for the comet assay as detailed in Chapter 2, Section 2.5.1. Replicate slides were made for each treatment condition, and the protocol detailed in Chapter 2, Sections 2.5.1 to 2.5.4 followed.

3.2.3.3 Validation of the Comet Assay with Hydrogen Peroxide (H_2O_2)

84BR cells at 70-80 % confluence were aliquoted into 500 µl cell suspensions made in centrifuge tubes and exposed to various concentrations (0, 10, 50 and 100 µM) of H_2O_2 for 20 minutes at room temperature. Cells were prepared onto CometSlides™ and treated as reported in Chapter 2, Sections 2.5.1 and 2.5.2, followed by unwinding (40 minutes) and electrophoresis (24 minutes). Unwinding and electrophoresis times were based on studies with this cell type reported by Cornwall Dermatology Research (CDR) (Morley *et al.*, 2005).

3.2.4 Micronucleus (Mn) Assay

The micronucleus assay process was followed as detailed in Chapter 2, Section 2.6 with the following modifications. Initially the micronucleus assay was optimised with Cyto B. This was followed by validation with EMS on a separate occasion. CHO-K1 cells were

seeded at a density of 4 x 10^5 cells ml^{-1} in 25 cm^2 flasks and incubated at 37 ± 1 °C for 24 hours to allow for cell attachment to the growth substrate. EPCA1 cells were seeded at a density of 1 x 10^6 cells ml^{-1}, RTG-2 were seeded at 4 x 10^5 cells ml^{-1} in 25 cm^2 flasks and cells incubated at their optimum growth temperature of 21 ± 1 °C for 24 hours in 5 % CO_2. Cyto B was added at 0.0, 1.5, 3.0, 4.5 and 6.0 µg ml^{-1} per flask in GM. EMS was added to the cell monolayer at various concentrations (0.0, 0.8, 1.6 and 3.2 mM) prepared in medium as described in Section 3.2.2 before adding to the cell monolayer. The flasks were incubated at 37 ± 1 °C for 24 ± 1 hours (CHO-K1) or incubated at 21 ± 1 °C for 48 ± 1 hours in 5 % CO_2 (EPCA1 and RTG-2). After the exposure period had elapsed, the medium was discarded and the monolayer washed twice with PBS. Cyto B at optimal concentration in solvent (DMSO) was added to the cells in GM and the CHO-K1 flasks incubated at 37 ± 1 °C for 24 ± 1 hours, whilst EPCA1 and RTG-2 flasks were incubated at 21 ± 1 °C for 48 ± 1 hours in 5 % CO_2. After 24 (CHO-K1) or 48 hours (EPCA1 and RTG-2) exposure to Cyto B, the cells were removed from the incubator, and treated as Chapter 2, Section 2.6.1 (Giemsa staining).

3.2.4.1 Validation of the Mn Assay using Colchicine and the Anti-Kinetochore Stain

Concentrations of colchicine (COL) used in this study were followed from current literature (Jie & Jie, 2001) and set at 0.1, 1.0 and 1.8 µg ml^{-1} for validation. A stock solution of COL was prepared at 1 mg ml^{-1} in distilled water and diluted to 10 µg ml^{-1} in medium to obtain the working solution. Serial dilutions were made in medium containing 1 % FBS and added to cell monolayers. Cells were seeded as before (Section 3.2.4) and COL was added to the cell monolayer at various concentrations (0.0, 0.1, 1.0 and 1.8 µg ml^{-1}). The flasks were incubated at 37 ± 1 °C for 24 ± 1 hours for CHO-K1. EPCA1 and RTG-2 cells were incubated at 21 ± 1 °C for 48 ± 1 hours in 5 %

CO_2. After the exposure period had elapsed, the medium was discarded and the monolayer washed twice with PBS. Cyto B in solvent (DMSO) was added to the cells at the optimised concentration for each cell line in GM. CHO-K1 cells were incubated at 37 ± 1 °C for 24 ± 1 hours, whilst EPCA1 and RTG-2 cells were incubated at 21 ± 1 °C for 48 ± 1 hours in 5 % CO_2. After 24 (CHO-K1) or 48 hours (EPCA1, RTG-2) exposure to Cyto B, the cells were removed from the incubator, and treated as in Chapter 2, Section 2.6.2 and 2.6.3.

3.2.5 ESR Background Measurements

ESR measurements were made according to protocol in Chapter 2, Section 2.8.1. Preliminary experiments were made without adding live cells (Section 3.3.7).

3.3 Results

3.3.1 Assessment of Cell Viability with Trypan Blue

Prior to all comet assay experiments cell viability was assessed using trypan blue exclusion dye. This test relies on membrane integrity to distinguish between viable or non-viable cells. Percentage viabilities were above 90 % in all cases.

3.3.2 Cytotoxicity Using NRR and Dual Stain (Calcein AM/EthD III)

The dual stain assay using Calcein AM/EthD III was carried out according to the method outlined in Chapter 2, Section 2.4.2 for CHO-K1, EPCA1 and RTG-2 cell lines using various concentrations of EMS (0.0, 0.8, 1.6, 3.2 and 10.0 mM) and COL (0.0, 0.1, 1.0 and 1.8 $\mu g\ ml^{-1}$). Results for EMS and COL were all over 95 % viability (data not shown). The NRR experiment was used first to validate the NRR assay with EMS and second to investigate any differences between the CHO-K1, EPCA1 and RTG-2 cell lines that may indicate their relative sensitivities to the chemicals used. Cells were treated with various concentrations of EMS (0.0, 0.8, 1.6, 3.2 and 10.0 mM) for 24 hours. NRR results are presented for these cell lines in Figure 3.1. The data were normalised to a percentage (for example, the average of the control for EPCA1 was 0.95 neutral red absorbance whilst the average for 10 mM EMS was 0.79 neutral red absorbance). CHO-K1 showed a significant difference between the control and all EMS doses tested (Mann-Whitney U test, $p < 0.05$). EPCA1 cells had no significant difference between the control and all EMS doses tested (Mann-Whitney U test, $p > 0.05$) except between the control and 10 mM EMS (Mann-Whitney U test, $p < 0.05$). RTG-2 showed no significant difference between the control and EMS doses tested up to 1.8 mM (Mann-Whitney U test, $p > 0.05$), but there were significant differences between the control and 3.2 mM EMS and the control and

10 mM EMS (Mann-Whitney U test, $p < 0.01$). Exposure of all cell types to EMS gave no significant difference between cell lines (Mann-Whitney U test, $p > 0.05$). In all cell lines, viability was decreased to approximately 80 % with 10 mM EMS.

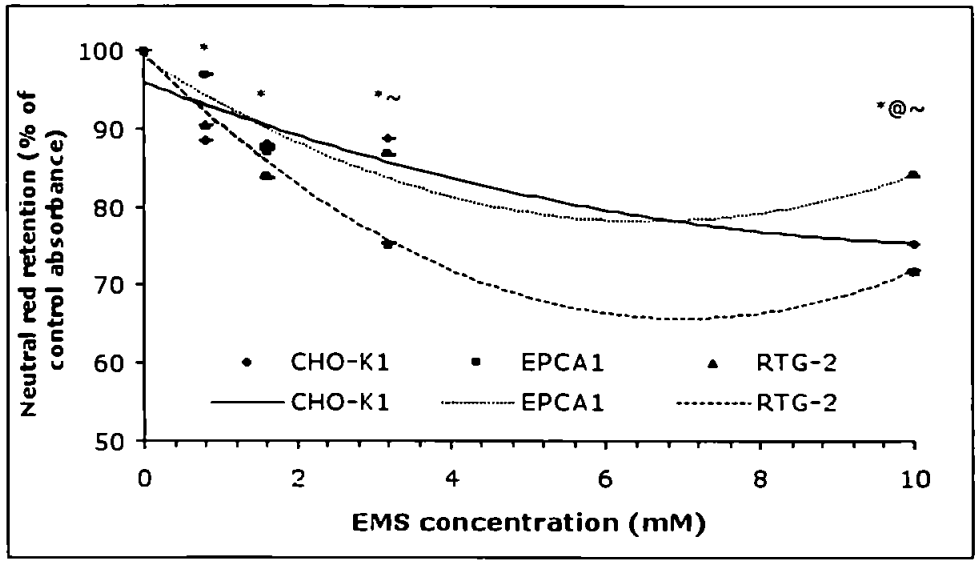

Figure 3.1 Cell viability assessed through the uptake of neutral red dye by CHO-K1, EPCA1 and RTG-2 cells following exposure of cells to 24 hour EMS at various concentrations (0.0, 0.8, 1.6, 3.2 and 10.0 mM). Cell viability is expressed as a percentage of the control (% control), with the control value being 100 %. Data points are represented by 10 replicates. The observed damages at all the EMS concentrations are indicated as significantly different (*) from the control for CHO-K1 (*) (Mann-Whitney U test, $p<0.05$), EPCA1 ($^{@}$) (Mann-Whitney U test, $p<0.05$) and RTG-2 (~) (Mann-Whitney U test, $p<0.01$)

3.3.3 Single Cell Gel Electrophoresis (comet assay)

3.3.3.1 Comet Assay Optimisation

Preliminary experiments were conducted to optimise the comet assay. In order to determine the unwinding and electrophoresis times for the three cell lines (CHO-K1, EPCA1, RTG-2) hydrogen

peroxide (H_2O_2) was used as the positive control and cells were treated to a concentration of 100 μM H_2O_2 for 20 minutes. Various unwinding (10, 20, 30 and 40 minutes) and electrophoresis (10, 20, 30 and 40 minutes) times were investigated. DNA damage was measured by the percentage tail DNA (Tail DNA %) migrated (Morley *et al.*, 2005). In order to identify any significant differences between the unwinding times and the electrophoresis times within the data the non-parametric Mann-Whitney *U* Rank Sum test was performed using MINITAB.

3.3.3.1.1 CHO-K1

In CHO-K1 cells it was clear that significantly greater DNA damage ($p < 0.05$) was observed in the positive control groups compared with the non H_2O_2 exposed groups (Figure 3.2). There was no significant difference between the unwinding times for the different electrophoresis times or between the electrophoresis times for different unwinding times ($p > 0.05$). Therefore 40 minutes unwinding time and 20 minutes electrophoresis time, giving a background of about 15 % DNA damage was chosen for the duration of this study. This agreed with findings reported in the literature, as well as the findings from research in this laboratory on mammalian cell lines (Raissudin & Jha, 2004). From these experiments it was shown that through positive control exposure to H_2O_2 increased DNA damage could be adequately detected through these experimental conditions. The results for the different unwinding and electrophoresis times for the CHO-K1 cell line are presented in Figure 3.2.

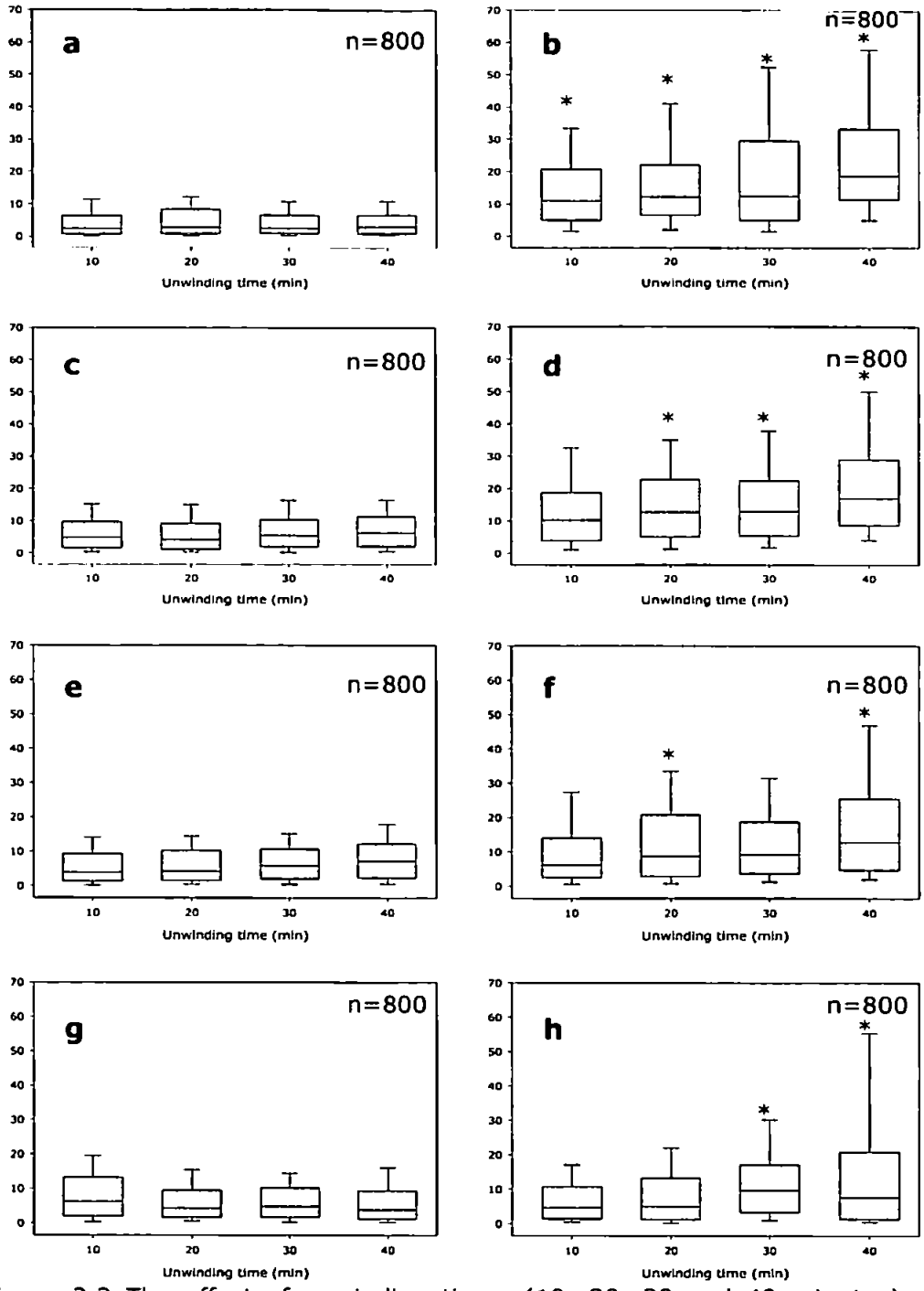

Figure 3.2 The effect of unwinding times (10, 20, 30 and 40 minutes) with 40 (Figure 3.2 a,b), 30 (Figure 3.2 c,d), 20 (Figure 3.2 e,f) or 10 (Figure 3.2 g,h) minutes electrophoresis times on the Tail DNA (%) migrated in CHO-K1 cells following negative control (left plots) or exposure to 20 minutes H_2O_2 (100 µM) (right plots). Significant differences (Mann-Whitney U test, $p < 0.05$) between the H_2O_2 positive controls and the corresponding negative controls are indicated (*). There were no significant differences between the unwinding times for different electrophoresis times or between the electrophoresis times for different unwinding times ($p > 0.05$). Each box represents 200 replicate cells (total n = 800).

3.3.3.1.2 EPCA1

In EPCA1 cells there was no significant difference ($p > 0.05$) between 10 and 20 minutes unwinding times, therefore 20 minutes unwinding time (with a background of about 30 % DNA damage) and 20 minutes electrophoresis time was chosen for the duration of this study due to the agreement with current literature on fish cell lines (Nehls & Segner, 2001; Raisuddin & Jha, 2004). The results reported here show that there is a significant effect from using H_2O_2 as a positive control allowing this assay to adequately detect DNA damage using these experimental conditions. The results for the different unwinding and electrophoresis times for the EPCA1 cell line are presented in Figure 3.3.

3.3.3.1.3 RTG-2

In RTG-2 cells there was no significant difference ($p > 0.05$) shown between the unwinding times therefore 20 minutes unwinding time was chosen as it created a background of about 30 % DNA damage and 20 minutes electrophoresis time was chosen for the duration of this study due to the agreement with current literature on fish cell lines (Nehls & Segner, 2001; Raisuddin & Jha, 2004). The experimental results showed that the positive control to H_2O_2 was successful in allowing the detection of DNA damage through the use of these experimental conditions. The results for the different unwinding and electrophoresis times for the RTG-2 cell line are presented in Figure 3.4.

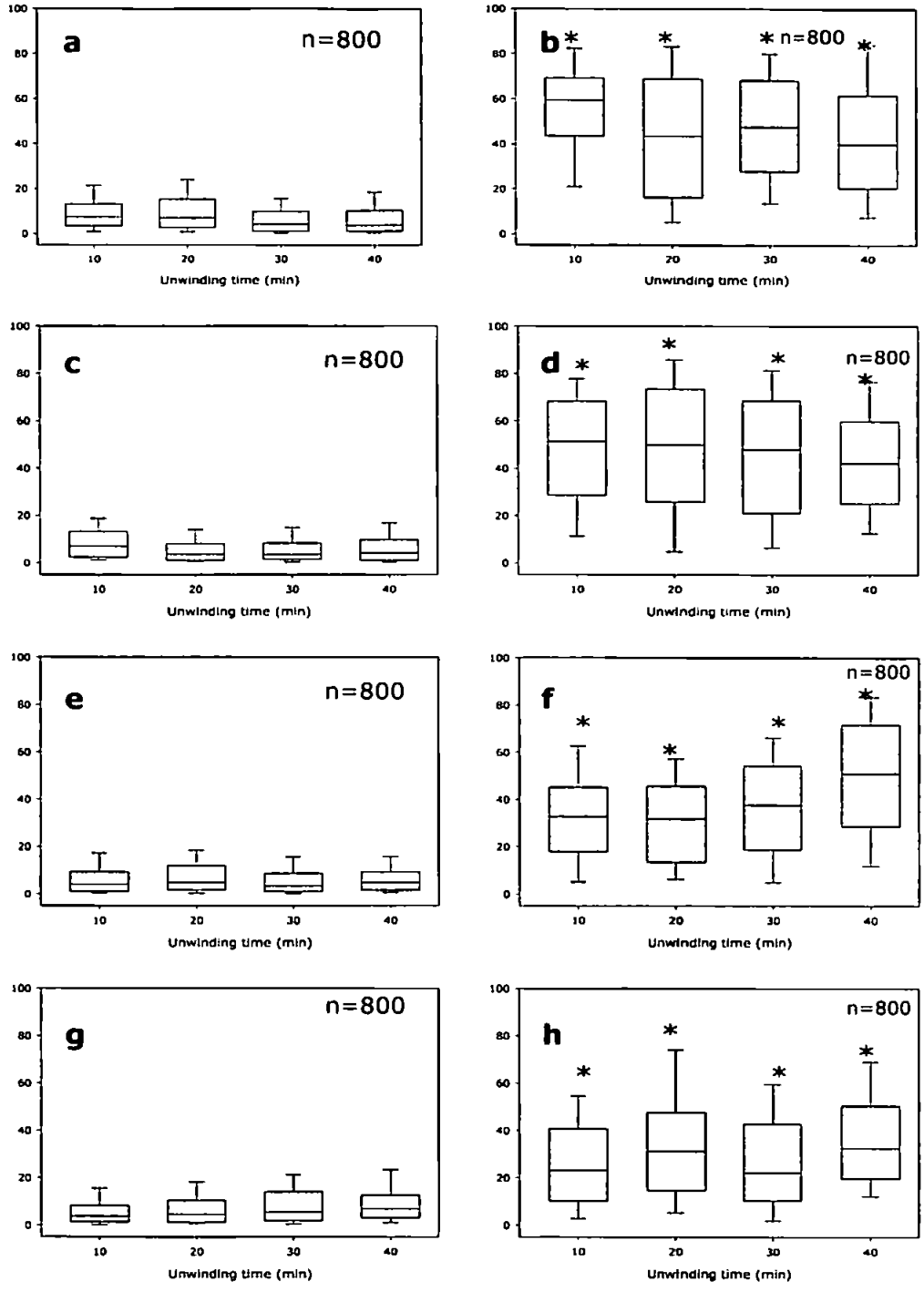

Figure 3.3 The effect of unwinding times (10, 20, 30 and 40 minutes) with 40 (Figure 3.3 a,b), 30 (Figure 3.3 c,d), 20 (Figure 3.3 e,f) or 10 (Figure 3.3 g,h) minutes electrophoresis time on DNA damage (Tail DNA (%)) to EPCA1 cells following negative control (left plots) or exposure to 20 minutes H_2O_2 (100 μM) (right plots). Significant differences (Mann-Whitney U test, $p<0.05$) between the H_2O_2 positive controls and the corresponding negative controls are indicated (*). There were no significant differences between the unwinding times for different electrophoresis times or between the electrophoresis times for different unwinding times ($p>0.05$). Each box represents 200 cells (total n=800).

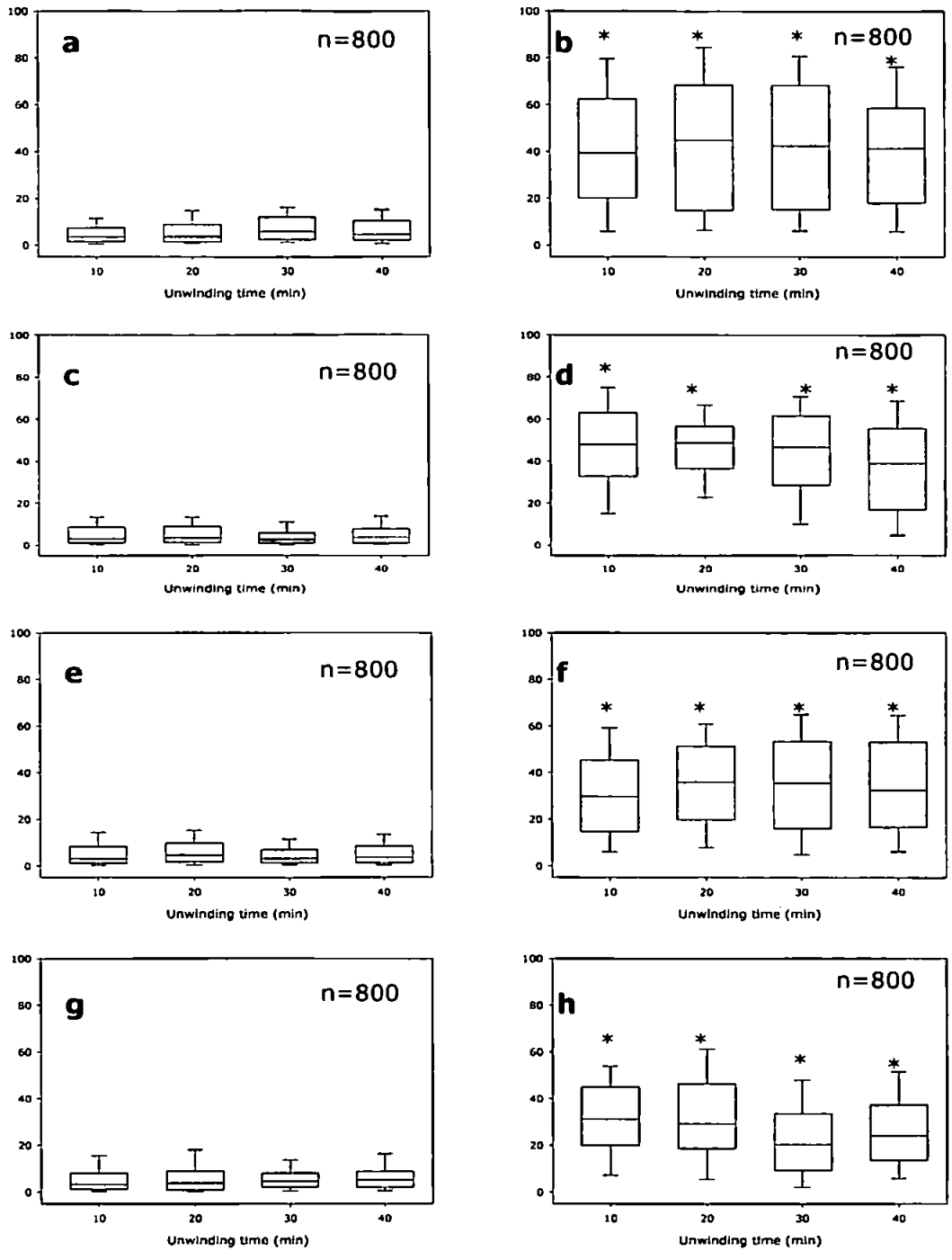

Figure 3.4 The effect of unwinding times (10, 20, 30 and 40 minutes) with 40 (Figure 3.4 a,b), 30 (Figure 3.4 c,d), 20 (Figure 3.4 e,f) or 10 (Figure 3.4 g,h) minutes electrophoresis time on median DNA damage to RTG-2 cells following negative control (left plots) or exposure to 20 minutes H_2O_2 (100 µM) (right plots). Significant differences (Mann-Whitney U test, $p<0.05$) between the H_2O_2 positive controls and the corresponding negative controls are indicated (*). There were no significant differences between the unwinding times for different electrophoresis times or between the electrophoresis times for different unwinding times ($p>0.05$). Each box represents 200 cells (total n=800).

3.3.3.2 Validation of the Comet Assay using Ethyl Methanesulphonate (EMS)

To validate the comet assay, the effect of the known genotoxin EMS was investigated. All cell lines were exposed to EMS at concentrations of 0.0, 0.8, 1.6 and 3.2 mM for 6 hours (following recommendations set out by Tice *et al.,* 2000) following which the comet assay was performed. DNA damage was measured by the Tail DNA (%). The non-parametric Mann-Whitney *U* Rank Sum test was performed on the data using MINITAB and p-values indicated a significant difference between the control and all EMS concentrations (Mann-Whitney U test, $p < 0.001$) for CHO-K1 (Figure 3.5a), EPCA1 (Figure 3.5b) and RTG-2 (Figure 3.5c). There was also a significant difference in response to EMS between the CHO-K1 and RTG-2 cell lines (Mann-Whitney U test, $p < 0.001$) but no significant difference between RTG-2 and EPCA1 cell lines (Mann-Whitney U test, $p > 0.05$). These results showed that there was a dose-dependent effect of EMS on DNA damage which was observed in all the cell lines tested. This indicated that EMS was effective as a positive control for further experiments.

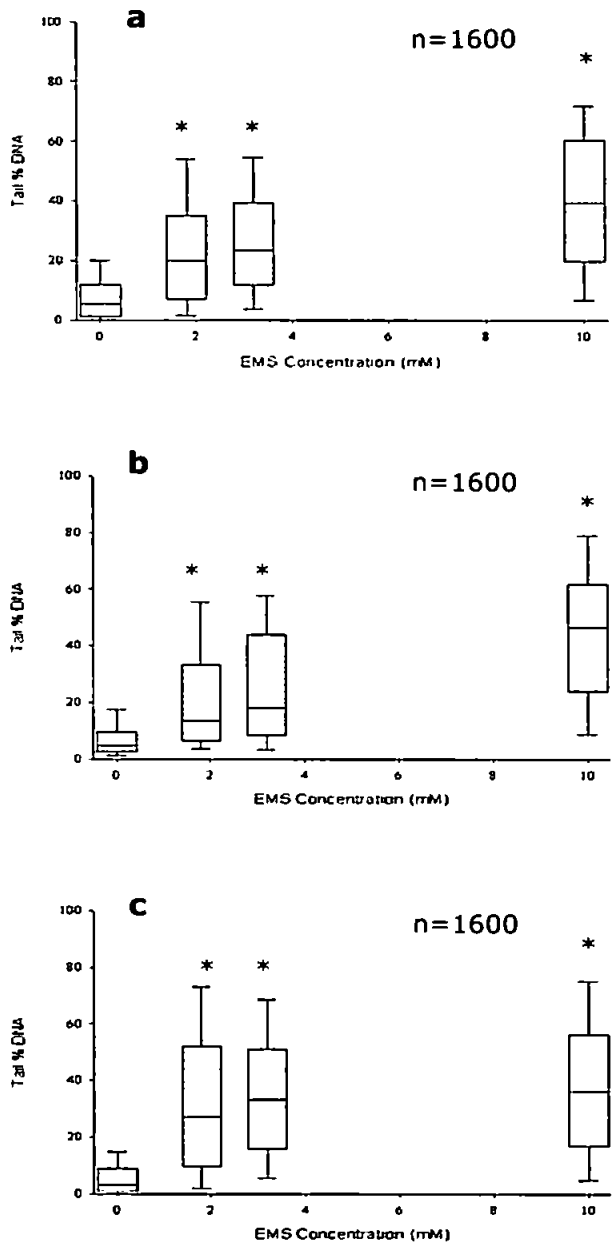

Figure 3.5 Median DNA damage observed in CHO-K1 (Figure 3.5a), EPCA1 (Figure 3.5b) and RTG-2 (Figure 3.5c) cells following 6 hour exposure to EMS at various concentrations (0.0, 0.8, 1.6 and 3.2 mM). DNA damage is assessed by the Tail DNA (%) migrated. The observed damages at all the EMS concentrations are significantly different (*) from the control (Mann-Whitney U test, $p < 0.001$). Each box represents 400 cells (total n=1600).

3.3.3.3 Validation of the Comet Assay using Hydrogen Peroxide (H_2O_2)

To further validate the comet assay, the effect of H_2O_2 was investigated at various concentrations in 84BR cells. 84BR cells were exposed to H_2O_2 for 20 minutes at various concentrations (0, 10, 50 and 100 μM). As measured by Tail DNA (%) (Figure 3.6) there was a significant dose response increase in DNA damage from the control and all H_2O_2 concentrations tested (Mann-Whitney U test, $p < 0.0001$) as well as between all the doses tested (Mann-Whitney U test, $p < 0.0001$).

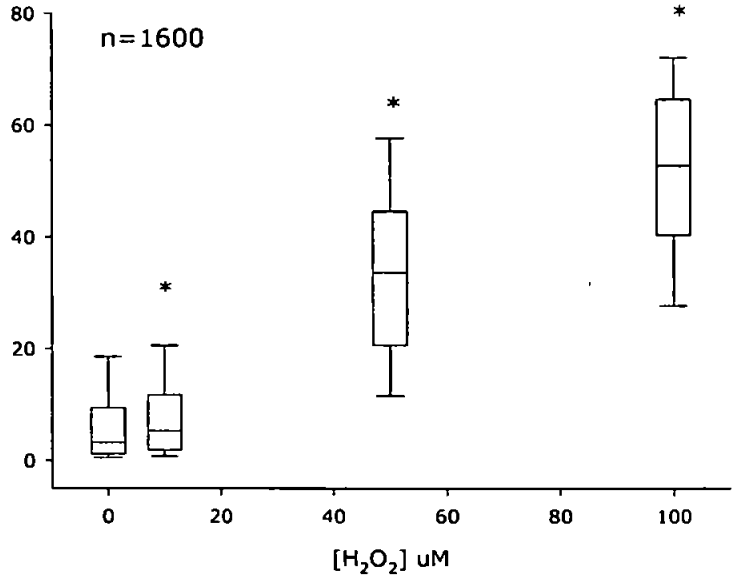

Figure 3.6 DNA damage to 84BR cells following exposure to 20 minutes H_2O_2 at various concentrations (0, 10, 50 and 100 μM). DNA damage is assessed by the Tail DNA (%) migrated. The DNA damages produced by all the H_2O_2 concentrations were significantly different (*) from that of the control (Mann-Whitney U test, $p < 0.0001$). Each box represents 400 cells (total n=1600).

3.3.4 Micronucleus (Mn) Assay

3.3.4.1 Optimisation of the Mn Assay with Cytochalasin B (Cyto B).

Various concentrations of Cyto B (0.0, 1.5, 3.0, 4.5 and 6.0 μg ml^{-1}) were tested in all cell lines (CHO-K1, EPCA1, RTG-2). Cell viabilities were above 90 % for all Cyto B exposures measured through trypan blue unless indicated otherwise. Cells were manually scored using Giemsa stain and results are presented in Table 3.1.

3.3.4.1.1 CHO-K1

Results showed that the frequency of binucleate cells increased significantly (Mann-Whitney U test, $p < 0.05$) with increasing concentrations of Cyto B to a concentration of 3.0 μg ml^{-1} (mean of 653.67 ± 35.08) (which was significantly different from the control (Mann-Whitney U test, $p < 0.05$)). At 4.5 μg ml^{-1} and 6.0 μg ml^{-1} Cyto B the number of binucleate cells dropped slightly to a plateau but also remained significantly different from the control (Mann-Whitney U test, $p < 0.05$). Associated with this was a gradual reduction in the frequencies of mononucleate cells observed with increasing concentrations of Cyto B. There was a small increase in micronuclei frequency seen with increasing the Cyto B concentration from no response seen at 0.0 μg ml^{-1} Cyto B to a mean of 1.33 ± 0.58 at a concentration of 6.0 μg ml^{-1} Cyto B however, this was not significantly different from the control (Mann-Whitney U test, $p > 0.05$). In this work, a maximum generation of binucleate cells with minimum background micronuclei was produced at 3.0 μg ml^{-1} Cyto B so this concentration was chosen for further experiments. This dose also produced significantly (Mann-Whitney U test, $p < 0.05$) more binucleate cells from the other doses.

3.3.4.1.2 EPCA1

Results for EPCA1 cells showed the generation of binucleate cells increased significantly (Mann-Whitney U test, $p < 0.05$) with increasing concentrations of Cyto B to a mean of 838.00 ± 9.90 at a concentration of 1.5 μg ml^{-1} Cyto B. The concentration 1.5 μg ml^{-1} Cyto B produced significantly more (Mann-Whitney U test, $p < 0.05$) binucleate cells than the lowest and highest concentrations (0.5 or 6.0 μg ml^{-1}) of Cyto B. Associated with the occurrence of binucleate cells with the addition of Cyto B were sharp reductions in mononucleate cells (e.g. a mean of 352.5 ± 96.87 with 0.5 μg ml^{-1} Cyto B) from the control mononucleated cell occurrence (a mean of 909.0 ± 94.75). There was a large increase in micronuclei frequency seen with increasing Cyto B concentration from no observed micronuclei at 0.0 μg ml^{-1} Cyto B to a mean of 11.5 ± 2.12 at a concentration of 6.0 μg ml^{-1} Cyto B that was significantly different from the control value above 0.5 μg ml^{-1} Cyto B (Mann-Whitney U test, $p < 0.05$). A maximum generation of binucleate cells with minimum background micronuclei was produced at 1.5 μg ml^{-1}, so this concentration was chosen for further experiments with this cell type.

3.3.4.1.3 RTG-2

Results for RTG-2 cells showed the generation of binucleate cells increased significantly (Mann-Whitney U test, $p < 0.05$) with increasing concentrations of Cyto B to a mean of 636.5 ± 48.79 (1.5 μg ml^{-1}) and a reduction in the frequencies of mononucleate cells with increasing concentration of Cyto B from the control (a mean of 980.5 ± 2.12) to 1.5 μg ml^{-1} (a mean of 469.5 ± 9.19) (Table 3.3). Frequencies of micronuclei remained low and not significantly different from the control (Mann-Whitney U test, $p > 0.05$), to a maximum mean observed micronuclei frequency of 1.5 ± 0.71 at 1.5

μg ml^{-1} (Mann-Whitney U test, $p > 0.05$). However, cytotoxicity was observed through extensive cell detachment at concentrations of 3.0 μg ml^{-1} and above in this cell line. Bearing this effect in mind, the maximum generation of binucleate cells with minimum background micronuclei was produced at 1.5 μg ml^{-1} (significantly different from the control and 0.5 μg ml^{-1} Cyto B) and this concentration was chosen for further experiments.

Table 3.1 Effect of various concentrations of Cyto B on the mean (±SE) number of binucleate cells and micronuclei produced in CHO-K1, EPCA1 and RTG-2 cell lines (n=33,613) using the Giemsa stain. Significant differences from the control are indicated (*) (Mann Whitney U test, $p < 0.05$).

CHO-K1	Mononucleate cells	Binucleate cells	Micronuclei
[Cyto B] (μg ml^{-1})			
0.0	946.33 ± 30.01	56.33 ± 25.70	Not observed
1.5	874.67 ± 11.24	125.33 ± 11.24	0.33 ± 0.58
3.0	356.33 ± 35.08	653.67 ± 35.08*	1.00 ± 0.00
4.5	491.33 ± 3.21	508.67 ± 3.21*	1.33 ± 0.58
6.0	496.67 ± 7.57	503.33 ± 7.57*	1.33 ± 0.58
EPCA1			
[Cyto B] (μg ml^{-1})			
0.0	909.0 ± 94.75	97.50 ± 77.07	Not observed
0.5	352.5 ± 96.87	690.50 ± 71.42*	2.0 ± 2.83
1.5	236.0 ± 31.11	838.00 ± 9.90*	3.5 ± 0.71
3.0	198.5 ± 62.93	824.00 ± 21.21*	5.0 ± 2.83
4.5	207.5 ± 47.38	815.00 ± 53.74*	6.0 ± 1.41
6.0	299.5 ± 135.06	778.00 ± 49.50*	11.5 ± 2.12*
RTG-2			
[Cyto B] (μg ml^{-1})			
0.0	980.5 ± 2.12	30.5 ± 2.12	Not observed
0.5	837.5 ± 17.68	175.0 ± 16.97*	Not observed
1.5	469.5 ± 9.19*	636.5 ± 48.79*	1.5 ± 0.71

3.3.4.2 Validation of the Micronucleus Assay with EMS

The effects of various concentrations of EMS 0.0, 0.1, 1.0, 1.8 and 3.2 mM (Giemsa stain, Table 3.2) or 0.0, 1.8 mM (anti-kinetochore stain, Table 3.3) were observed for the CHO-K1, EPCA1 and RTG-2 cells in order to investigate genomic instability through the activity of this clastogenic compound.

3.3.4.2.1 CHO-K1

The effect of EMS in CHO-K1 cells was investigated using Giemsa to detect micronuclei, and using the anti-kinetochore stain for clastogenic and aneugenic effects. Results using Giemsa stain showed that 1.8 mM EMS caused a significant increase ($p < 0.05$) in the frequencies of mean micronuclei seen (7.00 ± 1.15) from 0.0 mM EMS. There was no significant increase (Mann-Whitney U test, $p > 0.05$) between the control and the other EMS doses tested (0.1, 1.0 and 3.2 mM). The number of micronuclei generated with 3.2 mM EMS was the same as observed with 1.0 mM EMS and the lack of an increase in the number of micronuclei at the highest tested dose could be due to excessive damage outside the detection range for this assay at this concentration (Table 3.2). Results using the anti-kinetochore stain (Table 3.3) indicated that numbers of mononucleate cells reduced slightly and not significantly (Mann-Whitney U test, $p > 0.05$) within a scoring protocol of 1000 binucleate cells, from a mean of 87.5 ± 7.78 to a mean of 79.0 ± 5.66 when EMS was applied. The frequency of K- micronuclei observed increased significantly (Mann-Whitney U test, $p < 0.05$) with EMS exposure. There were no K+ micronuclei detected in CHO-K1 cells.

3.3.4.2.2 EPCA1

In EPCA1 cells the effect of EMS was investigated using Giemsa to detect micronuclei, and using the anti-kinetochore stain to investigate clastogenic and aneugenic effects. Results using the Giemsa stain showed that frequencies of micronuclei increased when EMS was present. This increase was significant with 1.0 mM and 3.2 mM EMS ($p < 0.05$). Results using the anti-kinetochore stain indicated that numbers of mononucleate cells increased significantly ($p < 0.05$) within a scoring protocol of 1000 binucleate cells, from a mean of 78 ± 8.49 (control) to a mean of 212.5 ± 54.45 when EMS was present. The frequency of K- micronuclei observed increased significantly ($p < 0.05$) to a mean of 6.5 ± 2.12 with EMS exposure. There were no K+ micronuclei detected in EPCA1 cells.

3.3.4.2.3 RTG-2

In RTG-2 cells the effect of EMS was investigated using Giemsa to detect micronuclei, and the anti-kinetochore stain to investigate clastogenic and aneugenic effects. Results using the Giemsa stain showed that frequencies of micronuclei increased significantly ($p < 0.05$) from 1.67 ± 0.58 in the control to 5.00 ± 1.00 (1.0 mM EMS). The frequency of micronuclei at the highest concentration used here (4.00 ± 0.00 micronuclei at concentration 1.8 mM EMS) was slightly lower than the highest frequency seen (5.00 ± 1.00 in 1.0 mM EMS) but this was not a significant difference ($p > 0.05$). This frequency was lower than seen in Sections 3.3.4.2.1 and 3.3.4.2.2 for the same dose (1.8 mM EMS) but this was not significantly different indicating that an increase in EMS concentration may generate excessive damage in these cells that is beyond the appropriate detection range of the assay and suggesting that RTG-2 cells are more sensitive to the effects of EMS than CHO-K1 or EPCA1. Results using the anti-kinetochore stain indicated that within a scoring protocol of 1000

binucleate cells numbers of mononucleate cells reduced slightly ($p > 0.05$), from 80 ± 7.07 to 76 ± 9.90 when EMS was applied. The frequency of K- micronuclei observed increased significantly ($p < 0.05$) with EMS exposure. There were no K+ micronuclei detected but a significant induction of K- micronuclei that suggest a loss of chromosome fragments (clastogenic mechanism).

Table 3.2 Effect of various concentrations of EMS on the mean number of micronuclei produced in the CHO-K1, EPCA1 or RTG-2 cell lines using the Giemsa stain (n=56,000). Significant differences are indicated (*) between the tested doses and the control (Mann Whitney U test, $p < 0.05$).

[EMS] (mM)	0.0	0.1	1.0	1.8	3.2
Cellular Response-CHO-K1					
Binucleate	1000.0 ± 0.00	1000.0 ± 0.00	1000.0 ± 0.00	1000.0 ± 0.00	1000.0 ± 0.00
Micronuclei	0.50 ± 0.58	3.00 ± 0.82	4.00 ± 1.83	7.00 ± 1.15*	4.00 ± 3.00
Cellular Response-EPCA1					
Binucleate	1000.0 ± 0.00	1000.0 ± 0.00	1000.0 ± 0.00	1000.0 ± 0.00	1000.0 ± 0.00
Micronuclei	1.0 ± 1.41	2.5 ± 0.71	5.0 ± 0.00*	6.5 ± 0.71*	5.5 ± 7.78*
Cellular Response-RTG-2					
Binucleate	1000.00 ± 0.00	1000.00 ± 0.00	1000.00 ± 0.00	1000.00 ± 0.00	N/A
Micronuclei	1.67 ± 0.58	1.00 ± 0.00	5.00 ± 1.00*	4.00 ± 0.00	N/A

Table 3.3 Effect of various concentrations of EMS on the mean number of micronuclei produced in the CHO-K1, EPCA1 or RTG-2 cell lines using the anti-kinetochore stain (n=26,349). Significant differences are indicated (*) between the tested dose and the control (Mann Whitney U test, $p < 0.05$).

[EMS] (mM)	0.0	1.8
Cellular Response-CHO-K1		
Mononucleate	87.5 ± 7.78	79.0 ± 5.66
Binucleate	1000.0 ± 0.00	1000.0 ± 0.00
K+ 1000 Bn cells	Not observed	Not observed
K- 1000 Bn cells	0.5 ± 0.71	7.5 ± 0.71*
Cellular Response-EPCA1		
Mononucleate	78.0 ± 8.49	212.5 ± 54.45
Binucleate	1000.0 ± 0.00	1000.0 ± 0.00
K+ 1000 Bn cells	Not observed	Not observed
K- 1000 Bn cells	0.5 ± 0.71	6.5 ± 2.12*
Cellular Response-RTG-2		
Mononucleate	80.0 ± 7.07	76.0 ± 9.90
Binucleate	1000.0 ± 0.00	1000.0 ± 0.00
K+ 1000 Bn cells	Not observed	Not observed
K- 1000 Bn cells	0.5 ± 0.71	5.5 ± 0.71*

3.3.4.3 Investigation of Micronuclei Induction with Colchicine (COL)

Three cell lines (CHO-K1, EPCA1, RTG-2) were exposed to COL (Section 3.2.3) at various concentrations (0.0, 0.1, 1.0 and 1.8 μg ml^{-1}) and the results are presented in Tables 3.4. The effects of COL were investigated using the anti-kinetochore stain, to identify any clastogenic and/or aneugenic effects.

3.3.4.3.1 CHO-K1

Results show that for the CHO-K1 cell line in the presence of COL, numbers of mononucleate cells increased within a scoring protocol of 1000 binucleate cells, ranging from 83 ± 15.56 for the control to 279 ± 19.80 with 1.0 μg ml^{-1} COL exposure ($p < 0.05$). The results from anti-kinetochore staining show that there is significant increase ($p < 0.05$) in the numbers of micronuclei produced following CHO-K1 exposure to COL. Of these induced micronuclei, there was a small (but insignificant ($p > 0.05$)) response in K- micronuclei frequency from the K- control (0.5 ± 0.71) to COL at the lowest concentration of 0.1 μg ml^{-1} (1.0 ± 0.00 (K-)) observed whereby a plateau response was then observed for 1.0 μg ml^{-1} (0.5 ± 0.71) and 1.8 μg ml^{-1}. These results suggest that COL has small clastogenic activity, however when the K+ micronuclei results are taken into account, there was a large and significant increase ($p < 0.05$) in K+ micronuclei at 0.1 μg ml^{-1} (12.5 ± 0.71) which then reduced at 1.0 μg ml^{-1} (8.0 ± 1.41) and 1.8 μg ml^{-1} (7.0 ± 1.41) respectively. These results suggest that COL has significant aneugenic activity at all the concentrations tested. However, greater insight into the activity of COL appears when looking at the data obtained with multinucleated cells. At the highest concentration of COL that was used (1.8 μg ml^{-1}) there are significantly more ($p < 0.05$) multinucleated cells (frequency of 18.5 ± 2.12).

3.3.4.3.2 EPCA1

Results show that in the presence of COL the numbers of mononucleate cells increase significantly ($p < 0.05$) within a scoring protocol of 1000 binucleate cells, ranging from 76.5 ± 23.33 (control) to 292 ± 16.97 (1.8 μg ml^{-1} COL). These results from anti-kinetochore staining show that there is small but statistically insignificant ($p > 0.05$) response in K- micronuclei frequency from the K- control (1.0 ± 1.41) and at the lowest concentration of COL (0.1 μg ml^{-1} - 1.0 ± 0.00 (K-)). A plateau response is then observed for 1.0 μg ml^{-1} and 1.8 μg ml^{-1} respectively (1.5 ± 0.71). There is also a large, significant ($p < 0.05$) increase in K+ micronuclei at 0.1 μg ml^{-1} (8.0 ± 0.00) but this declines with increasing concentrations of COL. At the higher concentrations of COL (1.0 and 1.8 μg ml^{-1}) there are more multinucleated cells (frequencies of 4.5 ± 2.12 and 8.5 ± 0.71 respectively) (significantly different from the control ($p < 0.05$)) than those observed with the lower concentrations of COL and than those observed within the control group.

3.3.4.3.3 RTG-2

Results show that the numbers of mononucleate cells increase significantly ($p < 0.05$) within a scoring protocol of 1000 binucleate cells, ranging from 85 ± 8.49 (0.00 μg ml^{-1} COL) to 300.5 ± 4.95 (1.8 μg ml^{-1} COL). Results from anti-kinetochore staining show that there is small and statistically insignificant ($p > 0.05$) increase in K- micronuclei frequency from the K- control (0.5 ± 0.71) at the lowest concentration of COL (0.1 μg ml^{-1} - 1.0 ± 1.41 (K-)) whereby the response of micronuclei does not increase as concentrations of COL increase. For K+ micronuclei, there is a large and significant ($p < 0.05$) increase in K+ micronuclei at a concentration of 0.1 μg ml^{-1} (8.0 ± 0.00) the frequency of which then declines at 1.0 μg ml^{-1} (5.5 ± 2.12) and 1.8 μg ml^{-1} (5.5 ± 0.71) COL. At the higher

concentrations of COL (1.8 μg ml^{-1}) there are more multinucleated cells (frequency of 6.5 ± 0.71; statistically different from the control ($p < 0.05$)) than observed with the lower concentrations of COL and within the control group.

Table 3.4 Effect of various concentrations of COL on the mean number of micronuclei produced in the CHO-K1, EPCA1 and RTG-2 cell lines (n=56,592) using the anti-kinetochore stain. Significant differences from the control are indicated (*) (Mann Whitney U test, $p < 0.05$).

[COL] ($\mu g\ ml^{-1}$)	0.0	0.1	1.0	1.8
Cellular Response-CHO-K1				
Mononucleate	83.0 ± 15.56	139.0 ± 52.33*	279.0 ± 19.80*	253.5 ± 89.80*
Binucleate	1000.0 ± 0.00	1000.0 ± 0.00	1000.0 ± 0.00	1000.0 ± 0.00
K+ 1000 Bn cells	Not observed	12.5 ± 0.71*	8.0 ± 1.41*	7.0 ± 1.41*
K-1000 Bn cells	0.5 ± 0.71	1.0 ± 0.00	0.5 ± 0.71	0.5 ± 0.71
Multinucleate cells	Not observed	4.5 ± 2.20*	12.5 ± 3.54*	18.5 ± 2.12*
Cellular Response-EPCA1				
Mononucleate	76.5 ± 23.33	104.0 ± 1.41*	217.0 ± 32.53*	292.0 ± 16.97*
Binucleate	1000.0 ± 0.00	1000.0 ± 0.00	1000.0 ± 0.00	1000.0 ± 0.00
K+ 1000 Bn cells	Not observed	8.0 ± 0.00*	6.5 ± 2.12*	5.5 ± 0.71*
K- 1000 Bn cells	1.0 ± 1.41	1.0 ± 0.00	1.5 ± 0.71	1.5 ± 2.12
Multinucleate cells	Not observed	1.0 ± 0.00	4.5 ± 2.12*	8.5 ± 0.71*
Cellular Response-RTG-2				
Mononucleate	85.0 ± 8.49	116.5 ± 17.68*	241.0 ± 50.91*	300.5 ± 4.95*
Binucleate	1000.0 ± 0.00	1000.0 ± 0.00	1000.0 ± 0.00	1000.0 ± 0.00
K+ 1000 Bn cells	Not observed	8.0 ± 0.00*	5.5 ± 2.12*	5.5 ± 0.71*
K- 1000 Bn cells	0.5 ± 0.71	1.0 ± 1.41	1.0 ± 1.41	0.5 ± 0.71
Multinucleate cells	Not observed	1.5 ± 0.71	3.0 ± 1.41*	6.5 ± 0.71*

3.3.5 UVR Background Measurements

UVR measurements were taken in triplicate at the start of the work reported here in order to assess the spectral output of the UVB and UVA lamps and the UVR chamber. Measurements were taken throughout practical experimentation (Chapter 2, Section 2.7) to check UV irradiance levels, whereby any fluctuations could be modified to ensure that cells received correct UVR doses. The free standing UVB lamp produced a mainly UVB output which also continued into the UVA wavelength, but at greatly reduced intensity (Figure 3.9a). The UVR chamber produced UVR light strongly in the region of visible light, at reduced intensity in the UVA region and at low levels in the UVB region (Figure 3.9a). The intensity of the UVA output in the UV cabinet was below 0.05 W m^{-2} s^{-1} and would be too weak to generate sufficient damage to the cells under experimentally realistic conditions or times. Figure 3.9b illustrates the output of the free-standing UVA lamp which emitted UVA strongly at an intensity of approximately 2.25 W m^{-2} s^{-1}. This provided a more useful working output of UVA and was chosen as the UVA source for future experiments. The spectral outputs of the light sources used are illustrated below in Figure 3.9.

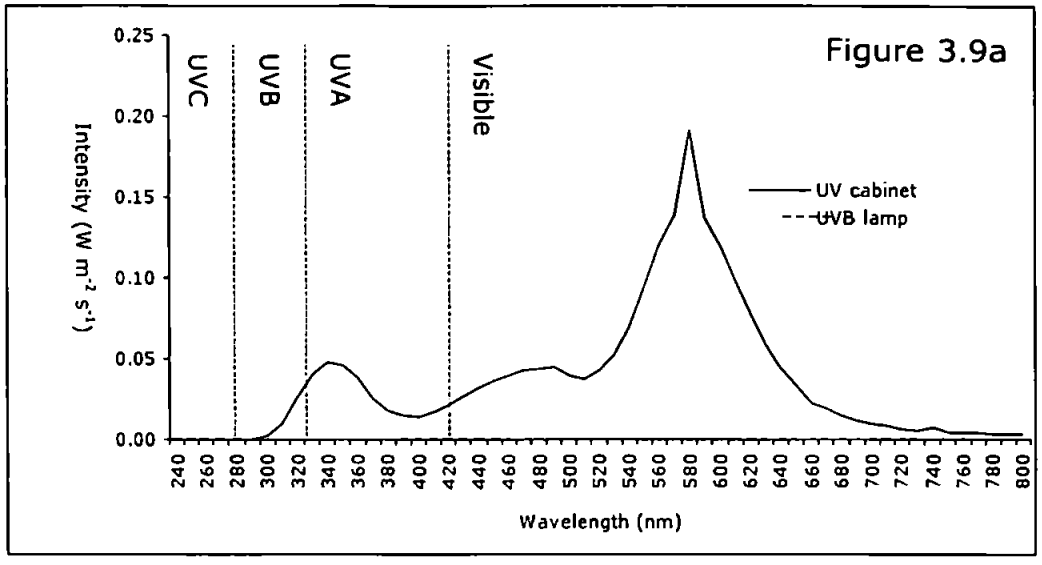

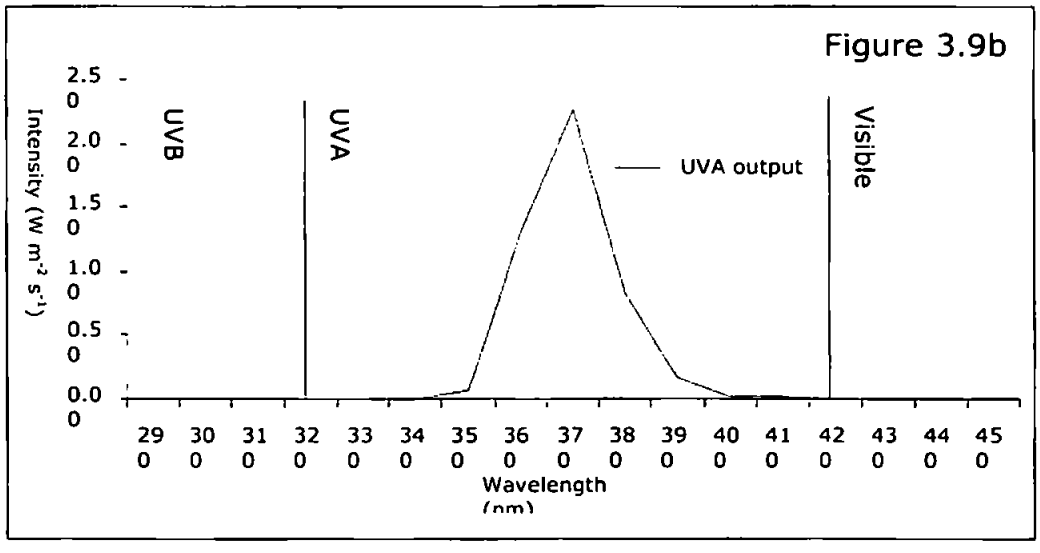

Figure 3.9 (a) Mean spectral distribution in the UV cabinet and produced by the free-standing UVB lamp indicating the wavelengths and wavelength intensities produced by each (triplicate measurements). (b) Mean spectral distribution of the free-standing UVA lamp indicating the wavelength and wavelength intensity emitted (triplicate meansurements).

3.3.6 Electron Spin Resonance (ESR) Background Measurements

As with most experimental systems the first step in using ESR for the examination of a particular radical species is to establish the experimental conditions for effective spin-trapping to occur. In this study 50 ml of a solution of B(a)P in dimethylsulphoxide (DMSO) (1 mg ml^{-1}) was added to 0.5 ml of various spin traps (Tiron, DMPO, TMPol, POBN) dissolved in PBS and then exposed to UVA irradiation. Tiron (4,5-dihydroxy-1,3-benzene-disulphonic acid disodium salt) was found to be photosensitive to UVA and could therefore not be used as it gave a false positive response for superoxide (it is reportedly sensitive to superoxide radical anions only (McRae *et al.,* 1982)). Under irradiation, the spin trap 5,5-dimethyl-1-pyrroline-N-oxide (DMPO) formed an OH adduct, characterised by a 1:2:2:1 quartet with $a_N = a_H{}^{\beta} = 1.49$ mT. However, the DMPO-OH adduct can be formed either by direct trapping of hydroxyl radicals or from the decomposition of the superoxide adduct, DMPO-OOH (Pou *et al.,* 1994). This can produce difficulties with interpretation of data since the source of the hydroxyl radical could be either from superoxide or hydroxyl. Use of an iron chelator (i.e diethylenetriaminetetraacetic acid (DETAPAC) (Pou *et al.,* 1994) Section 4.3.4) is then necessary to distinguish the source of the DMPO-OH adduct by ensuring that trace metal impurities (e.g. iron) were removed. TMPol, a trap for singlet oxygen gave no signal on irradiation of the aqueous solution but in contrast, in a DMSO solution of B(a)P and TMPol, an intense 3-line signal with $a_N = 1.58$ mT was observed, indicating the formation of singlet oxygen in a non-aqueous environment which is probably due to the presence of DMSO. Irradiation of an aqueous solution of α-(4-pyridyl 1-oxide)-N-*tert*-butylnitrone (POBN) containing B(a)P showed a weak 3x2 signal with $a_N = 1.597$ mT and $a_H = 0.268$ mT, which can be assigned to POBN-CH_3. When ethanol was added to the solution, irradiation produced a different 3x2 signal with $a_N = 1.566$ mT and $a_H = 0.244$ mT, due to POBN-$CH(OH)CH_3$. These radical adducts (POBN-

CH_3 and POBN-CH(OH)CH_3) can be ascribed to the reaction of hydroxyl radicals with DMSO and ethanol respectively (Buettner & Mason, 2003) (the addition of ethanol can increase the detection of hydroxyl radicals however ethanol can be damaging when used with cells) and make the use of this spin trap unsuitable due to the use of DMSO in the system used to dissolve B(a)P. On the basis of these observations DMPO was used in this work (Elliott *et al.,* 1986) (Sections 4.3.4 and 5.3.4.4).

3.4 Discussion

When the dual stain technique was applied following cellular exposure to EMS or COL no cytotoxicity was detected in any of the cell lines. Using the NRR assay, CHO-K1 cells showed greater sensitivity than the fish cells (EPCA1 and RTG-2) to the effects of EMS, with all EMS concentrations significantly reducing cell viability indicating a disruption to lysosomal membrane stability. However, in RTG-2 cells there was only significant cytotoxicity given at the highest two doses (3.2 and 10 mM EMS) and in EPCA1 cells only the highest dose tested (10 mM EMS) gave a significant reduction cell viability. There was no significant difference between the responses of the different cell lines to the same concentrations of EMS; although viability was reduced at the highest EMS dose (10 mM EMS) tested in all cell lines suggesting that this dose was cytotoxic at this concentration to all cell lines. The NRR assay has been successfully applied in ecotoxicological studies to various cell lines including RTG-2 cells and primary cell lines derived from gold fish skin cells (Reeves *et al.*, 2008; Sánchez-Fortún *et al.*, 2005) and it is recommended for use with regulatory phototoxicity evaluation of chemicals by OECD (Spielmann *et al.*, 1998). The NRR results suggested that this assay could be used for further experimentation alongside the comet and micronucleus assays to establish levels of cytotoxicity (for example, non – specific DNA damage is associated with cell death (Tice *et al.*, 2000; Kwak *et al.*, 2001)). Therefore, the evidence from these experiments suggests that testing for cell viability with these assays will ensure that responses shown from experiments with either the comet assay or the micronucleus assay would be unlikely to be due to cytotoxicity and more likely would occur as a result of genetic damage.

Initially, the effects of two comet parameters (unwinding times and electrophoresis times) were investigated. The outcome of these experiments was a standardised approach to both the unwinding and

electrophoresis time parameters in experiments for each cell type employed. Tice *et al.* (2000) have illustrated the importance of optimising different parameters for the specific cell line and that comparisons are made between the extent of DNA migration in both the control and the treated cells under different unwinding times. These recommendations by Tice *et al.* (2000) suggest that there is some migration induced from control cells. The data reported here show that 40 minutes unwinding and 20 minutes electrophoresis (Figure 3.2) were most suitable for the mammalian cell line (CHO-K1), whilst 20 minutes unwinding and 20 minutes electrophoresis were most appropriate for both the fish cell lines (EPCA1 and RTG-2) (Figures 3.3 and 3.4 respectively) and so these were the parameters selected for the rest of the experimentation undertaken.

Published work with human cells shows a wide range of both the unwinding and the electrophoresis times used in the comet assay. The results presented here for the mammalian cells (CHO-K1) show comparable unwinding and electrophoresis times (40 minutes unwinding and 20 minutes electrophoresis) to other work. For example, Pouget *et al.* (2000) used 45 minutes unwinding and 20 minutes electrophoresis times and other studies use longer unwinding times of up to 1 hour (Bock *et al.*, 1998), whilst others use shorter times such as 20 minutes unwinding and 15 min minutes electrophoresis (Myllyperkiö *et al.*, 2000). Fish erythrocytes have been used in comet assay testing under the same time parameters as used in this study (20 minutes unwinding and 20 minutes electrophoresis) (Villarini *et al.*, 1998). However, other workers using blood samples have used 10 minutes unwinding and 15 or 20 minutes electrophoresis (Andrade *et al.*, 2004). The EPC cell line has been used for genotoxicity testing with the comet assay in other studies and experimental conditions were comparable to the ones reported here. For instance, Kammann *et al.* (2001) exposed EPC cells to marine sediments containing PAH and used 20 minutes

unwinding and 15 minutes electrophoresis for comet assay testing. So, the unwinding and electrophoresis times chosen for this work have been optimised in this laboratory and are consistent with those reported in the literature.

Using this optimised system with EMS gave results from the comet assay that showed that EMS significantly increased DNA damage in all cell types in a clear dose – related manner. EMS as well as other, related, weakly mutagenic compounds, such as methyl methanesulfonate (MMS) act through alkylation of several positions on DNA: the N^1, N^3, N^6 and N^7 position of adenine; N^1, N^2, N^3, N^7 and O^6 of guanine; the N^3, N^4 and O^2 position of cytosine; and the N^3, O^2 and O^4 position of thymine (Horváthová *et al.,* 1998). Base modification by DNA alkylation then causes weakening of the *N*-glycosylic bonds which leads to depurination/depyrimidination and the appearance of alkali – labile abasic sites (AP sites). AP sites may also be formed as a result of the excision of some forms of base damage initiated by specific DNA glycosylases. AP sites are removed by AP endonucleases, which cleave DNA adjacent to AP sites and create single strand breaks (SSBs) in DNA (Horváthová *et al.,* 1998). However, the use of EMS employed in this thesis was not intended to differentiate amongst the different mechanisms of DNA damage, or to investigate repair mechanisms. For this reason, the increase in DNA damage as shown through increasing strand breaks with increasing concentrations of EMS, gives only an indication of the nature of the interactions between EMS and the cell lines investigated here but does provide a measure to which the level of DNA damage initiated by B(a)P and UV (both singly and together) can be compared. Similarly, in order to simply validate the comet assay, with 84BR cells H_2O_2 was used and showed a dose related significant increase in DNA damage.

The Cyto B results indicated that the greatest sensitivity is shown by the EPCA1 cell line for the generation of micronuclei, followed by the RTG-2 and CHO-K1 cell lines (i.e. EPCA1 > RTG-2 > CHO-K1). Cyto B also appeared to be cytotoxic to RTG-2 cells at increased concentrations. These results suggest that fish cell lines have greater sensitivity to Cyto B than the mammalian CHO-K1 cell line. The results from this study indicate that 3 μg ml^{-1} Cyto B is an appropriate concentration to use with the CHO-K1 cell line whilst a lower concentration of 1.5 μg ml^{-1} is more suitable for the fish cell lines, EPCA1 and RTG-2. The chosen concentration for the CHO-K1 cell line is in agreement with published literature for Chinese hamster cultures (Ellard *et al.,* 1991), and human fibroblasts (Antoccia *et al.,* 1993). However, whilst there is copious published work on *in vivo* micronucleus studies using fish for biomonitoring studies, there is little information or use of established fish cell lines with this assay in ecogenotoxicological testing, and this is currently a unique instance of using fish cells with the CBMN assay.

Following optimisation of the CBMN assay, EMS was used to validate the assay using Giemsa staining to detect micronuclei frequencies, CHO-K1 cells gave a significant increase in micronuclei frequency up to 1.8 mM EMS but no significant difference between the control and 3.2 mM EMS. This could be related to the significant disruption in membrane stability seen using the NRR assay however, this data was obtained within a scoring protocol of 1000 binucleate cells therefore any damaged cells may have died and detached before detection using the CBMN assay giving a lower frequency of micronucleated cells. In EPCA1 cells there was a significant increase in micronuclei in all doses tested and also a significant increase in the mononucleate cells with EMS. The increase in mononucleate cells may be due to a delay in the cell cycle due to DNA damage and indicates genomic instability (Kaufmann & Paules, 1996). These results suggest that the greatest sensitivity was shown by RTG-2 cells to the effects of

EMS followed by EPCA1 and CHO-K1 however there was no significant difference between the micronuclei produced at the same doses.

Using anti-kinetochore staining in all cell lines (CHO-K1, EPCA1 and RTG-2) the results for the EMS exposures indicated that EMS significantly increased the frequency of K- micronuclei which was a clastogenic effect in all three cell lines because no K+ micronuclei were detected. There was no significant difference between the responses of the cell lines tested indicating that this compound acts in a broadly similar way across different cell types. Consistent with these data is the use of EMS as a positive clastogenic control in published literature (Frieauff *et al.,* 1998; Raisuddin & Jha, 2004). The results from this investigation indicate that EMS is a good positive control for further studies in the Mn assay, due to its induction of a strong dose-related clastogenic response in all cell lines. Following validation with EMS, the micronucleus assay was also validated with COL. These results indicated a positive response to COL that was not linearly dose dependent. Higher doses of COL caused a lower frequency of micronuclei than the lower doses of COL but there was a positive dose dependent increase in multinucleated cells observed in all cell lines. COL is well known for its aneugenic mode of action at low doses (Antoccia *et al.,* 1993; Schmid *et al.,* 1999; Schriever-Schwemmer *et al.,* 1997) and the results presented showed that COL induced the highest frequency of micronuclei at the lowest dose tested (0.1 μg ml^{-1}) compared to the larger doses used in all cell lines. There was no statistically significant difference between the cells lines in the micronuclei that were produced. For example, the EPCA1 results showed a lower frequency of micronuclei than the CHO-K1 cells, but a similar response was seen between the EPCA1 and the RTG-2 cells in all COL concentrations but these responses were not statistically different. COL has been shown to produce a dose-related increase in micronuclei in human fibroblasts (Antoccia *et al.,* 1993) whilst Zijno *et al.* (1996) reported that

treatments with COL produced a significant increase of micronucleated cells only at the highest dose (20 ng ml^{-1}) tested. The results here indicate that a significant majority of micronuclei induced by COL contained K+ signals, indicating that COL had a mainly aneugenic effect at the lowest dose used which suggests that the observed micronuclei were created from part or the whole chromosome. In partial agreement with our results, Jie & Jie (2001) showed that following treatment with COL at the same concentration as used in these experiments (0.1 µg ml^{-1}) 74.5 % of the micronuclei induced displayed centromeric signals and several telomeric signals, indicating that micronuclei induced by COL were mainly composed of whole chromosomes. Yang & Cao (2000) also concluded that the majority of COL-induced micronuclei contained whole chromosomes.

In addition to the assessment of micronuclei, other parameters (mononucleate and binucleate cell induction) were investigated. There was a significant increase in mononucleate cells detected in all cell lines following treatment with COL. This increase in mononucleated cells may be due to a cell cycle delay resulting in late cytokinesis. For example, cell cycle delays are indicative of DNA damage responses that may have occurred to provide more time for repair before the critical stages of DNA replication (Kaufmann & Paules, 1996). The work reported here shows that at the higher concentrations of COL used, there were lower frequencies of micronucleated cells, but higher frequencies of multinucleated cells. Antoccia *et al.* (1993) also showed that higher COL concentrations (2.25×10^{-8} M) produced higher frequencies of multinucleated cells (Antoccia *et al.*, 1993). COL is also used as a spindle blocking agent at higher doses (Dybowski, 2000) and it has been reported that its combined use with Cyto B can reduce binucleate cell frequencies with the appearance of tetra- and poly-nucleated cells (Antoccia *et al.*, 1993). The observations of poly-nucleated cells here suggest that its

use as a positive aneugen should be restricted to the lower doses tested.

In conclusion, the preliminary studies with the Mn assay, provided data which demonstrate that each cell line shows a broadly similar response to EMS or COL treatment. Anti-kinetochore antibody treatment demonstrated differences in the induction of micronuclei-containing chromosome fragments and whole chromosomes with chemicals such as EMS and COL. These preliminary experiments showed the Mn assay to be suitable for use with compounds such as B(a)P and UVR to investigate clastogenic and aneugenic mechanisms. The CHO-K1 cell line provided a suitable mammalian model to use and of the two fish cell lines used, the RTG-2 cell line is more suitable for use in the Mn assay than the EPCA1 cell line due to its larger cell size and the relative ease of staining. With regard to the different cell lines used, it was shown that following cytotoxicity experiments, mammalian (CHO-K1) and fish cells (EPCA1 and RTG-2) exhibited similar sensitivities to chemicals with different modes of action i.e. clastogenic EMS and aneugenic COL. After genotoxicity studies with the comet assay, the importance of optimising and validating variables was demonstrated and the parameters chosen were consistent with those reported in the literature. It was also shown with the Mn assay that all the cell lines exhibited a similar response to EMS and COL and the use of the anti-kinetochore stain provided an approach with which to distinguish between clastogenic and aneugenic effects in the cell. The following table (Table 3.5) details the advantages and disadvantages of all three cell lines for use in the work reported here.

Table 3.5 Summary of the advantages and disadvantages of the cell lines CHO-K1, EPCA1 and RTG-2 in ecotoxicological testing for the purposes of this work.

Cell line	Advantages	Disadvantages
CHO-K1	- Commonly used in genotoxicity studies (Huynh-Delerme *et al.*, 2003; Raisuddin & Jha, 2004) -Easy to work with large cells in this work, 24 h cell cycle - Visually clear in Mn assay in this work - Widely used in Mn assay (Liu *et al.*, 2005)	- No metabolic function – requires an exogenous metabolic system (Ellard *et al.*, 1991; Ellard & Parry, 1993) - Lower response observed for comet assay to B(a)P than fish cells in this work
EPCA1	- Widely used in environmental toxicology studies (Kammen *et al.*, 2001; Ruiz-Leal & George, 2004) - Cells derived from epithelial tissue – relevant to interactive toxicity work - Basic metabolic present (Wright *et al.*, 2000) - Sensitive response observed for the comet assay in this work	- Transformed cell line (papilloma) (Wolf & Mann, 1980) - 48 h cell cycle (Wolf & Mann, 1980) - Small cells, difficult to perform the Mn assay in this work due to poor staining
RTG-2	- Widely used in environmental toxicology testing (Castano & Becerril, 2004; Nehls & Segner, 2001) - Easy to work with in this work as they are large cells - Basic metabolic function present (Castano *et al.*, 1996; Fent, 2001; Nehls & Segner, 2001; Segner, 1998) - Established ability to metabolise B(a)P (Castano *et al.*, 2000; Kolpoth *et al.*, 1999 - Sensitive response in BOTH comet and Mn assay in this work – Respond to both aneugenic and clastogenic effects of tested chemicals (Mn) at similar doses to mammalian cells without the addition of exogenous metabolic activity (Sanchez *et al.*, 2000) - Visually clear in Mn assay in this work - Well characterised for use in Mn assay (Kolpoth *et al.*, 1999; Sanchez *et al.*, 2000)	- 48 h cell cycle (Wolf & Quimby, 1962)

In preparation for the next stage of the work planned, it was necessary to examine the most suitable cell lines with which to continue research for the subsequent studies. With regards to the fish cell lines, it was decided to limit the investigations into B(a)P and UV mainly to the RTG-2 cell line, and execute only preliminary experiments with B(a)P to the EPCA1 cell line to avoid excessive and unnecessary repetitions of the investigations. The use of the RTG-2 cell line provides an excellent foundation from which to develop a tiered approach to the investigation of interactions between B(a)P and UVB/UVA. Additionally, the RTG-2 cell line is commonly used in environmental ecotoxicological studies (for references see Table 3.5) and has been optimised and validated within this project. The CHO-K1 cell line was also selected to produce baseline B(a)P and UV data for mammalian data, and to enable comparisons to be made with data from the primary human 84BR cells introduced later in the project (Chapter 5).

CHAPTER IV – THE INTERACTIVE EFFECTS OF B(a)P AND UVR ON CELLS DERIVED FROM AQUATIC ORGANISMS

4.1 Introduction

Aquatic environments are subject to a massive outfall of organic pollutants especially in built-up areas (Liu *et al.*, 2005) and of these organic pollutants PAHs present one of the largest threats to marine life (Secco *et al.*, 2005; Vidal-Martinez *et al.*, 2006). Water is rarely pristine and organisms may be exposed to low levels of PAH pollution in complex mixtures (Donkin *et al.*, 2003; Kilemade *et al.*, 2004a). Long-term low level exposures to PAHs will allow these compounds to build-up within tissues due to their lipophilic nature; B(a)P metabolites have been detected in muscle and liver extracts in flatfish (Gmur & Varanasi, 1982) and in bile and liver extracts from ictalurid catfish (Willett *et al.*, 2000). Although exposure concentrations may not be lethal, PAH accumulation in tissue may reduce immune function (Hoeger *et al.*, 2004) or reproductive ability (Monteiro *et al.*, 2000), or cause them to become vulnerable to additional stressors such as temperature change. Early life stages may be particularly vulnerable (Diamond *et al.*, 2006), and detrimental effects such as low hatch weights, retarded development, lower growth rates and increased susceptibility to mortality due to stress have been observed (Luchenbach *et al.*, 2003). Exposure to PAHs has been shown to increase apoptotic cell death in larval pink salmon (*Oncorhynchus gorbuscha*) skin cells and gonads (Marty *et al.*, 1997). Chronic exposure to PAHs may also cause deformities, oedemas, reduced growth, swimming impairment and mortality (Barron *et al.*, 2004).

Responses like this will over time reduce the overall fitness of the species through population declines and mortalities.

UVR may also cause many detrimental effects. In aquaculture fish are held in high stocking densities, often in shallow waters, with little or no shade and hence there is the potential for greater exposure to solar radiation than in the wild. For instance, many studies have been conducted on fish egg and larval stages, showing that solar and artificial UVB may induce a stress response in affected individuals, such as unusually high ventilation rates and impaired respiratory control in larvae and juveniles (Steeger *et al.,* 2001). For example, solar and artificial UVR exposure also produces DNA damage (e.g. high CPD loads) (Armstrong *et al.,* 2002; Malloy *et al.,* 1997), reduced fertilisation success (indicated by impaired sperm quality and motility) in sea urchin larvae (Au *et al.,* 2002), loss of positive buoyancy in plaice eggs (*Pleuronectes platessa*) (Steeger *et al.,* 2001), photohaemolysis of erythrocytes (Kumar & Joshi, 1992), cataract formation in rainbow trout (*Onchorynchus mykiss*) (Cullen *et al.,* 1994), embryonic malformation, such as spinal deformations for Patagonian freshwater fish *Galaxias maculates* (Battini *et al.,* 2000) and inhibited swimming and detrimental effects on development (Pennington & Emlet, 1986). UVB irradiation can cause wavelength dependent mortalities to both eggs and embryonic stages in fish (Battini *et al.,* 2000; Béland *et al.,* 1999; Keller *et al.,* 1997; Kouwenberg *et al.,* (1999a); Pennington & Emlet, 1986; Steeger *et al.,* 2001) and mortality may be dependent on when in the life history the organism is exposed to UVB, for example, there is increased mortality observed if plaice eggs (*Pleuronectes platessa*) are UVB irradiated before gastrulation (Steeger *et al.,* 2001). Other workers showed that

the mortality of cod embryos following exposure to UVB was suggested to have been caused by a direct interaction with DNA and stimulation of apoptotic pathways and also found that the eggs had a photo-repair mechanism, which could increase cod egg survival in UVB exposed groups (Kouwenberg *et al.*, 1999a).

In the past decade, interest has focused on the interaction of UVR and PAHs and the potential for these interactions to induce mutagenicity. UVA has not demonstrated mortality effects on its own (Béland *et al.*, 1999) but UVR has been shown to combine with other environmental factors that may result in additive or synergistic effects, which may or may not lead to detrimental results (Laycock *et al.*, 2000). PAHs can absorb UVR (Newsted & Giesy, 1987) and this results in a unique interaction that may on the one hand enhance their degradation but on the other may also increase their toxicity (Shemer & Linden, 2007; Weinstein *et al.* 1997). Degradation of PAHs is mainly via photolysis as PAHs absorb sunlight in the visible (400-760 nm) and ultraviolet (100-400 nm) regions of the electromagnetic spectrum. However, this absorption has led to growing evidence that at all but the most extreme exposures the real hazard from PAHs to aquatic organisms may be due to their photo-enhanced toxicity following exposure to the UV component of light rather than by any direct effect (Diamond *et al.*, 2003; Diamond *et al.*, 2006). Photo-enhanced toxicity has been demonstrated in a range of aquatic systems and has shown a variety of effects at the organism level, from acute skin lesions to carcinogenesis. For instance, photoinduced toxicity of sediment-associated PAHs was demonstrated with the marine amphipod *Rhepoxynius abronius*. Toxicity was explained through the photo-activation of pyrene and fluoranthene (Swartz *et al.*, 1997). The eyes

of teleost fish have shown sensitivity to a combination of PAH and UVR in laboratory trials which may lead to cataract formation (Laycock *et al.*, 2000). Weinstein *et al.* (1997) showed that in the absence of UVR, fluoranthene was not acutely toxic to juvenile fathead minnows (*Pimephales pomelas*) below its water solubility, but became toxic in the presence of artificial UVR. As a complement to this research, Weinstein and co-workers performed a histological examination of the gill lamellae, which revealed that the mode of action of photo-induced fluoranthene toxicity was a disruption of the mucosal cell membrane function and integrity, which eventually resulted in respiratory stress and death (Weinstein *et al.*, 1997). The general mechanism behind the phototoxicity of PAHs may be due to a photosensitisation mechanism whereby PAHs accumulate in membranes and generate ROS upon exposure to UVR causing membrane damage (Choi & Oris, 2000b; Zhang *et al.*, 2004). Studies at the cellular level have indicated that co-exposure to PAHs and UVR causes the formation of free-radicals and oxidative stress (Choi & Oris, 2000b; Liu *et al.*, 1998) although the nature of the radical species generated is uncertain (Zhang *et al.*, 2004).

4.1.1 Aims and Objectives

The aim of the work reported in this chapter was to investigate the effects of B(a)P, UVB and UVA and their interaction to two fish cell models: EPCA1 and RTG-2, under *in vitro* conditions.

The specific objectives were:

a) To investigate the cytotoxicity and genotoxicity of B(a)P in EPCA1 and RTG-2 cell lines with and without metabolic activation (S9) in the comet assay (DNA damage) and to use the Mn assay (chromosomal changes) to investigate the clastogenic and aneugenic effect of B(a)P.
b) To study the effects of UVB (EPCA1 and RTG-2) and UVA (RTG-2) irradiation on cell viability, DNA damage (comet assay) and chromosome damage/cell cycles (micronucleus assay). To compare the responses of the cell lines used.
c) To examine the cytotoxicity (NRR) and DNA damage (comet assay) of B(a)P followed by UVB or UVA in RTG-2 cells and to examine the potential interactive toxicity of B(a)P and UVA using the micronucleus (Mn) assay (RTG-2) to investigate chromosome damage or cell cycle changes. To explore whether oxidative stress is involved in the interaction between B(a)P and UVA (RTG-2) using ESR.

4.2 Materials and Methods

4.2.1 Cells and B(a)P Exposure Conditions

The EPCA1 and RTG-2 cell lines were cultured under the cell culture conditions set out in Chapter 2, Section 2.3. EPCA1 and RTG-2 cells at 70-80 % confluence were exposed to various concentrations of B(a)P (0.00, 0.05, 0.10, 0.32, 1.00 and 3.20 μg ml^{-1}) in medium containing 1 % FBS (prepared as stated in Chapter 2, Section 2.5.5). Metabolic activation of B(a)P was conducted as stated in Chapter 2, Section 2.5.6.

4.2.2 Assays of Cell Viability and Cytotoxicity

Dual staining and Annexin V-FITC apoptosis detection were conducted according to the method described in Chapter 2, Sections 2.4.2 and 2.4.3. Results were expressed as a percentage where applicable except in the pilot study with Annexin V-FITC apoptosis detection. This pilot study looked at a basic time course (2 h, 4 h and 6 h post irradiation) following irradiation with 50 J m^{-2} UVB and was taken because of the difficulties in preparing cells for the micronuclei assay following UVB irradiation (Section 4.2.6.2). The results are presented in Figure 4.5 (Section 4.3.2.4). The NRR assay was carried out as outlined in Chapter 2, Section 2.4.4 with the modification (because of the growth requirements of fish cells) that the initial incubation of EPCA1 and RTG-2 cells was carried out at 21 ± 1 °C in a humid atmosphere in 5 % CO_2 for 48 hours. EPCA1 and RTG-2 cells were treated with various concentrations (0.0, 0.1, 1.0 and 3.2 μg ml^{-1}) of B(a)P for 24 hours. Irradiation of the RTG-2 cells was conducted in

PBS to various doses of UVB (0*, 100 and 200 J m^{-2}) or UVA (0*, 500, 2000 and 4000 J m^{-2}) and the plates immediately transferred onto ice before processing with the NRR assay. For uptake of the neutral red, the plates were incubated for 3 hours at room temperature. Results were expressed as a percentage of the control (Babich *et al.*, 1988).

4.2.3 Comet Assay

Unless stated, viability for comet assay experiments was always over 90 % in accordance with the recommendations of Tice *et al.* (2000) as measured by trypan blue (Chapter 2, Section 2.4.1) (data not shown). The comet assay was conducted as stated in the protocol in Chapter 2, Sections 2.5.1 to 2.5.4 with the following modifications based on the optimisation results in Chapter 3, Section 3.3.3.1.2 and 3.3.3.1.3. For example, unwinding times for both EPCA1 and RTG-2 was 20 minutes, with 20 minutes electrophoresis. Replicate slides were made for each treatment condition, and experiments were conducted in duplicate at separate times.

For comet assay experiments using B(a)P, EPCA1 and RTG-2 cells at 70-80 % confluence were exposed to various concentrations (0.0, 0.1, 1.0 and 3.2 µg ml^{-1}) of B(a)P in medium (prepared as stated in Chapter 2, Section 2.5.5). The cells were incubated for 6 hours (with and without metabolic activation (Chapter 2, Section 2.5.6)) or 24 hours (without metabolic activation) at 21 ± 1 °C according to the recommendations of Tice *et al.* (2000) and then treated according to Chapter 2, Sections 2.5.2 to 2.5.4. For experiments using UVR, RTG-2 and EPCA1 cells were prepared onto slides for the comet assay and exposed to various doses of UVB (RTG-2: 0*, 25, 50, 75, 100, 200,

350 and 500 J m^{-2}, EPCA1: 0*, 200, 350 and 500 J m^{-2}) including a sham irradiated control (0* sham irradiated for the same time as 500 J m^{-2} UVB). RTG-2 cells were treated with various doses of UVA (0*, 500, 1000, 2000, 4000, 6000 or 8000 J m^{-2}) including a sham irradiated control (0* sham irradiated for the same time as 8000 J m^{-2} UVA). For treatments of interactive toxicity of B(a)P and UVR, RTG-2 cells at 70-80 % confluence were exposed to various concentrations (0.00, 0.05, 0.10, 0.32, 1.00 and 3.20 µg ml^{-1}) of B(a)P in medium for 24 hours (without metabolic activation) as detailed above. Following B(a)P treatment, cells were washed twice with PBS, trypsinised and resuspended in GM, before being prepared onto CometSlides™ and treated as detailed in Chapter 2, Section 2.5.1. Following this, RTG-2 cells were exposed to various doses of UVB (0*, 25, 50, 75, 100 and 200 J m^{-2}) or UVA (0*, 25, 50, 100 and 200 J m^{-2}) then immediately placed on ice. Both these included a sham irradiated control (0* sham irradiated for the same time as 200 J m^{-2} UVB or 200 J m^{-2} UVA respectively). Immediately following irradiation slides were transferred to chilled lysing solution (Section 2.5.1) and processed according to Chapter 2, Sections 2.5.2 to 2.5.4. The UVR sources used are detailed in Chapter 2, Section 2.7.

4.2.4 Micronucleus Assay

For all experiments, EPCA1 cells were seeded at a density of 1 x 10^6 cells ml^{-1} and RTG-2 cells were seeded at a density of 4 x 10^5 cells ml^{-1} in GM both in 25 cm^2 flasks and incubated at 21 ± 1 °C for 48 hours in 5 % CO_2. For experiments using B(a)P, B(a)P was added to the cell monolayers at various concentrations (EPCA1: 0.0, 0.1, 1.0 and 3.2 µg ml^{-1} and RTG-2: 0.00, 0.05, 0.10, 1.00 and 3.20 µg ml^{-1}) prepared in

medium as described in Chapter 2, Section 2.5.5 and the flasks incubated at 21 ± 1 °C for 48 ± 1 hours in 5 % CO_2. Experiments scored 1000 binucleate cells per treatment group, with two treatment groups; and the experiments were duplicated. For experiments using UVR, RTG-2 cells were seeded in GM at a density of 4 x 10^5 cells ml^{-1} in petri dishes in a 5 % CO_2 atmosphere for 48 hours and then were washed twice with PBS and treated with various doses of UVA (0*, 25, 50 and 100 J m^{-2}). For experiments involving interactive toxicity, RTG-2 cells were seeded in GM at a density of 4 x 10^5 cells ml^{-1} in petri dishes and incubated at 21 ± 1 °C for 48 hours in 5 % CO_2. Cells were washed twice with PBS and incubated with B(a)P (0.025 µg ml^{-1}) for 6 hours. Following this incubation period, the cells were washed twice with PBS and treated with various doses of UVA (0*, 25, 50 and 100 J m^{-2}). After the exposure period had elapsed, the medium was discarded and the monolayer washed twice with PBS. Cyto B (1.5 µg ml^{-1}) in solvent (DMSO) was added to the cells in growth medium and the flasks incubated at 21 ± 1 °C for 48 ± 1 hours in 5 % CO_2. Following the exposure periods the cells were then treated as Chapter 2, Sections 2.6.1, 2.6.2 and 2.6.2.1 for both Giemsa and anti-kinetochore staining respectively. The UVR source used is detailed in Chapter 2, Section 2.7.

4.2.5 ESR Measurements on B(a)P and UV Treated RTG-2 Cells

ESR measurements were made according to protocol in Chapter 2, Section 2.6.4.1. RTG-2 cells were pre-treated for 24 hours with B(a)P (3.2 µg ml^{-1}). Cells from each 25 ml culture flask were trypsinised and re-suspended in GM and the cell suspension was divided into two before being centrifuged at 800 rpm for 8 minutes. The cell pellet was

washed 3 times with PBS to remove serum and free B(a)P and the cell pellet from each half was re-suspended in 50 µl of 250 mM DMPO in PBS prior to irradiation (UVA: 500 J m^{-2}). The spin traps TMPol and POBN were both used at a concentration of 50 mM. The samples were then placed in the microwave cavity of the spectrometer and acquisition of spectra started within 1 minute of the end of irradiation (UVB: (Phillips, UK), UVA: (XX-40 FB, Spectroline, USA)) (Chapter 3, Section 3.3.6).

4.2.6 Statistics

Each experiment was performed twice and contained duplicate treatments. NRR data and comet assay data were collected from Excel and transferred into MINITAB software for statistical analysis. Non-parametric Mann-Whitney U-tests were performed on the data to compare the cell responses to the untreated controls. For micronucleus experiments, the results are presented as means (±SE) tables to show the data and statistical analysis was performed on the means. For all tests a significant difference was taken at a p-value of $p < 0.05$.

4.3 Results

4.3.1 The Effects of Benzo(a)Pyrene Alone on Fish Cell Lines (EPCA1, RTG-2)

4.3.1.1 Cytotoxicity Assays for Benzo(a)Pyrene Effects on Fish Cell Lines (EPCA1, RTG-2)

Trypan blue and dual staining viability assays were conducted as described in Chapter 2, Sections 2.4.1 and 2.4.2 respectively. The results showed over 90 % percentage cell viability in all control and B(a)P treated groups for both viability techniques for both the EPCA1 and RTG-2 cell lines (results not shown). The NRR assay was conducted as described in Chapter 2, Section 2.4.4, with the modifications described above in Section 4.2.4. The NRR investigation considered B(a)P cytotoxicity in EPCA1 and RTG-2 cells. After exposure of EPCA1 and RTG-2 cells to various B(a)P concentrations (0.0, 0.1, 1.0 and 3.2 μg ml^{-1}) for 24 hours the viability of the cells was examined using NRR. The results of this assay (Figure 4.1) revealed a reduction in cell viability to approximately 90 % for the EPCA1 cell line at a concentration of 3.2 μg ml^{-1}. Cell viability was reduced to approximately 65 % in the RTG-2 cell line at the highest concentration (3.2 μg ml^{-1}) from the raw data average neutral red absorbance of 0.624 (control) to 0.400 (3.2 μg ml^{-1}). However the differences observed in the EPCA1 cells were not significantly different ($p > 0.05$) between the control and all doses tested. Neither were those in the RTG-2 cells except when exposed to the highest dose of B(a)P ($p < 0.05$) between the control and 3.2 μg ml^{-1} B(a)P. A significant difference was observed between the observations with

EPCA1 and RTG-2 cells ($p < 0.001$). This suggests that RTG-2 cells exhibit a greater sensitivity to the effects of B(a)P than the EPCA1 cells in the NRR assay.

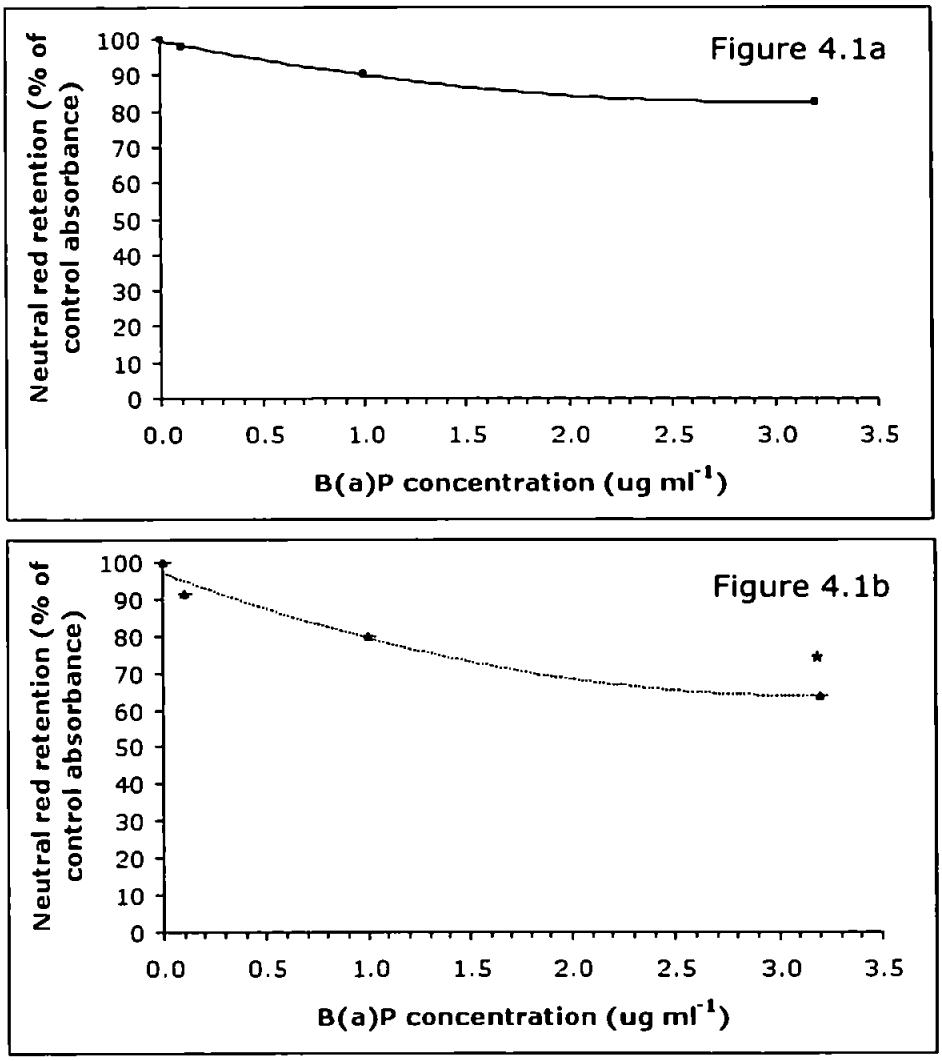

Figure 4.1 Cell viability assessed through the uptake of neutral red dye by EPCA1 (Figure 4.1a) and RTG-2 cells (Figure 4.1b) following exposure of cells to 24 hour B(a)P at various concentrations (0.0, 0.1, 1.0 and 3.2 μg ml^{-1}). Each data point represents 12 replicates for each variable. Cell viability is expressed as a percentage of the control (% control), with the control value being 100 %. Asterisk (*) indicates a significant difference from the control in RTG-2 cells ($p < 0.05$).

4.3.1.2 The Comet Assay for Benzo(a)Pyrene Effects on Fish Cell Lines (EPCA1, RTG-2)

The comet assay was used to investigate the effect of various concentrations of B(a)P (0.0, 0.1, 1.0 and 3.2 μg ml^{-1}) on DNA damage in EPCA1 and RTG-2 cells. DNA damage was measured by % Tail DNA migrated. Due to the indirect action of this compound (e.g. B(a)P requires enzymatic activity to be converted to reactive electrophilic metabolites (Section 1.2.1)) an exogenous metabolic agent (S9) was used in conjunction with some of the B(a)P exposures, up to recommended exposure times (Tice *et al.*, 2000). EPCA1 and RTG-2 cells were treated for 6 hours (with or without metabolic activation (S9)), or 24 hours (without S9).

4.3.1.2.1 The Comet Assay for Benzo(a)Pyrene Effects on the EPCA1 Cell Line

In EPCA1 cells, the results showed that there was a significant increase in DNA damage ($p < 0.001$) between the control and all exposures for B(a)P with and without S9 activation for both the 6 hour (Figures 4.2a and 4.2b) and 24 hour (Figure 4.2c) treatments. However, EPCA1 cells treated for 6 hours with B(a)P used in conjunction with S9 showed greater DNA damage than cells treated with B(a)P without S9. Cells treated with B(a)P (without S9) showed DNA damage that ranged up to 25 % tail DNA, whilst B(a)P treated cells (with S9) showed DNA damage that ranged up to approximately 45 %. EPCA1 cells treated with B(a)P for 6 hours in combination with S9 had no significant difference between the tested concentrations ($p > 0.05$) whilst those cells treated with B(a)P without the addition of S9, showed a

significant increase in DNA damage as B(a)P concentration increased ($p < 0.05$). Cells treated with B(a)P and S9 gave significantly higher DNA damage than those cells treated with B(a)P without S9 at the same concentrations ($p < 0.001$). When EPCA1 cells were treated with B(a)P for 24 hours (without S9), the results gave a clear response to B(a)P that was significantly different from the control value ($p < 0.001$) and increased DNA damage was significantly related to an increase in the B(a)P concentration ($p < 0.001$). Values here ranged from to 45 % for the highest concentration of B(a)P used (3.2 μg ml^{-1}).

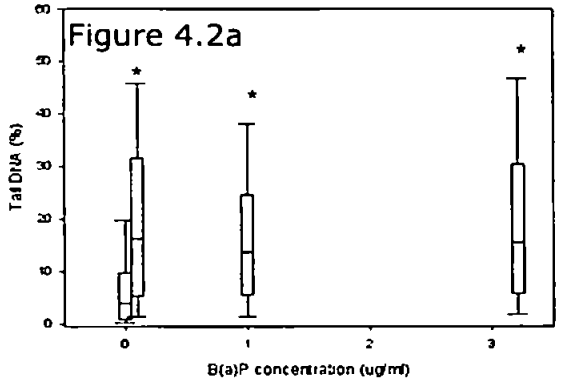

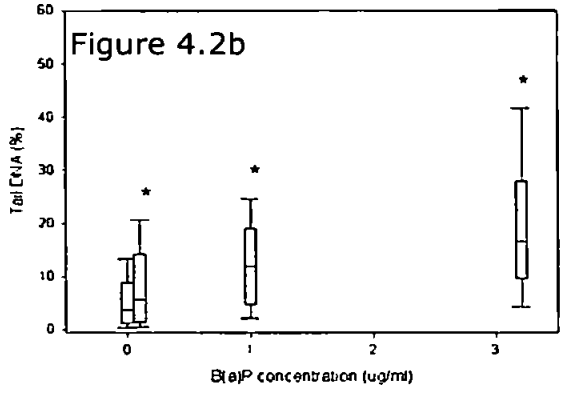

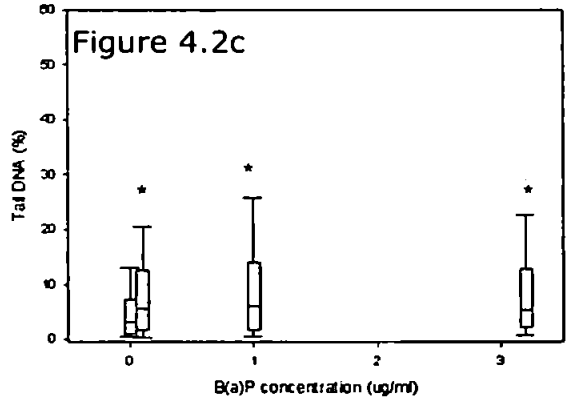

Figure 4.2 DNA damage to EPCA1 cells following exposure to 6 hour B(a)P at various concentrations (0.0, 0.1, 1.0 and 3.2 μg ml^{-1}) without (Figure 4.2a) exogenous metabolic activation (S9), with S9 (Figure 4.2b) or following exposure to 24 hour B(a)P (0.0, 0.1, 1.0 and 3.2 μg ml^{-1}) without S9 (Figure 4.2c). DNA damage is assessed by the Tail DNA (%). (Data marked with *(all concentrations) are significantly different to the control at $p < 0.0001$).

4.3.1.2.2 The Comet Assay for Benzo(a)pyrene Effects on the RTG-2 Cell Line

In RTG-2 cells, the results showed that there was a significant difference in observable % Tail DNA between the control and all exposures for B(a)P concentrations for both the 6 hour (with and without S9 activation) (Figures 4.3a and 4.3b respectively) and 24 hour (without S9) ($p < 0.0001$) (Figure 4.3c) treatments. RTG-2 cells treated for 6 hours with B(a)P (without S9) showed a relatively weak response with all concentrations which was significantly different from the control ($p < 0.0001$). There was a range of DNA damage from 10 % (0.0 μg ml^{-1}) to up to 30 % (1.0 μg ml^{-1}) and DNA damage reached a maximum of 22 % at the highest concentration tested (3.2 μg ml^{-1}). However, when B(a)P was used in conjunction with S9 the results gave a clearly higher dose response (which was significantly higher at each concentration than B(a)P without S9 ($p < 0.001$)), with all tested concentrations being significantly different from the control ($p < 0.0001$). A range of maximal DNA damage from 30 % (0.1 μg ml^{-1}) up to 90 % (3.2 μg ml^{-1}) was observed with B(a)P plus S9. RTG-2 cells treated with B(a)P for 24 hours (without S9) again showed a clear and significant increase in DNA damage ($p < 0.001$). These results (24 hours) gave significantly higher DNA damage than those observed for 6 hours (without S9) at all doses ($p < 0.001$) except 0.1 μg ml^{-1} B(a)P ($p > 0.05$). However, these results (24 hours) were of a significantly lower magnitude of DNA damage than those observed in cells treated with B(a)P and S9 for 6 hours ($p < 0.05$). Values here ranged from a maximum of 15 % at the lowest concentration used (0.1 μg ml^{-1}), through 30 % (1.0 μg ml^{-1}), to plateau at 35 % for the highest concentration used (3.2 μg ml^{-1}).

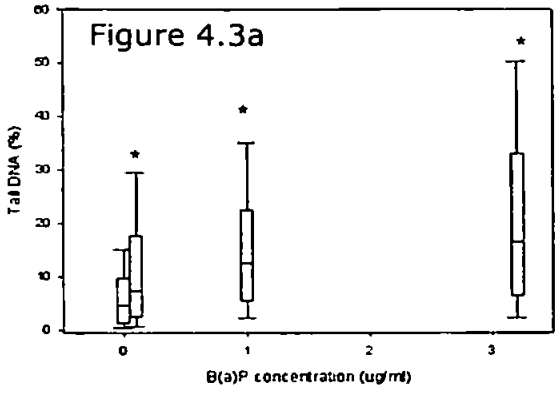

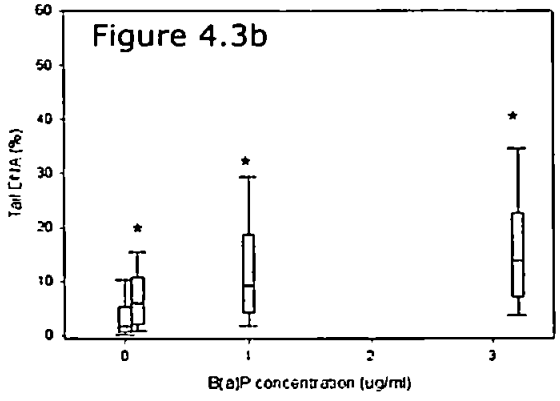

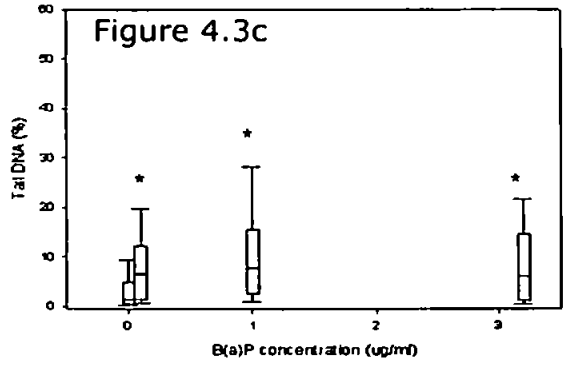

Figure 4.3 DNA damage to EPCA1 cells following exposure to 6 hour B(a)P at various concentrations (0.0, 0.1, 1.0 and 3.2 μg ml^{-1}) without (Figure 4.3a) exogenous metabolic activation (S9), with S9 (Figure 4.3b) or following exposure to 24 hour B(a)P (0.0, 0.1, 1.0 and 3.2 μg ml^{-1}) without S9 (Figure 4.3c). DNA damage is assessed by the Tail DNA (%). (Data marked with *(all concentrations) are significantly different to the control at $p < 0.0001$).

4.3.1.3 The Micronucleus Assay for Benzo(a)pyrene Effects on Fish Cell Lines (EPCA1, RTG-2)

4.3.1.3.1 The Micronucleus Assay for Benzo(a)pyrene Effects on EPCA1 Cells

EPCA1 cells were exposed to various concentrations of B(a)P (0.0, 0.1, 1.0 and 3.2 μg ml^{-1}) for 24 hours. The results for EPCA1 cells are presented in Table 4.1 and 4.2. Results using Giemsa stain show that the numbers of mononucleate cells varied slightly within a scoring protocol of 1000 binucleate cells, increasing from 96 ± 8.49 (0.0 μg ml^{-1} B(a)P) to 133.5 ± 16.26 (1.0 μg ml^{-1} B(a)P). Numbers of mononucleate cells did not appear to vary much between doses from 113 ± 26.87 (0.0 μg ml^{-1} B(a)P) to 131.5 ± 4.95 in the highest concentration of B(a)P used (3.2 μg ml^{-1} B(a)P) which was not a significant difference ($p > 0.05$). Micronuclei were manually scored in 1000 binucleate cells following recommended scoring procedures for this assay (Surrales *et al.,* 1994) and indicated a weak linear increase in the number of micronuclei as the concentration of B(a)P increased from 7.0 ± 2.83 (1.0 μg ml^{-1} B(a)P) to 9.5 ± 2.12 (3.2 μg ml^{-1} B(a)P) which were significantly different from the control in all experimental concentrations of B(a)P ($p < 0.05$). There were no nucleoplasmic bridges (NPB), multinucleated cells, or cases of multiple micronuclei observed for all the experimental doses.

Following these experiments with Giemsa, the use of anti-kinetochore stain was employed to further investigate the action of B(a)P on the EPCA1 cell line (Table 4.2). Again, it was possible to score 1000 binucleate cells and the numbers of mononucleate cells displayed a

greater increase than with Giemsa staining, from 111.5 ± 13.44 (0.0 μg ml^{-1} B(a)P) to 234.5 ± 40.31 (3.2 μg ml^{-1} B(a)P) which was significantly different ($p < 0.05$). As before using Giemsa stain, no NPB were observed in this cell line at these doses tested.

Micronuclei were detected by a significant increase ($p < 0.05$) in both mononucleate and binucleate cells, with the majority of K+ micronuclei detected within a binucleate cell, giving a strong positive response ($p < 0.05$). Micronuclei ranged from 5.5 ± 0.71 (0.1 μg ml^{-1} B(a)P), although the largest total frequency of micronuclei observed within binucleate cells was 22 ± 0.00 (3.2 μg ml^{-1} B(a)P) that was significantly different from the control ($p < 0.05$). These frequencies were significantly higher ($p < 0.05$) than observed in the control group (1.5 ± 0.71). A much lower frequency of micronuclei was detected within mononucleate cells (maximum of 2 ± 1.41 in the concentration 1.0 μg ml^{-1} B(a)P), this response was barely above the baseline level seen in the controls (0.0 ± 0.00) and was not a significant increase ($p > 0.05$). Of the binucleate and mononucleate cells containing a micronucleus, a larger proportion of micronuclei were located in the B(a)P treated cells within a binucleate cell and of the micronuclei detected within a binucleate cell, 14 ± 2.83 (3.2 μg ml^{-1} B(a)P) were K+ micronuclei, indicating a strongly aneugenic mode of action. However, as micronuclei were also detected with kinetochore negative (K-) signals, it would suggest that B(a)P acts on these cells in both a clastogenic and aneugenic way.

Table 4.1 Effect of B(a)P on the mean generation of micronuclei (±SE) in the EPCA1 cell line using Giemsa or anti-kinetochore stain (n=27,383). No nucleoplasmic bridges, incidences of 2, 3 or 4+ nuclei or multinucleated cells were observed. Significant differences (Mann Whitney U-test $p<0.05$) for each cellular response from the control are indicated (*).

[B(a)P] (μg ml^{-1})	0.0	0.1	1.0	3.2
Cellular Response–Giemsa Stain				
Mononucleate	96.0 ± 8.49	113.0 ± 26.87	133.5 ± 16.26	131.5 ± 4.95
Binucleate	1000.0 ± 0.00	1000.0 ± 0.00	1000.0 ± 0.00	1000.0 ± 0.00
Micronucleus/Binucleate	Not observed	7.0 ± 2.83*	7.5 ± 2.12*	9.5 ± 2.12*
Cellular Response–Antikinetochore stain				
Mononucleate	111.5 ± 13.44	140.5 ± 17.68	189.0 ± 22.63	234.5 ± 40.31*
Binucleate	1000.0 ± 0.00	1000.0 ± 0.00	1000.0 ± 0.00	1000.0 ± 0.00
Micronucleus/Mononucleate	Not observed	0.5 ± 0.71	1.5 ± 0.71	2.0 ± 1.41
Micronucleus/Binucleate	1.5 ± 0.71	5.5 ± 0.71*	14.5 ± 6.36*	22.0 ± 0.00*
K+ Mononucleate cells	Not observed	0.5 ± 0.71	1.0 ± 1.41	1.5 ± 0.71
K- Mononucleate cells	Not observed	Not observed	0.5 ± 0.71	0.5 ± 0.71
K+ Binucleate cells	Not observed	4.0 ± 1.41	10.5 ± 0.71	14.0 ± 2.83
K- Binucleate cells	1.5 ± 0.71	1.5 ± 2.12	4.0 ± 5.66	8.0 ± 2.83

4.3.1.3.2 The Micronucleus Assay for Benzo(a)pyrene Effects on RTG-2 Cells

RTG-2 cells were exposed to various concentrations of B(a)P (0.00, 0.05, 0.10, 1.00 and 3.20 μg ml^{-1}) for 24 hours and the Mn assay conducted to potential genomic instability produced. The effects of B(a)P on micronucleus formation were investigated using the two different staining techniques (Giemsa and anti-kinetochore). The results for RTG-2 cells are presented in Table 4.2. Results using the Giemsa stain show that within a scoring protocol of 1000 binucleate cells numbers of mononucleate cells varied widely, increasing from 120 ± 5.66 (0.05 μg ml^{-1} B(a)P) to 445 ± 65.05 (3.2 μg ml^{-1} B(a)P) which was a significant difference ($p < 0.05$) in all concentrations except between the control and 0.05 μg ml^{-1} B(a)P ($p > 0.05$). Micronuclei were scored in 1000 binucleate cells and indicated a significant ($p < 0.05$) increase from base levels in the number of micronuclei as the concentration of B(a)P increased, from 7.0 ± 1.41 (0.1 μg ml^{-1} B(a)P) to 14 ± 5.66 (3.2 μg ml^{-1} B(a)P). However there was no significant increase in micronuclei induction following treatment with 0.05 μg ml^{-1} B(a)P ($p > 0.05$). There were no nucleoplasmic bridges (NPB) or cases of multiple micronuclei observed throughout these experimental doses. However, multinucleate cells were detected at two treatment doses (1.0 μg ml^{-1} (not a significant increase $p > 0.05$) and 3.2 μg ml^{-1} B(a)P) to a maximum detected frequency of 2.5 ± 0.71 (3.2 μg ml^{-1} B(a)P) which was a significant increase ($p < 0.05$).

Following these experiments with Giemsa, the use of anti-kinetochore stain was employed to further investigate the action of B(a)P on the RTG-2 cell line. Again, it was possible to score 1000 binucleate cells

and the numbers of mononucleate cells observed displayed a smaller range than with Giemsa staining, from 114.5 ± 24.75 (0.0 μg ml^{-1} B(a)P) to 197 ± 2.83 (3.2 μg ml^{-1} B(a)P) although this did increase with B(a)P exposure in comparison with the control group ($p < 0.05$) except for exposure to 0.05 μg ml^{-1} B(a)P ($p > 0.05$). As before using Giemsa stain, no NPB were observed in this cell line at these doses tested. With anti-kinetochore staining, micronuclei were detected in both mononucleate and binucleate cells, with the majority of micronuclei detected within a binucleate cell, giving a strong dose-response (increasing number with increasing B(a)P concentration) which was a significant increase ($p < 0.05$). Micronuclei ranged from 1.5 ± 0.71 (0.05 μg ml^{-1} B(a)P), with no significant increase ($p > 0.05$) at the lowest dose of B(a)P tested (0.05 μg ml^{-1}) although the largest frequency of micronuclei observed within binucleate cells was 29 ± 11.31 (3.2 μg ml^{-1} B(a)P). These frequencies were significantly higher ($p < 0.05$) than observed in the control group (1.5 ± 0.75). A much lower and insignificant ($p > 0.05$) frequency of micronuclei was detected within mononucleate cells (0.5 ± 0.71 with the concentration 3.2 μg ml^{-1} B(a)P). This response was barely above the baseline level seen in the control (no micronuclei observed). Of the binucleate and mononucleate cells containing micronuclei, the vast majority of micronuclei were located in the B(a)P treated groups and contained a K+ signal located within a binucleate cell; of the micronuclei detected within a binucleate cell, 27 ± 8.49 (3.2 μg ml^{-1} B(a)P) were K+ micronuclei ($p < 0.05$), indicating a strongly aneugenic mode of action. However, as significant micronuclei (1.0 and 3.2 μg ml^{-1} B(a)P $p < 0.05$) were also detected with K- signals, it would suggest that B(a)P acts on these cells in both a clastogenic and aneugenic way.

Table 4.2 Effect of various doses of B(a)P on the mean generation (±SE) of micronuclei in the RTG-2 cell line using Giemsa or anti-kinetochore stain (n=30,849). There were no incidences of nucleoplasmic bridges, K- mononucleated cells or 2, 3 or 4+ nuclei observed. Significant increases (Mann-Whitney *U* test $p<0.05$) in cellular responses from the control are indicated (*).

[B(a)P] (μg ml^{-1})	0.00	0.05	0.10	1.00	3.20
Cellular Response - Giemsa					
Mononucleate	159.5 ± 10.61	120.0 ± 5.66	139.5 ± 50.20*	322.0 ± 33.94*	445.0 ± 65.05*
Binucleate	1000.0 ± 0.00	1000.0 ± 0.00	1000.0 ± 0.00	1000.0 ± 0.00	1000.0 ± 0.00
Micronucleus/Binucleate	Not observed	Not observed	7.0 ± 1.41*	5.0 ± 1.41*	14.0 ± 5.66*
Multinucleate cells	Not observed	Not observed	Not observed	1.0 ± 1.41	2.5 ± 0.71*
Cellular Response – Anti-kinetochore stain					
Mononucleate	114.5 ± 24.75	165.0 ± 31.11	131.5 ± 13.44*	144.0 ± 2.83*	197.0 ± 2.83*
Binucleate	1000.0 ± 0.00	1000.0 ± 0.00	1000.0 ± 0.00	1000.0 ± 0.00	1000.0 ± 0.00
Micronucleus/Mononucleate	Not observed	Not observed	Not observed	Not observed	0.5 ± 0.71
Micronucleus/Binucleate	1.5 ± 0.75	1.5 ± 0.71	7.0 ± 2.83*	14.5 ± 0.71*	29.0 ± 11.31*
K+ Mononucleate cells	Not observed	Not observed	Not observed	Not observed	0.5 ± 0.71
K+ Binucleate cells	Not observed	1.0 ± 0.00	2.0 ± 1.41	14.5 ± 0.71*	27.0 ± 8.49*
K- Binucleate cells	1.5 ± 0.75	0.5 ± 0.71	5.0 ± 4.24*	Not observed	2.0 ± 2.83*

In summary, the experiments with B(a)P showed that DNA damage was induced in both EPCA1 and RTG-2 cells shown by the comet assay and the Mn assay. Cell viability was > 90 % in all control groups and experimental concentrations of B(a)P for both cell lines using dual staining and trypan blue. However, B(a)P showed a significant increase in cytotoxic response (NRR) at the highest concentration tested (3.2 μg ml^{-1} B(a)P) in the RTG-2 cells only. The RTG-2 cells gave a significantly higher response in cytotoxicity than the EPCA1 cells in the NRR assay ($p < 0.001$).

Data obtained through use of the comet assay showed that a significant increase in DNA damage was induced through exposure to B(a)P in comparison with the control groups for cells treated both with and without exogenous metabolic action (S9) and for 24 hours treatment with B(a)P. There was no significant increase ($p > 0.05$) in DNA damage for B(a)P used without S9 at the same concentrations between EPCA1 and RTG-2 cells except at 1.0 μg ml^{-1} B(a)P ($p < 0.05$). When cells were treated with B(a)P and S9 DNA damage in EPCA1 cells was significantly higher from RTG-2 cells at the concentration 0.1 μg ml^{-1} B(a)P ($p < 0.05$) but not between the other concentrations tested ($p > 0.05$). With 24 hours exposure to B(a)P, EPCA1 cells gave significantly higher DNA damage only at the concentration 3.2 μg ml^{-1} B(a)P ($p < 0.01$) but not between the other concentrations ($p > 0.05$). These data suggest no broad differences in DNA damage between the cell lines tested here following treatment with B(a)P.

Additionally, experiments using the micronucleus assay showed significant increases in micronuclei frequencies and suggested that the action of B(a)P was due to both aneugenic and clastogenic

mechanisms (Mn assay) in both the fish cell lines due to the significant generation of both K+ and K- micronuclei respectively (Tables 4.2 and 4.4). There was no significant difference ($p > 0.05$) between the cell lines tested for any of the parameters except the RTG-2 cells showed significantly higher generation of mononucleate cells than EPCA1 using Giemsa staining at concentrations 1.0 and 3.2 μg ml^{-1} B(a)P ($p < 0.05$). These data suggest that RTG-2 cells are more sensitive than EPCA1 cells in the NRR assay possibly due to differences in lysosomal membrane stability (Section 2.4.5).

4.3.2 The Effects of Solar Radiation (UVR) Alone on Fish Cell Lines EPCA1 and RTG-2

4.3.2.1 Cytotoxicity Assays for UVB Effects on the Fish Cell Lines EPCA1 and RTG-2

The effects of UVB on cell viability and cytotoxicity were assessed in EPCA1 and RTG-2 cells. Cell viability was initially assessed with trypan blue dye and the dual stain fluorescence dye. In RTG-2 cells, trypan blue results showed no loss in cell viability (viability > 98 %) up to 500 J m^{-2} UVB after which cell viability was reduced to 75 % at both 625 and 750 J m^{-2} UVB. Cell viability dropped to 40 % at a dose of 1000 J m^{-2} UVB (Figure 4.4a). In EPCA1 cells, trypan blue results showed cell viability remained above 90 % at 625 J m^{-2} UVB, which dropped down to 33 % at 1000 J m^{-2} UVB (Figure 4.4a). There was no significant difference between the responses of the two cell lines in this assay ($p > 0.05$). For RTG-2 cells, dual stain fluorescence was also used to investigate cell viability. Results showed a decrease in cell viability from 94 % at 0* J m^{-2} UVB to 1 % viability at 1000 J m^{-2} UVB. Cell

viability was reduced to approximately 59 % at 625 J m^{-2} UVB (Figure 4.4b). For EPCA1 cells, dual stain fluorescence showed cell viability remained over 94 % at 500 J m^{-2} UVB, dropping down to 34.5 % at the highest UVB dose of 1000 J m^{-2} (Figure 4.4b). There was a significant difference between the responses of the two cell lines in this assay with doses > 500 J m^{-2} UVB ($p < 0.05$). Cytotoxicity was also investigated through the NRR assay (Figure 4.4c). After exposure of EPCA1 and RTG-2 cells to various UVB doses (0*, 200, 500, 625, 750, 875 and 1000 J m^{-2}), the viability of the cells was analysed. In EPCA1 cells, the results indicate significant differences between the sham irradiated control (0*) and all doses tested ($p < 0.05$). In RTG-2 cells, there was no significant difference between the control and 200, 500 J m^{-2} ($p > 0.05$), whilst in doses of 625 to 1000 J m^{-2} UVB, cell viability was reduced significantly ($p < 0.001$). Additionally there was no significant difference ($p > 0.05$) between the results from the two cell lines for the same doses (200 and 500 J m^{-2} UVB suggesting that RTG-2 cells are more sensitive than EPCA1 cells at UVB doses greater than 500 J m^{-2} (Section 4.3.1.1). Trypan blue, dual stain fluorescence and NRR results for EPCA1 and RTG-2 cells are presented in Figure 4.4. The pilot study using Annexin V to investigate apoptosis looked at a basic time course (2, 4 and 6 hours post irradiation) following irradiation with 50 J m^{-2} UVB. The results are presented in Figure 4.5 and suggest that apoptosis is occurring within 6 hours.

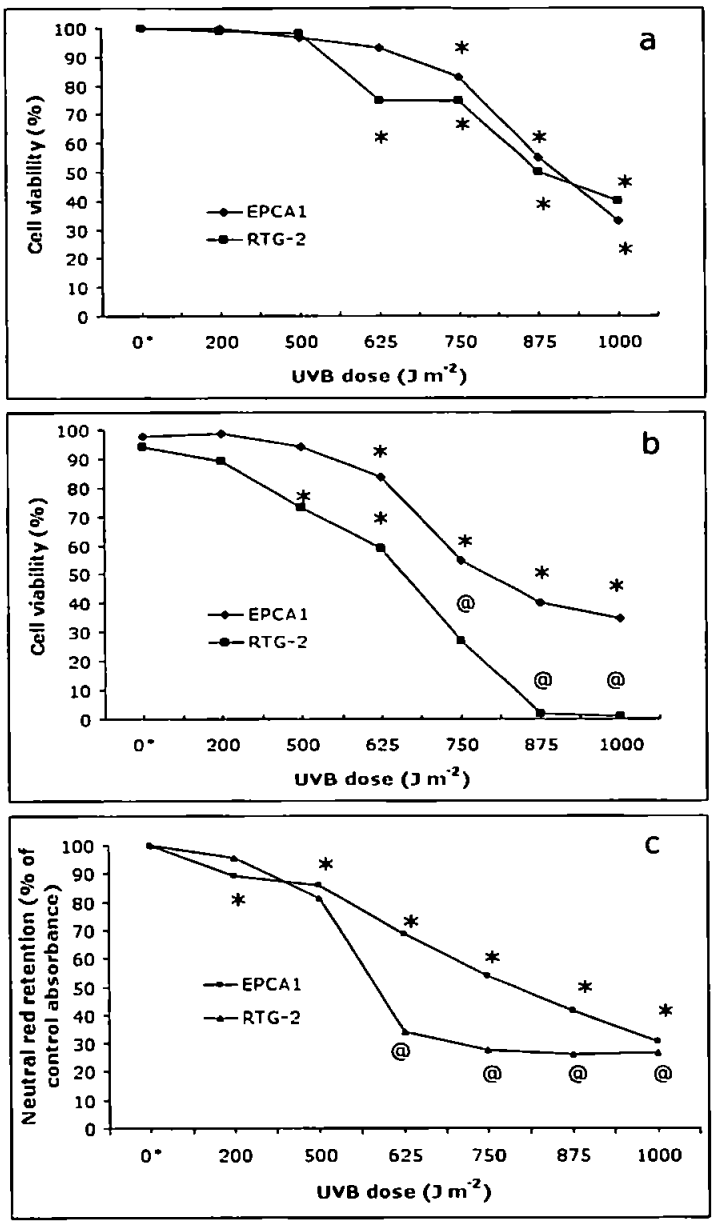

Figure 4.4 Cell viability assessed through (a) trypan blue, (b) dual stain fluorescence or (c) NRR in EPCA1 and RTG-2 cells following exposure to UVB (0*, 200, 500, 625, 750, 875, 1000 J m^{-2}). Cell viability is expressed as percentage viability (%) (trypan blue and dual stain fluorescence) or as a percentage of the control absorbance (NRR) (control values are 100 %). Significant difference (Mann-Whitney U-test) from the control is indicated by * ($p < 0.05$) or @ ($p < 0.001$). Results are from replicate studies.

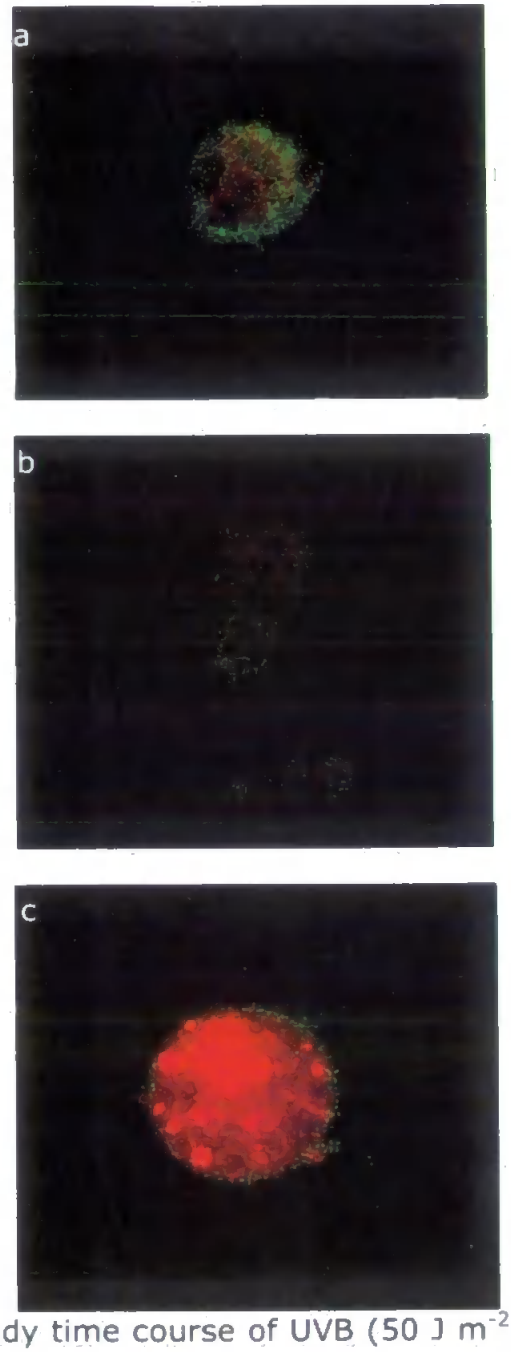

Figure 4.5 Pilot study time course of UVB (50 J m^{-2} UVB). (a) 2 hours post irradiation (b) 4 hours post irradiation and (c) 6 hours post irradiation with Annexin V using RTG-2 cells to identify apoptosis or necrosis. The figure illustrates the onset of apoptosis at 6 hours post irradiation due to the red colouration.

4.3.2.2 Cytotoxicity Assays for UVA Effects on a Fish Cell Line (RTG-2)

Cell viability and the cytotoxicity of various doses of UVA (0*, 500, 2000 and 4000 J m^{-2}) were tested with trypan blue, dual stain fluorescence and NRR assays in RTG-2 cells. Results with trypan blue and dual staining were over 98 % viability at all doses for both cell types and are not presented here. Using the NRR assay, RTG-2 showed a cytotoxic response at 2000 J m^{-2} and 4000 J m^{-2} UV A ($p < 0.05$). Results for RTG-2 cells are presented in Figure 4.6.

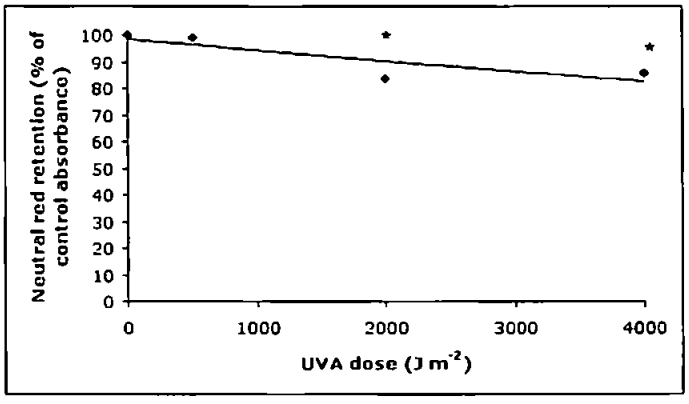

Figure 4.6 Cell viability assessed through the uptake of neutral red dye by RTG-2 cells following exposure of cells to various doses of UVA (0*, 500, 2000 and 4000 J m^{-2}). Cell viability is expressed as a percentage of the control absorbance, with the control value being 100 %. Significant difference (Mann-Whitney U-test) from the control indicated by (*) in RTG-2 cells ($p < 0.05$).

4.3.2.3 The Comet Assay for UVR effects on Fish Cell Lines (EPCA1, RTG-2)

4.3.2.3.1 Comet Assay for UVB Effects with the EPCA1 Cell Line

The effect of various doses of UVB (0*, 200, 350 and 500 J m^{-2}) on the EPCA1 cell line was investigated using the comet assay. The doses were selected to investigate the less cytotoxic doses (less than 500 J m^{-2}) as measured through trypan blue, dual stain fluorescence and NRR assay (Section 4.3.2.1). The comet assay experiments showed a significant effect ($p < 0.0001$) between the sham irradiated control (0*) and all UVB doses tested (200, 350 and 500 J m^{-2}). A significant ($p < 0.0001$) increase was initially observed between 0* J m^{-2} and 200 and 350 J m^{-2} (Figure 4.7). The comet assay response dropped off at the highest dose tested (500 J m^{-2}) suggesting a loss of sensitivity in the assay at this dose due to excessive DNA damage.

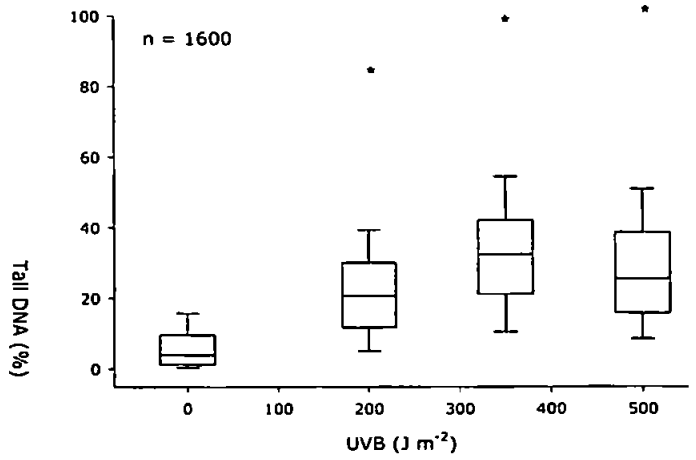

Figure 4.7 DNA damage to EPCA1 cells (n=1600) following exposure to various doses of UVB (0*, 200, 350 and 500 J m^{-2}). DNA damage was assessed by the Tail DNA (%). All UVB doses were significantly different (*) to the control (Mann-Whitney U-test $p < 0.0001$). N.B. control (0.0*) was sham irradiated for the same time period as 500 J m^{-2}.

4.3.2.3.2 Comet assay for UVB/UVA effects with the RTG-2 cell line

The effect of various doses of UVB (0*, 200, 350 and 500 J m^{-2}) or UVA (0*, 500, 1000, 2000, 4000, 6000 and 8000 J m^{-2}) on the RTG-2 cell line was investigated using the comet assay. The UVB doses were selected to investigate the lower less cytotoxic doses (less than 500 J m^{-2} UVB) as measured through trypan blue, dual stain fluorescence and NRR assay in Section 4.3.2.1. The comet assays showed a significant effect ($p < 0.0001$) between the sham irradiated control (0*) and all UVB doses tested (0*, 200, 350 and 500 J m^{-2}) (Figure 4.8a). There was no clear dose response shown, with a strong increase in DNA damage shown initially between 0 J m^{-2} and 200 J m^{-2} ($p < 0.0001$) which then appeared to steadily plateau at a median value of approximately 35 % and is probably due to a loss of sensitivity in this assay at these doses. Due to this plateau response to UVB, the dose was dropped to investigate DNA damage in RTG-2 cells at UVB doses lower then 200 J m^{-2} (Figure 4.8b). These results clearly demonstrate the steady response of the cells from increasing the UVB dose from 0* J m^{-2} through to 100 J m^{-2}. At 200 J m^{-2} the comet assay response is greatly reduced, again suggesting a lack of sensitivity in the comet assay due to greatly enhanced DNA damage beyond the detection range of the assay. Results indicate a significant increase in DNA damage from the control to 25, 50, 75 and 100 J m^{-2} UVB ($p < 0.0001$). Additionally, there was no significant difference in response between the EPCA1 and RTG-2 cell lines following UVB irradiation ($p < 0.001$) suggesting a similar response between the two cell types to this insult. This is consistent with the results obtained in Section 4.3.2.1. (Figure 4.4) which shows no significant difference between the cell lines at doses 200 and 500 J m^{-2} UVB.

Figure 4.8a

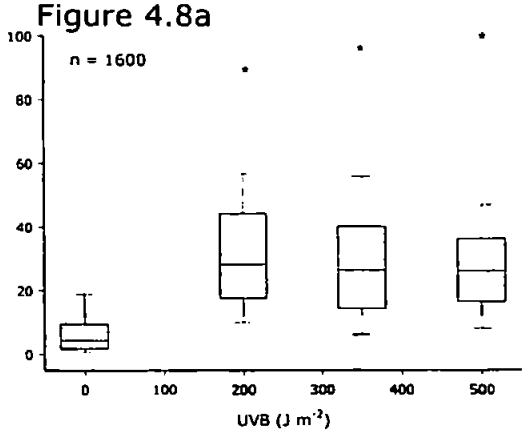

Figure 4.8b

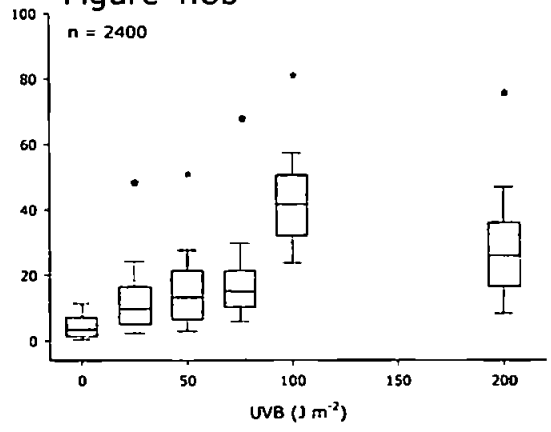

Figure 4.8 DNA damage to RTG-2 cells following exposure to various doses of UVB (0*, 200, 350 and 500 J m^{-2}) (Figure 4.8a) or (0*, 25, 50, 75, 100 and 200 J m^{-2}) (Figure 4.8b). DNA damage was assessed by the Tail DNA (%). All UVB doses tested were significantly different (*) to the control (Mann-Whitney U-test, $p < 0.0001$). N.B. control (0*) was sham irradiated for the same time period as 500 J m^{-2} (Figure 4.8a) or 200 J m^{-2} (Figure 4.8b).

With UVA, no significant effect (Mann-Whitney U-test, $p > 0.05$) was shown between the sham irradiated control (0*) and all UVA doses tested (500, 1000, 2000, 4000, 6000 and 8000 J m^{-2}). There was no clear dose response in median DNA damage shown; however there is a wide range of DNA damage indicated by the outliers (Figure 4.9).

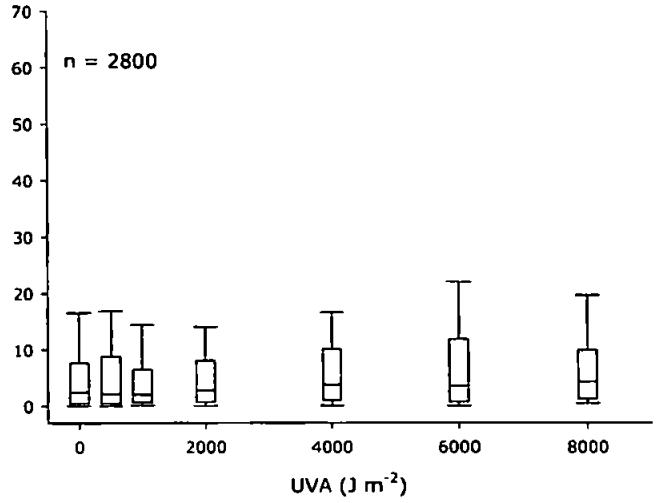

Figure 4.9 DNA damage to RTG-2 cells following exposure to various doses of UVA (500, 1000, 2000, 4000, 6000 and 8000 J m^{-2}). DNA damage was assessed by the percentage tail DNA (Tail DNA %) migrated. No UVA doses tested caused DNA damage that was significantly different to the control (Mann-Whitney U-test, $p > 0.05$). N.B. control (0*) was sham irradiated for the same time period as 8000 J m^{-2}.

4.3.2.4 The Micronucleus Assay for UVA Effects on RTG-2 Cells

There was no significant difference shown (Mann-Whitney U-test, $p > 0.05$) between the EPCA1 and RTG-2 cell lines for NRR assay (Chapter 3, Section 3.3.2), comet assay response with EMS (Chapter 3, Section 3.3.4.2), NRR assay with doses ≤ 500 J m^{-2} UVB (although RTG-2 showed a significantly more sensitive response with doses greater than 500 J m^{-2} UVB) (Section 4.3.2.1) or the comet assay with UVB (Section 4.3.2.3). Therefore only the larger RTG-2 cells were used for investigation of UVA with the Mn assay which is also in agreement with the wide use of this cell line in ecogenotoxicological testing (Chapter 3, Table 3.13). Various doses of UVA (0*, 25, 50, 100 and 200 J m^{-2}) were tested in RTG-2 cells to investigate the effects of UVA by means of the micronucleus assay. The control (0*) was sham irradiated for

the same time as 200 J m^{-2} UVA. The effects of UVA on micronucleus formation were investigated using two staining techniques (Giemsa and anti-kinetochore) to investigate the potential mechanisms of action (clastogenic or aneugenic, respectively) following UVA exposure. Experiments scored 1000 binucleate cells per treatment group where possible, and the experiments were duplicated. The results for RTG-2 cells are presented in Table 4.3. At a dose of 0* J m^{-2} UVA it was possible to retain the standard protocol employed for the previous micronucleus experiments by counting micronuclei within 1000 binucleate cells (1000 ± 0.00 J m^{-2}). However, as UVA doses were introduced, the frequencies of mononucleate cells observed increased compared to the control. Hence it was decided to count a total of 1000 binucleate and mononucleate cells in order to investigate the ratio of the two cell types to each other (and therefore if there were any significant differences), and to be able to detect as many micronuclei as possible in both mononucleate and binucleate cells (Fenech *et al.,* 2003a; Fenech *et al.,* 2003b; Rosefort *et al.,* 2004) (expanded in Section 4.4.2). The results using Giemsa stain show that numbers of mononucleate cells vary widely within a scoring protocol of a total of 1000 binucleate and mononucleate cells, ranging from 200.5 ± 31.82 (0.00 J m^{-2}) to 451.5 ± 16.34 (200 J m^{-2}) which was a significant difference ($p < 0.05$). The numbers of binucleate cells scored also varied with the addition of UVA, from 621 ± 29.70 (25 J m^{-2}) to 751.5 ± 17.25 (50 J m^{-2}). These doses were significantly different from each other ($p < 0.05$) except between 50 and 100 J m^{-2} UVA ($p > 0.05$). Micronuclei were scored in mononucleate and binucleate cells and indicate a strong dose-responsive increase in the total micronuclei induced ($p < 0.05$). The number of micronuclei in mononucleate cells increased as the UVA dose increased and were

significantly different from the control ($p < 0.05$) and each other ($p < 0.05$) except for between 100 and 200 J m^{-2} UVA ($p > 0.05$). Micronuclei were detected in mononucleate cells in the highest frequency (10.50 ± 1.91) at the highest dose used (200 J m^{-2}). In binucleate cells, the highest frequency of micronuclei was 8.0 ± 0.82 (100 J m^{-2}), but numbers of micronuclei showed no clear relationship to UVA dose. Frequencies of NPB were significantly enhanced in all UVA doses compared to the control ($p < 0.05$), to a maximum observed number of 4.75 ± 0.96 (200 J m^{-2}). Equally interesting, throughout these experiments many incidences of more than one micronucleus observed within the cell was detected at all UVA doses. These incidences were mainly limited to appearances of 2 nuclei at a frequency of 6.75 ± 0.50 (200 J m^{-2}) which were all significantly different from the control ($p < 0.05$). With an occurrence of three micronuclei in the cell, only 50 J m^{-2} UVA was significantly different from the control ($p < 0.05$). Occurrences of four or more micronuclei within a cell were small and limited to 50 J m^{-2} and 100 J m^{-2} (0.25 ± 0.50 for each dose) and not significantly different from the control ($p > 0.05$). Following these experiments, the use of anti-kinetochore stain was employed to investigate the mechanisms of action of UVA on the RTG-2 cell line. Again, it was not possible to score 1000 binucleate cells alone with the addition of UVA because the frequencies of mononucleate cells to binucleate cells observed became almost indistinguishable by eye, so micronuclei were scored in a total of 1000 mononucleate and binucleate cells. The numbers of mononucleate cells ranged from 197 ± 26.87 (0.0 J m^{-2}) to 695 ± 9.90 (25 J m^{-2}) which were significantly different from the control ($p < 0.05$). There were some differences in the numbers of micronuclei observed between mononucleate or binucleate cells. In both types of cell, the

micronuclei frequencies increased significantly in a dose responsive way ($p < 0.05$). The largest frequency of micronuclei observed within a mononucleate cell was 13.5 ± 0.71 (200 J m^{-2}), whilst the highest frequency in a binucleate cell was 11 ± 2.83 (100 J m^{-2}) which were both significantly different from the control ($p < 0.05$). Of the cells containing micronuclei, a larger proportion of micronuclei detected contained a K+ signal but were located in both mononucleate and binucleate cells. The greatest frequency of micronuclei was 8.5 ± 0.71 detected with a K+ signal in a mononucleate cell (200 J m^{-2}). These results indicate a strongly aneugenic mode of action. However, as micronuclei were also detected significantly ($p < 0.05$) with K- signals, it would suggest that UVA induces both a clastogenic and aneugenic response in these cells.

Although it was possible to show genotoxicity of UVB through using the comet assay, it was not possible to generate any Mn data for UVB irradiated cells. It was considered that with the comet assay the cells were irradiated and processed immediately for the assay. However to generate cells for the Mn assay there is a 48 hour period between irradiation with UVB and processing due to the cytokinesis block method with Cyto B. At some point after irradiation with UVB the cells most probably undergo apoptosis or necrosis. This was considered in this pilot study with RTG-2 cells using Annexin V (method detailed in Chapter 2, Section 2.4.3) and the results of this pilot study are presented in Figure 4.5. These results indicate through a time course the onset of apoptosis at 6 hours post irradiation. These data although preliminary would indicate why it was not possible to generate micronuclei following exposure to UVB.

Table 4.3 Effect of various doses of UVA on the mean generation (±SE) of micronuclei in the RTG-2 cell line (n=23,506) using Giemsa or anti-kinetochore stain. There were no multinucleate cells observed. Significant increases (Mann-Whitney *U* test $p<0.05$) in the cellular responses from the control are indicated (*).

UVA dose (J m^{-2})	**0***	**25**	**50**	**100**	**200**
Cellular Response-Giemsa					
Mononucleate	200.5 ± 31.82	390 ± 15.56	333.5 ± 14.36	337.25 ± 35.57	451.5 ± 16.34*
Binucleate	1000 ± 0.00	621 ± 29.70	751.5 ± 17.25	728 ± 18.81	633.75 ± 6.24*
Micronucleus/Mononucleate	Not observed	1.5 ± 0.71	4.0 ± 0.82*	7.5 ± 1.29*	10.50 ± 1.91*
Micronucleus/Binucleate	0.5 ± 0.71	3.0 ± 1.41*	5.75 ± 0.96*	8.0 ± 0.82*	4.75 ± 1.71*
Nucleoplasmic Bridge	Not observed	0.5 ± 0.71	2.0 ± 0.8*2	3.0 ± 1.41*	4.75 ± 0.96*
2 nuclei	Not observed	0.5 ± 0.71	2.75 ± 0.50*	4.75 ± 1.71*	6.75 ± 0.50*
3 nuclei	Not observed	Not observed	1.75 ± 0.50*	1.5 ± 1.29	1.25 ± 0.96
4+ nuclei	Not observed	Not observed	0.25 ± 0.50	0.25 ± 0.50	Not observed
Cellular Response-anti-kinetochore stain					
Mononucleate	197.0 ± 26.87	695.0 ± 9.90*	436.0 ± 9.90*	546.0 ± 14.14*	567.5 ± 41.72*
Binucleate	1000.0 ± 0.00	326.5± 20.51*	584.5± 16.26*	460.5 ± 26.16*	469 ± 22.63*
Micronucleus/Mononucleate	Not observed	0.5 ± 0.71	4.5 ± 0.71*	10.5 ± 0.71*	13.5 ± 0.71*
Micronucleus/Binucleate	0.5 ± 0.71	2.0 ± 1.41*	9.0 ± 1.41*	11.0 ± 2.83*	10.0 ± 1.41*
K+ Mononucleate cells	Not observed	0.5 ± 0.71	2.5 ± 0.71*	6.5 ± 0.71*	8.5 ± 0.71*
K- Mononucleate cells	Not observed	Not observed	2.0 ± 0.00*	4.0 ± 0.00*	5.0 ± 1.41*
K+ Binucleate cells	Not observed	1.5 ± 0.71	5.5 ± 0.71*	6.5 ± 0.71*	5.5 ± 0.71*
K- Binucleate cells	0.5 ± 0.71	0.5 ± 0.71	3.5 ± 0.71*	4.5 ± 2.12*	4.5 ± 0.71*

4.3.3 Interactive Toxicity for B(a)P and UVR effects on Fish Cells (EPCA1, RTG-2).

4.3.3.1 The NRR assay data for the interactive toxicity of B(a)P and UVB/UVA effects on RTG-2 cells.

The NRR assay was conducted as described in Chapter 2, Section 2.4.4, with the modifications described above in Section 4.2.4. The experiment was designed to examine the interactive cytotoxicity of B(a)P (0.0, 0.1, 1.0 and 3.2 μg ml^{-1}) (Section 4.3.1.1) and UVB (0*, 100 and 200 J m^{-2}) (Section 4.3.2.1) or UVA (0*, 500, 2000 and 4000 J m^{-2}) (Section 4.3.2.2) in RTG-2 cells. The results are presented in Figure 4.10. RTG-2 cells pre-treated with B(a)P for 24 hours and irradiated with UVB (Figure 4.10a) showed no significant reduction in cell viability ($p > 0.05$) for all B(a)P concentrations or UVB doses except 3.2 μg ml^{-1} and 100 J m^{-2} UVB ($p < 0.01$). There was no significant difference between the responses in cell viability for each concentration at each dose ($p > 0.05$). With UVA, cells treated with 0.1 μg ml^{-1} B(a)P and irradiated with 4000 J m^{-2} UVA showed a significant reduction in cell viability to 43 % (4000 J m^{-2}, $p < 0.05$), whilst in cells treated with 1.0 μg ml^{-1}, cell viability was reduced down to 66 % (500 J m^{-2}), 63 % (2000 J m^{-2}) and 35 % (4000 J m^{-2}), which were all significant ($p < 0.05$) (Figure 4.10b). The results of this assay also revealed a reduction in cell viability for all UVA doses at a concentration of 3.2 μg ml^{-1} B(a)P down to 60 % (500 J m^{-2}), 59 % (2000 J m^{-2}) and 22 % (4000 J m^{-2}), which were all significant ($p < 0.05$). The negative control values (sham irradiated for each UVA dose) were all 100 %.

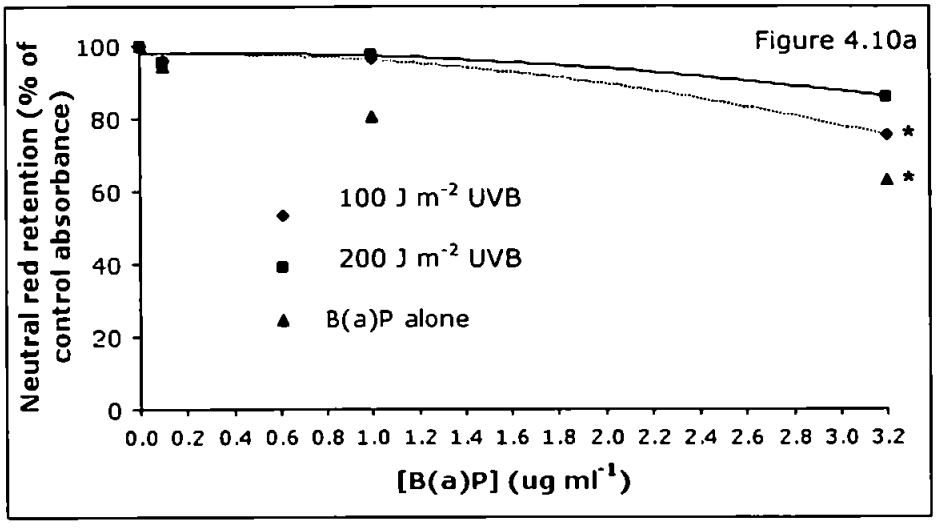

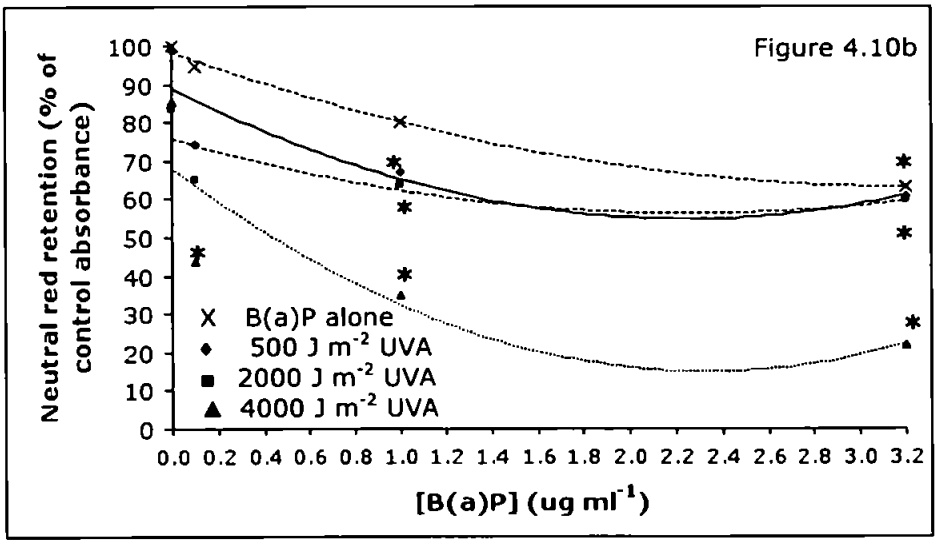

Figure 4.10 Cell viability assessed through the uptake of neutral red dye by RTG-2 cells following pre-treatment with B(a)P for 24 hours at various concentrations (0.0, 0.1, 1.0 and 3.2 µg ml^{-1}) and then exposure to various doses UVB (100 and 200 J m^{-2}) (Figure 4.10a) or UVA (500, 2000 and 4000 J m^{-2}) (Figure 4.10b). Cell viability was expressed as a percentage of the control absorbance, with the control value being 100 %. Significant effects are indicated (*) (Mann Whitney U-test, $p < 0.05$) (NB control (0*) for each experiment was

sham irradiated for the same time as either 100 or 200 J m^{-2} UVB or 500, 2000 or 4000 J m^{-2} UVA).

4.3.3.2 An investigation for the interactive toxicity of B(a)P and UVB/UVA in RTG-2 cells employing the comet assay.

The results of UVB dose on DNA damage (comet assay) was investigated in the RTG-2 cell line. UVB results (Section 4.3.2.2.2) showed a strong DNA damage response to UVB with a large increase in Tail DNA (%) from the control and 100 and 200 J m^{-2} UVB. The drop off in observed DNA damage with 200 J m^{-2} UVB appeared indicative of loss of sensitivity from the assay. Therefore, interactive effects of B(a)P and UVB were investigated in RTG-2 cells at various UVB doses (0* (sham irradiated control for the same time as 200 J m^{-2}), 25, 50, 75, 100 and 200 J m^{-2}) following pre-incubation with B(a)P (0.0, 0.1, 1.0 and 3.2 µg ml^{-1}). The results are presented in Figure 4.11.

Pre-exposure of RTG-2 cells to B(a)P (24 h), followed by exposure of cells to 200 J m^{-2} UVB resulted in an apparent increase in median DNA damage when compared to the sham irradiated control ($p < 0.0001$) and to the B(a)P concentrations used (Figure 4.11). However, when compared to the irradiated control (200 J m^{-2} UVB), there was no significant increase ($p > 0.05$) in median DNA damage following pre-treatment with 0.1 µg ml^{-1} and 3.2 µg ml^{-1} B(a)P + 200 J m^{-2} UVB because this response may have exceeded the range of insult but there was a significant increase in median DNA damage with 1.0 µg ml^{-1} B(a)P + 200 J m^{-2} UVB ($p < 0.05$). A similar response was seen when cells treated with B(a)P were irradiated with 100 J m^{-2} UVB. In this case, there was an increase in median DNA damage that was

significantly different ($p < 0.0001$) from the sham irradiated control and all B(a)P concentrations used. However, when compared to 100 J m^{-2} UVB, the damage was significant only at 0.1 µg ml^{-1} B(a)P ($p < 0.0001$).

The effect of irradiating cells with 75 J m^{-2} UVB, following pre-treatment with B(a)P was investigated. This result showed that there was a significant ($p < 0.001$) increase in median DNA damage with all concentrations of B(a)P compared to the sham irradiated control or 75 J m^{-2} UVB and all B(a)P and 75 J m^{-2} UVB doses tested ($p < 0.0001$) i.e. at 75 J m^{-2} UVB in the presence of B(a)P (all concentrations) it was observed that there was a significant ($p < 0.0001$) increase in DNA damage from the combined B(a)P and UVB doses when compared to B(a)P and UVB.

An investigation into the effects of 50 J m^{-2} UVB showed a significant increase in DNA damage between the negative controls and the interactive doses tested ($p < 0.0001$). There was no significant difference ($p > 0.05$) between 50 J m^{-2} UVB and 50 J m^{-2} UVB + 0.1 µg ml^{-1} B(a)P, but a significant effect between 50 J m^{-2} and 50 J m^{-2} UVB + 1.0 µg ml^{-1} ($p < 0.01$) and 50 J m^{-2} UVB + 3.2 µg ml^{-1} ($p < 0.001$). There was a significant increase in DNA damage between B(a)P alone at all doses and the interactive UVB and B(a)P doses ($p < 0.01$).

Irradiation of RTG-2 cells with 25 J m^{-2} UVB following pre-treatment with B(a)P showed a significant response between the sham irradiated control and all B(a)P and UVB doses tested ($p < 0.0001$). There was a significant difference between 25 J m^{-2} UVB and all combined B(a)P and UVB doses tested ($p < 0.001$). Following pre-treatment with

B(a)P, and irradiation with 25 J m^{-2} UVB, there was a significant increase in DNA damage between the B(a)P and combined UVB and B(a)P doses ($p < 0.001$) except for between 3.2 µg ml^{-1} B(a)P and 25 J m^{-2} UVB and 3.2 µg ml^{-1} B(a)P ($p > 0.05$) suggesting that this is exceeding the applicable range for the assay.

Interactive effects of B(a)P and UVA were investigated in RTG-2 cells at various UVA doses (0*, 500, 1000, 2000, 4000, 6000 and 8000 J m^{-2}) following pre-incubation with B(a)P (0.00, 0.05, 0.10, 0.32, 1.00 and 3.20 µg ml^{-1}) (Figure 4.11b). Pre-exposure of RTG-2 cells to B(a)P, followed by exposure of cells to 8000 J m^{-2} UVA resulted in an increase in DNA damage at 0.1 µg ml^{-1}, from B(a)P alone at this concentration, but there was a subsequent plateau in DNA damage and a reduction in the measured DNA damage as the B(a)P dose increased to 3.2 µg ml^{-1}. This was considered an effect due to excessive DNA damage which made the comet assay an inappropriate technique. A similar effect was seen with 6000 J m^{-2} UVA; at a dose of 3.2 µg ml^{-1} there appeared to be a reduction in DNA damage, but all results were significant ($p < 0.01$). When 4000 J m^{-2} UVA was investigated, there was no significant difference seen between the control and 4000 J m^{-2} UVA ($p > 0.05$), but when cells were pre-treated with B(a)P, results showed a significant increase in DNA damage ($p < 0.0001$) with increasing B(a)P. Similarly, there was no significant difference seen between the control and lower UVA doses of 500, 1000 or 2000 J m^{-2} UVA ($p > 0.05$), but when cells were pre-treated with B(a)P, results showed a significant increase in DNA damage following UVA irradiation ($p < 0.0001$) at all B(a)P concentrations. In all cases, with UVA alone, there is no effect on DNA damage between the control and all UVA doses tested ($p > 0.05$).

However, 24 hours pre-treatment with B(a)P did cause a significant increase in DNA damage. In RTG-2 cells pre-treated for 24 hours with B(a)P there is a significant increase in DNA damage with all UVA doses investigated. These data suggest that there is an additive effect from pre-treating the cells with B(a)P and then exposure to UVA at various doses.

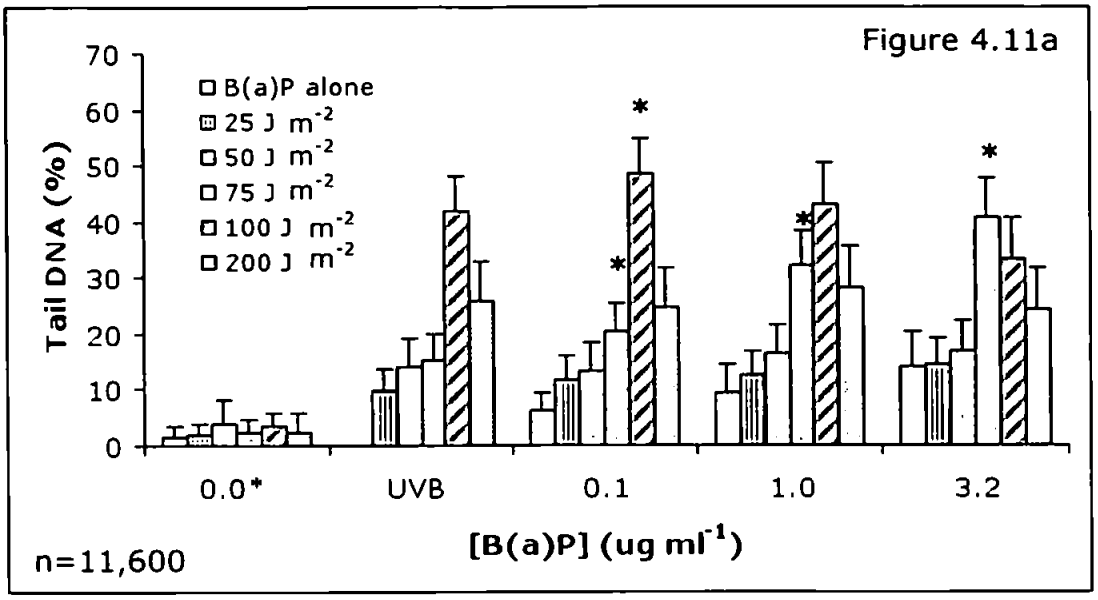

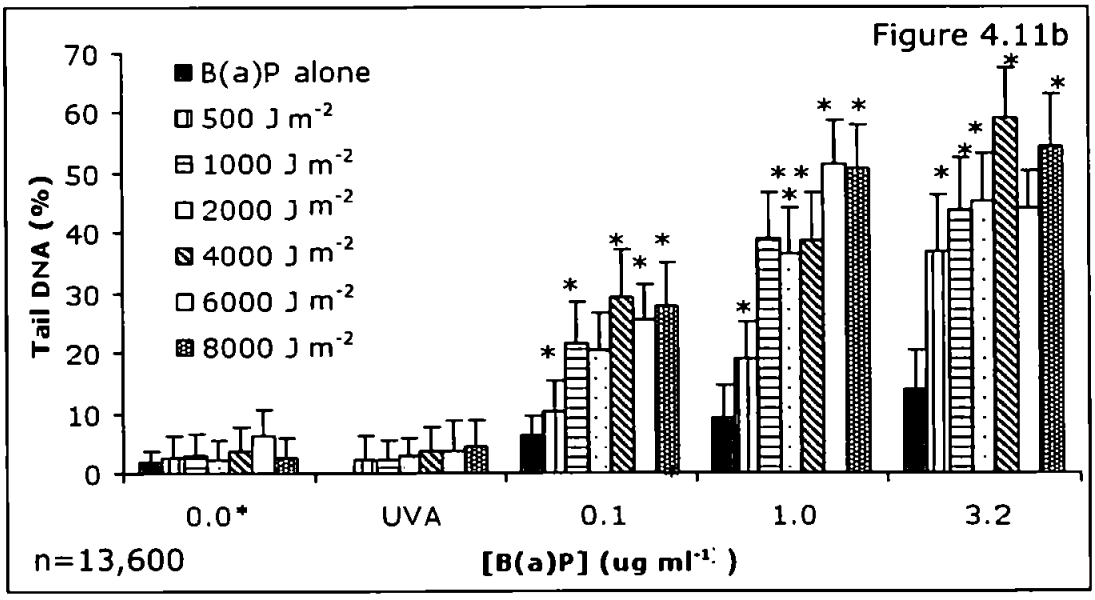

Figure 4.11 Median DNA damage to RTG-2 cells following pre-incubation for 24 hours with B(a)P (0.0, 0.1, 1.0 and 3.2 µg ml^{-1}) and exposure to UVB (0*, 25, 50, 75, 100 and 200 J m^{-2}) (Figure 4.11a) or UVA (0*, 500, 1000, 2000, 4000, 6000 and 8000 J m^{-2}) (Figure 4.11b). DNA damage was assessed by the Tail DNA (%) (0* is the sham irradiated control for each experiment, and controls were sham irradiated for the same time as each UVB or UVA dose). Significant differences (Mann-Whitney-*U* test, $p<0.001$) from the additive B(a)P and UVB/UVA irradiated response are indicated (*).

4.3.3.3 The NRR assay for the interactive toxicity of (and recovery from) B(a)P and UVA effects on fish cells (RTG-2).

It was decided to investigate cell viability and recovery following pre-treatment with B(a)P and exposure to various doses of UVA. Hence, B(a)P treated RTG-2 cells were irradiated with various doses of UVA as above (500, 2000 and 4000 J m^{-2}), and then incubated in GM for 0, 1, 6 or 24 hours. At zero hours post incubation there was no significant difference between the sham irradiated control and 500 J m^{-2} UVA ($p > 0.05$) but a significant difference between the sham irradiated control and 2000 or 4000 J m^{-2} UVA ($p < 0.05$). There was a significant reduction in cell viability from the sham irradiated control and all B(a)P and UVA combinations tested ($p < 0.05$). At 1 hour post-treatment there was a significant reduction in cell viability between the sham irradiated control and all UVA doses tested ($p < 0.05$). All combinations of B(a)P and UVA tested displayed a significant reduction in cell viability ($p < 0.05$) from the same UVA doses tested with the exception of 0.1 µg ml^{-1} B(a)P and 500 J m^{-2} UVA ($p > 0.05$). At 6 hours post-incubation, there was no significant difference between the sham irradiated control and 500 J m^{-2} UVA ($p > 0.05$) however there was a significant reduction in cell viability between the control and all combinations of B(a)P and UVA tested in all cases ($p < 0.05$). With 24 hours incubation in growth medium results showed there was no significant effect in cytotoxicity between the control and 4000 J m^{-2} UVA ($p > 0.05$) but a significant reduction in cell viability ($p < 0.05$) at all combinations of B(a)P and UVA tested with the exceptions of 0.1 µg ml^{-1} B(a)P + 500 J m^{-2} UVA where there was no significant effect ($p > 0.05$) which may have been too low an effect to measure. Results are presented in Figure 4.12.

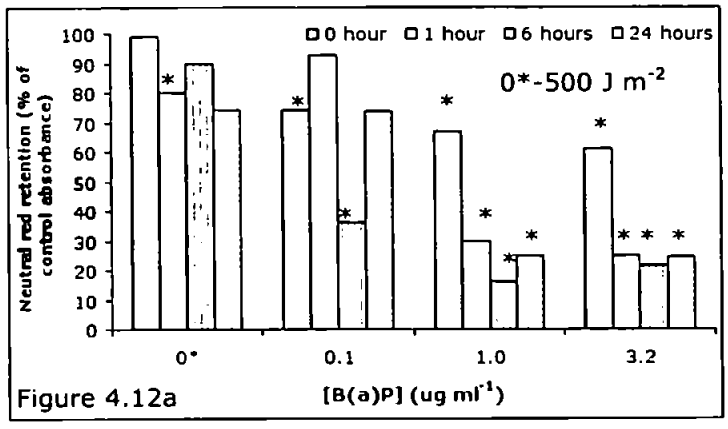

Figure 4.12a

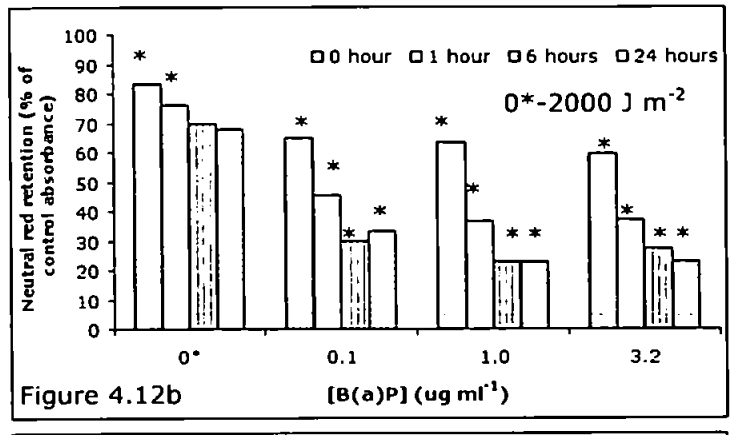

Figure 4.12b

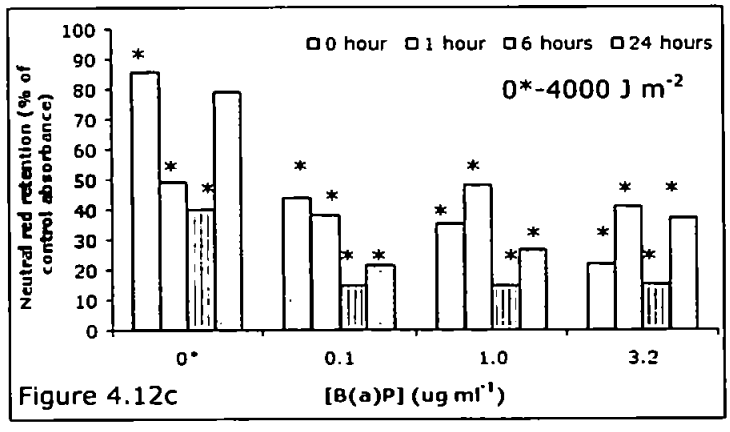

Figure 4.12c

Figure 4.12 Cell viability assessed through the uptake of neutral red dye by RTG-2 cells following pre-treatment with B(a)P at various doses (0.1, 1.0 and 3.2 μg ml^{-1}) and then exposure to UVA (500 (Figure 4.12a), 2000 (Figure 4.12b), or 4000 J m^{-2} (Figure 4.12c). 0* is UVA dose indicated in specific figures. Cells were then incubated for various times (0, 1, 6, 24 hours) in GM. Significant differences (Mann-Whitney-U test, $p < 0.05$) from the control are indicated (*).

4.3.3.4 The micronucleus assay for interactive toxicity for B(a)P and UVA effects on fish cells (RTG-2).

Various doses of UVA (0*, 25, 50 and 100 J m^{-2}) were tested in RTG-2 cells following their incubation with 0.05 µg ml^{-1} B(a)P to investigate possible interactive effects by means of the micronucleus assay. Interactive effects on micronucleus formation were investigated using both Giemsa and anti-kinetochore staining techniques to investigate the potential mechanisms of action (clastogenic or aneugenic, respectively). Experiments scored 1000 binucleate cells per treatment group, or 1000 cells and experiments were duplicated. The results for RTG-2 cells are presented in Table 4.4. In the previous section (Section 4.3.1.3.2) there was no significant increase in micronuclei induced following incubation with 0.05 µg ml^{-1} B(a)P. Without pre-incubation with 0.05 µg ml^{-1} B(a)P and at a dose of 0* J m^{-2} UVA, it was possible to remain with the standard protocol employed for the previous micronucleus experiments by counting micronuclei within 1000 binucleate cells. At this concentration level (no pre-incubation and 0* J m^{-2} UVA), 212 ± 9.90 mononucleate cells were counted within 1000 ± 0.00 binucleate cells. However, as UVA doses were introduced to the B(a)P pre-incubated cells, the frequencies of mononucleate cells visibly increased so it was decided to count a total of 1000 binucleate and mononucleate cells in order to investigate the ratio of the two cell types to each other, and to be able to detect as many micronuclei as possible.

The results using Giemsa stain show that numbers of mononucleate cells vary widely within a scoring protocol of a total of 1000 binucleate and mononucleate cells, ranging from 656.25 ± 32.48 (0.05 µg ml^{-1} B(a)P + 25 J m^{-2}) to 742.5 ± 39.53 (0.05 µg ml^{-1} B(a)P + 50 J m^{-2})

which were both significantly different from the control ($p < 0.05$). The numbers of binucleate cells scored also varied with exposure to UVA, in this case dropping with increasing UVA dose from 408.75 ± 13.89 (0.05 μg ml^{-1} B(a)P + 25 J m^{-2}) to 279.5 ± 37.83 (0.05 μg ml^{-1} B(a)P + 50 J m^{-2}) which were both significantly different from the control ($p < 0.05$). Micronuclei scored in mononucleate and binucleate cells did not show much variation in terms of frequencies of micronuclei but both increased significantly from the control ($p < 0.05$) and in the total frequency induced ($p < 0.05$). In mononucleate cells a maximum of 9.5 ± 2.65 were detected (0.05 μg ml^{-1} B(a)P + 100 J m^{-2}). In binucleate cells, there was no observed increase with dose ($p > 0.05$) and the maximum frequency detected was 11.5 ± 2.65 (0.05 μg ml^{-1} B(a)P + 100 J m^{-2}). Along with the increase in micronuclei observed, there were many incidences of more than one micronucleus observed within the cell at all UVA doses. The greatest frequencies were detected at the lowest combined doses (0.05 μg ml^{-1} B(a)P + 25) although all combinations (0.05 μg ml^{-1} B(a)P + 25, 50 or 100 J m^{-2}) were significantly different from the control ($p < 0.05$), with the highest frequency of 6.0 ± 0.82 (0.05 μg ml^{-1} B(a)P + 25 J m^{-2}) in cells containing 3 micronuclei which was significantly different from the control ($p < 0.05$). Multiple micronuclei were observed at all doses and the effects were significantly higher than B(a)P alone for RTG-2 cells ($p < 0.05$) but there was no significant difference in the presence of multiple micronuclei between the interactive dose and the UVA dose alone ($p > 0.05$) suggesting that UVA is the more mutagenic agent. An increase of NPB was observed at all interactive doses, to a maximum observed number of 2.0 ± 0.82 (0.05 μg ml^{-1} B(a)P + 50 J m^{-2}); marginally lower than the response seen to UVA or B(a)P alone

in this cell line and not significantly different from the control ($p > 0.05$).

Following these experiments with Giemsa, the use of anti-kinetochore stain was employed to investigate the mechanisms of action of interactive toxicity on the RTG-2 cell line (Table 4.4). Again, it was not possible to score 1000 binucleate cells alone, so micronuclei were scored in a total of 1000 mononucleate and binucleate cells. At the control dose, 182.5 ± 21.92 mononucleate cells were scored alongside 1000 binucleate cells. When cells were exposed to B(a)P and UVA the numbers of mononucleate cells ranged from 560 ± 4.24 (0.05 μg ml^{-1} B(a)P + 50 J m^{-2}) to 688.5 ± 19.09 (0.05 μg ml^{-1} B(a)P + 100 J m^{-2}) which were all significantly different from the control ($p < 0.05$). The numbers of binucleate cells did not increase steadily with dose but ranged from 417.5 ± 3.54 (0.05 μg ml^{-1} B(a)P + 25 J m^{-2}), to 468.5 ± 4.24 (0.05 μg ml^{-1} B(a)P + 50 J m^{-2}) down to 332.0 ± 28.28 (0.05 μg ml^{-1} B(a)P + 100 J m^{-2}) (these data are probably outside the useful range of the assay) which were all significantly different from the control ($p < 0.05$).

Again, as with Giemsa staining, there was little difference in the numbers of micronuclei observed in either a mononucleate or a binucleate cell. The largest frequency of micronuclei observed within a mononucleate cell was 13 ± 2.83 (0.05 μg ml^{-1} B(a)P + 100 J m^{-2}), whilst 14 ± 1.41 and 14 ± 2.83 were detected within a binucleate cell (0.05 μg ml^{-1} B(a)P + 50 J m^{-2} and 0.05 μg ml^{-1} B(a)P + 100 J m^{-2}, respectively). All the micronuclei induced were significantly different from the control ($p < 0.05$). These results are similar to the results found with Giemsa staining, but the exposure groups 0.05 μg ml^{-1}

B(a)P + 25 J m^{-2} and 0.05 µg ml^{-1} B(a)P + 50 J m^{-2} again have significantly higher induction of micronuclei than the results seen for UVA or B(a)P alone hence a synergistic effect is demonstrated ($p < 0.05$). Numbers of micronuclei induced were significantly different from the control ($p < 0.05$) and of the cells containing micronucleus, a larger proportion of micronuclei detected contained a K+ signal but were located in both mononucleate and binucleate cells. These results indicate an aneugenic mode of action. However, as micronuclei were also detected with K- signals, it would suggest that B(a)P and UVA induce both a clastogenic and aneugenic response in RTG-2 cells.

Table 4.4 Effect of interactive toxicity following pre-incubation with 0.05 μg ml^{-1} B(a)P with various doses of UVA on the mean generation (±SE) of micronucleus in RTG-2 cells (n=17,445) using Giemsa or anti-kinetochore stain. There were no multinucleate cells observed. Significant differences (Mann-Whitney *U* test $p<0.05$) from the control are indicated (*).

	0.00 μg ml^{-1} B(a)P + 0* J m^{-2} UVA	**0.05 μg ml^{-1} B(a)P + 25 J m^{-2} UVA**	**0.05 μg ml^{-1} B(a)P + 50 J m^{-2} UVA**	**0.05 μg ml^{-1} B(a)P + 100 J m^{-2} UVA**
Cellular Response-Giemsa				
Mononucleate	212.0 ± 9.90	656.25 ± 32.48*	742.50 ± 39.53*	706.25 ± 25.04*
Binucleate	1000.0 ± 0.00	408.75 ± 13.89*	279.50 ± 37.83*	355.25 ± 45.22*
Micronucleus/Mononucleate	0.5 ± 0.71	7.50 ± 1.29*	7.75 ± 0.96*	9.50 ± 2.65*
Micronucleus/Binucleate	Not observed	10.00 ± 1.41*	9.75 ± 0.96*	11.50 ± 2.65*
Nucleoplasmic Bridge	Not observed	1.75 ± 1.26	2.00 ± 0.82	1.50 ± 1.29
2 nuclei	Not observed	5.75 ± 0.96*	4.25 ± 3.50*	2.25 ± 1.71*
3 nuclei	Not observed	6.00 ± 0.82*	3.25 ± 2.06*	4.25 ± 1.71*
4+ nuclei	Not observed	4.25 ± 1.71*	1.00 ± 0.82	2.75 ± 1.71*
Cellular Response-anti-kinetochore stain				
Mononucleate	182.5 ± 21.92	601.0 ± 2.83*	560.0 ± 4.24*	688.5 ± 19.09*
Binucleate	1000.0 ± 0.00	417.5 ± 3.54*	468.5 ± 4.24*	332.0 ± 28.28*
Micronucleus/Mononucleate	Not observed	6.5 ± 0.71*	7.5 ± 0.71*	13.0 ± 2.83*
Micronucleus/Binucleate	0.5 ± 0.71	8.5 ± 0.71*	14.0 ± 1.41*	14.0 ± 2.83*
K+ Mononucleate cells	Not observed	2.5 ± 0.71*	5.0 ± 0.00*	8.0 ± 1.41*
K- Mononucleate cells	Not observed	4.0 ± 1.41*	2.5 ± 0.71*	5.0 ± 1.41*
K+ Binucleate cells	Not observed	4.0 ± 1.41*	10.0 ± 1.41*	9.0 ± 1.41*
K- Binucleate cells	0.5 ± 0.71	4.5 ± 0.71*	3.5 ± 0.71*	5.0 ± 1.41*

4.3.4 ESR

The samples of DMPO, as obtained from Sigma contained traces of paramagnetic impurity which could not readily be removed (for example by shaking the DMPO solutions with activated charcoal). Since preliminary experiments confirmed that these trace impurities were unaffected by B(a)P and/or UVA the background spectra were subtracted from all experimental spectra presented here. The effect of untreated RTG-2 cells in the presence of UVA (500 J m^{-2}) shows an insignificant signal (Figure 4.13a). When RTG-2 cells incubated with 3.2 µg ml^{-1} B(a)P (24 hours) (data not shown) were irradiated with UVA (500 J m^{-2}) in the presence of the spin trap DMPO (Elliott *et al.*, 1986), the major species detectable by ESR is DMPO-OH (Figure 4.13b). This supports the interpretation that the combination of UVA and B(a)P is necessary to produce ·OH radicals.

In order to determine whether hydroxyl or superoxide is responsible for the observed signal, various agents were used to interfere with the production of these species (Thornalley & Dodd, 1985). One mM diethylenetriaminetetraacetic acid (DETAPAC) strongly chelates any free iron and inhibits decomposition of H_2O_2 to ·OH (Fenton processes) after UVA. Figure 4.14a shows the signal from B(a)P and UVA treated RTG-2 cells that contained DETAPAC and the strong spin adduct suggests that a Fenton reaction is not involved. As shown, the spin adduct is greatly reduced, strongly suggesting that UVA/B(a)P is causing the direct production of hydroxyl radicals. This indicated the formation of either ·OH or O_2^{-}·radicals. However, addition of either mannitol (which readily reacts with ·OH and competes with DMPO) to the B(a)P-treated cells prior to irradiation greatly decreased the yield

of DMPO-OH (Figure 4.14b). Addition of SOD, which converts superoxide to H_2O_2 had little effect (Figure 4.14c). Addition of catalase, which converts H_2O_2 to water, also had a small effect (Figure 4.14d). This indicated that the major radical product is ·OH, formed directly rather than from H_2O_2 and that superoxide is not involved in ·OH production. In the presence of TMPol, B(a)P treated cells showed no evidence of the formation of singlet oxygen on irradiation (Lion *et al.*, 1980). Similarly no ESR signal was observed when POBN was used as spin trap, unless 10 % by volume of ethanol was also added, in which case the POBN-$CH(OH)CH_3$ radical was detected (Chapter 3, Section 3.3.7). This provides further evidence of the formation of hydroxyl radicals.

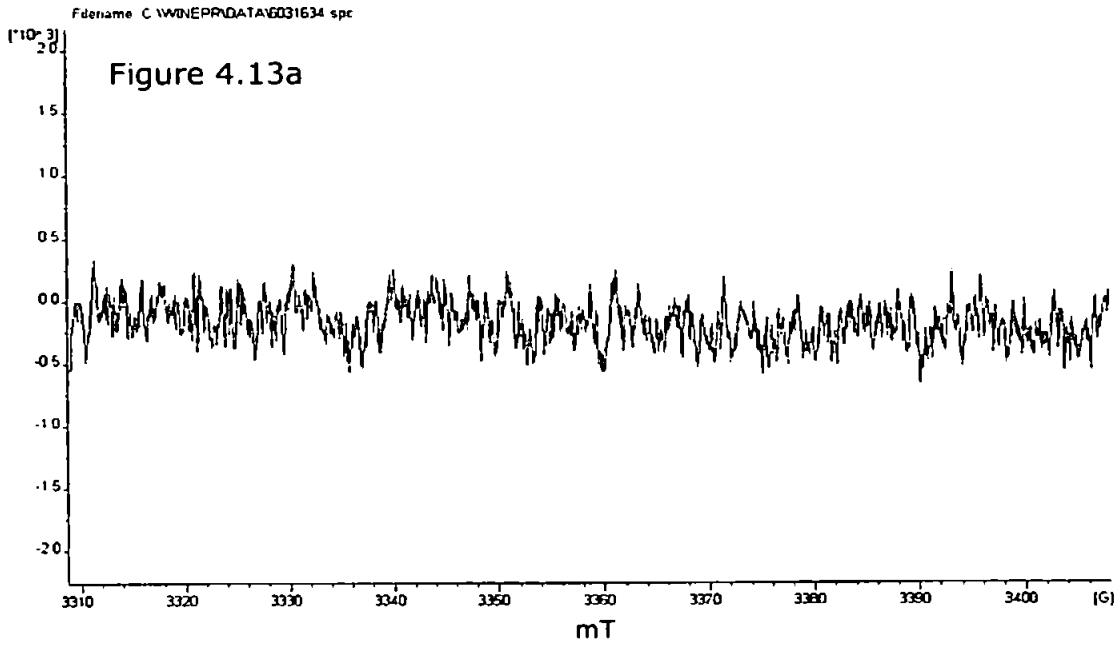

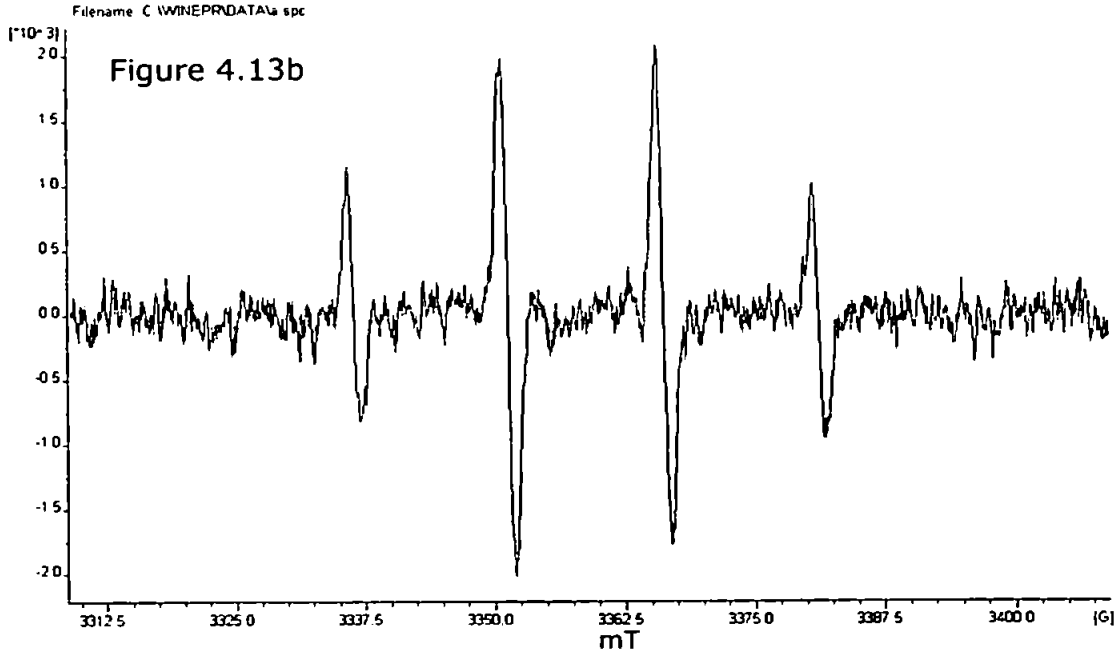

Figure 4.13 The effect of UVA irradiation on RTG-2 cells (Figure 4.13a). Figure 4.13b shows the clear DMPO-OH signal after UVA irradiation (500 J m^{-2}) of the B(a)P treated (3.2 µg ml^{-1}) RTG-2 cells.

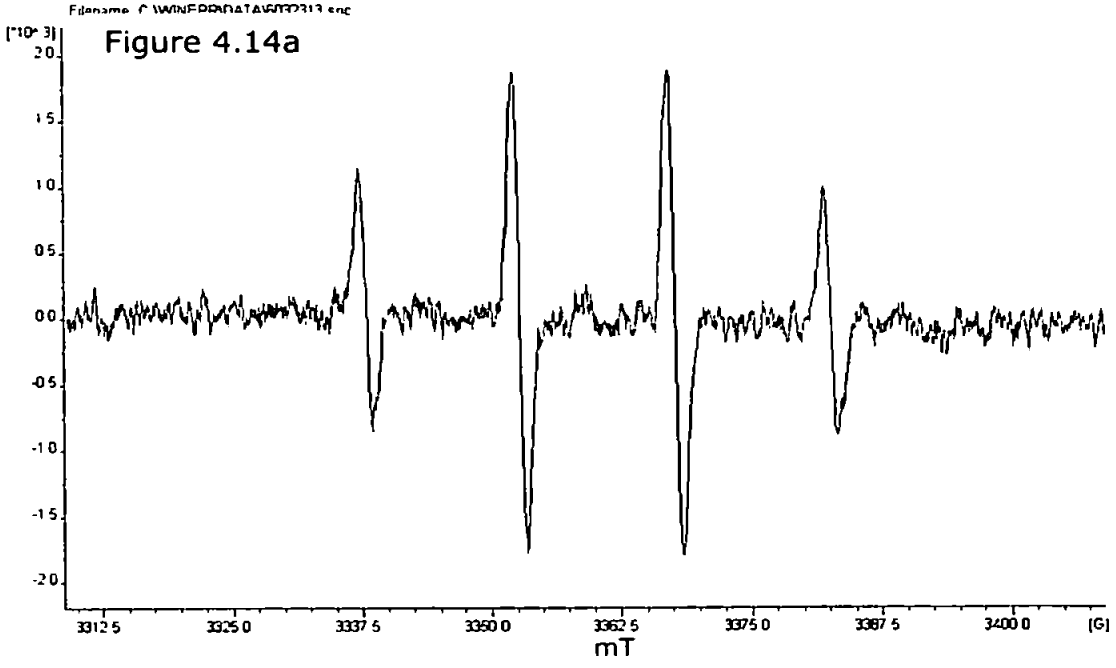
Figure 4.14a
[*10^ 3]
20
15
10
05
00
-05
-10
-15
-20
3312 5
3325 0
3337 5
3350 0
3362 5
3375 0
3387 5
3400 0
[G]
mT

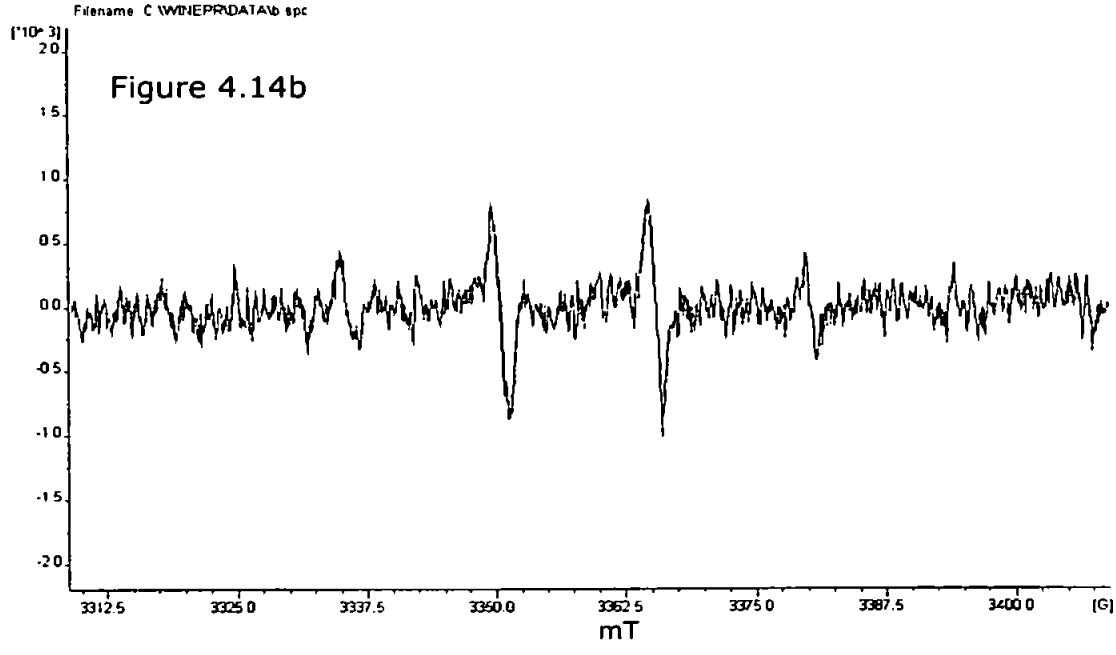
Filename C \WINEPRDATA\b spc
Figure 4.14b
[*10^ 3]
20
15
10
05
00
-05
-10
-15
-20
3312.5
3325 0
3337.5
3350.0
3362 5
3375 0
3387.5
3400 0
[G]
mT

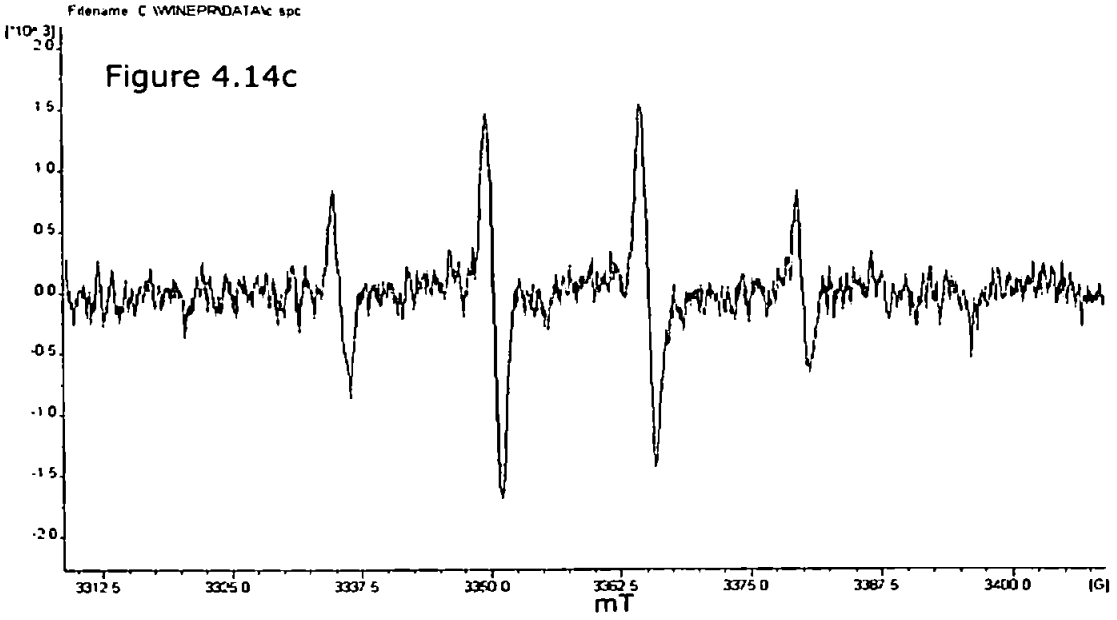

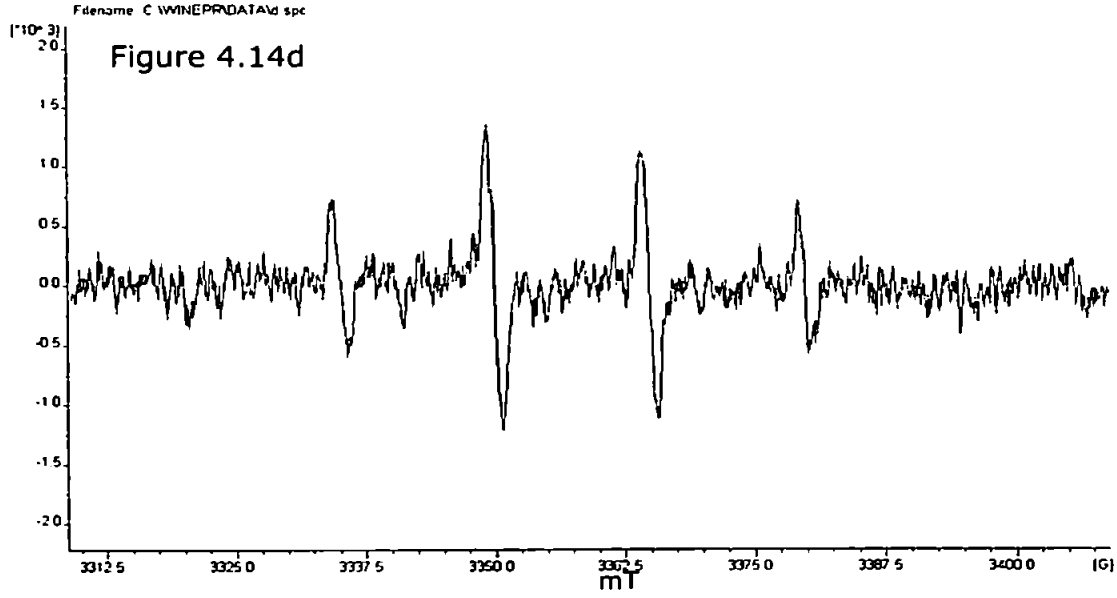

Figure 4.14 Treatment of RTG-2 cells with 3.2 μg ml^{-1} B(a)P (24 hours) followed by UVA (500 J m^{-2}) with the addition of DETAPAC (Figure 4.14a), mannitol (which greatly decreased the yield of DMPO-OH) (Figure 4.14b). Addition of SOD had little effect (Figure 4.14c). Addition of catalase also had a small effect (Figure 4.14d). This indicated that the major radical product is ·OH.

4.4 Discussion

There are few data published about the combined effects of PAHs such as B(a)P and UVA in cellular systems, however there is a wealth of data regarding the effects of crude oils (containing PAHs) and their phototoxicity with UVA and/or sunlight (Duesterloh *et al.*, 2002). For example, the use of chemical dispersants in the environment following oil spills may accelerate PAH dissolution into the aqueous phase, which may increase its bioavailability (Barron *et al.*, 2003). This increased bioavailability causes negative consequences by building up in the tissues and in combination with UVA or sunlight damages smaller aquatic organisms like herring eggs causing problems such as yolk sac oedema (Barron *et al.*, 2003). This leads to the hypothesis that UVA both with and without PAHs may be a significant and causative factor in early life stage mortalities in fish (Barron *et al.*, 2003; Duesterloh *et al.*, 2002). *In vivo*, fish lethality tests have limitations, for example in terms of growing economical costs and ethical concerns therefore it is increasingly important to explore alternative experimental techniques that search for ways to apply the ideals of replacement, reduction and refinement (Hutchinson *et al.*, 2003). The largest reductions in cell viability of 10 % and 35 % were observed in EPCA1 and RTG-2 cells respectively following treatment with 3.2 μg ml^{-1} B(a)P and suggested the RTG-2 cells showed a greater sensitivity than the EPCA1 cells, a finding that supports those reported elsewhere. For instance, in a study with EPC and RTG-2 cells using the NRR assay, RTG-2 cells were found to be more suitable for testing estuarine aqueous elutriate samples due to their tolerance to osmolality effects (Davoren *et al.*, 2005). The different cytotoxic response observed in this work could be due to the different enzyme activities in the two cell types as

metabolic activation of PAHs (such as B(a)P) have been suggested to reduce cell viability *in vitro* (Babich *et al.*, 1988). Araújo and co-workers (2000) did not observe any cytotoxicity in the RTG-2 cell line following 24 hours incubation with B(a)P doses of 0.625 to 20 μg ml^{-1} and suggested that insufficient amounts of B(a)P were metabolised to give a cytotoxic response. The actual levels of enzymatic activity may differ between the cell lines therefore influencing cytotoxic responses (Kammann *et al.*, 2001; Sanchez *et al.*, 2000). For example, a 35 % reduction in cell viability in RTG-2 cells was only observed with 10 μg ml^{-1} B(a)P after 144 hours treatment (Araújo *et al.*, 2000). However, Martin-Alguacil and co-workers (1991) found that RTG-2 cells metabolised sufficient amounts of B(a)P in 24 hours to reduce cell viability (NRR assay) which could explain the greater reduction in cell viability in RTG-2 due to a higher enzymatic activity than EPCA1 cells. RTG-2 cells have been shown to possess CYP1A activity indicated from ethoxyresorufin-O-deethylase (EROD) measurements (Nehls & Segner, 2001). Elevated EROD activities in fish cells have not only indicated exposure to PAHs but have been associated with significant biological effects (Au *et al.*, 2004) and significantly correlated to increases in lysosome accumulation (Yuen *et al.*, 2006).

B(a)P also caused increased DNA damage and genomic instability in both EPCA1 and RTG-2 cells. Greater variability in DNA damage was displayed in cells with the use of an exogenous metabolic source (S9) than in those cells treated to B(a)P without S9. Kammann and co-workers (2001) observed that 2.5 ng ml^{-1} B(a)P caused a significant genotoxic effect when used in conjunction with a fish enzyme suspension. This concentration is about 100 times less than the lowest concentration used in the work here (0.1 μg ml^{-1}) which gave a

significant genotoxic effect in both EPCA1 and RTG-2 cells. The RTG-2 cells demonstrated increased DNA damage than that of the EPCA1 cells to 0.1 μg ml^{-1} B(a)P for the 6 hour (with S9) group and to 1.0 μg ml^{-1} B(a)P for the 6 hour (without S9) group. Nehls and Segner (2001) investigated the genotoxicity of B(a)P to RTG-2 and RTL-W1 (liver epitheloid tissue from rainbow trout) using the comet assay following 2 hour exposures to various concentrations of B(a)P (0.94-50 μmol l^{-1}) and differences in sensitivity to B(a)P were observed between the two cell lines. This was related to EROD activity associated with cytochrome P4501A (CYP1A) monooxygenase, which is involved in phase I biotransformation of B(a)P to the ultimate carcinogen (Nehls & Segner, 2001). The study indicated that the effects of prototype CYP1A inducer, ß-naphthoflavone (BNF) were higher with RTL-W1 cells than with RTG-2 cells, which could form an important explanation not only for the different responses of these two cell lines, but also for the interpretation of results obtained from exposure experiments using other established cell lines (Nehls & Segner, 2001). The results discussed above indicate the importance of metabolic conversion in enhancing the toxicity of B(a)P and point up the variations which can exist in PAH metabolisms between cell lines. This has important ramifications in relation to the choice of cell lines for PAH-related assays and whether these differences are related to cytochrome monooxygenase activity is most and requires further study.

Significant increases in micronuclei were detected in EPCA1 and RTG-2 cells following treatment with B(a)P (except 0.05 μg ml^{-1} B(a)P in RTG-2). Significant frequencies of K+ micronuclei were detected indicating an aneugenic mode of action of B(a)P. There were no significant differences between the EPCA1 and RTG-2 cells in micronuclei

induction. In agreement with the results reported here with RTG-2, Sanchez and co-workers (2000) detected no micronuclei in RTG-2 cells with 0.05 μg ml^{-1} B(a)P but increasing the concentration to 0.5 and 1.0 μg ml^{-1} B(a)P induced micronuclei (Sanchez *et al.*, 2000). However, they only detected micronuclei with 0.1 μg ml^{-1} B(a)P after 72 hours treatment (Sanchez *et al.*, 2000) which suggests that our technique was more sensitive. In the work presented here diverse nuclear abnormalities were not observed in EPCA1 or RTG-2 cells following exposure to B(a)P. *In vivo* investigations by other workers have shown that B(a)P is a potent inducer of both erythrocytic micronuclei and nuclear abnormalities in juvenile sea bass (Gravato & Santos, 2002). However, B(a)P caused significant increases in mononucleate cells in RTG-2 cells which may indicate an alteration in cell cycle and along with the positive induction of micronuclei could suggest genomic instability. In agreement with the work presented Sanchez and co-workers (2000) concluded that B(a)P increased micronuclei frequencies, but significantly delayed cell-cycle progression in RTG-2 cells. Micronuclei have also been detected in RTG-2 cells following exposure to 5-25 μmol B(a)P (Kolpoth *et al.*, 1999). Using a random amplified polymorphic DNA (RAPD) technique a 24 hour treatment with 0.1 μg ml^{-1} B(a)P or 0.5 μg ml^{-1} B(a)P increased instability of the DNA in RTG-2 cells (Castano & Becceril, 2004).

Micronuclei were detected in both mononucleate and binucleate cells indicating that it was valuable to include the scoring of micronuclei within mononucleate cells (as observed previously, Fenech *et al.*, 2003a) to detect all damaged cells. Research has indicated that aneugens (such as COL) may also induce micronuclei in mononucleate cells and additional value is added to the micronucleus assay by

scoring mononucleate cells (Rosefort *et al.*, 2004). By scoring micronuclei within both mononucleate and binucleate cells the detection of pre-existing DNA damage as well as micronuclei expressed during culture as a result of chromosome breaks is enabled (Fenech *et al.*, 2003b).

A significant reduction in cell viability with UVA (> 2000 J m^{-2}) in RTG-2 cells and UVB in EPCA1 cells (> 200 J m^{-2}) and RTG-2 cells (> 625 J m^{-2}) was observed. Using similar doses of UVR and in agreement with the work presented here, O'Reilly and Mothersill (1997) investigated the *in vitro* effects of UVA and UVB on clonogenic survival of a fish cell line which was found to be sensitive to UVB (> 200 J m^{-2}) and UVA (> 3000 J m^{-2}). It has been suggested that cells are stimulated to undergo a cell death mechanism such as apoptosis following UVB treatment (Nishigaki *et al.*, 1999). UVB has been shown to induce apoptosis in medaka fish cells (OCP13) as well as bring about morphological changes such as cell shrinkage and a reduction in the number of nucleoli at 4 hours post UVB (Nishigaki *et al.*, 1999). Morphological changes were observed in 30-40 % of cells treated with 200-400 J m^{-2} UVB (Nishigaki *et al.*, 1999). In agreement with these data, the pilot study using Annexin V with RTG-2 suggested that apoptosis was induced 6 hours post UVB irradiation although this requires further study to elucidate.

UVB significantly increased DNA damage in both EPCA1 and RTG-2 cells at all doses tested however, there was no significant increase in DNA damage to RTG-2 cells from exposure to UVA. High dose effects of UVB made the comet assay difficult creating an apparent reduction in DNA damage at the highest UVB dose used (500 J m^{-2}) however this

could be a false result due to the assay losing sensitivity through extensive DNA damage. For example, Nishigaki and co-workers (1999) observed changes in cellular distributions, and distortion to the nuclei 4 hours post-200 J m^{-2} UVB irradiation.

In the work presented here, reducing the UVB dose gave a clearer dose-related response indicating that the damage was not so extensive at these doses. This suggests that the damage is so extensive at the higher doses of UVB that the DNA fragments are small so they disperse making 'comets' undetectable and therefore immeasurable. This effect is therefore in part due to a technical effect rather than a mechanistic effect. Similarly, Armstrong and co-workers (2002) demonstrated that exposure to 2.7 – 5.87 mW m^{-2} UVB caused extensive DNA fragmentation in larval Japanese medaka (*Oryzias latipes*) and significant necrosis suggesting an inability to photoreactivate and therefore repair the DNA damage.

A positive increase in the frequencies of micronuclei were observed following exposure to UVA in RTG-2 cells. This was associated with a delayed cell cycle manifested through a reduction in the number of cells entering cytokinesis and therefore being detected as binucleate cells (thus a significant increase in mononucleate cells was observed). A delayed or arrested cell cycle is a general response of cells to DNA damage and the detection of mononucleate cells after UVA irradiation would indicate significant genotoxic damage. Cell cycle checkpoint defects may also cause the formation of micronuclei (Fenech, 2006). A larger proportion of micronuclei were detected in mononucleate cells showing a clear relationship to UVA dose than in binucleate cells. Other workers have produced data which suggests that micronuclei in

mononucleate cells may be useful to distinguish clastogenic agents from aneugenic agents and increase the sensitivity of the test as aneugens are most commonly detected in mononucleate cells (Elhajouji *et al.,* 1998). However there was no clear distinction between mononucleate or binucleate cells with relation to K+ micronuclei (that would indicate an aneugenic effect). An increase in multinucleate cells and nucleoplasmic bridges (NPBs) with UVA dose was also observed. The induction of multinucleated cells has been reported elsewhere for human cells and was suggested to be due to two mechanisms: the fusion of two or more cells shortly after 150 kJ m^{-2} UVA of early G_1 cells, or an impairment of cytokinesis causing delayed formation of multinucleated cells after UVA irradiation in S and G_2 phases (Bråthen *et al.,* 2000). NPBs are indicative of DNA mis-repair, chromosome rearrangement or telomere end-fusions because they are thought to originate from dicentric chromosomes whereby the centromeres have been pulled to the opposite poles of the cell at anaphase and may break to form micronuclei (Fenech, 2006). These data indicate not only the formation of micronuclei following exposure to UVA from aneugenic and clastogenic mechanisms but also suggest other more complex cellular defects (such as inhibition of DNA synthesis (Bånrud *et al.,* 1995; de Laat *et al.,* 1996) that warrant further investigation in order to fully elucidate the mechanisms of UVA induced DNA and cellular damage. This is one of the first applications of anti-kinetochore staining to RTG-2 cells, and the work reported here demonstrates that this technique will be a useful tool in aquatic ecotoxicology.

Increased effects on cell systems by PAHs in the presence of UVR are expected. For example, the repercussions of photocytotoxicity have

been demonstrated *in vivo* to larval stages of oysters when embryos were simultaneously exposed to 5 μg l^{-1} PAH and 6.3 μW cm^{-2} UVB or 456.2 μW cm^{-2} UVA (Lyons *et al.,* 2002) and newt larvae following exposure to > 25 ppb B(a)P and 250 μW cm^{-2} UVA (Fernandez & l'Haridon, 1994). Other studies have shown a significant decrease in bacterial bioluminescence from 1, 5, 50 and 100 ppb B(a)P and 1, 5, 50 and 100 ppb phenanthrene co-exposure followed by 5.8 μW cm^{-2} UVB in developing sea urchins that lead to a significant dose-dependent decrease in growth rates (Steevens *et al.,* 1999). In the work reported here, pre-exposure to B(a)P followed by UVB did not show significant reductions in cell viability however, pre-exposure to B(a)P followed by UVA showed significant reductions in cell viability in all combinations of B(a)P and UVA tested. This has been observed elsewhere for example, the photocytotoxicity of creosote was shown to be 35-fold higher than creosote alone which was suggested to be due to photomodification of the aromatic hydrocarbons in creosote (Schirmer *et al.,* 1999). The potential cellular recovery following pre-treatment with B(a)P and exposure to various doses of UVA was investigated and was of interest because cells have been shown to repair DNA damage following 500 kJ m^{-2} UVA (Bock *et al.,* 1998). However, results suggested a progressive reduction in cell viability over time following treatment with B(a)P and UVA that would imply no cellular recovery. Whether this is related to apoptotic or necrotic mechanisms requires further study.

The effects of UVB alone showed large increases in DNA damage and the interactive effects of B(a)P and higher UVB doses (e.g. 200 and 100 J m^{-2}) showed a lack of consistent evidence to suggest significant increases in DNA damage compared to the high DNA damage caused

by the UVB alone. This was probably due to the detection range of the assay being exceeded and the results did not reflect the effects of the incorporation of B(a)P into the system. Significant DNA damage was observed with UVB > 75 J m^{-2} and B(a)P. Some interactions (e.g. 75 J m^{-2} and 1.0 or 3.2 µg ml^{-1} B(a)P) indicated a synergistic response. However, lower UVB doses (50 and 25 J m^{-2}) with B(a)P suggested additive effects. Work of this nature has been performed on human cells but not previously on fish cells (Crallan *et al.*, 2005). For example, the addition of Fpg enzyme (which enables the detection of oxidised purine bases through the conversion of the DNA base damage to SSBs) caused a noticeable increase in the Tail DNA (%) indicating the presence of oxidative lesions from the combined exposure to 5 µM B(a)P and 100 kJ m^{-2} UVB (Crallan *et al.*, 2005). This data is significant to the work reported here, as it made it possible to detect small but significant increases in DNA damage, indicating that although the precise mechanisms of DNA damage remains unclear, additive effects and some synergistic effects are possible with a combination of B(a)P and UVB. *In vivo*, this data has shown relevance with studies involving the eye, for example an investigation using the comet assay showed that exposure of bovine retinal pigment epithelial (RPE) cells to 100 µM B(a)P rendered them more susceptible to DNA damage induced by 0.09 J cm^{-2} UVB (Patton *et al.*, 2002) suggesting that the repair enzyme systems might be overwhelmed, which may have consequence for fish held in high stocking densities in shallow polluted waters such as some aquaculture facilities.

In the work presented here a range of exposures to B(a)P all significantly increased DNA damage when cells were then exposed to UVA. B(a)P concentration dependent increases in DNA damage were

observed when cells were pre-exposed with B(a)P followed by UVA < 6000 J m^{-2} and results suggested a synergistic effect from B(a)P or UVA alone. Whilst pre-exposure with B(a)P followed by either 8000 or 6000 J m^{-2} UVA caused a significant increase in DNA damage there was no B(a)P concentration related response seen and some of the data was confounded by the effects of large amounts of damage making the comet assay inappropriate or small amounts of damage making the signal to noise ratio too small. Evidence in environmental studies points to the phototoxic components of oil specifically being 3-5 ring PAHs which would include B(a)P (Barron & Ka'aihue, 2001). The data presented here indicate that even low doses of B(a)P are capable of inducing a significant increase in DNA damage under a range of UVA doses. In the field the risks of tissue accumulation of PAHs such as B(a)P depend on factors such as food web accumulation as well as the solubility limited physical bioavailability of the PAH (Barron *et al.*, 2003; Moermond *et al.*, 2007; Verweij *et al.*, 2004). Nevertheless the synergisms between B(a)P and UVA suggest that small amounts of PAHs may well have a profound impact on ecosystem health.

Significant increases in micronuclei frequencies were observed that were higher than either UVA or B(a)P alone. Only the highest combination (0.05 µg ml^{-1} B(a)P + 100 J m^{-2}) tested did not show this effect from B(a)P or UVA which could be due to exceeding the useful damage range for measurements. Significant increases in mononucleated cells following combined exposure as well as increases in nuclear abnormalities such as NPBs and poly-nucleated cells in RTG-2 were observed following exposure to B(a)P and UVA. These data suggested considerable changes in the cell cycle from combined exposures. Interesting results were also seen from the increases in

multiple micronuclei from the lowest B(a)P and UVA combination used which could signify a heritable and possibly unstable mutation. There is no published literature for established fish cell lines comparable to these data with regard to cell cycle delays and nuclear abnormalities following treatment with B(a)P and UVA. However, *in vivo* studies have assessed nuclear abnormalities such as blebbed, notched or lobed nuclei in minnow erythrocytes (Ayllon & Garcia-Vasquez, 2000) and in peripheral erythrocytes following treatment with effluents from a petroleum refinery (Cavas & Ergene-Gözükara, 2005). As demonstrated in the work presented factors other than micronuclei (e.g. nuclear abnormalities or cell cycle alterations) give useful indications to the precise nature of responses to toxicity exposure. For example, Cavas and Ergene-Gözükara (2005) showed that measuring both micronuclei and nuclear abnormalities increased the sensitivity of the micronucleus test system. Additionally, anti-kinetochore staining showed that the interaction between B(a)P and UVA acts both aneugenically and clastogenically (micronuclei were detected with both K+ and K- signals respectively) suggesting a loss of both whole chromosomes and chromosomal fragments. The RTG-2 cell line has been used in ecotoxicological screening for environmental pollutants in combination with other techniques (Castano *et al.*, 2000; Kolpoth *et al.*, 1999; Raisuddin & Jha, 2004) but the use of anti-kinetochore staining has not been previously applied to fish cell lines for use in assessing the genotoxicity of PAHs and/or UVR. From the data reported here RTG-2 cells are a good tool for ecotoxicological testing with the micronucleus assay and anti-kinetochore staining.

The major radical formed from co-exposure to B(a)P and UVA was shown to be hydroxyl ($^{\cdot}OH$). The DMPO-OH spin adduct decays with

time (Finkelstein *et al.*, 1982), most likely because it is metabolised by the cells and, in fact, later samples, which were no doubt less viable, gave a larger spin adduct signal. DMPO-OH can be formed by trapping ·OH radicals, formed directly or from H_2O_2 via the Fenton reaction. In contrast, if superoxide was produced in the system, it would have been initially trapped as DMPO-OOH, but would then rapidly decay to DMPO-OH, so the appearance of the DMPO-OH signal is not unequivocal proof of direct formation of ·OH in the B(a)P/UVA system. Further experiments supported that this radical was being formed directly. A variety of agents (DETAPAC, mannitol, superoxide dismutase, catalase) was used to see whether or not they would be able to determine the ROS produced. Results showed that ROS were not produced via Fenton processes or from superoxide. These data suggested that oxidative stress is a major part of the DNA damage involved in the interaction between B(a)P and UVA. ESR has not been employed previously to the production of ROS from PAHs or UVR in fish cell lines.

These data confirmed the mutagenicity of B(a)P to EPCA1 and RTG-2 cells through reductions in cell viability, increased DNA damage and altered cellular functions that were from aneugenic and clastogenic mechanisms. Irradiation with UVB caused significant reductions in cell viability (potentially involving apoptosis) and increased DNA damage in EPCA1 and RTG-2. However, RTG-2 cells irradiated with UVA showed no significant reductions in cell viability or increased DNA damage but significant increases in cell cycle function and cellular abnormalities. Incubation with B(a)P followed by irradiation with UVA synergistically reduced cell viability, increased DNA damage and altered cellular mechanisms that may be due to both aneugenic and clastogenic

mechanisms. Oxidative activity for the direct formation of hydroxyl radical was shown to be a key element in these processes.

CHAPTER V – THE INTERACTIVE EFFECTS OF B(a)P AND UVR ON CELLS DERIVED FROM MAMMALIAN ORGANISMS

5.1 Introduction

Exposure to chemical mutagens is generally assumed to be the major cause of cellular mutation (Allen-Hoffman & Rheinwald, 1984; Durant *et al.*, 1996; Durant *et al.*, 1999); however, increased or excessive exposure to UVR is well known to induce direct acute and chronic reactions in both human and animal skin (Ichihashi *et al.*, 2003; Seité *et al.*, 2006b). In humans sun behaviour is complex and often linked to particular societies. In Caucasian populations people with Type I skin type (very fair, burns easily) are at greater risk of developing sun related skin damage but may be more likely to take precautions in the sun as opposed to people with Type IV skin (tans easily, rarely burns) who may take more risks in the sun (Thieden *et al.*, 2005). For example, in Europeans, risk behaviour outside the beach in northern Europe, gave a median value of 2.5 solar erythemal doses (SED; 1 SED equates to 100 J m^{-2} normalised to 298 nm) per day (ranging from 0.3-15.8 SEDs per day) compared to risk behaviour at the beach which gave a median value of 4.6 SEDs per day (ranging between 0.3-25.9 SEDs per day) (Thieden *et al.*, 2004). In southern Europe, compared with the beach in northern Europe, the daily UVR doses were almost double (6.9 SEDs per day; ranging from 0.4-32.6 SEDs per day), with adolescents receiving 11.0 SEDs per day (ranging from 4.1-18.3 SEDs per day) and children receiving 44 % of their total measured dose at the beach (Thieden *et al.*, 2004). UVA is known to induce alterations in immune functioning, increase pigmentation and cause other aspects of photoaging (Fourtanier *et al.*, 2008; Moyal & Fourtanier, 2002; Moyal & Fourtanier, 2008; Nghiem *et al.*, 2001; Seite *et al.*, 2006b). For example, 3.4 J cm^2 of UV-solar simulated radiation (290–400 nm) may induce acute

alterations of erythema, induction of SCC in the epidermis, nuclear accumulation of p53, and thymine dimers in the skin (Seité *et al.*, 2006a). UVR has the potential to damage many biological targets and genotoxicity can be induced through DNA damage (Ikehata *et al.*, 2003; Morales *et al.*, 2003; Tsilimigaki *et al.*, 2003), by interactions with other components of the cell (Iordanov *et al.*, 2002) and also when photosensitising chemicals are present (Danaee *et al.*, 2004; Lim & Stern 2005; Vander *et al.*, 2001; Young *et al.*, 1990). Onset of carcinogenesis may also be stimulated by viruses and evidence has suggested that infection with certain human papillomavirus groups may have enhanced the rates of SCC because the virus acted as a cofactor (Ateenyi-Agaba *et al.*, 2004). The therapeutic use of coal tars in many dermatitic disorders has been implicated in the development of skin cancer when combined with UVR (Pion *et al.*, 1995) which has been attributed to the high PAH content in coal tars. PAHs are ubiquitous in urban air pollution and vehicle exhaust emissions contain particulate matter including PAHs (Durant *et al.*, 1996; Liu *et al.*, 2005). PAH concentrations in air may range from < 1 ng m^{-3} in a rural environment to 1-10 ng m^{-3} in urban areas, whilst some occupational environments may have PAH concentrations > 1000 ng m^{-3} (Grimmer, 1983). Four- to six-ring PAHs (including B(a)P) in aerosol particles have a major size range peak at 1.1 μm and PAHs associated with the particles within this size range are easily transported through the upper respiratory tract into the bronchioles and alveoli of the lungs where they can pose a direct adverse health impact (Zhou *et al.*, 2005). These products can circulate around the body and they can be detected in skin, hair and urine (Zhang *et al.*, 2007). The toxicity of some PAHs has been demonstrated to increase in the presence of UVA causing cytotoxic and genotoxic responses (Besaratinia & Pfeifer, 2003; Crallan *et al.*, 2005; Ekunwe *et al.*, 2005; Zheng *et al.*, 2004). For example, concommitant exposure to 0.75, 2.00, or 5.00 μM fluoranthene with 6.1 ± 0.07 J m^{-2}

UVA caused a significant increase in DNA damage and cytotoxicity in HaCaT (human keratinocyte) cells (Zheng *et al.*, 2004). An understanding of the effects of combinations of insults such as PAHs and sunlight may be key in interpreting the huge epidemiological database which has built up on skin cancer and its causes.

5.1.1 Aims and Objectives

The aim of this chapter was to investigate the effects of B(a)P and UVR separately and their interactions in two mammalian cell models: CHO-K1 and 84BR, under *in vitro* conditions. The specific objectives were:

a) To investigate the cytotoxicity of B(a)P (CHO-K1), UVB (CHO-K1) or UVA (CHO-K1 and 84BR) and the potential interactive cytotoxicity of B(a)P and UVA using the NRR assay (CHO-K1 and 84BR).
b) To examine the DNA damage or chromosomal changes caused by B(a)P (CHO-K1 (with and without metabolic activation (S9) in the comet assay) and 84BR), UVB (CHO-K1) or UVA (CHO-K1 and 84BR) using genotoxicity assays.
c) To explore the possible interactions between B(a)P exposed CHO-K1 cells and UVB or UVA radiation using genotoxic assays (comet and micronucleus assays) to examine potential DNA damage or cellular changes including clastogenic or aneugenic effects and to use a primary human cell type (84BR) to further investigate these effects and to consider possible similarities or differences between it and CHO-K1 cells.
d) To examine potential oxidative stress from these interactions in CHO-K1 and 84BR cells using ESR.

5.2 Materials and Methods

5.2.1 Cells and B(a)P Exposure Conditions

The CHO-K1 cell line and 84BR cells were cultured under the cell culture conditions set out in Chapter 2, Section 2.3. CHO-K1 and 84BR cells at 70-80 % confluence were exposed to various concentrations of B(a)P (0.00, 0.05, 0.10, 0.32, 1.00 and 3.20 μg ml^{-1}) in medium containing 1 % FBS (prepared as stated in Chapter 2, Section 2.5.5). Metabolic activation of B(a)P was conducted as stated in Chapter 2, Section 2.5.6.

5.2.2 Assays of Cell Viability and Cytotoxicity

To assess cell viability prior to comet experiments, trypan blue was used as described in Chapter 2, Section 2.4.1. Dual staining and Annexin V-FITC Apoptosis Detection were conducted according to the methods in Chapter 2, Sections 2.4.2 to 2.4.3. Results were expressed as a percentage where applicable. The NRR assay was conducted as stated in Chapter 2, Section 2.4.4. CHO-K1 cells were exposed to various concentrations of B(a)P (0.0, 0.1, 1.0 and 3.2 μg ml^{-1}) or UVB doses (0*, 200, 500, 625, 750, 875 and 1000 J m^{-2}). CHO-K1 and 84BR cells were also exposed to various doses of UVA (0*, 500, 1000 and 4000 J m^{-2}) or B(a)P (0.0, 0.1, 1.0 and 3.2 μg ml^{-1}) and UVA (0*, 500, 1000 and 4000 J m^{-2}). Results were expressed as a percentage of the control (Babich *et al.*, 1988).

5.2.3 Comet Assay

Unless stated, cell viability for comet assay experiments was always over 90 % in accordance with the recommendations of Tice *et al.* (2000) as measured by trypan blue (Chapter 2, Section 2.4.1). The comet

assay was conducted as stated in the protocol in Chapter 2, Sections 2.5.1 to 2.5.4 with the modifications determined through optimisation in Chapter 3. For example, unwinding times and electrophoresis times for CHO-K1 cells were 40 minutes and 20 minutes, respectively. Only cells at 70-80 % confluence were used, replicate slides were made for each treatment condition, and experiments were conducted in duplicate. The UVR sources used are detailed in Chapter 2, Section 2.7. For experiments using B(a)P, CHO-K1 and 84BR cells were exposed to various concentrations of B(a)P (0.0, 0.1, 1.0 and 3.2 μg ml^{-1}) in medium (Chapter 2, Section 2.5.5). The cells were incubated for 6 hours (with and without metabolic activation (Chapter 2, Section 2.5.6)) or 24 hours (without metabolic activation) at 37 ± 1 °C according to the recommendations set out by Tice *et al.* (2000). For experiments using UVR, CHO-K1 cells were prepared onto slides (Chapter 2, Section 2.5.1) and exposed to various doses of UVB (0*, 200, 350 and 500 J m^{-2}). The comet assay protocol was then adhered to (Chapter 2, Section 2.5) with the following modifications. Immediately following irradiation, slides were transferred to chilled lysing solution (Section 2.5.1) and processed (Chapter 2, Sections 2.5.2 to 2.5.4). For experiments to investigate interactive toxicity, CHO-K1 and 84BR cells were exposed to various concentrations (0.00, 0.05, 0.10, 0.32, 1.00 and 3.20 μg ml^{-1}) of B(a)P in medium for 24 hours (without metabolic activation) (Chapter 2, Section 2.5.5) and prepared onto CometSlides™ (Chapter 2, Section 2.5.1). Following this, CHO-K1 and 84BR cells were exposed to various doses of UVA (0*, 25, 50, 100 and 200 J m^{-2}), then immediately placed on ice. Slides were transferred to chilled lysing solution (Chapter 2, Section 2.5.1) and processed according to Chapter 2, Sections 2.5.2 to 2.5.4.

5.2.4 Micronucleus Assay

CHO-K1 cells were seeded at a density of 4 x 10^5 cells ml^{-1} in growth medium in 25 cm^2 flasks for B(a)P experiments or Petri dishes for UVA or interactive toxicity experiments and incubated at 37 ± 1 °C for 24 hours. 84BR cells were seeded at a density of 1 x 10^6 cells ml^{-1} in growth medium in 25 cm^2 flasks for B(a)P experiments or Petri dishes for UVA or interactive toxicity experiments and incubated at 37 ± 1 °C for 48 hours in 5 % CO_2. B(a)P was added to the CHO-K1 cell monolayer at various concentrations (0.000, 0.025, 0.100, 1.000 and 3.200 µg ml^{-1}), and to the 84BR cells at 0.00 and 0.05 µg ml^{-1} prepared in medium as described in Chapter 2, Section 2.5.5. Cells were incubated at 37 ± 1 °C for 24 ± 1 hours (CHO-K1) or 48 ± 1 hours in 5 % CO_2 (84BR). After the exposure period had elapsed, the medium was discarded and the monolayer washed twice with PBS. Cyto B (3 µg ml^{-1}) in solvent (DMSO) was added to the cells in growth medium and the flasks incubated at 37 ± 1 °C for 24 ± 1 hours (CHO-K1) and 48 ± 1 hours in 5 % CO_2 (84BR). For UVA investigations, cells were washed twice with PBS and treated with various doses of UVA (0*, 25, 50 and 100 J m^{-2}). Cyto B (3 µg ml^{-1}) in solvent (DMSO) was immediately added to the cells in GM following irradiation and the dishes incubated at 37 ± 1 °C for 24 ± 1 hours (CHO-K1) or 48 hours in 5 % CO_2 (84BR cells). For experiments into interactive toxicity, cells were washed twice with PBS and incubated with B(a)P (0.025 µg ml^{-1}) for 6 hours, washed twice with PBS and treated with various doses of UVA (0*, 25, 50 and 100 J m^{-2}). Cyto B (3 µg ml^{-1}) in solvent (DMSO) was immediately added to the cells with growth medium and the dishes incubated at 37 ± 1 °C for 24 ± 1 hours (CHO-K1) and 48 hours in 5 % CO_2 (84BR). Following these incubation periods and treatments, the cells were removed from the incubator, and treated as Chapter 2, Sections 2.6.1 to 2.6.2.1 for Giemsa and anti-kinetochore staining.

5.2.5 ESR Measurements on B(a)P and UVR Treated Cells (CHO-K1, 84BR)

ESR measurements were made according to the protocol in Chapter 2, Section 2.6.4.1. CHO-K1 and 84BR cells were treated for 24 hours with B(a)P (3.2 μg ml^{-1}). Cells from each 25 ml culture flask were trypsinised and re-suspended in GM and the cell suspension was divided into two before being centrifuged at 800 rpm for 8 minutes. The cell pellet was washed 3 times with PBS to remove serum and free B(a)P and the cell pellet from each half was re-suspended in 50 μl of 250 mM DMPO in PBS prior to irradiation. The spin traps TMPol and POBN were both used at a concentration of 50 mM. The samples were then placed in the microwave cavity of the spectrometer and acquisition of spectra started within 1 minute of the end of irradiation (UVB: (Phillips, UK), UVA: (XX-40 FB, Spectroline, USA)).

5.2.6 Statistics

For comet assay data, the data were collected from Excel and transferred into MINITAB for statistical analysis. Comet assay data was non-parametric, therefore, the median was used for comparisons. Mann-Whitney U tests were performed on the data to investigate the level of significant difference between the medians. The data was then transferred into SigmaPlot to make box and whisker plots. For micronucleus experiments, the results are presented in tables and Mann-Whitney U tests performed on the data to investigate the level of significant difference between the medians.

5.3 Results

5.3.1 The Effects of B(a)P Alone on Mammalian Cell Lines CHO-K1 and 84BR.

These experiments were designed to investigate the baseline effects of the PAH B(a)P on mammalian cells (CHO-K1, 84BR). The effects of B(a)P were assessed through a suite of assays; NRR, comet and micronucleus, and a study with ESR in CHO-K1 cells. The effects of B(a)P were also investigated in 84BR cells, using the comet assay and the micronucleus assay, for comparison purposes with data obtained from studies with B(a)P and UVR. Interactive toxicity (i.e. B(a)P and UVR) was also investigated in both cell types using ESR. Results are presented below (Sections 5.3.1.1 to 5.3.4.4).

5.3.1.1 The NRR Cytotoxicity Assay for B(a)P Effects on the CHO-K1 Cell Line.

Initially, B(a)P cytotoxicity was investigated for CHO-K1 cells using the NRR assay to assess cell viability through the retention of neutral red dye in the lysosomes. After exposure of CHO-K1 cells to B(a)P for 24 hours at various concentrations (0.0, 0.1, 1.0 and 3.2 $\mu g\ ml^{-1}$) the viability of the cells was examined. Results indicated that 0.1 and 1.0 $\mu g\ ml^{-1}$ B(a)P reduced cell viability to approximately 96 % ($p > 0.05$) and 88 % ($p > 0.05$) respectively (no significant differences). B(a)P at 3.2 $\mu g\ ml^{-1}$ reduced cell viability to approximately 68 % ($p < 0.05$). Results for this assay are presented in Figure 5.1.

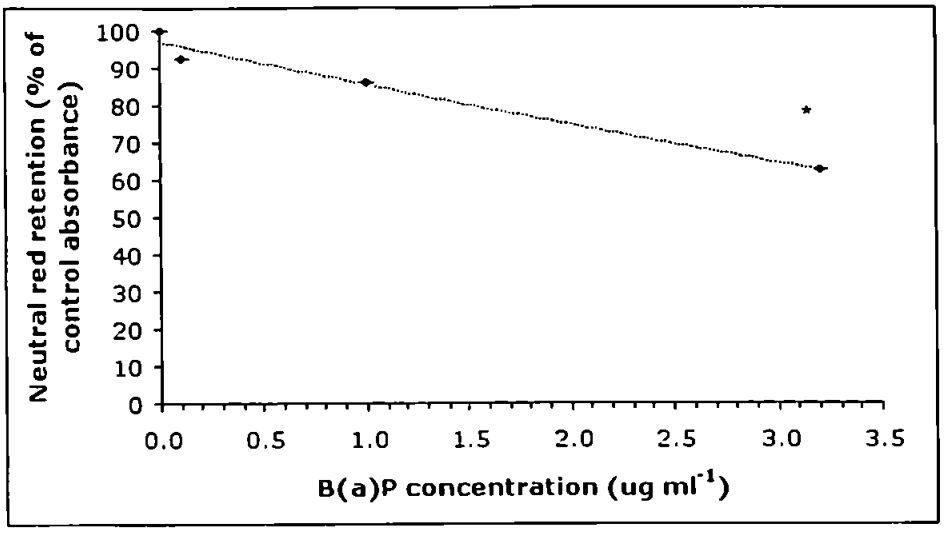

Figure 5.1 Cell viability assessed through the uptake of neutral red dye by CHO-K1 cells following exposure of cells to 24 hour B(a)P at various concentrations (0.0, 0.1, 1.0 and 3.2 μg ml^{-1}). Cell viability is expressed as a percentage of the control (% control) with the control value being 100 %. Asterisks (*) indicate a significant difference from the control (Mann-Whitney U test, $p < 0.05$).

5.3.1.2 The Comet Assay for B(a)P Effects on Mammalian Cell Lines (CHO-K1 and 84BR).

5.3.1.2.1 CHO-K1

The comet assay was performed after treating CHO-K1 cells for 6 hours (with or without metabolic activation (S9)) or 24 hours (without S9) with B(a)P (0.0, 0.1, 1.0 and 3.2 μg ml^{-1}). DNA damage was measured by the % Tail DNA. Percentage tail DNA revealed that DNA was not significantly ($p > 0.05$) damaged following 6 hour exposure to 0.1 μg ml^{-1} B(a)P without exogenous metabolic activation (S9) (Figure 5.2a). However, there was significant ($p < 0.05$) DNA damage to cells following 6 hours exposure to 1.0 and 3.2 μg ml^{-1} B(a)P (without S9) (Figure 5.2a). Results showed that there was a significant difference ($p < 0.05$)

between the control and all exposures for the B(a)P group with S9 (Figure 5.2a), with a higher significance ($p < 0.0001$) than the group without S9, although the S9 exposures displayed no dose response (Figure 5.2b). For CHO-K1 cell exposed to B(a)P for 24 hours (without S9), there a dose-response was shown, and a significant difference from the control ($p < 0.0001$) shown for all tested concentrations (Figure 5.2c).

5.3.1.2.2 84BR

The comet assay was performed after treating 84BR cells for 24 hours (without S9 exogenous metabolic activation) with B(a)P (0.00, 0.05, 0.10, 0.32, 1.00 and 3.20 μg ml^{-1}). DNA damage was measured as the % Tail DNA. Percentage Tail DNA revealed that DNA was not significantly damaged ($p > 0.05$) following 24 hour exposure to 0.05 μg ml^{-1} B(a)P. There was significant DNA damage ($p < 0.001$) to cells following 24 hours exposure to 0.1, 1.0 and 3.2 μg ml^{-1} B(a)P, and significant DNA damage ($p < 0.01$) to cells treated with 0.32 μg ml^{-1} B(a)P. The results for 84BR cells are presented in Figure 5.3.

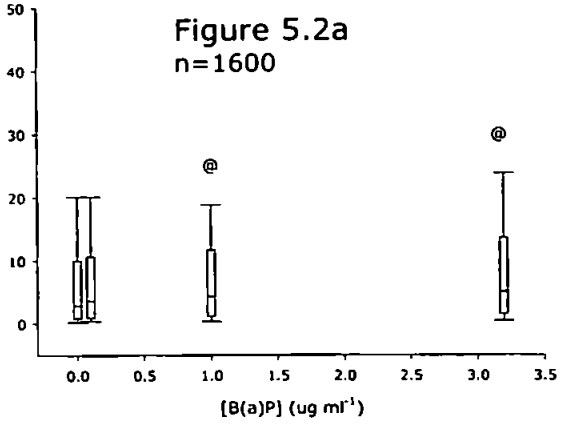

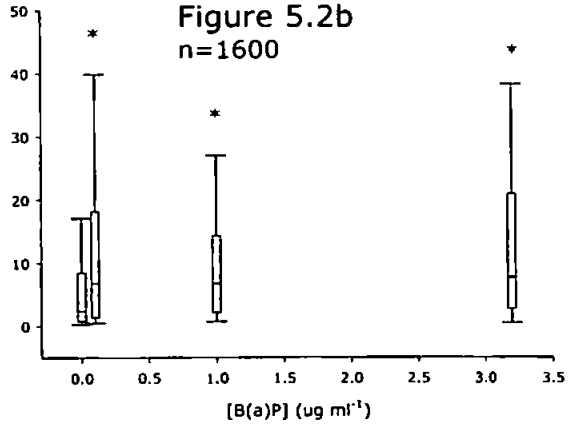

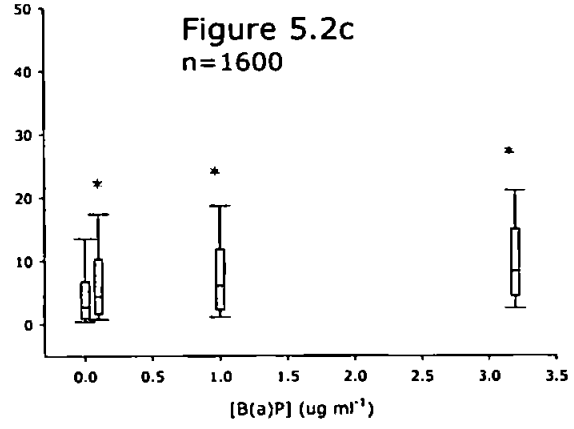

Figure 5.2 Median DNA damage to CHO-K1 cells following exposure to 6 hour B(a)P at various concentrations (0.0, 0.1, 1.0 and 3.2 μg ml^{-1}) without (Figure 5.2a) exogenous metabolic activation (S9), with S9 (Figure 5.2b) or following exposure to 24 hour B(a)P (0.0, 0.1, 1.0 and 3.2 μg ml^{-1}) without S9 (Figure 5.2c). Data marked with @ are significantly different to the control (Mann-Whitney U test, $p < 0.05$) or with * are significantly different to the control (Mann-Whitney U test, $p < 0.0001$).

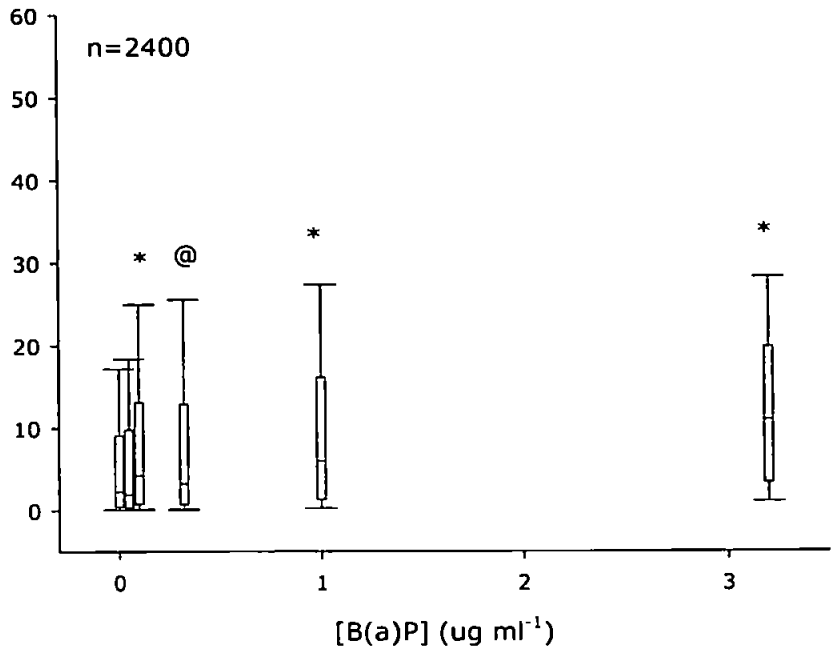

Figure 5.3 Median DNA damage to 84BR cells following exposure to 24 hour B(a)P at various concentrations (0.00, 0.05, 0.10, 0.32, 1.00 and 3.20 μg ml^{-1}). DNA damage is assessed by the % Tail DNA. Data marked with @ are significantly different to the control (Mann-Whitney U test, $p < 0.01$) or with * are significantly different to the control (Mann-Whitney U test, $p < 0.001$).

5.3.1.3 The Micronucleus Assay for B(a)P Effects on Cell Lines CHO-K1 and 84BR.

5.3.1.3.1 CHO-K1

Various concentrations of B(a)P were tested (0.00, 0.05, 0.10, 1.00 and 3.20 μg ml^{-1}) in CHO-K1 cells to investigate genomic instability by means of the micronucleus assay. The effects of B(a)P on micronuclei formation were examined using two different staining techniques to investigate the potential mechanisms of action following B(a)P exposure.

One thousand binucleate cells were scored per treatment group in each experiment, and the experiments were carried out in duplicate. The results for CHO-K1 cells are presented in Table 5.1. Results from Giemsa staining showed that numbers of mononucleate cells vary slightly within a scoring protocol of 1000 binucleate cells, ranging from 127.5 ± 10.61 (0.05 μg ml^{-1}) to 208 ± 16.97 (0.00 μg ml^{-1}) and all treatment groups were significantly lower than the control ($p < 0.05$). Micronuclei were manually scored in 1000 binucleate cells and indicated a weak increase in the number of micronuclei as the concentration of B(a)P increased to a maximum of 7.0 ± 1.41 at the highest concentration used (3.20 μg ml^{-1}) which was significantly different from the control ($p < 0.05$). Associated with this increase was a slight enhancement of multinucleated cells and the maximum number of multinucleated cells seen here was 2.0 ± 2.83 (3.20 μg ml^{-1}); which was significantly different from the control ($p < 0.05$). There were no nucleoplasmic bridges (NPB) observed throughout these experiments and few incidences of more than one micronucleus being observed within the cell (0.05 μg ml^{-1}).

Using the anti-kinetochore stain, 1000 binucleate cells were scored and the numbers of mononucleate cells ranged from 90.5 ± 4.95 (0.00 μg ml^{-1}) to 199.5 ± 2.12 (3.20 μg ml^{-1}). All treatment groups were significantly different from the control ($p < 0.05$). As before using Giemsa stain, no NPB were observed in this cell line using this stain. There was a significant increase ($p < 0.05$) in total induced micronuclei following exposure to all concentrations of B(a)P. The majority of micronuclei were detected within a binucleate cell (3.20 μg ml^{-1} B(a)P gave an average of 29.5 ± 2.12 micronuclei), but were also detected within mononucleate cells, for example 1.5 ± 0.71 micronuclei at 1.00 μg ml^{-1} B(a)P and 2.0 ± 1.41 at 3.20 μg ml^{-1} B(a)P.

5.3.1.3.2 84BR

B(a)P (0.00, 0.05 μg ml^{-1}) was tested with 84BR cells to investigate the effect of B(a)P alone at these doses, prior to testing interactive effects with UVA by means of the micronucleus assay, thus all doses used with CHO-K1 were not tested in these cells. As before, the effects of B(a)P on micronucleus formation were examined using two different staining techniques (Giemsa and anti-kinetochore antibody) to investigate the responses following B(a)P exposure. Experiments scored 1000 binucleate cells per treatment group, and were duplicated in separate experiments. The results for 84BR cells are presented in Table 5.2. Results from the Giemsa stain showed that numbers of mononucleate cells varied slightly within a scoring protocol of 1000 binucleate cells, ranging from 147.5 ± 13.44 (0.00 μg ml^{-1}) down to 138 ± 9.90 (0.05 μg ml^{-1}) which was not a significant difference ($p > 0.05$). Micronuclei were scored in 1000 binucleate cells, but mononucleate cells containing micronuclei were also counted. Results indicated a weak increase in the number of micronuclei with the addition of 0.05 μg ml^{-1} B(a)P into the system to 1.0 ± 0.00 micronuclei in mononucleate cells and to 0.5 ± 0.71 micronucleus in binucleate cells but neither of these results was significantly different to the control ($p > 0.05$). There were no NPB or multinucleated cells observed throughout these experiments and no incidence of more than one micronucleus observed within the cell. Using anti-kinetochore antibody, 1000 binucleate cells were scored and the numbers of mononucleate cells ranged from 129 ± 16.97 (0.00 μg ml^{-1}) to 162 ± 4.24 (0.05 μg ml^{-1}). No micronuclei were observed within a mononucleate cell, and only 1.0 ± 0.00 micronuclei was detected within a binucleate cell containing a K+ signal, again indicating an aneugenic mode of action for this chromosomal effect, even at this low dose, although none of these results were significantly different from the control ($p > 0.05$).

Table 5.1 Effect of various concentrations of B(a)P (0.00, 0.05, 0.10, 1.00 and 3.20 μg ml^{-1}) on the mean generation (±SE) of micronuclei in the CHO-K1 cell line (n=32,064) using Giemsa or anti-kinetochore stain. There were no nucleoplasmic bridges or incidences of 2 or 4+ nuclei. Significant differences (Mann-Whitney U-test $p<0.05$) from the control are indicated (*).

[B(a)P]	0.00 μg ml^{-1}	0.05 μg ml^{-1}	0.10 μg ml^{-1}	1.00 μg ml^{-1}	3.20 μg ml^{-1}
Cellular Response-Giemsa					
Mononucleate	208.0 ± 16.97	127.5 ± 10.61*	161.0 ± 5.66*	160.0± 74.23*	141.5 ± 17.68*
Binucleate	1000.0 ± 0.00	1000.0 ± 0.00	1000.0 ± 0.00	1000.0 ± 0.00	1000.0 ± 0.00
Micronucleus/Binucleate	2.0 ± 1.41	1.0 ± 1.41	2.5 ± 0.71	3.5 ± 1.10*	7.0 ± 1.41*
3 nuclei	Not observed	0.5 ± 0.71	Not observed	Not observed	Not observed
Multinucleate cells	Not observed	Not observed	0.5 ± 0.71	2.0 ± 0.94*	2.0 ± 2.83*
Cellular Response-anti-kinetochore stain					
Mononucleate	90.5 ± 4.95	141.0 ± 15.56*	120.5± 23.33*	178.0 ± 7.07*	199.5 ± 2.12*
Binucleate	1000.0 ± 0.00	1000.0 ± 0.00	1000.0 ± 0.00	1000.0 ± 0.00	1000.0 ± 0.00
Micronucleus/Mononucleate	Not observed	Not observed	Not observed	1.5 ± 0.71	2.0 ± 1.41
Micronucleus/Binucleate	2.0 ± 1.41	0.5 ± 0.71	8.5 ± 3.54*	19.5 ± 6.36*	29.5 ± 2.12*
K+ Mononucleate	Not observed	Not observed	Not observed	1.5 ± 0.71	1.5 ± 2.12
K- Mononucleate	Not observed	Not observed	Not observed	Not observed	0.5 ± 0.71
K+ Binucleate	Not observed	Not observed	8.0 ± 2.83*	17.5 ± 3.54*	28.0 ± 4.24*
K- Binucleate	2.0 ± 1.41	0.5 ± 0.71	0.5 ± 0.71	2.5 ± 3.54	1.5 ± 2.12

Table 5.2 Effect of B(a)P (0.00 and 0.05 μg ml^{-1}) on the generation of micronuclei in 84BR cells (n=13,730) using Giemsa or anti-kinetochore stain. There were no nucleoplasmic bridges, incidences of 2 or 3 nuclei, multinucleate cells or micronuclei in mononucleate cells detected using anti-kinetochore stain.

[B(a)P]	0.00 μg ml^{-1}	0.05 μg ml^{-1}
Cellular Response-Giemsa stain		
Mononucleate	147.5 ± 13.44	138.0 ± 9.90
Binucleate	1000.0 ± 0.00	1000.0 ± 0.00
Micronucleus/Mononucleate	Not observed	1.0 ± 0.00
Micronucleus/Binucleate	0.5 ± 0.71	0.5 ± 0.71
Cellular Response-anti-kinetochore stain		
Mononucleate	129.0 ± 16.97	162.0 ± 4.24
Binucleate	1000.0 ± 0.00	1000.0 ± 0.00
Micronucleus/Binucleate	Not observed	1.0 ± 0.00
K+ Binucleate cells	Not observed	1.0 ± 0.00

5.3.2 The Effects of UVR on the CHO-K1 and 84BR Cell Lines.

5.3.2.1 The Effects of UVB (CHO-K1) and UVA (CHO-K1 and 84BR) on Cell Viability.

The effects on cell viability and the cytotoxicity effects of UVB were assessed in CHO-K1 cells. Cell viability was initially assessed with trypan blue dye (Figure 5.4a). Results showed no loss in cell viability which remained at 100 % up to 750 J m^{-2} UVB where cell viability dropped off to 70 %. Cell viability dropped to 45 % at 1000 J m^{-2} UVB and 50 % at 875 J m^{-2} UVB. Dual stain fluorescence was also used to investigate viability. Results of dual staining showed a dose-dependent decrease in cell viability from 100 % at 0.0 J m^{-2} UVB to 20 % viability at 1000 J m^{-2} UVB. Cell viability was reduced to approximately 50 % at 625 J m^{-2} UVB (Figure 5.4a). Using the NRR assay, exposure of CHO-K1

cells to various UVB doses (0*, 200, 500, 625, 750, 875 and 1000 J m^{-2}), indicated significant differences between the sham irradiated control (0*) and all doses tested ($p < 0.01$). Doses above 500 J m^{-2} reduced cell viability to less than 50 %, with 200 J m^{-2} reducing viability to approximately 80 %. NRR results for the CHO-K1 cells are presented in Figure 5.4b.

Following these experiments with UVB, cell viability and the cytotoxicity of various doses of UVA (0*, 500, 2000 and 4000 J m^{-2}) were tested with trypan blue, dual stain fluorescence and NRR assays in CHO-K1 and 84BR cells. Results with trypan blue and dual staining were over 97 % viability at all doses for both cell types and are not presented here. Results of the NRR assay show little difference between the cell types and little reduction in cell viability. There was no significant difference between the control and 500 J m^{-2} ($p > 0.05$) in CHO-K1 cells. CHO-K1 viability was reduced significantly at 2000 J m^{-2} ($p = 0.046$, $p < 0.05$) and also dropped to 84 % ($p < 0.05$) at 4000 J m^{-2}. Cell viability in 84BR cells was above 90 % and there was no significant difference ($p > 0.05$) between the control and in all UVA doses tested. Results for CHO-K1 and 84BR cells are presented in Figure 5.5.

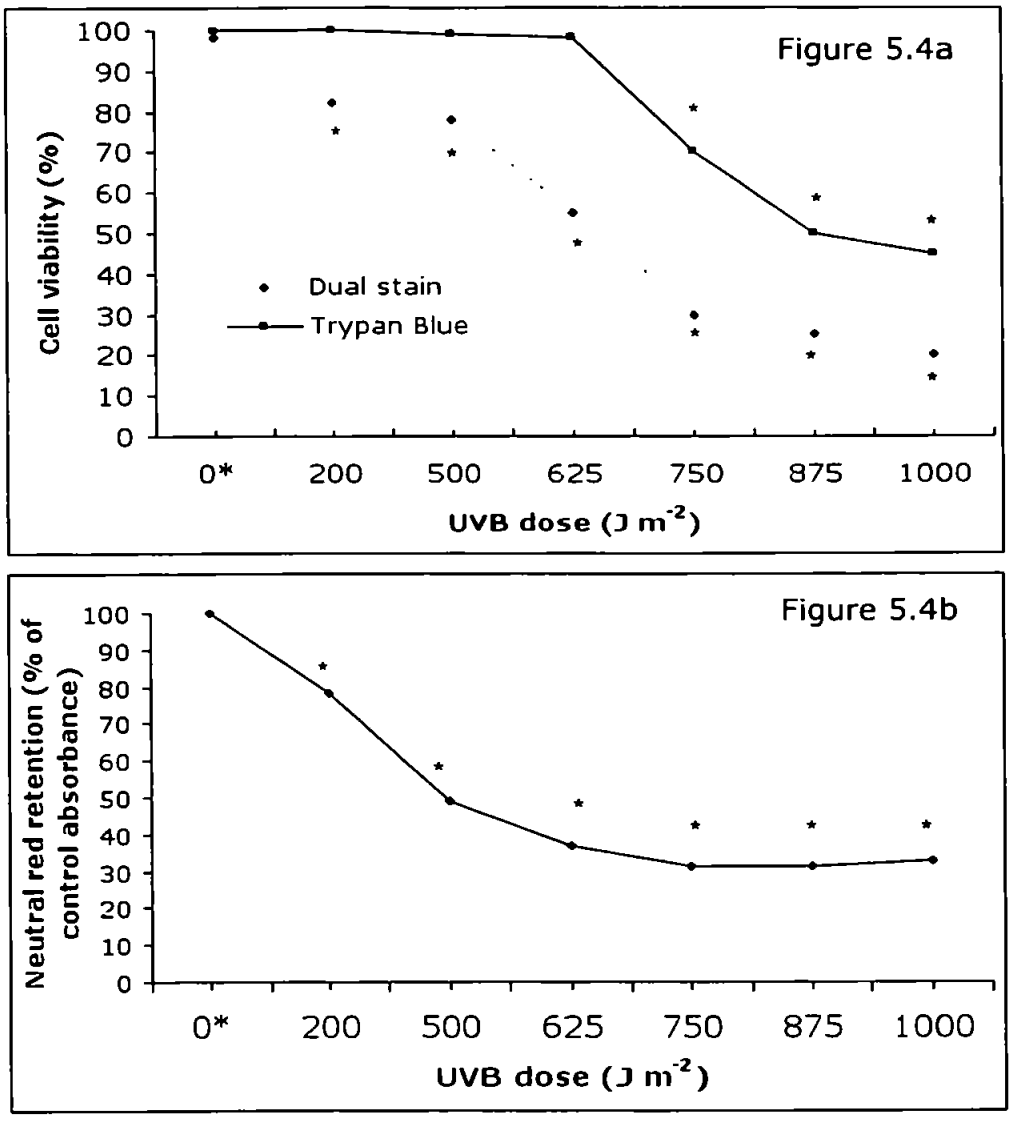

Figure 5.4. Cell viability in CHO-K1 cells assessed through trypan blue and dual stain fluorescence technique (Figure 5.4a) or neutral red retention (NRR) assay (Figure 5.4b) following exposure to various doses of UVB (0*, 200, 500, 625, 750, 875 and 1000 J m^{-2}). Cell viability is expressed as percentage viability (%) for trypan blue and dual stain fluorescence assays or as a percentage of the control (%) for the NRR assay where control values are 100 %. 0* value is sham irradiated (Data marked with * are significantly different to the control, Mann-Whitney U test, $p < 0.01$).

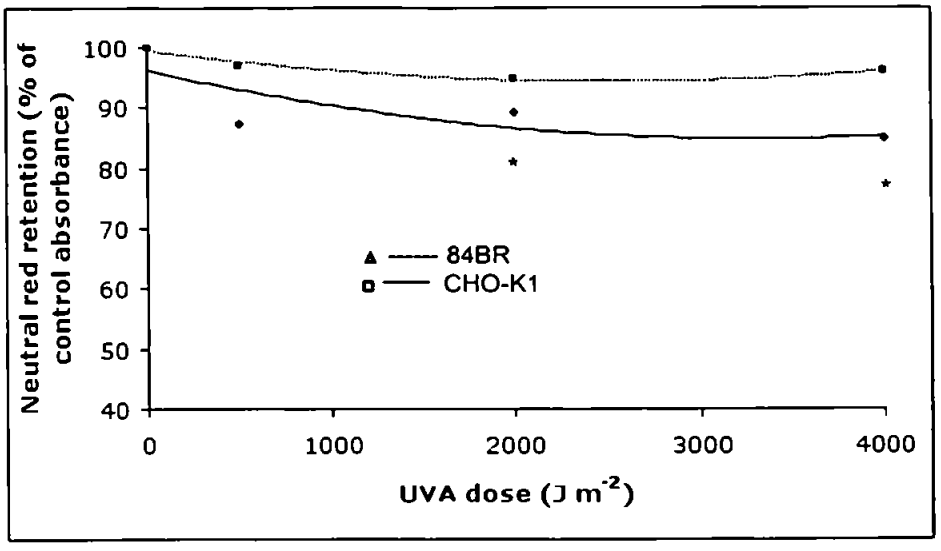

Figure 5.5. Cell viability in CHO-K1 and 84BR cells following exposure to various doses of UVA (0*, 500, 2000 and 4000 J m^{-2}). 0* value is sham irradiated. Cell viability is assessed through NRR assay and values are presented as a percentage of the control value. Data marked with * (CHO-K1) are significantly different to the control (Mann-Whitney U test, $p < 0.05$).

5.3.2.2 The Comet Assay for UVR Effects on CHO-K1 (UVB and UVA) and 84BR (UVA) Cells.

Following the cytotoxicity studies, experiments were carried out on the CHO-K1 cell line to investigate the genotoxic effect of UVB (0*, 200, 350 and 500 J m^{-2}) using the comet assay on the lower less cytotoxic UVB doses as measured through trypan blue, dual stain fluorescence and NRR assay in Section 5.3.2.1 or UVA (0*, 500, 2000 and 4000 J m^{-2}). The comet assay experiments showed a significant effect ($p < 0.0001$) between the sham irradiated control (0*) and all UVB doses tested (200, 350 and 500 J m^{-2}) (Figure 5.6a). There was no clear dose response shown, with a significant increase initially between 0* J m^{-2} and 200 J m^{-2} from a median of 6 % (0*) to a median value of 27 % (200 J m^{-2}) and

then a linear response in the level of DNA damage observed to a median of 30 % (500 J m^{-2}). There was no significant difference in the median DNA damage caused between any of the UVB doses tested ($p > 0.05$). Following the responses to UVB, the dose was dropped to investigate DNA damage at UVB doses lower then 200 J m^{-2} and investigated in the RTG-2 cell line (Chapter 4, Section 4.3.2.2). For UVA, there was a significant increase ($p < 0.01$) in DNA damage between the sham irradiated control (0*) and 2000 and 4000 J m^{-2} UVA and all doses tested increased dose dependently ($p < 0.0001$) with increasing UVA (Figure 5.10) in CHO-K1 cells (Figure 5.6b). In 84BR cells there was no significant increase ($p > 0.05$) in DNA damage between the sham irradiated control (0*) and all UVA doses tested (0*, 500, 2000 and 4000 J m^{-2}) with no dose dependent response ($p > 0.05$) with increasing UVA (Figure 5.7).

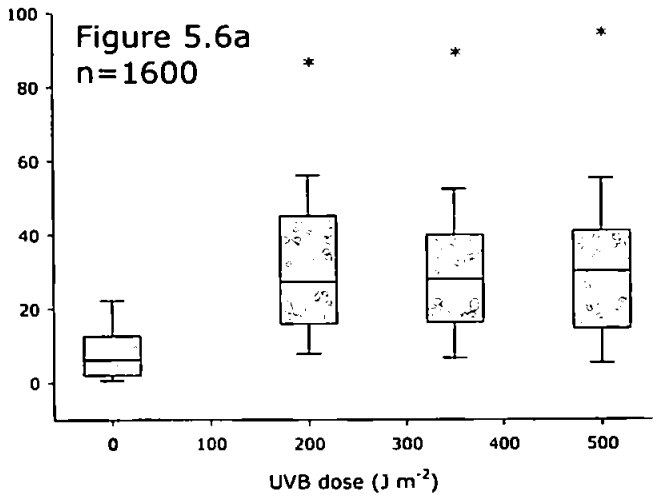

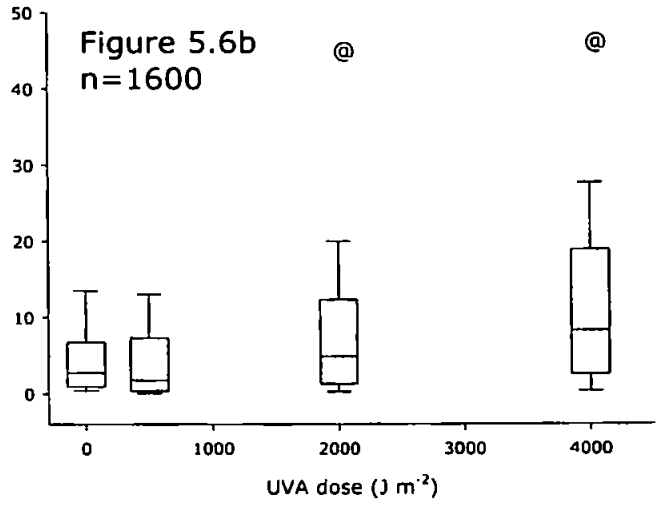

Figure 5.6 DNA damage to CHO-K1 cells following exposure to various doses of UVB (0*, 200, 350 and 500 J m^{-2}) (Figure 5.6a) or UVA (0*, 500, 2000 and 4000 J m^{-2}) (Figure 5.6b). DNA damage is assessed by the % Tail DNA. All UVB doses tested are significantly different (*) (Mann-Whitney U test, $p < 0.0001$) from the sham irradiated control (0*) but not significantly different from each other (Mann-Whitney U test, $p > 0.05$). UVA doses which are significantly different (Mann-Whitney U test, $p < 0.01$) from the sham irradiated control (@) are indicated and all doses are significantly different from each other (Mann-Whitney U test, $p < 0.0001$).

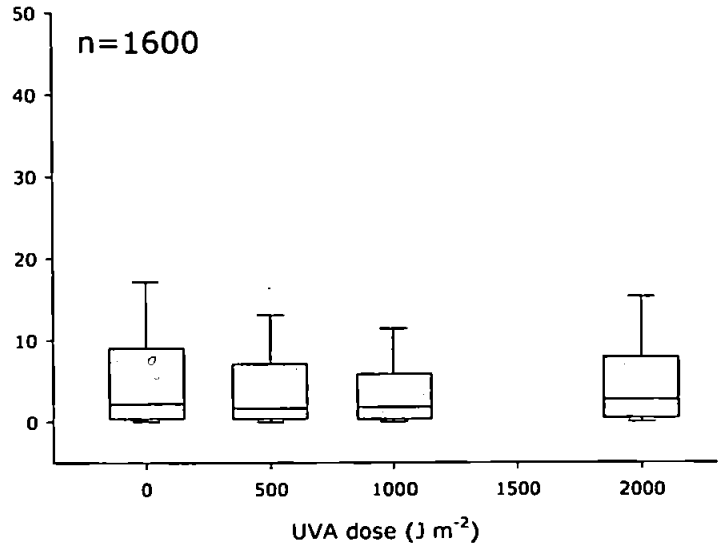

Figure 5.7 DNA damage to 84BR cells following exposure to various doses of UVA (0*, 500, 1000 and 2000 J m^{-2}). DNA damage is assessed by the % Tail DNA. There was no significant difference (Mann-Whitney U test, $p > 0.05$) between the sham irradiated control (0*) or any of the UVA doses tested.

5.3.3 The Micronucleus Assay for UVA effects on Mammalian Cells CHO-K1 and 84BR.

5.3.3.1 CHO-K1

Various doses of UVA (0*, 25, 50, 100 and 200 J m^{-2}) were used to irradiate CHO-K1 cells in order to investigate the subsequent occurrence of genomic instability as evaluated by means of the micronucleus assay. Experiments scored at least 1000 cells per treatment group, and the experiments were duplicated. The results for CHO-K1 cells are presented in Table 5.3. The results from using the Giemsa stain showed that numbers of mononucleate cells varied widely within a scoring protocol of a total of 1000 binucleate and mononucleate cells, ranging

from 205 ± 9.90 (0* J m^{-2}) to 527.25 ± 97.06 (100 J m^{-2}) and for all exposure groups, the frequencies of mononucleate cells were significantly different from the control value ($p < 0.05$). The numbers of binucleate cells scored also varied with exposure to UVA, from 1000 ± 0.00 (0* J m^{-2}) to 636.5 ± 21.92 (25 J m^{-2}). All exposure groups tested were significantly different from the control ($p < 0.05$).

Micronuclei were scored in mononucleate and binucleate cells and scores indicate a large and significant increase in the number of micronuclei in both mononucleate and binucleate cells as the UVA dose increases ($p < 0.05$). Associated with this increase is an interesting enhancement of NPB at all UVA doses, to a maximum observed number of 6.0 ± 2.45 (100 J m^{-2}) which was significantly different from the control ($p < 0.05$). Equally interesting, throughout these experiments were the many incidences of more than one micronucleus which were observed within cells at all UVA doses. These incidences ranged from 0.5 ± 0.71 (25 J m^{-2}) which was not a significant increase from the control ($p > 0.05$) to a 7.0 ± 4.08 frequency of 2 nuclei (100 J m^{-2}) which was a significant increase from the control ($p < 0.05$). There was also a significant increase ($p < 0.05$) in the frequency of 2 nuclei at the highest dose tested (200 J m^{-2}). Occurrences of four or more micronuclei within a cell were limited to 100 J m^{-2} and 200 J m^{-2} (2.25 ± 1.71 and 2.5 ± 2.08 respectively) and were not significantly different from the control ($p > 0.05$). Using the anti-kinetochore antibody, micronuclei were scored in a total of 1000 mononucleate and binucleate cells due to the observed increased frequency in mononucleate cells. The numbers of mononucleate cells ranged from 200.5 ± 4.95 (0* J m^{-2}) to 420.5 ± 7.78 (50 J m^{-2}) which were significantly different from the control ($p < 0.05$). The numbers of binucleate cells scored also varied with the addition of UVA, from 1000 ± 0.00 (0* J m^{-2}) to 588.5 ± 13.44 (50 J m^{-2}) and all exposure groups tested were significantly different from the

control ($p < 0.05$). There was not a significant difference in the numbers of micronuclei observed in either a mononucleate or a binucleate cell ($p > 0.05$). The largest frequency of micronuclei observed within a mononucleate cell was 11 ± 1.41 (200 J m^{-2}), whilst 10 ± 1.41 were detected within a binucleate cell (100 J m^{-2}). There was no significant difference in the induction of micronuclei following 25 J m^{-2} UVA ($p > 0.05$), but the other doses tested were all significantly different from the control ($p < 0.05$) in both mononucleate and binucleate cells. Of the cells containing micronuclei, a larger proportion of micronuclei were detected that contained a K+ signal ($p < 0.05$) but these were located in both mononucleate and binucleate cells indicating a strongly aneugenic mode of action. However, as micronuclei were also detected with K- signals in significant frequencies ($p < 0.05$), it would suggest that UVA induces both a clastogenic and aneugenic response in these cells.

Table 5.3 Effect of various doses of UVA on the mean generation (±SE) of micronuclei in the CHO-K1 cell line (n=28,444) using Giemsa or anti-kinetochore stain. There were no multinucleate cells observed. Significant differences (Mann-Whitney *U* test $p<0.05$) from the control are indicated (*).

UVA dose (J m^{-2})	**0***	**25**	**50**	**100**	**200**
Cellular Response-Giemsa					
Mononucleate	205.0 ± 9.90	381.5 ± 20.51*	429.00 ± 16.21*	527.25 ± 97.06*	467.50 ± 29.00*
Binucleate	1000.0 ± 0.00	636.5 ± 21.92*	636 ± 17.68*	495.00±106.08*	601.00 ± 28.65*
Micronucleus/Mononucleate	0.5 ± 0.71	1.5 ± 0.71	4.00 ± 0.82*	6.25 ± 1.71*	11.75 ± 2.06*
Micronucleus/Binucleate	0.5 ± 0.71	2.5 ± 0.71*	5.00 ± 0.82*	9.50 ± 3.00*	7.50 ± 1.00*
Nucleoplasmic Bridge	Not observed	0.5 ± 0.71	1.25 ± 0.96	6.00 ± 2.45*	4.00 ± 2.94*
2 nuclei	Not observed	0.5 ± 0.71	2.25 ± 0.96	7.00 ± 4.08*	4.25 ± 2.22*
3 nuclei	Not observed	0.5 ± 0.71	2.25 ± 1.26	4.50 ± 5.20*	1.50 ± 1.91
4+ nuclei	Not observed	Not observed	Not observed	2.25 ± 1.71	2.50 ± 2.08
Cellular Response-anti-kinetochore stain					
Mononucleate	200.5 ± 4.95	380.0 ± 22.63*	420.5 ± 7.78*	390.5 ± 9.19*	333.0 ± 18.38*
Binucleate	1000.0 ± 0.00	641.5 ± 13.44*	588.5 ± 13.44*	645.0 ± 18.38*	673.0 ± 15.56*
Micronucleus/Mononucleate	0.5 ± 0.71	1.5 ± 0.71	5.5 ± 0.71*	7.5 ± 0.71*	11.0 ± 1.41*
Micronucleus/Binucleate	Not observed	2.5 ± 0.71	5.0 ± 1.41*	10.0 ± 1.41*	6.5 ± 0.71*
K+ Mononucleate cells	Not observed	1.0 ± 0.00	2.5 ± 0.71*	5.5 ± 0.71*	7.0 ± 1.41*
K- Mononucleate cells	0.5 ± 0.71	0.5 ± 0.71	3.0 ± 1.41*	2.0 ± 0.00*	4.0 ± 0.00*
K+ Binucleate cells	Not observed	1.5 ± 0.71	3.5 ± 0.71*	6.0 ± 1.41*	4.0 ± 0.00*
K- Binucleate cells	Not observed	1.0 ± 0.00	1.5 ± 0.71	3.5 ± 0.71*	2.5 ± 0.71*

5.3.3.2 84BR

A systematically increasing series of doses of UVA (0*, 25, 50, 100 and 200 J m^{-2}) were used to irradiate 84BR cells in order to investigate any consequent genomic instability as identified by the micronucleus assay. The effects of UVA on micronucleus formation were investigated using both Giemsa and anti-kinetochore staining techniques to investigate the potential mechanisms of action (clastogenic or aneugenic, respectively) following UVA exposure. Experiments scored at least 1000 cells per treatment group, and the experiments were duplicated. The results for 84BR cells are presented in Table 5.4. The results using Giemsa stain showed that numbers of mononucleate cells varied widely within a scoring protocol of a total of 1000 binucleate and mononucleate cells, ranging from 196 ± 28.28 (0* J m^{-2}) to 496 ± 14.76 (200 J m^{-2}) which was a significant difference from the control value ($p < 0.05$). The numbers of binucleate cells scored also varied significantly ($p < 0.05$) with the addition of UVA, from 1000 ± 0.00 (0* J m^{-2}) to 735.5 ± 21.61 (50 J m^{-2}). Micronuclei were scored in mononucleate and binucleate cells and indicated a strong and significant increase in the number of micronuclei in both mononucleate and binucleate cells and in the total frequencies of micronuclei induced as the UVA dose increases ($p < 0.05$). Associated with this increase is an interesting enhancement of NPB in all UVA doses (except for exposure to 25 J m^{-2} UVA which was not a significant response: $p > 0.05$), to a maximum observed number of 4.0 ± 3.37 at the maximum UVA dose used (200 J m^{-2}) which was a significant difference from the control value ($p < 0.05$). Throughout these experiments many incidences of more than one micronucleus were observed within the cell at all UVA doses. These incidences ranged from 0.25 ± 0.50 (50 J m^{-2}) which was not significantly different to the control ($p > 0.05$) to a 4.25 ± 1.71 frequency of 2 nuclei (100 J m^{-2}) which was a significant difference from the control value ($p < 0.05$).

Occurrences of four or more micronuclei within a cell were limited to 50 J m^{-2}, 100 J m^{-2} and 200 J m^{-2} (0.25 ± 0.50 ($p > 0.05$), 2.25 ± 2.06 ($p < 0.05$) and 1.25 ± 1.50 ($p > 0.05$) respectively). There was only one incidence of multinucleated cells observed of 0.25 ± 0.50 (100 J m^{-2}) which was not significant ($p > 0.05$).

Using the anti-kinetochore staining technique, micronuclei were scored in a minimum of 1000 mononucleate and binucleate cells per treatment group and experiments were duplicated. The numbers of mononucleate cells ranged from 193.5 ± 23.33 (0* J m^{-2}) to 532.5 ± 4.95 at the highest UVA dose used (200 J m^{-2}) which was a significant difference from the control value ($p < 0.05$). Frequencies of binucleate cells ranged from 629.5 ± 9.19 at 25 J m^{-2}, down to 495 ± 8.49 at the highest dose used (200 J m^{-2}) which was a significantly less than the control value ($p < 0.05$). There was no significant difference in the numbers of micronuclei observed in either a mononucleate or a binucleate cell and the total micronuclei induced were significantly higher than the control value in all concentrations tested ($p < 0.05$). The largest frequency of micronuclei observed within a mononucleate cell was 12.5 ± 2.12 (200 J m^{-2}), whilst 10.5 ± 2.12 micronuclei were detected within a binucleate cell (100 J m^{-2}) which were all significantly higher than the control ($p < 0.05$). Of the cells containing micronuclei, a larger and significant proportion ($p < 0.05$) of micronuclei detected contained a K+ signal but were located in both mononucleate and binucleate cells. These results indicate a strongly aneugenic mode of action. However, as micronuclei were also detected in significant frequencies ($p < 0.05$) with K- signals, it would suggest that UVA induces both a clastogenic and aneugenic response in these cells.

Table 5.4 Effect of various doses of UVA on the mean generation (±SE) of micronuclei in 84BR cells using Giemsa or anti-kinetochore stain (n=42,318). Significant differences (Mann-Whitney *U* test $p<0.05$) from the control are indicated (*).

UVA dose (J m^{-2})	0*	25	50	100	200
Cellular Response-Giemsa					
Mononucleate	196.0 ± 28.28	387.0 ± 12.73*	344.50 ± 26.46*	448.75 ± 24.13*	496.00 ± 14.76*
Binucleate	1000.0 ± 21.61	633.5 ± 12.02*	735.50 ± 21.61*	617.50 ± 15.63*	584.75 ± 62.91*
Micronucleus/Mononucleate	Not observed	2.5 ± 0.71	4.25 ± 1.26*	5.50 ± 1.29*	10.00 ± 2.16*
Micronucleus/Binucleate	Not observed	1.5 ± 0.71	5.00 ± 0.82*	8.75 ± 2.22*	7.50 ± 1.29*
Nucleoplasmic Bridge	Not observed	0.5 ± 0.71	2.25 ± 0.50	3.00 ± 1.41	4.00 ± 3.37*
2 nuclei	Not observed	0.5 ± 0.71	2.25 ± 1.71	4.25 ± 1.71*	2.75 ± 0.96
3 nuclei	Not observed	Not observed	1.25 ± 0.96	1.50 ± 1.29	2.50 ± 1.91
4+ nuclei	Not observed	Not observed	0.25 ± 0.50	2.25 ± 2.06	1.25 ± 1.50
Multinucleate cells	Not observed	Not observed	Not observed	0.25 ± 0.50	Not observed
Cellular Response-anti-kinetochore stain					
Mononucleate	193.5 ± 23.33	389.5 ± 3.54*	391.5 ± 9.19*	442.5 ± 20.51*	532.5 ± 4.95*
Binucleate	1000.0 ± 0.00	629.5 ± 9.19*	625.0 ± 1.41*	584.5 ± 7.78*	495.0 ± 8.49*
Micronucleus/Mononucleate	Not observed	1.5 ± 0.71	4.0 ± 1.41*	9.0 ± 1.41*	12.5 ± 2.12*
Micronucleus/Binucleate	0.5 ± 0.71	3.5 ± 0.71*	5.5 ± 0.71*	10.5 ± 2.12*	8.0 ± 1.41*
K+ Mononucleate cells	Not observed	1.0 ± 0.00	2.5 ± 0.71	6.0 ± 1.41*	7.5 ± 0.71*
K- Mononucleate cells	Not observed	0.5 ± 0.71	1.5 ± 0.71	3.0 ± 0.00*	5.0 ± 1.41*
K+ Binucleate cells	Not observed	2.5 ± 0.71	3.5 ± 0.71*	6.5 ± 2.12*	4.5 ± 0.71*
K- Binucleate cells	0.5 ± 0.71	1.0 ± 0.00	2.0 ± 0.00	4.0 ± 0.00*	3.5 ± 0.71*

5.3.4 Interactive Toxicity for B(a)P and UVA Effects on Mammalian Cells (CHO-K1, 84BR).

5.3.4.1 The NRR Assay for Assessing the Interactive Cytotoxicity of B(a)P and UVA in the Mammalian Cells CHO-K1 and 84BR.

The cytotoxicity of interactions between B(a)P and UVA was assessed for CHO-K1 and 84BR cells through the NRR assay. After exposure of CHO-K1 or 84BR cells for 24 hours to various concentrations of B(a)P (0.0, 0.1, 1.0 and 3.2 μg ml^{-1}) and then various UVA doses (0*, 500, 2000 and 4000 J m^{-2}) the viability of the cells was analysed. CHO-K1 cells showed a small reduction in cell viability at all concentrations of B(a)P interacting with 500 J m^{-2}, which was significant in the two highest B(a)P concentrations, reducing cell viability down to 89 % (1.0 μg ml^{-1}, $p < 0.05$) and 84 % ($p < 0.05$) at the highest B(a)P dose used (3.2 μg ml^{-1}) (Figure 5.8a). B(a)P concentrations with higher UVA (2000 and 4000 J m^{-2}) caused a greater interactive effect, and reduced cell viability significantly at all combinations ($p < 0.05$). Exposure to the highest dose of B(a)P (3.2 μg ml^{-1}) interacting with 2000 and 4000 J m^{-2} UVA resulting in 68 % ($p < 0.05$) and 50 % ($p < 0.05$) cell viability respectively (Figure 5.8a). In 84BR cells, cell viability was significantly reduced at all B(a)P and UVA combinations ($p < 0.05$) except for 0.1 μg ml^{-1} B(a)P interacting with 4000 J m^{-2} ($p > 0.05$). Viability was reduced to 40 % ($p < 0.05$) in the highest combined exposure (3.2 μg ml^{-1} + 4000 J m^{-2}) (Figure 5.8b). The results of the NRR assay were used to select suitable doses for use in comet assay experiments; UVA doses could be selected on the basis of observed cytotoxicity. Those doses that reduced viability to less than 60 % were omitted from the experiment (3.2 μg ml^{-1} + 4000 J m^{-2}).

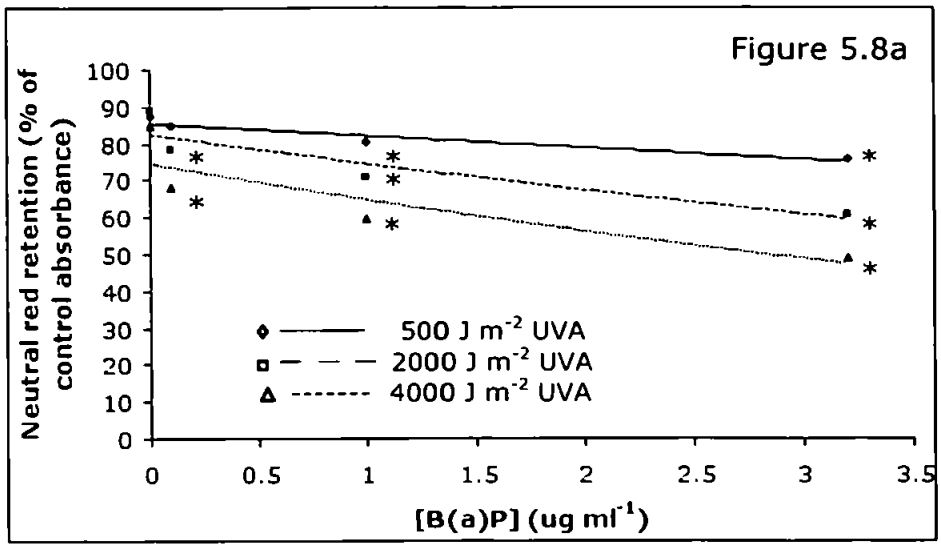

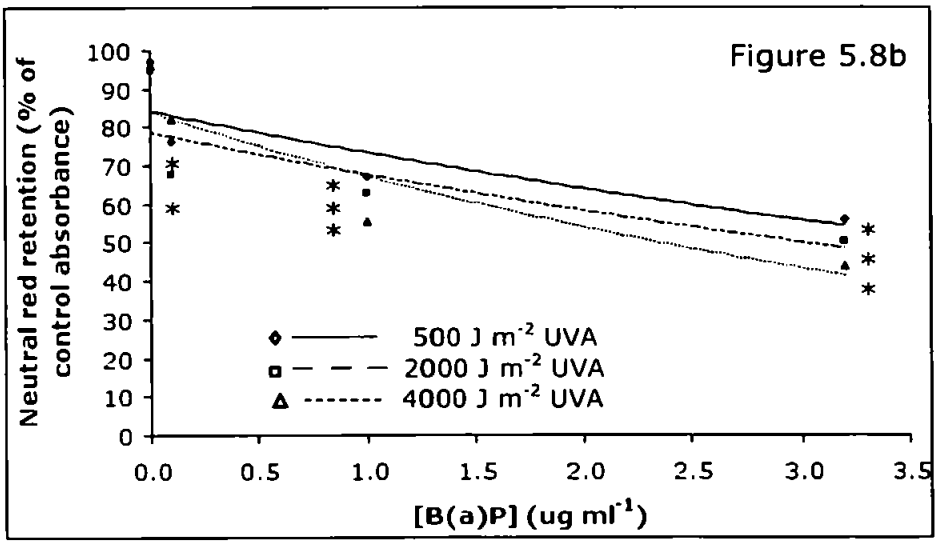

Figure 5.8 Cytotoxicity in CHO-K1 (Figure 5.8a) and 84BR (Figure 5.8b) cells following 24 hours pre-incubation with B(a)P (0.0, 0.1, 1.0 and 3.2 μg ml^{-1}) and exposure to various doses of UVA (0*, 500, 2000 and 4000 J m^{-2}). 0* value is sham irradiated for the same time as 4000 J m^{-2} UVA. Cytotoxicity is assessed through NRR assay and values are presented as a percentage of the control value. All CHO-K1 data are significantly different (*) to the control (Mann-Whitney U test, $p < 0.05$) with the exception of 0.1 μg ml^{-1} interacting with 500 J m^{-2} (Mann-Whitney U test, $p > 0.05$) whilst all 84BR data are significantly different (*) to the control (Mann-Whitney U test, $p < 0.05$) with the exception of 0.1 μg ml^{-1} B(a)P interacting with 4000 J m^{-2} (Mann-Whitney U test, $p > 0.05$).

5.3.4.2 The Comet Assay for Assessment of the Interactive Toxicity Between B(a)P and UVA in the Mammalian Cells CHO-K1 and 84BR.

Following the cytotoxicity experiments (Section 5.3.4.1) UVA doses were selected (500, 1000 and 2000 J m^{-2}) for use in comet assay experiments. The comet assay was performed after treating CHO-K1 for 24 hours with B(a)P (0.0, 0.1, 1.0, 2.0 and 3.2 µg ml^{-1}), and 84BR cells for 24 hours with B(a)P (0.00, 0.05, 0.10, 0.32, 1.00 and 3.20 µg ml^{-1}), and subsequent exposure to UVA (0*, 500, 1000 and 2000 J m^{-2}). Cell viability was assessed prior to all comet assay experiments with trypan blue dye and cell viability was over 90 % in all cases (data not shown). DNA damage was measured as the % Tail DNA.

5.3.4.2.1 CHO-K1

Results for CHO-K1 cells showed a gradual increase in DNA damage as exposure to UVA was increased with the appearance of a plateau response with increasing concentrations of B(a)P (Figure 5.9). Median values of % Tail DNA for CHO-K1 cells are maximised at 2000 J m^{-2} with B(a)P, at values between 34 % (3.2 µg ml^{-1} B(a)P and 2000 J m^{-2} UVA) and 37 % (0.1 µg ml^{-1} B(a)P and 2000 J m^{-2} UVA). All results of interactive toxicity between B(a)P and UVA showed a significant increase from the control ($p < 0.0001$).

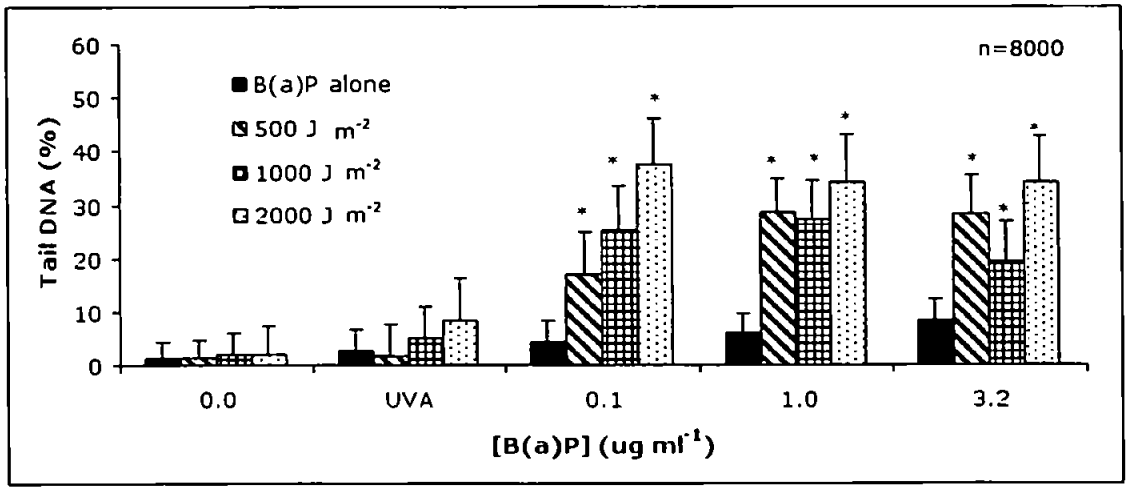

Figure 5.9 DNA damage to CHO-K1 cells following pre-incubation for 24 hours with B(a)P (0.0, 0.1, 1.0 and 3.2 μg ml^{-1}) and exposure to various doses of UVA (0*, 500, 1000 and 2000 J m^{-2}). DNA damage is assessed by the % Tail DNA. Significant differences (Mann-Whitney-U test, $p<0.0001$) from the combined B(a)P and UVA irradiated response are indicated (*). Plots for B(a)P alone are significantly different to the control (Mann-Whitney U test, $p < 0.0001$) at all concentrations.

5.3.4.2.2 84BR

84BR cells pre-treated with B(a)P for 24 hours before UVA exposure showed a statistically significant increase ($p < 0.001$) in DNA damage above the damage seen with B(a)P alone (Figure 5.10). There was no significant difference between the controls or UVA treated cells ($p > 0.05$), but damage was significant in cells treated with B(a)P and exposure to UVA ($p < 0.001$). The greatest damage was observed at the combined highest doses received by the cells (1.0 and 3.2 μg ml^{-1} + 2000 J m^{-2}), with the same level of damage seen at the next highest dose (3.2 μg ml^{-1} + 1000 J m^{-2}), here DNA damage reached 100 % ($p < 0.0001$). At combinations of 1.0 and 3.2 μg ml^{-1} + 2000 J m^{-2} and 3.2 μg ml^{-1} + 1000 J m^{-2}, cells became too damaged to score, in some cases,

it was not possible to score the damage, so DNA damage was measured as 100 %.

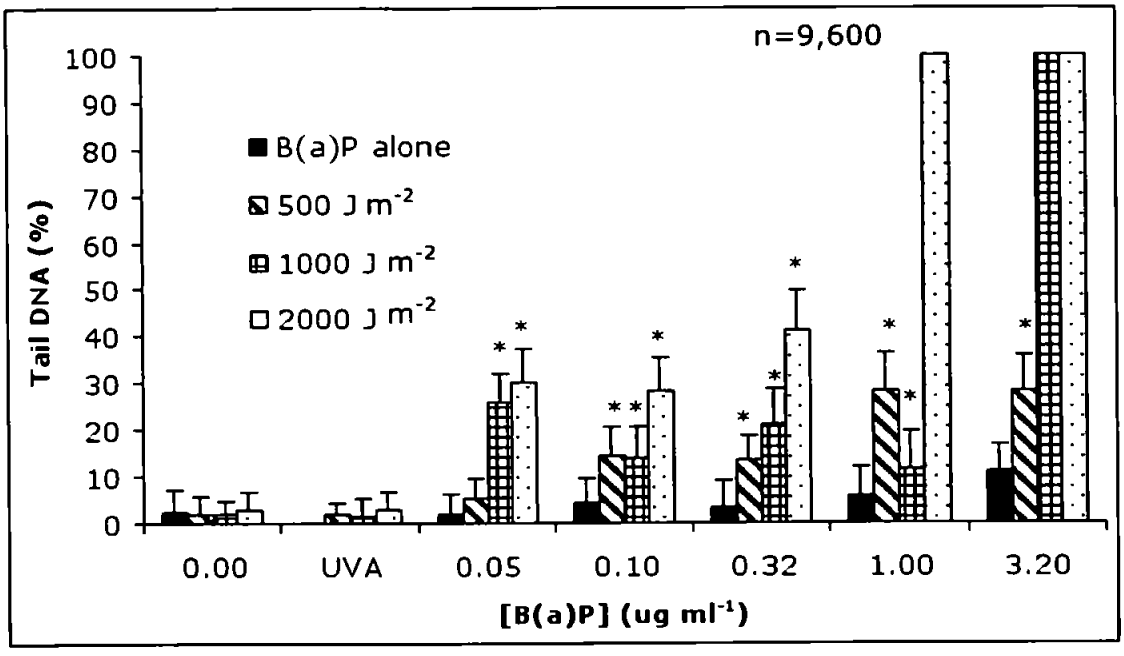

Figure 5.10 DNA damage to 84BR cells following pre-incubation for 24 hours with B(a)P (0.00, 0.05, 0.10, 0.32, 1.00 and 3.20 μg ml^{-1}) and exposure to various doses of UVA (0*, 500, 1000 and 2000 J m^{-2}). DNA damage is assessed by the % Tail DNA. Significant differences (Mann-Whitney-U test, $p<0.001$) from the combined B(a)P and UVA irradiated response are indicated (*).

5.3.4.3 The Micronucleus Assay for Interactive Toxicity of B(a)P and UVA Effects on the Mammalian Cells CHO-K1 and 84BR.

5.3.4.3.1 CHO-K1

Various doses of UVA (0*, 25, 50 and 100 J m^{-2}) were tested in CHO-K1 cells following their incubation with 0.05 μg ml^{-1} B(a)P to investigate interactive effects by means of the micronucleus assay. As previously, interactive effects on micronucleus formation were examined using both

Giemsa and anti-kinetochore staining techniques to investigate the potential mechanisms of action (clastogenic or aneugenic, respectively). Experiments scored 1000 binucleate cells per treatment group, and the experiments were duplicated. The results for CHO-K1 cells are presented in Table 5.5. With no pre-incubation with 0.05 μg ml^{-1} B(a)P and a dose of 0* J m^{-2} UVA, it was possible to remain with the standard protocol employed for the previous micronucleus experiments by counting micronuclei within 1000 binucleate cells. At this dose level, 205.5 ± 12.02 mononucleate cells were counted within 1000 ± 0.00 binucleate cells. However, as UVA doses were introduced to the B(a)P pre-incubated cells a total of 1000 binucleate and mononucleate cells were scored in order to investigate the ratio of the two cell types to each other and to be able to detect as many micronuclei as possible. The results from using Giemsa stain show that numbers of mononucleate cells vary widely within a scoring protocol of a total of 1000 binucleate and mononucleate cells, appearing to range dose responsively from 533.5 ± 34.45 (0.05 μg ml^{-1} B(a)P + 25 J m^{-2}), through 644.75 ± 35.77 (0.05 μg ml^{-1} B(a)P + 50 J m^{-2}) to 725.5 ± 32.91 (0.05 μg ml^{-1} B(a)P + 100 J m^{-2}) which were all significantly different from the control ($p < 0.05$). These increases in mononucleate cells from combined exposure were significantly higher than with UVA alone ($p < 0.05$). The numbers of binucleate cells scored also varied with exposure to UVA dropping proportionately with increasing UVA dose from 510.5 ± 7.51 binucleate cells (0.05 μg ml^{-1} B(a)P + 25 J m^{-2}), through to 402.25 ± 62.97 binucleate cells (0.05 μg ml^{-1} B(a)P + 50 J m^{-2}), to 332.75 ± 46.36 (0.05 μg ml^{-1} B(a)P + 100 J m^{-2}) which were all significantly different from the control ($p < 0.05$). Micronuclei were scored in mononucleate and binucleate cells and indicate a significant increase in the total number of micronuclei induced ($p < 0.05$) and also in both mononucleate and binucleate cells to a maximum of 12.25 ± 1.26 (mononucleate cells: 0.05 μg ml^{-1} B(a)P + 100 J m^{-2}) and 12.75 ± 2.06

(binucleate cells: 0.05 μg ml^{-1} B(a)P + 100 J m^{-2}) as the UVA dose increases. These responses are a significant increase ($p < 0.05$) in total micronuclei from either UVA or B(a)P alone in the CHO-K1 cell line and all combined doses tested demonstrated a synergistic effect from the combination of B(a)P and UVA. Along with the increase in micronuclei observed, there were many incidences of two micronuclei observed within a cell at all UVA doses. These incidences ranged from 1.75 ± 0.50 (0.05 μg ml^{-1} B(a)P + 25 J m^{-2}) to a 9.0 ± 1.41 frequency of 2 nuclei (0.05 μg ml^{-1} B(a)P + 100 J m^{-2}) which were all significantly different from the control ($p < 0.05$). There was a significant increase in the frequency of three micronuclei detected in the cell at all interactive doses tested, whereas with four or more micronuclei, only the dose 0.05 μg ml^{-1} B(a)P + 25 J m^{-2} produced significantly more micronuclei ($p < 0.05$). Multiple micronuclei were observed at all doses and the effects in treatment groups 0.05 μg ml^{-1} B(a)P + 25 J m^{-2} and 0.05 μg ml^{-1} B(a)P + 50 J m^{-2} were significantly higher than the multiple micronuclei observed in either UVA alone or B(a)P alone in CHO-K1 cells ($p < 0.05$). As with the effects seen in CHO-K1 cells following UVA irradiation alone, an increase of NPB was observed at all interactive doses, to a maximum observed number of 4.0 ± 0.82 (0.05 μg ml^{-1} B(a)P + 100 J m^{-2}) but only doses 0.05 μg ml^{-1} B(a)P + 25 J m^{-2} and 0.05 μg ml^{-1} B(a)P + 100 J m^{-2} gave a significant increase from the control ($p < 0.05$). This response appears marginally lower than the response seen for UVA alone or B(a)P alone in this cell line but there is no significant difference ($p > 0.05$) in the induction of NPB by a combined dose of B(a)P and UVA. Use of the anti-kinetochore stain was employed to investigate the mechanisms of action of interactive toxicity to the CHO-K1 cell line. Again, due to the observed increases in mononucleate cells, micronuclei were scored in a total of 1000 mononucleate and binucleate cells. At the control dose, 182.5 ± 26.16 mononucleate cells were scored alongside 1000 binucleate cells. With

interactive toxicity, the numbers of mononucleate cells ranged from 464 ± 15.56 (0.05 μg ml^{-1} B(a)P + 25 J m^{-2}) to 722.5 ± 14.85 (0.05 μg ml^{-1} B(a)P + 100 J m^{-2}) which was significantly higher than the control value ($p < 0.05$). The numbers of binucleate cells scored also varied with the addition of UVA, in this case dropping proportionately with increasing UVA dose from 556.5 ± 7.78 binucleate cells (0.05 μg ml^{-1} B(a)P + 25 J m^{-2}), through to 413.0 ± 16.97 binucleate cells (0.05 μg ml^{-1} B(a)P + 50 J m^{-2}), to 300.5 ± 4.95 (0.05 μg ml^{-1} B(a)P + 100 J m^{-2}) which were all significantly different from the control ($p < 0.05$). These figures are similar to the Giemsa stained cells. Again there was little difference in the numbers of micronuclei observed in either a mononucleate or a binucleate cell and the results indicate a significant increase in the number of total micronuclei induced ($p < 0.05$). The largest frequency of micronuclei observed within a mononucleate cell was 12.5 ± 0.71 (0.05 μg ml^{-1} B(a)P + 100 J m^{-2}), whilst 12.5 ± 2.12 were detected within a binucleate cell (0.05 μg ml^{-1} B(a)P + 100 J m^{-2}) and all of the results were significantly higher than the control value ($p < 0.05$). These results are similar to the results found with using Giemsa staining, but again the induction of total micronuclei using anti-kinetochore staining was significantly higher than the micronuclei results seen for UVA or B(a)P alone ($p < 0.05$). Of the cells containing a micronucleus, a significantly larger proportion of micronuclei detected contained a K+ signal but were located in both mononucleate and binucleate cells ($p < 0.05$). These results indicate a strongly aneugenic mode of action. However, as micronuclei were also detected with significantly increased ($p < 0.05$) K- signals, it would suggest that B(a)P and UVA induce both a clastogenic and aneugenic response in CHO-K1 cells.

Table 5.5 Effect of interactive toxicity following pre-incubation with 0.05 μg ml^{-1} B(a)P with various doses of UVA (0*, 25, 50 and 100 J m^{-2}) on the mean (±SE) generation of micronuclei in CHO-K1 cells (n=34,949) using Giemsa or anti-kinetochore stain. There were no multinucleate cells observed. Significant differences (Mann-Whitney *U* test $p<0.05$) from the control are indicated (*).

Dose	0.00 μg ml^{-1} B(a)P + 0* J m^{-2} UVA	0.05 μg ml^{-1} B(a)P + 25 J m^{-2} UVA	0.05 μg ml^{-1} B(a)P + 50 J m^{-2} UVA	0.05 μg ml^{-1} B(a)P + 100 J m^{-2} UVA
Cellular Response-Giemsa stain				
Mononucleate	205.5 ± 12.02	533.50 ± 34.45*	644.75 ± 35.77*	725.50 ± 32.91*
Binucleate	1000.0 ± 0.00	510.50 ± 7.51*	402.25 ± 62.97*	332.75 ± 46.36*
Micronucleus/Mononucleate	Not observed	8.25 ± 0.96*	9.75 ± 2.87*	12.25 ± 1.26*
Micronucleus/Binucleate	Not observed	11.25 ± 0.96*	10.00 ± 2.94*	12.75 ± 2.06*
Nucleoplasmic Bridge	Not observed	2.25 ± 0.50*	2.00 ± 1.41	4.00 ± 0.82*
2 nuclei	Not observed	7.75 ± 0.96*	9.75 ± 0.96*	9.00 ± 1.41*
3 nuclei	Not observed	5.50 ± 1.73*	6.25 ± 1.89*	7.75 ± 1.71*
4+ nuclei	Not observed	6.75 ± 0.96*	1.75 ± 0.50	2.25 ± 0.96
Cellular Response-anti-kinetochore stain				
Mononucleate	182.5 ± 26.16	464.0 ± 15.56*	643.5 ± 43.13*	722.5 ± 14.85*
Binucleate	1000.0 ± 0.00	556.5 ± 7.78*	413.0 ± 16.97*	300.5 ± 4.95*
Micronucleus/Mononucleate	0.5 ± 0.71	7.0 ± 1.41*	8.5 ± 2.12*	12.5 ± 0.71*
Micronucleus/Binucleate	0.5 ± 0.71	10.5 ± 0.71*	11.5 ± 0.71*	12.5 ± 2.12*
K+ Mononucleate cells	Not observed	4.5 ± 0.71*	6.0 ± 1.41*	6.0 ± 1.41*
K- Mononucleate cells	0.5 ± 0.71	2.5 ± 0.71	2.5 ± 0.71	6.5 ± 0.71*
K+ Binucleate cells	Not observed	8.0 ± 1.41*	8.5 ± 0.71*	8.0 ± 1.41*
K- Binucleate cells	0.5 ± 0.71	2.5 ± 0.71	3.0 ± 0.00*	4.5 ± 0.71*

5.3.4.3.2 84BR

Various doses of UVA (0*, 25, 50 and 100 J m^{-2}) were used to irradiate 84BR cells following their incubation with 0.05 µg ml^{-1} B(a)P in order to investigate interactive effects by means of the micronucleus assay using both Giemsa and anti-kinetochore staining techniques to investigate the potential mechanisms of action (clastogenic or aneugenic, respectively). Experiments scored 1000 binucleate cells per treatment group, and the experiments were duplicated. The results for 84BR cells are presented in Table 5.6. With no pre-incubation with 0.05 µg ml^{-1} B(a)P and at a dose of 0* J m^{-2} UVA, 230 ± 62.23 mononucleate cells were counted within 1000 ± 0.00 binucleate cells. However, when UVA doses were used to irradiate the B(a)P pre-incubated cells the results showed that numbers of mononucleate cells varied widely within a scoring protocol of a total of 1000 binucleate and mononucleate cells, appearing to range from 624.25 ± 16.46 (0.05 µg ml^{-1} B(a)P + 25 J m^{-2}), through 646.75 ± 48.69 (0.05 µg ml^{-1} B(a)P + 50 J m^{-2}) to 554 ± 114.47 (0.05 µg ml^{-1} B(a)P + 100 J m^{-2}) in mononucleate cells, and these results were all significantly higher than the control ($p < 0.05$). These increases in mononucleate cells from the combined exposure were significantly higher than with UVA alone ($p < 0.05$) except at one combination (0.025 µg ml^{-1} B(a)P + 100 J m^{-2} UVA) ($p > 0.05$). In binucleate cells, there was again a significant reduction in the frequencies of binucleate cells scored ($p < 0.05$). Similarly, the numbers of binucleate cells scored varied with the irradiation of UVA, again showing no pattern with increasing UVA dose from 426.75 ± 24.19 (0.05 µg ml^{-1} B(a)P + 25 J m^{-2}), through 395.25 ± 49.22 (0.05 µg ml^{-1} B(a)P + 50 J m^{-2}), to 509.75 ± 81.99 (0.05 µg ml^{-1} B(a)P + 100 J m^{-2}). Micronuclei scored in mononucleate and binucleate cells indicated a significant ($p < 0.05$) increase in the number of total micronuclei in both mononucleate and binucleate cells and a maximum of 10.25 ± 2.63 in mononucleate cells

(0.05 μg ml^{-1} B(a)P + 100 J m^{-2}), which is slightly lower than the frequency observed for CHO-K1 cells. In binucleate cells, the maximum frequency seen was 12.25 ± 1.71 (0.05 μg ml^{-1} B(a)P + 100 J m^{-2}) which was similar to the CHO-K1 response at this dose. These total responses in micronuclei induction are significantly greater ($p < 0.05$) than the responses from exposure to either UVA or B(a)P alone. Incidences of more than one micronucleus observed within the cell were detected at all doses, although these effects were not dissimilar from UVA or B(a)P alone for 84BR cells there was only a significant increase in the production of multiple micronuclei with combined dose 0.05 μg ml^{-1} B(a)P + 25 J m^{-2} ($p < 0.05$). Frequencies of multiple micronuclei ranged from 1.25 ± 0.50 (0.05 μg ml^{-1} B(a)P + 100 J m^{-2}) with 4 or more micronuclei (no doses were significantly different from the control $p > 0.05$) to a 3.75 ± 1.50 frequency (0.05 μg ml^{-1} B(a)P + 50 J m^{-2}) which was significantly different from the control ($p < 0.05$). With the incidence of 2 micronuclei only the lowest combined dose produced a significant increase ($p < 0.05$). Frequencies of NPB were observed at all interactive doses and were only significantly increased ($p < 0.05$) from the control at the highest combined doses (0.05 μg ml^{-1} B(a)P + 50 J m^{-2} and 0.05 μg ml^{-1} B(a)P + 100 J m^{-2}) to a maximum observed number of 3.75 ± 1.71 (0.05 μg ml^{-1} B(a)P + 50 J m^{-2}), although there was no significant difference ($p > 0.05$) at these doses there was a significant increase in NPB induction at the lowest combined dose (0.05 μg ml^{-1} B(a)P + 25 J m^{-2}) when compared to both UVA and B(a)P alone ($p < 0.05$). However, there was no significant difference ($p > 0.05$) between NPB induction and UVA alone for the highest doses tested (0.05 μg ml^{-1} B(a)P + 50 or 100 J m^{-2}) but these highest doses were significantly different from B(a)P alone ($p < 0.05$). From using the ant-kinetochore antibody micronuclei were scored in a total of 1000 mononucleate and binucleate cells. At the control dose, 129 ± 2.83 mononucleate cells were scored alongside 1000 binucleate cells. The numbers of

mononucleate cells showed little range with the maximum frequency observed at 610 ± 45.25 (0.05 μg ml^{-1} B(a)P + 100 J m^{-2}); figures that were similar to the Giemsa stained cells but all were significantly higher than the control ($p < 0.05$). With the binucleate cells, there was a significant decrease ($p < 0.05$) from the control in the frequencies of cells detected. Again there was little difference in the frequencies of total micronuclei observed in both mononucleate or binucleate cells and all the doses tested induced a significant increase in micronuclei ($p < 0.05$). The largest frequency of micronuclei observed within a mononucleate cell was 10.5 ± 0.71 (0.05 μg ml^{-1} B(a)P + 100 J m^{-2}), whilst 14 ± 1.41 were detected within a binucleate cell (0.05 μg ml^{-1} B(a)P + 100 J m^{-2}) and all these doses were significantly different from the control ($p < 0.05$). These results are similar to the results found with Giemsa staining, however, the results of the total combined doses (0.05 μg ml^{-1} B(a)P + 25, 50 or 100 J m^{-2}) are significantly higher ($p < 0.05$) than the corresponding results for UVA or B(a)P alone. Of the cells containing a micronucleus, a significantly ($p < 0.05$) larger proportion of micronuclei were detected that contained a K+ signal but were located in both mononucleate and binucleate cells. These results indicate a strongly aneugenic mode of action following interactive toxicity. However, as micronuclei were also detected in significant frequencies with K- signals, it would suggest that B(a)P and UVA induce both a clastogenic and aneugenic response in 84BR cells.

Table 5.6 Effect of interactive toxicity following pre-incubation with 0.05 μg ml^{-1} B(a)P with various doses of UVA (0*, 25, 50 and 100 J m^{-2}) on the mean (±SE) generation of micronuclei in 84BR cells (n=34,392) using Giemsa or anti-kinetochore stain. There were no multinucleate cells observed. Significant differences (Mann-Whitney *U* test $p<0.05$) from the control are indicated (*).

Dose	0.00 μg ml^{-1} B(a)P + 0* J m^{-2} UVA	0.05 μg ml^{-1} B(a)P + 25 J m^{-2} UVA	0.05 μg ml^{-1} B(a)P + 50 J m^{-2} UVA	0.05 μg ml^{-1} B(a)P + 100 J m^{-2} UVA
Cellular Response-Giemsa stain				
Mononucleate	230.0 ± 62.23	624.25 ± 16.46*	646.75 ± 48.69*	554.00 ± 114.47*
Binucleate	1000.0 ± 0.00	426.75 ± 24.19*	395.25 ± 49.22*	509.75 ± 81.99*
Micronucleus/Mononucleate	Not observed	6.50 ± 1.29*	7.25 ± 0.96*	10.25 ± 2.63*
Micronucleus/Binucleate	Not observed	8.75 ± 1.71*	8.75 ± 0.96*	12.25 ± 1.71*
Nucleoplasmic Bridge	Not observed	3.00 ± 1.63*	3.75 ± 1.71*	3.50 ± 1.29*
2 nuclei	Not observed	3.75 ± 2.06*	2.50 ± 2.08	2.00 ± 1.63
3 nuclei	Not observed	3.00 ± 2.45*	3.75 ± 1.50*	1.50 ± 1.29
4+ nuclei	Not observed	2.75 ± 3.20	2.00 ± 1.83	1.25 ± 0.50
Cellular Response-anti-kinetochore stain				
Mononucleate	129.0 ± 2.83	601.0 ± 5.66*	574.0 ± 16.97*	610.0 ± 45.25*
Binucleate	1000.0 ± 0.00	408.0 ± 11.31*	467.0 ± 43.84*	424.5 ± 38.89*
Micronucleus/Mononucleate	Not observed	5.5 ± 0.71*	7.5 ± 2.12*	10.5 ± 0.71*
Micronucleus/Binucleate	0.5 ± 0.71	6.5 ± 0.71*	8.5 ± 2.12*	14.0 ± 1.41*
K+ Mononucleate cells	Not observed	3.5 ± 0.71*	4.5 ± 2.12*	6.0 ± 0.00*
K- Mononucleate cells	Not observed	2.0 ± 0.00	3.0 ± 0.00	4.5 ± 0.71*
K+ Binucleate cells	Not observed	4.5 ± 0.71*	5.0 ± 1.41*	9.5 ± 2.12*
K- Binucleate cells	0.5 ± 0.71	2.0 ± 0.00	3.5 ± 0.71	4.5 ± 0.71*

5.3.4.4 ESR

The effects of B(a)P and UVA both alone and in combination were investigated using ESR. Background spectra (presented in Chapter 4, Section 4.3.4) were subtracted from all experimental spectra presented here. Figure 5.11 shows the effects of UVA irradiation (500 J m^{-2}) (Figure 5.11a) or B(a)P (24 hours) (3.2 µg ml^{-1}) without UVA irradiation (500 J m^{-2}) in CHO-K1 cells and demonstrates no significant signals (Figure 5.11b). CHO-K1 cells treated with 3.2 µg ml^{-1} B(a)P (24 hours) and irradiated with UVA (500 J m^{-2}) in the presence of DMPO gave an intense signal of DMPO-OH, which was not observed with untreated cells (Figure 5.11c). 84BR cells treated with 3.2 µg ml^{-1} B(a)P (24 hours) and irradiated with UVA (500 J m^{-2}) in the presence of DMPO gave an intense signal of DMPO-OH (Figure 5.12b), which was not observed with untreated cells (Figure 5.12a). Agents (mannitol, SOD, catalase) were incorporated into the CHO-K1 system (Figures 5.13b to 5.13d respectively) on cells treated for 24 hours with B(a)P (3.2 µg ml^{-1}) followed by UVA (500 J m^{-2}) (Figure 5.13a). The reduction produced by mannitol (Figure 5.13b) is what one would expect from competition for hydroxyl, whilst SOD (converts superoxide to hydrogen peroxide) had no significant effect. Catalase (converts H_2O_2 to water) reduced the signal but may be competing for hydroxyl. If the catalase was destroying H_2O_2 to prevent secondary hydroxyl formation the reduction expected may have been greater than that observed. Results obtained with TMPol and POBN (data not shown) were similar to those obtained with RTG-2 cells (Chapter 3, Section 3.3.7 and Chapter 4, Section 4.3.5). It can be concluded that the presence of B(a)P in cells causes direct formation of hydroxyl radicals on exposure to UVA.

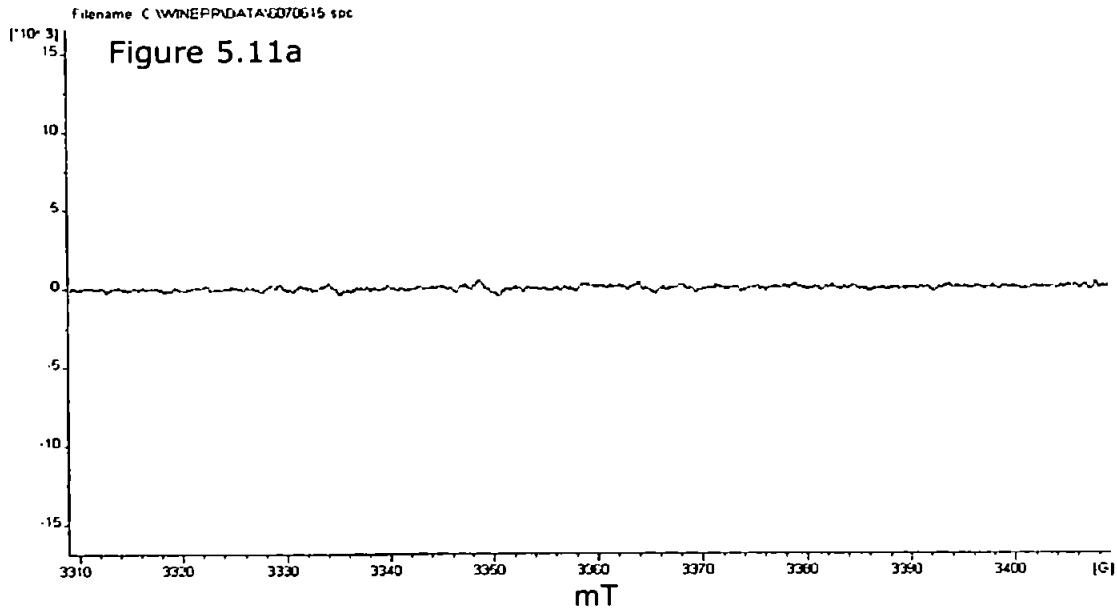

Figure 5.11a

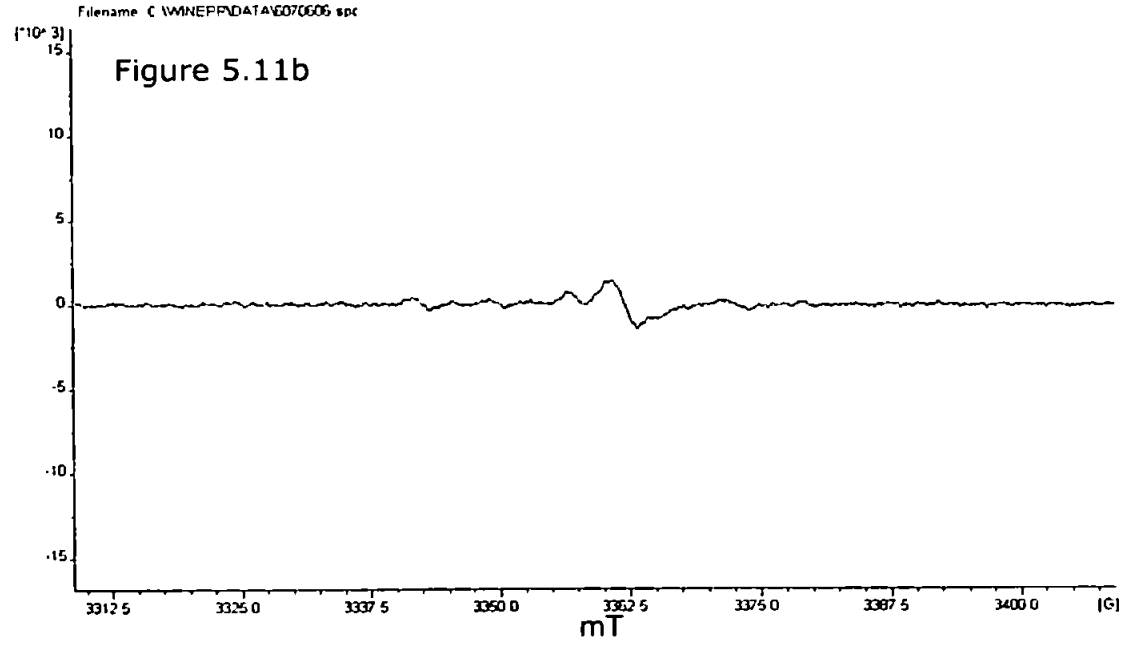

Figure 5.11b

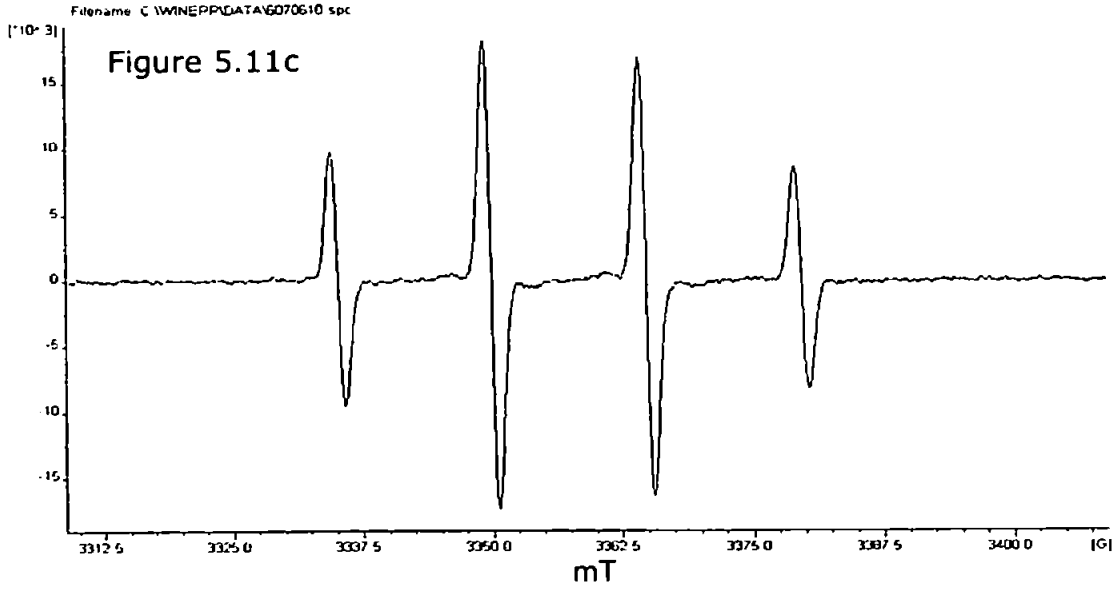

Figure 5.11 The effect of UVA (500 J m^{-2}) (no B(a)P) (Figure 5.11a), 24 hours treatment with B(a)P (3.2 µg ml^{-1}) without UVA treatment (500 J m^{-2}) (Figure 5.11b). Figure 5.11c shows B(a)P treated (24 hours) CHO-K1 cells after UVA irradiation (500 J m^{-2}).

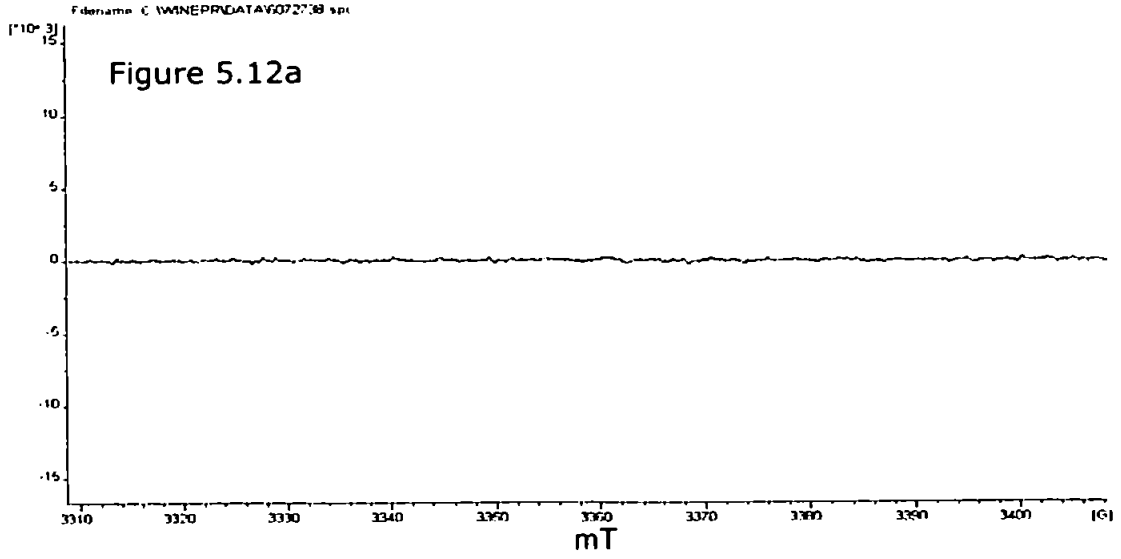

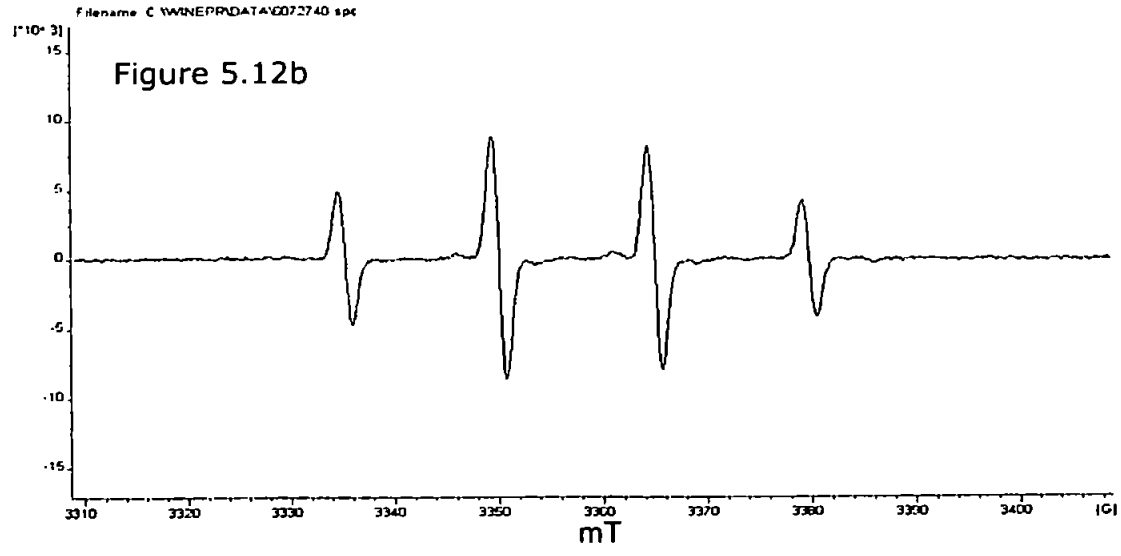

Figure 5.12 The effect of UVA irradiated (500 J m^{-2}) DMPO control (Figure 5.12a) on 84BR cells. Figure 5.12b shows the effects of treatment (24 hours) with B(a)P (3.2 µg ml^{-1}) with UVA (500 J m^{-2}) on free radical formation in 84BR cells.

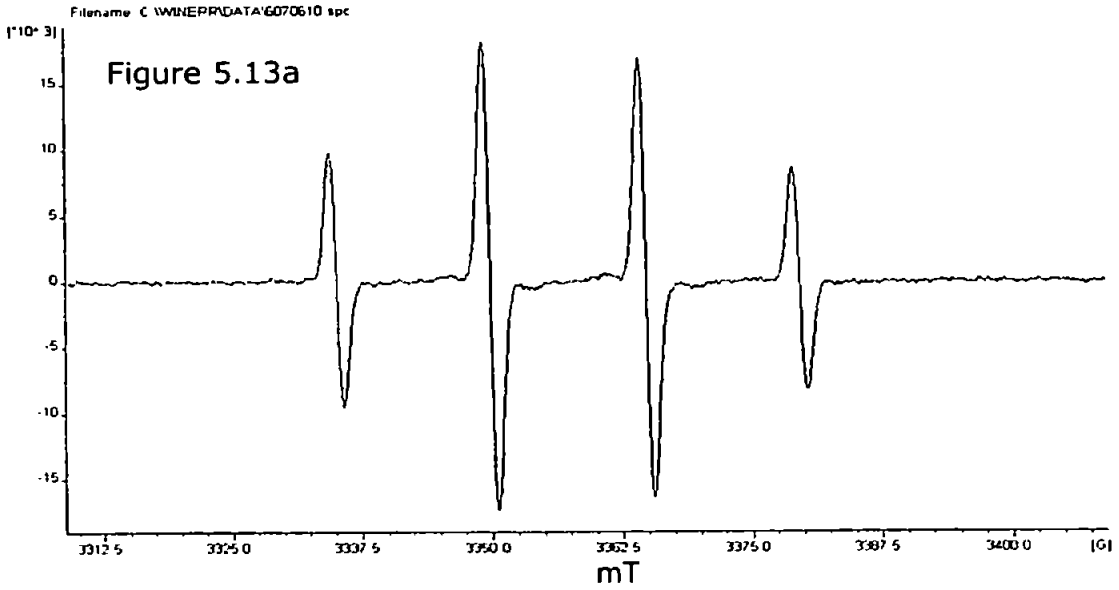
Filename C:\WINEPR\DATA\6070610.spc
Figure 5.13a
15
10
5
0
-5
-10
-15
3312.5
3325.0
3337.5
3350.0
3362.5
3375.0
3387.5
3400.0
[G]
mT

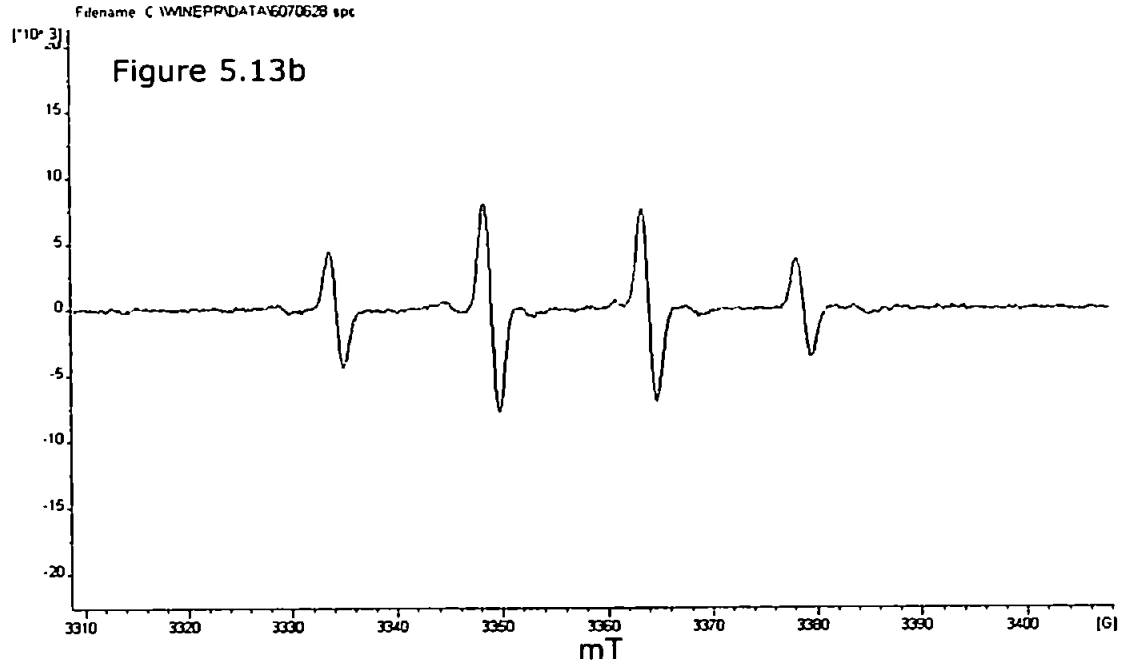
Filename C:\WINEPR\DATA\6070628.spc
Figure 5.13b
15
10
5
0
-5
-10
-15
-20
3310
3320
3330
3340
3350
3360
3370
3380
3390
3400
[G]
mT

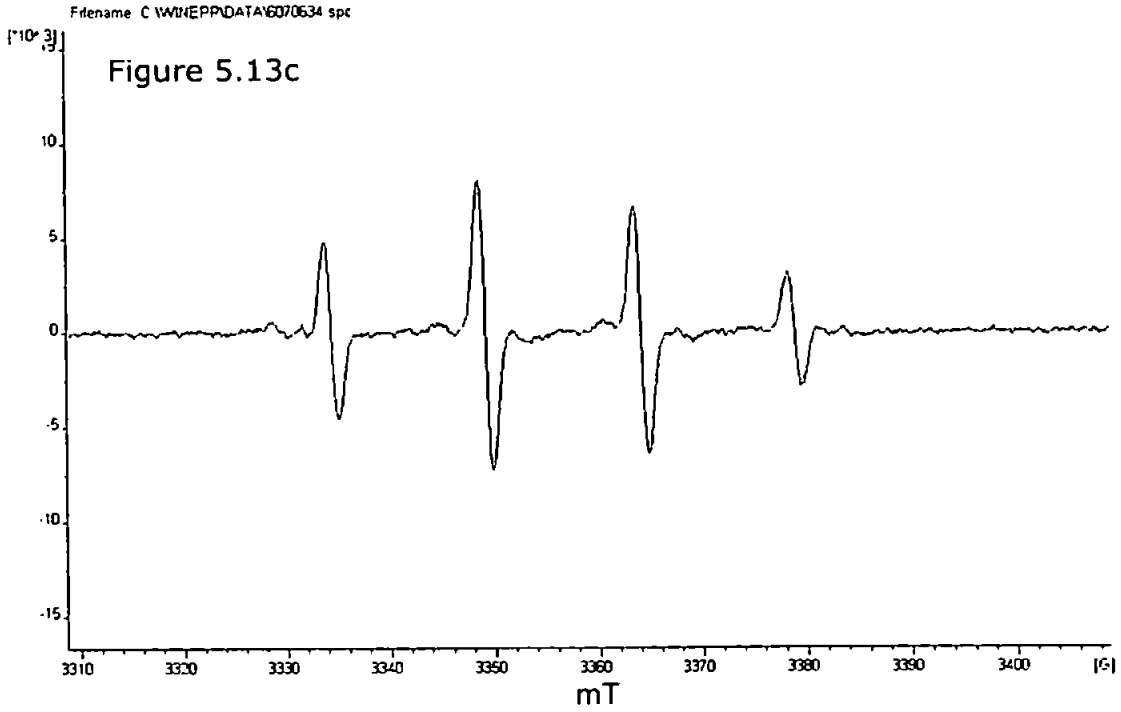

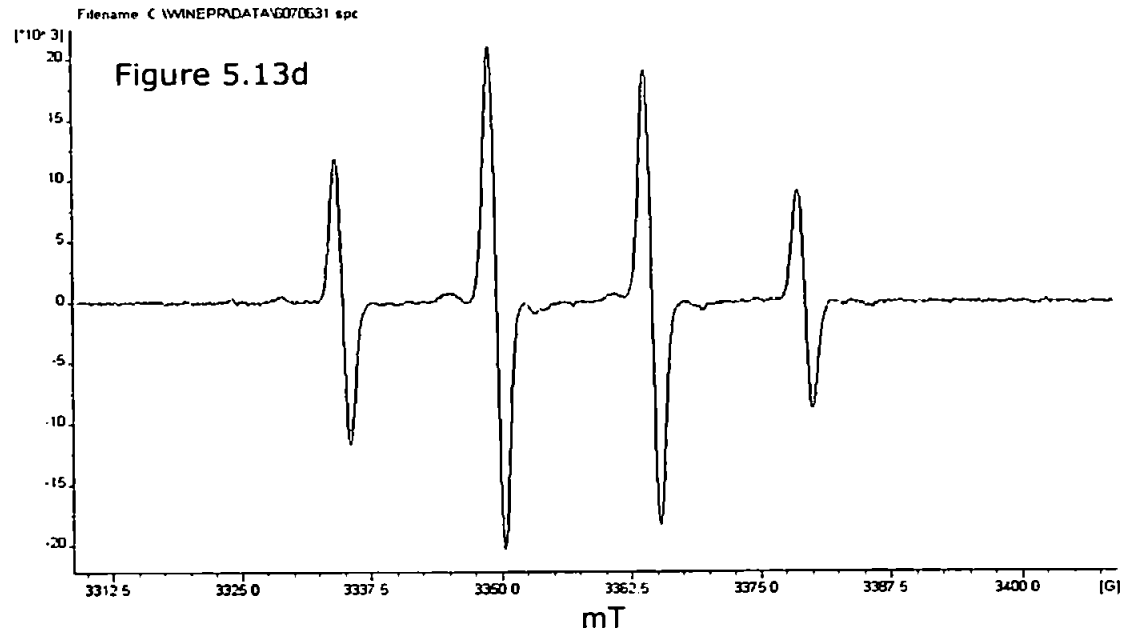

Figure 5.13 The effect of mannitol (Figure 5.13b), catalase (Figure 5.13c) and superoxide dismutase (Figure 5.13d) on cells treated with B(a)P (3.2 μg ml^{-1}) followed by UVA (500 J m^{-2}) (Figure 5.13a) on free radical formation.

5.4 Discussion

Over the past few decades there has been an increase in interest in the harmful effects of UVR to human skin and UVR is implicated in aging (Ma *et al.*, 2001; Wlaschek *et al.*, 2001), sunburn and skin carcinogenesis (Kowalczuk *et al.*, 2006). However, there is little evidence into the effects of UVR in conjunction with other environmental contaminants in mammalian models and human skin. The effects of B(a)P and UVR were investigated separately and together using *in vitro* models. CHO-K1 cells lack the enzymes necessary to metabolise certain xenobiotics (including B(a)P) so other workers have tried to address this problem by using exogenous metabolic activation systems (such as Arochlor 1254 (an S9 simulator)) or by using cells with inherent metabolic capability (Babich *et al.*, 1988). However, B(a)P reduced cell viability to approximately 68 % in CHO-K1 cells at a concentration of 3.2 μg ml^{-1} B(a)P in the work presented here. In agreement with our findings, other researchers used a hepatocellular tumour cell line (HepG2) and exposed these cells to B(a)P at concentrations ranging from 0.05 to 5.00 μg ml^{-1} for 1, 2 or 3 days. They observed cytotoxicity after 1 day (24 hours) of exposure to concentrations 2.00 and 5.00 μg ml^{-1} with cell survival reduced by 35 % (Babich *et al.*, 1988). Kiefer and co-workers (1988) observed maximum cytotoxicity in metabolically capable human lung tumour cells (NCI-H322) with 5-10 μM B(a)P and suggested the cytotoxicity was related to the metabolites produced as the cytotoxicity of anti-7,8-dihydroxy-7,8-dihydrobenzo(a)pyrene (7,8-diol-BP) was greater than B(a)P which was greater than 3-hydroxybenzo(a)pyrene (3-OH-BP) (Kiefer *et al.*, 1988).

Commercially available S9 was used to activate B(a)P to its metabolites in CHO-K1 cells which follows the experiences of previous workers (Johnson *et al.*, 1996) who have used both human and rat S9 to

activate a range of pro-mutagens (including B(a)P: 20 – 300 μM) in CHO cells. B(a)P caused significant increases in DNA damage to CHO-K1 with median tail DNA damage of 7 % with and without S9) and 10 % in 84BR cells (without S9). DNA damage ranged up to 40 % with the additional use of S9 in CHO-K1 cells. These observations are consistent with results from other workers. The increased mutagenicity of B(a)P in the presence of exogenous metabolic activation probably involves an AhR inducible CYP1A1-dependent pathway (Annas *et al.,* 2000). PAHs are known to induce the CYP1A pathway by ligand binding at the cytosolic Ah-receptor which is associated with other proteins (Whitlock, 1990) but Annas and co-workers (2000) demonstrated that whilst 10 μM B(a)P was shown to induce significant DNA damage in human umbilical vein endothelial cells (HUVEC) without an exogenous metabolic activation system, more extensive damage was observed from cells that had been pre-treated with β–naphthoflavone (BNF) a well known AhR agonist which induces cytochrome P-450 (CYP) enzymes. This binding may increase the mutagenic effects of B(a)P such as those reported here. Machala and co-workers (2001), investigated the activation of aryl hydrocarbon receptor (AhR) by a range of PAH, determined by the chemical-activated luciferase expression (CALUX) assay. Using the rat hepatoma H411E cell line they demonstrated that AhR-mediated metabolism of PAHs could significantly contribute to their mutagenic effects (Machala *et al.,* 2001). These results suggest possible mechanisms by which increased DNA damage is observed when an exogenous metabolic agent (S9) is incorporated into the system with CHO-K1 cells. There may be deleterious effects of using exogenous metabolic activation. A study using HepG2 cells exposed to 2 or 3 days B(a)P in the presence of Arochlor 1254 showed only 10 % survival due to the increased metabolic activity (Babich *et al.,* 1988). However, it is also possible that this 10 % survival could be due to toxicity from long term exposure to the S9 exogenous metabolic system which is not

recommended for long term exposures (Kirsch-Volders *et al.*, 2003). To overcome the difficulties of using exogenous metabolising agents (such as Arochlor 1254) studies including *in vivo* systems (Garry *et al.*, 2003) or cell lines containing inherent metabolic activation (e.g. human bronchoalveolar cells (Jiang *et al.*, 2006) and the 84BR cells used here) may provide a simpler system for the detection of genotoxins dependent on metabolic activation (Dagher *et al.*, 2005) to prevent any deleterious effects from the incorporation of an exogenous metabolic agent (Babich *et al.*, 1988; Kirsch-Volders *et al.*, 2003).

Weak but significant increases in the induction of micronuclei were indicated in CHO-K1 and 84BR cells following treatment with B(a)P. The mode of action of B(a)P appeared to be influenced through aneugenic mechanisms because a significant majority of micronuclei displayed a kinetochore positive signal – indicating a loss of whole chromosomes. The majority of micronuclei were detected within a binucleate cell; however, micronuclei (both K+ and K-) were also detected within mononucleate cells indicating that it is valuable to include scoring of micronuclei within mononucleate cells in agreement with current literature (Fenech *et al.*, 2003) to detect all damaged cells, such as those that have already expressed DNA damage before they were put into culture with Cyto B. Scoring micronuclei with both mononucleate and binucleate cells enables the detection of pre-existing DNA damage as well as micronuclei expressed during culture as a result of chromosome breaks from the test compound (Fenech *et al.*, 2003). The consequences of aneugenic and clastogenic activity may have serious implications (Kamiguchi & Tateno, 2002) such as the accumulation of DNA adducts (Lee *et al.*, 2002) or inhibiting the progression of meiotic divisions in human spermatozoa (Georgellis *et al.*, 1990). These data are important as they highlight the mutagenicity of B(a)P not only to somatic cells, but also to the gametes, having potentially significant

consequences for reproduction. Environmental studies using cultured human lymphocytes have demonstrated the induction of aneugenic activity from extracts of diesel exhaust particulates (Odagiri *et al.,* 1994) that contain PAH compounds such as B(a)P.

UVB caused a significant reduction in cell viability with all UVB doses in CHO-K1 cells. In agreement with the work presented here, a dose-related decrease in cell survival from exposure to 60, 120 or 180 J m^{-2} UVB was observed in lymphocytes (Keulers *et al.,* 1998) whilst 125 kJ m^{-2} UVB reduced clonogenic survival to 37 % in human breast cancer (MCF-7) cells (Koch-Paiz *et al.,* 2004). UVB has been shown to induce apoptosis in a variety of mammalian cell lines, demonstrated through changes in cellular morphology, phosphatidylserine (PS) exposure, oligonucleosomal DNA fragmentation and generation of hypochrome nuclei (Hagenhofer *et al.,* 1998). Conversely, the effects of UVA showed no reductions in cell viability in 84BR but reduced cell viability in CHO-K1 cells at the higher doses tested. Molecular studies have been carried out by other workers that indicate malfunctioning of the cellular apparatus following UVA radiation. He and co-workers (2004) demonstrated that 4 - 32 J m^{-2} UVA induced delayed and sustained extracellular signal-related kinase (ERK) activation that was epidermal growth factor receptor (EGFR) kinase activity dependent, but phospholipase C (PLC)/calcium/protein kinase C (PKC) mediated. This delayed and sustained activation serves to provide a survival signal for HaCaT keratinocytes. ERK is an important suppressive regulator of apoptosis, so activation of the ERK pathway would play a vital role in providing a survival signal to allow cells to escape from apoptosis and therefore increase the potential for a malignant transformation and tumourogenesis *in vivo* following UVA exposure (He *et al.,* 2004) and would require further investigation to elucidate.

UVB and UVA doses tested caused significant increases in DNA damage in CHO-K1 cells but there was no dose related response to UVB which may have been due to extensive damage at higher doses that overloaded the assay system. However, there was a significant and dose related increase in DNA damage in response to UVA suggesting that these two types of radiation may instigate different types of DNA damage. For example, the repair kinetics of UVA- and UVB-induced DNA damage have been shown to differ from each other, which would implicate the induction of different types of DNA lesions by UVA and UVB (Lehmann *et al.*, 1998). UVA (5 J m^{-2}) induced effects on DNA were shown to have been related to radical mediated strand breaks and DNA lesions which form alkali-labile sites whilst the effects of UVB (15 mJ cm^{-2}) mainly occurred as a consequence of excision repair-related strand breaks (Lehmann *et al.*, 1998). Horikawa-Miura and co-workers (2007) suggested DNA damage-dependent and independent pathways for the induction of cell death following UVB irradiation. Human embryonic fibroblast-like cells (HE49) irradiated with 240 J m^{-2} UVB generated equivalent amounts of DNA photoproducts and induced more clonogenic cell death, apoptosis, mitochondrial cytochrome C release and intracellular oxidative stress (Horikawa-Miura *et al.*, 2007). This would suggest biochemical pathways link the DNA damage and the associated reductions in cell viability observed in the work presented here.

UVA instigated genomic instability in both the CHO-K1 cell line and 84BR cells. This was shown through an inherited mutation on the chromosomal apparatus demonstrated through the significant induction of micronuclei. UVA has been shown to have an effect on genomic metabolism through alterations in cell cycle kinetics (de Laat *et al.*, 1996; Kowalczuk *et al.*, 2006). In the work reported here, UVA (25 – 200 J m^{-2}) caused a positive increase in the frequencies of micronuclei and altered cell cycle kinetics (a delayed cell cycle shown by the significantly

altered frequencies of mononucleated cells in both cell types (Fenech *et al.*, 2003a; Fenech *et al.*, 2003b; Rosefort *et al.*, 2004)). In partial agreement with these findings, Kowalczuk and co-workers (2006) showed that UVA slowed the cell cycle through the S phase in human melanocytes and arrested malignant melanoma cells in G1 indicating that UVA is able to induce strong cell cycle delays and considerably affect genomic metabolism or inhibit DNA synthesis (de Laat *et al.*, 1996). UVA (0-600 kJ m^{-2}) and UVB (0-80 J m^{-2}) have also been found to inhibit proliferation of mammalian cells in a fluence-dependent manner due to a temporary accumulation of cells in the S phase of the cell cycle (Bånrud *et al.*, 1995). This is consistent with the delayed cell cycle observed in the micronucleus assay reported here. The existence of two or more nuclei in the cell in significant frequencies was demonstrated in the work presented here. In agreement, Bånrud and co-workers (1995) showed that after exposure to 200 - 500 kJ m^{-2} UVA a large proportion of mammalian V79 cells were polyploid, with two or more nuclei.

Nucleoplasmic bridges (NPB) were observed throughout the scoring procedure in both CHO-K1 and 84BR cells and increased with increasing UVA dose. NPBs are suggested to form when the centromeres of dicentric chromosomes are pulled to opposite poles at anaphase and these abnormalities are detectable through the cytokinesis block micronucleus assay (CBMN) because cytokinesis is inhibited allowing the nuclear membrane to form around the binucleate daughter cells. They have been shown to be important biomarkers of DNA damage, chromosomal rearrangement, chromosomal breakage and translocation events, and can be identified without an antikinetochore staining procedure (Fenech & Crott, 2002; Thomas *et al.*, 2003). Shorrocks and co-workers (2004) demonstrated that although cells containing BRCA1 mutations had an abnormal cell cycle in response to 1 x 10^5 J m^{-2} UVA

(a defective G1/S checkpoint) genomic instability was not implicated as there was no corresponding increase in micronuclei as their data indicated that UVA-induced damage was repaired but remained error-prone (Shorrocks *et al.*, 2004). However, the work presented here supports the occurrence of genomic instability following UVA radiation due to the alterations in cell cycle, cellular abnormalities (NPB) and the corresponding increase in micronuclei.

Combined exposure to B(a)P and UVA significantly reduced the cell viability in CHO-K1 and 84BR cells. In CHO-K1 cells an approximately 10 % greater reduction in cell viability was seen from either B(a)P or UVA alone when cells were treated to B(a)P and 2000 J m^{-2} UVA. This effect increased to at least 20 % greater reduction in cell viability with cells treated with B(a)P and 4000 J m^{-2} UVA from either B(a)P or UVA alone. These results suggest an additive effect on the reduction in cell viability in CHO-K1. In 84BR cells, the reduction in cell viability was greater than that seen with CHO-K1 with reductions in cell viability of up to 40 % from UVA. These results suggest a synergistic effect on the reduction in cell viability in 84BR cells. Similarly, simultaneous treatment of human keratinocytes (HaCaT) with 1 µg ml^{-1} pyrene and 3.9 J cm^{-2} UVA resulted in a significant inhibition of cell proliferation (Ekunwe *et al.*, 2005) whilst exposure to 5 µM B(a)P and 1 kJ m^{-2} UVA caused a dramatic reduction in cell viability in human keratinocytes (Crallan *et al.*, 2005) which was greater than the effects of either B(a)P or UVA independently.

Additionally, the work presented here showed a significant increase in DNA damage from the combined exposure to B(a)P and UVA in both CHO-K1 cells and 84BR cells which suggests a synergistic effect from B(a)P or UVA alone. Zheng and co-workers (2004) demonstrated a dose responsive increase in DNA damage measured by the comet assay

from the interaction of fluoranthene (0.1 - 5 μM) and 6.1 J cm^{-2} UVA radiation in HaCaT cells. Zheng and co-workers (2004) supports similar findings as the work presented here, in that the DNA damage detected by the comet assay was associated with some cytotoxicity, implicating that the DNA damage observed could be a consequence of cellular toxicity mechanisms. Furthermore, other workers have shown that DSBs were generated following co-exposure to 10^{-6} M B(a)P and 1 J m^{-2} UVA in CHO-K1 cells and indicated again the relationship between DSBs and cytotoxicity (Toyooka *et al.,* 2004). In support of our finding of a synergistic effect, Crallan and co-workers (2005) demonstrated that exposure to 5 μM B(a)P followed by 1 kJ m^{-2} UVA caused a significant increase in DNA damage (up to 35 %) measured by the percentage tail DNA which was greater than either B(a)P or UVA alone (approximately 9 % and 10 % respectively). *In vivo*, combined B(a)P and UVA exposure has been shown to cause genetic damage that accumulated with time; BPDE-DNA adducts increased to approximately twice the level of B(a)P plus UVA whilst nuclear p53 expression increased, in conjunction with a parallel increase in 8-OHdG formation which was 300 % higher than B(a)P plus UVA (Saladi *et al.,* 2003). Notably, accumulations in DNA damage may be related to inherited mutations.

There were considerable increases in the frequencies of total micronuclei, multiple micronuclei and NPBs induced in both cell types (CHO-K1 and 84BR) used in this study from exposure to B(a)P followed by UVA. These increases were significantly higher than with B(a)P alone or UVA alone in all cases and often greater than B(a)P (alone) plus UVA (alone). These data may be indications of genomic instability caused by B(a)P followed by UVA in CHO-K1 and 84BR cells. There were substantial increases in micronuclei in mononucleated cells, and these contained both K+ and K- signals. A possible delayed cell cycle effect from combined exposure to B(a)P and UVA was demonstrated through the

significant increase in mononucleated cells. Although this was also shown with UVA treatment these increases from combined exposure were appreciably higher than with UVA alone. This is relevant as it demonstrates that the combination of B(a)P and UVA is an important factor in the increased genotoxic effects observed. Cell cycle delays have been demonstrated in human melanocytes and malignant melanoma cells when treated with UVA (Kowalczuk *et al.*, 2006) as well as in the work presented here with both CHO-K1 and 84BR cells. If the delay of progression through the cell cycle is inhibited before the critical stages of DNA replication, there may be an increase in spontaneous or induced gene mutation or chromosomal aberration contributing to genomic instability (Kaufmann & Paules, 1996). These data are an important contribution to the concept that in association with a delayed cell cycle, there are nuclear anomalies that may contribute to genomic instability in both CHO-K1 and 84BR cells (such as multiple micronuclei and NPBs).

Investigations into oxidative damage showed that when CHO-K1 and 84BR cells were incubated with B(a)P and then irradiated with UVA (in the presence of the spin trap DMPO), the major product was DMPO-OH. These data indicate the formation of either $^{\cdot}OH$ or $O_2^{\cdot-}$ radicals and suggest oxidative damage. When mannitol (which readily compete with DMPO or $^{\cdot}OH$) was added to the B(a)P treated CHO-K1 cells, prior to UVA irradiation, the yield of DMPO-OH was greatly decreased. Addition of catalase, which converts H_2O_2 to H_2O, had a small effect whilst addition of SOD, which converts superoxide indirectly to hydrogen peroxide radicals also had little effect. This indicates that the major radical product from the co-exposure of B(a)P and UVA is $^{\cdot}OH$, which is formed directly, rather than from H_2O_2, and that superoxide is not involved. The responses of the CHO-K1 and 84BR cells were generally indistinguishable from each other when cells were treated with B(a)P

and UVA. Shyong and co-workers (2003) treated cells with general ROS scavengers including catalase and observed significantly decreased H_2O_2 production from cells treated with 5 μg ml^{-1} B(a)P plus 10 kJ m^{-2} UVA, whereas scavengers of superoxide anion ($O_2^{\cdot-}$), hydroxyl radicals ($^{\cdot}OH$) and singlet oxygen ($^1O_2$) had minimal effects. They concluded that B(a)P synergistically enhanced the production of H_2O_2 in cultured cells by UVA (Shyong *et al.*, 2003). Gao and co-workers (2005) also suggested synergy between BPDE and UVA to produce ROS which in turn damage DNA. They used ROS scavengers and showed singlet oxygen and superoxide radical anion was involved in 8-OHdG formation (Gao *et al.*, 2005). Their findings agree with the findings reported here which suggest that ROS are produced in response to UVA following treatment with B(a)P. Toyooka and co-workers (2004) demonstrated that exposure to B(a)P followed by UVA radiation synergistically induced oxidative DNA damage in CHO-K1 cells but were unable to identify the radical species involved. This thesis suggests that $^{\cdot}OH$ is directly produced and is (to the best of our knowledge) a novel finding.

The results from this ESR study have significance as to date there has been no clear indication of the ROS species formed when PAHs and UVA interact in cellular systems. There have been reports that superoxide anion was the principal ROS produced by B(a)P and UVA (Liu *et al.*, 1998) but our data suggests that $^{\cdot}OH$ is produced directly. Ibuki and co-workers (2002) postulated that whereas hydroxyl radical and superoxide anion radical scavengers showed no effect, singlet oxygen quenchers significantly inhibited the formation of 8-OHdG from combined B(a)P and UVA exposure in human skin fibroblasts. The formation of 8-OHdG in DNA is significant as without proper repair, GC-TA transversions can occur (Feig *et al.*, 1994). However, this would suggest that 8-OHdG is a product of singlet oxygen whereas the work presented here in the cell types investigated suggests that singlet

oxygen is not involved. Kim and co-workers (2005) proposed that B(a)P could directly induce DNA adducts in the presence of light (370-750 nm), and that these DNA adducts could induce oxidative DNA damage. In partial agreement with these results (the work here looked at UVA specifically) the work presented here showed the induction of both DNA damage (comet, micronucleus assays) and oxidative damage (ESR) following B(a)P and UVA treatment in both CHO-K1 and 84BR cells. Interestingly, whilst CHO-K1 are not able to metabolise B(a)P, a strong DMPO-OH signal was generated giving a synergistic effect when cells were irradiated with UVA. This signal is slightly larger than seen with 84BR cells under the same conditions. Kim and co-workers (2005) proposed that B(a)P could be directly photoactivated to a mutagenic form. They suggested that a photoactivated form of B(a)P could bind to DNA resulting in a bulky lesion that would behave as a powerful photosensitiser to generate mutagenic oxidative damage (Kim *et al.*, 2005). This is supported by the synergistic effect observed in the comet assay in CHO-K1 cells. These reported data highlighted the broad range of effects that mixed environmental stressors can have on cells and this may affect risk assessment strategies for environmental pollutant exposure which are more complex than if a simple exposure to one type of mutagen was involved (Koch-Paiz *et al.*, 2004).

These studies and the work reported here confirms that B(a)P is an important mutagen in the environment which induces genotoxic damage through DNA strand breakage and aneugenic mechanisms, although its direct cytotoxicity is limited. UVB demonstrated considerable effects on cell viability and caused significant DNA damage, whilst UVA caused little effect on cell viability, limited DNA damage but significant increases in cellular alterations were observed in both cell types. CHO-K1 and 84BR cells incubated with B(a)P followed by irradiation with UVA showed reductions in cell viability, increases in DNA damage and altered cellular

mechanisms that may be due to both aneugenic and clastogenic mechanisms. This may make these effects more carcinogenic if inherited without repair as the cells survive the insult. Oxidative effects were observed that were shown to be a product of the hydroxyl radical (ESR). Exposure to combined B(a)P and UVA insult produced effects which were generally significantly greater than those produced by B(a)P and UVA independently.

CHAPTER VI – GENERAL DISCUSSION

The interactive toxicity of B(a)P and UVR was investigated in cell types of different phylogenetic origin (fish: EPCA1 and RTG-2 and mammalian: CHO-K1 and 84BR). From these results it may be valuable to compare the way in which the cell types reacted by generating a synthesis of the data. This can be done quantitatively and conceptually in order to stimulate new discoveries that could lead to future research and further hypothesis. The data chosen for comparison is the interactive toxicity of B(a)P and UVA using RTG-2, CHO-K1 and 84BR cells with the NRR, comet and micronucleus assays and is presented in Table 6.1. These data have been chosen because the purpose of the work presented here was to investigate the combined effect of B(a)P and UVA through various cytotoxic and genotoxic assays. The EC_{50} is added to the table as a general comparison between the cell types as it refers to the concentration which induces a response halfway between the baseline and maximum. Other data concerning the individual aspects of B(a)P or UVR have already been covered in detail in previous chapters and does not provide any added benefit to the investigation here.

Table 6.1 Comparison between the RTG-2, CHO-K1 and 84BR cells using NRR, Comet or Mn assays for the interactive toxicity of B(a)P and UVA. (* indicates that the DNA damage was too great to score, therefore 100 % DNA damage was measured). No noteworthy differences between the RTG-2, CHO-K1 or 84BR cells were detected for the comet or micronucleus assay.

	RTG-2	**CHO-K1**	**84BR**
B(a)P + UVA			
NRR (EC_{50})	0.1+4000 J m^{-2}	3.2+4000 J m^{-2}	3.2+4000 J m^{-2}
Comet assay (% Tail DNA)			
0.1 µg ml^{-1} B(a)P + 500 J m^{-2} UVA	10	17	15
1.0 µg ml^{-1} B(a)P + 500 J m^{-2} UVA	19	28	28
3.2 µg ml^{-1} B(a)P + 500 J m^{-2} UVA	37	28	28
0.1 µg ml^{-1} B(a)P + 1000 J m^{-2} UVA	22	25	14
1.0 µg ml^{-1} B(a)P + 1000 J m^{-2} UVA	39	27	12
3.2 µg ml^{-1} B(a)P + 1000 J m^{-2} UVA	44	19	100*
0.1 µg ml^{-1} B(a)P + 2000 J m^{-2} UVA	20	38	28
1.0 µg ml^{-1} B(a)P + 2000 J m^{-2} UVA	36	34	100*
3.2 µg ml^{-1} B(a)P + 2000 J m^{-2} UVA	45	34	100*
Micronucleus Assay (mean micronuclei per 1000 binucleate cells) using anti-kinetochore stain			
0.05 µg ml^{-1} B(a)P + 25 J m^{-2} UVA	8.5	10.5	6.5
0.05 µg ml^{-1} B(a)P + 50 J m^{-2} UVA	14	11.5	8.5
0.05 µg ml^{-1} B(a)P + 100 J m^{-2} UVA	14	12.5	14

From the table it can be seen that when comparing the cell groups an interesting pattern emerges where cell types reacted in a very similar way. For example, the EC_{50} value was 0.1 + 4000 J m^{-2} for RTG-2 cells and 3.2 + 4000 J m^{-2} for CHO-K1 and 84BR cells. The lower EC_{50} for the RTG-2 cells suggests a greater sensitivity of these cells to this combined insult when investigating cytotoxicity. Basal cytotoxicity reflects

adverse effects on cell structures and processes that are intrinsic to virtually all cells. Most cell systems should show a similar response, and also respond similarly when toxicity is measured by various viability criteria (Babich & Borenfreund, 1991; Babich *et al.,* 1991). The differential sensitivities of fish and mammalian cells have been suggested (Ahmed *et al.,* 1993; Castano & Gomez-Lechon, 2005; Raissudin & Jha, 2004) but these have mainly concerned genotoxicity assays. However there was no significant difference (Kruskal-Wallis, $p > 0.05$) between the median values in the RTG-2, CHO-K1 or 84BR cells for each B(a)P + UVA group in the comet assay data, or the mean micronuclei produced in the work presented here suggesting a similar effect of DNA damage across the different cell types to the combined genotoxic effect of B(a)P and UVA. Fish cells have been shown to have a low DNA repair capacity compared to mammalian cells, and they may therefore appear to be more sensitive to DNA damage (Ahmed *et al.,* 1993; Willett *et al.,* 2001). Other workers have reported an increased sensitivity of the RTG-2 cell line using the comet and micronucleus assays (Raissudin & Jha, 2004). The generalisation that fish cells are more sensitive than mammalian cells may need to be addressed in greater detail as this may not be applicable for all cytotoxic and genotoxic assays, and may also depend on the nature of the environmental contaminant being investigated.

The work presented here suggests that all cells react to B(a)P and UVA in a similar way as never previously documented with other research and possesses interesting avenues for further research. However when compared with some literature sources the results are contradictory (e.g. Ahmed *et al.,* 1993; Raissudin & Jha, 2004). This can be explained through technical limitations of the experiments used in this work and also with regard to the use of cultured cells. In order to clarify the

'knowledge gap' between our differing results specific follow up experiments could include the following.

1) Technical limitations:

- The NRR assay is a well established assay for looking at cell viability but it does not differentiate between the mechanism of cytotoxicity (e.g. necrosis or apoptosis) so a progression to this could be the detection of caspase activity and phosphatidylserine (PS) translocation to indicate apoptosis (Valencia and Kochevar, 2006).
- Similarly, the use of the comet assay could be expanded by incorporating the use of Fapy-DNA glycosylase enzyme incubation to detect oxidised purines and therefore oxidative DNA damage (Crallen *et al.*, 2005).
- With regards to the micronucleus assay it became apparent that there is no strict standardised protocol for the scoring of micronuclei that is adopted worldwide, although steps are being taken to rectify this (Kirsh-Volders *et al.*, 2003). The data presented investigated the production of micronuclei first (as recommended) in binucleated cells (Chapter 3) and second (as cellular responses altered) via a scoring practice of incorporating both the use of mononucleate and binucleate cells and other nuclear abnormalities (Chapters 4 and 5). This assay was further developed in the work presented here by examining parameters such as monunucleated cells and NPBs to increase the sensitivity of the system (Fenech *et al.*, 2003b). This data has been valuable in understanding the cellular changes occurring and increasing the sensitivity of the micronucleus assay as demonstrated. Other methods of automation may also increase the robustness of this assay (Varga *et al.*, 2004).

- The use of ESR was investigated with RTG-2 and CHO-K1 cells and results suggested direct formation of hydroxyl radicals. The generation of ·OH by B(a)P and UVA radiation may play an important part in oxidative DNA damage in cultured and primary cells. To continue this work, further research into other parameters of oxidative stress would be of value to investigate such as lipid peroxidation, glutathione or respiratory burst. The use of PCR to investigate gene expression would be a valuable continuation. Other avenues of interest include investigation into interleukins, apoptosis, phagocytosis or inflammatory changes to explore alterations in immune function. These would be an important addition to the work presented here, but this kind of research is expensive to conduct.

2) Limitations with regard the use of cultured cells:

- The use of primary cells has gained interest, but some primary cell systems have shown high levels of variability, and the conclusion is that cell lines appear to produce more reproducible responses (Scholz & Segner, 1999). The purposes of using the primary cell 84BR was to take the research to the next 'tier' and begin to investigate the combined effects of B(a)P and UVR to a cell type that potentially had an increased sensitivity and robustness (Morley *et al.*, 2005). It also maintained many metabolic functions that are often lost when working with established cell cultures. Although similar results were obtained (comet and micronucleus assays) through using the cultured cell lines as with the primary cells (84BR) extensive use of primary cells would be a positive progression to this work (e.g. by incorporating the effects of immune function which may or may not be related to the oxidative stress already shown in this work) as this would enable a

more realistic interpretation of effects further up the biological and ecological hierarchy (Moore *et al.*, 2004).

- The use of fish cells as a biomonitoring tool is of growing interest (Nehls & Segner, 2005) and the data presented here using anti-kinetochore staining and ESR is novel in its approach with its use of RTG-2 fish cells. The more practical handling of some fish cells (such as the 48 hour cell cycle, rudimentary cytochrome P-450-dependent monooxygenase activities and incubation at room temperature) means they would be a better alternative for replacing fish in bioassays than using mammalian cells (Castano & Gomez-Lechon, 2005) and as shown in this project, similar results would be gained from their use in ecotoxicology as with mammalian cells.
- The RTG-2 cell line would be a particularly useful tool to be adopted in future studies looking at biomonitoring in conjunction with *in vivo* practices (Castano *et al.*, 2003; Sanchez-Fortun *et al.*, 2005).

The findings of this research provide many opportunities for future novel avenues of research. The original hypothesis for this thesis was that B(a)P and UVR causes cytotoxicity and genotoxicity in fish and mammalian cells and the results of these studies showed that sequential exposure to B(a)P and UVA produced a synergistic enhancement of DNA damage, which was also represented by reductions in cell viability, increases in DNA damage, changes in cell cycle and increases in chromosomal damage as well as oxidative damage via the hydroxyl radical. The mechanism of this enhancement is however still unclear. B(a)P may induce bulky adducts when light (Kim *et al.*, 2005) or as presented in this work when UVA is present, inducing DNA damage as B(a)P absorption is in the UVA and visible light spectrum and has been previously shown to be photomutagenic (Yan *et al.*, 2004). Therefore

B(a)P or its metabolites may become activated by UVA to cause DNA damage. There is now the opportunity for future research to set a revised or new hypothesis. Possible research that can be extended from this paper have already been suggested but mainly concern the extension of the assays already used and greater detailed research into the up or down regulation of various key genes and further investigation into the effects of oxidative stress on genomic stability. A concise project would be able to concentrate on one particular cell type and delve deeper into the mechanisms causing cell mutation following treatment with B(a)P and UVA as the work presented here demonstrates that this combined insult affects cells ubiquitously.

In conclusion the authors study was successful in answering the questions posed within the limits of the techniques used and valuable patterns have emerged. This work opens opportunities into further research on interactive toxicity. The widespread occurrence of PAHs subject all exposed living cells to potential genotoxic stress and the knock-on effects of this insult combined with UVA appears to exacerbate the damage through direct and indirect mechanisms. The effects of combined exposure to B(a)P and UVA radiation involve oxidative stress, and cause inherited genomic instability which may account for the onset of carcinogenesis, as the mutations observed may be unstable yet not lethal. The consequences of this study are far-reaching and extend into many environmental areas, be they marine based, or involved in regulation of air pollution.

Appendix 1.1

Cell Culture Materials and Experimental Chemicals for Assays

Cell culture Materials

Reagent	Supplier	CAT No
Foetal Bovine Serum	Gibco	10186-151
Ham F12 nutrient mixture	Gibco	21765-037
Eagles Minimum Essential Medium (EMEM)	Gibco	31095-029
L-glutamine	Gibco	25030-024
Minimum Essential Medium (MEM) With Earles Salts, L-Glutamine	Gibco	31095-029
Minimum Essential Medium (MEM) With Earles Salts, without L-Glutamine, without phenol red	Gibco	51200-038
Phosphate Buffered Saline (PBS) Without Ca or Mg	Gibco	14190-086
Trypsin solution (0.25 %)	Gibco	25050-014
Versene 1:5000	Gibco	15040-033

List of Experimental Chemicals for Assays

Reagent	Supplier	CAS No
Benzo(a)pyrene (B(a)P)	Sigma	80-05-7
Colchicine (COL)	Sigma	C-9754
Hydrogen Peroxide (H_2O_2)	Fisher Chemicals	H/1800/15
Methansulfonic Acid Ethyl Ester (EMS)	Sigma	M-0880

List of Reagents for the Neutral Red Retention Assay (NRR)

Reagent	Supplier	CAS No
Acetic Acid	Sigma	64-19-7
Calcium Chloride ($CaCl_2$)	Sigma	10043-52-4
Ethanol	Sigma	64-17-5
Neutral Red	Sigma	553-24-2

List of Reagents for the Single Cell gel Electrophoresis ('Comet Assay')

Reagent	Supplier	CAS No
Dimethylsulfoxide (DMSO)	Fisher Chemicals	D-4121
0.5 M Ethylenediamine Tetraacetic Acid (EDTA), disodium salt	Sigma	E-7889
Ethidium Bromide	Sigma	E-1510
Low Melting Point Agarose (LMP)	Sigma	A-9414
Normal Melting Point Agarose (NMP)	Sigma	A-7174
Potassium Chloride (KCl)	Sigma	P-9541
Sodium Chloride (NaCl)	Sigma	S-3014
Sodium Hydroxide (NaOH)	BDH	102524X
Na_2EDTA	Sigma	E-1644
N-Lauryl-Sarcosine	Sigma	L-5125
Tris-Acetate	Sigma	T-1258

TRIS base	Sigma	Y-1503
TRITON-X-100	Sigma	T-8787
Trypan Blue Solution (0.4 %)	Sigma	T-8154

S9 activation system

NADPH Regensys 'A'	Moltox, Inc	1-0060-200-5
NADPH Regensys ,B'	Moltox, Inc	1-0060-201-5L
Aroclor 1254-induced S9	Moltox Inc	11-101

List of Reagents for the Micronucleus Assay

Reagent	**Supplier**	**CAS No**
Acetic Acid glacial 100 %	BDH	27013BV
Buffer Tablets pH 6.8	BDH	362242D
Cytochalasin B	Aldrich	1493-96-2
DPX Mountant, Dibutyl phthalate	BDH	360294H
Formaldehyde (37 % - Formalin)	Sigma	F-1635
Giemsa Stain Solution	BDH	350865P
Methanol	Fisher	M/3950/17
Potassium Chloride (KCl)	Sigma	P-9541
Human antinuclear antibody, centromere specific	Antibodies Inc. USA	15-134
Anti-Human IgG (Fc Specific) Cy3 conjugate	Sigma	C2571
DAPI antifade (0.1 µg ml^{-1} DAPI in antifade)	Appligene Oncor	S1373-3

Dual Staining

Name	**Supplier**	**Cat No**
Viability/Cytotoxicity Assay Kit for Animal Live & Dead Cells	Biotium Inc, USA	30002

Annexin V-FITC Apoptosis Detection

Name	**Supplier**	**Cat No**
Annexin V:FITC Apoptosis Detection Kit I	BD Biosciences	556547

Appendix 1.2
Preparation of buffers and solutions

S9 Metabolic Activation System (S9)

S9 Homogenate
S9 Homogenate aliquot (in 0.154 M KCl) into 1 ml vials and store at -70 °C

S9 Core
NADPH Regensys 'A' contains glucose-6-phosphate, $MgCl_2$/KCl in 0.1 M phosphate buffer, pH 7.4. 153 mg NADP NADPH Regensys 'B') added to 1 ml sterile distilled water and added to Regensys 'A'. Aliquot this into 5 ml vials and store at -20 °C.

Preparation:
This must be prepared immediately prior to use.
Mix:
0.15 ml S9 homogenate
0.60 ml S9 core
9.25 ml medium containing 1 % FBS and chemical under investigation (e.g. B(a)P)

This is added to the cell cultures and incubated for no longer than 3-6 hours.

Comet Assay
LMP agarose: 0.5 % in PBS

NMP agarose: 1 % in PBS

Lysing Solution (per 1 L): NaCl (2.5 M), Na_2EDTA (100 mM), Tris Base (10 mM), N-Lauryl-sarcosine (1 %), pH 10 in distilled water
TRITON-X (1 %) and DMSO (10 %) added immediately prior to use.

Electrophoresis Buffer (2 L): NaOH (1 M), EDTA (200 mM) in distilled water pH > 13

Neutralisation Buffer (1 L): Tris Base (0.4 M) in distilled water pH 7.5

Ethidium Bromide: 1/100 dilution in distilled water

Micronucleus Assay
Cytochalasin B : Cytochalasin B 100 µg ml^{-1} in DMSO

Potassium Chloride (KCl): 0.56 % KCl in distilled water

Fixative: 1:4 acetic acid: methanol

Giemsa Stain: 10 % Giemsa in Giemsa Buffer pH 6.8

References

Abe, S., Nemoto, N. and Sasaki, M. 1983. Comparison of aryl hydrocarbon hydroxylase activity and inducibility of sister chromatid exchanges by polycyclic aromatic hydrocarbons in mammalian cell lines. *Mutation Research*, **122**, 47-51.

Adams, N.L. and Shick, M.J. 1996. Mycosporine-like amino acids provide protection against ultraviolet radiation in eggs of the green sea urchin *Strongylocentrotus droebachiensis*. *Photochemistry and Photobiology* **64**, 149-158.

Agar, N.S., Halliday, G.M., Barnetson, R.S., Ananthaswamy, H.N., Wheeler, M. and Jones, A.M. 2004. The basal layer in human squamous tumors harbors more UVA than UVB fingerprint mutations: A role for UVA in human skin carcinogenesis. *Proceedings of the National Academy of Sciences of the U S A,* **101**, 4954-4959.

Agredano, Y.Z., Chan, J.L., Kimball, R.C. and Kimball, A.B. 2006. Accessibility to air travel correlates strongly with increasing melanoma incidence. *Melanoma Research*, **16**, 77-81.

Ahmed, F.E., Setlow, R.B., Grist, E. and Setlow, N. 1993. DNA repair, photorepair, and survival in fish and human cells exposed to UV radiation. *Environmental and Molecular Mutagenesis*, **22**, 18-25.

Albers, P.H. 1995. Petroleum individual polycyclic aromatic hydrocarbons. In: Hoffman DJ, Rattner BA, Burton GA Jr, Cairns JC Jr (eds) Handbook of ecotoxicology. Lewis Publishers, Boca Raton, FL, pp 330–355.

Albertini, R.J., Anderson, D., Douglas, G.R., Hagmar, L., Hemminki, K., Merlo, F., Natarajan, A., Norppa, H., Shoker, D.E.G., Tice, R., Waters, M.D. and Aitio, A. 2000. Special issue: IPCS guidelines for the monitoring of genotoxic effects of carcinogens in humans. *Reviews in Mutation Research*, **463**, 111-172.

Albès, B., Marguery, M.C., Schwarze, H.P., Journé, F., Loche, F. and Bazex, J. 2004. Prolonged photosensitivity following contact photoallergy to ketoprofen. *Dermatology*, **201**, 171-174.

Allen-Hoffmann, B.L. and Rheinwald, J.G. 1984. Polycyclic aromatic hydrocarbon mutagenesis of human epidermal keratinocytes in culture. *Proceedings of the National Academy of Sciences of the USA*, **81**, 7802-7806.

Alsbeih, M.G., Fertil, B., Arlett, C.F. and Malaise, E.P. 1996. High split-dose recovery in hypersensitive human fibroblasts: a case of induced radioresistance? *International Journal of Radiation Biology*, **69**, 225-239.

Anderson, S., Sadinski, W., Shugart, L., Brussard, P., Depledge, M., Ford, T., Hose, J., Stegeman, J., Suk, W., Wirgin, I. and Wogan, G. 1994. Genetic and molecular ecotoxicology: a research framework. *Environmental Health Perspectives*, **102**, 3-8.

Andrade, V.M., Silva, J., Silva, F.R., Heuser, V.D., Dias, J.F., Yoneama M.L. and Freitas, T.R.O. 2004. Fish as bioindicators to assess the effects of pollution in two southern Brazilian rivers using the comet assay and micronucleus test. *Environmental and Molecular Mutagenesis*, **44**, 459-468.

Annas, A., Brittebo, E. and Hellman, B. 2000. Evaluation of benzo(a)pyrene-induced DNA damage in human endothelial cells using alkaline single cell gel electrophoresis. *Mutation Research*, **471**, 145-155.

Antoccia, A., Tanzarella, C., Modesti, D. and Degrassi, F. 1993. Cytokinesis-block micronucleus assay with kinetochore detection in colchicine-treated human fibroblasts. *Mutation Research*, **287**, 93-99.

Aouadene, A., Di Giorgio, C., Sarrazin, L., Moreau, X., De Jong, L., Garcia, F., Thiery, A., Botta, A. and De Méo, M. 2008. Evaluation of the genotoxicity of river sediments from industrialized and unaffected areas using a battery of short-term bioassays. *Environmental and Molecular Mutagenesis*, **49**, 283-299.

Araújo, C.S., Marques, S.A., Carrondo, M.J., Gonçalves, L.M. 2000. *In vitro* response of the brown bullhead catfish (BB) and rainbow trout (RTG-2) cell lines to benzo(a)pyrene. *Science of the Total Environment*, **247**, 127-135.

Arfsten, D., Schaeffer, D. and Mulveny, D. 1996. The effects of near ultraviolet radiation on the toxic effects of polycyclic aromatic hydrocarbons in animals and plants: A review. *Ecotoxicology and Environmental Safety*, **33**, 1-24.

Armstrong, B.K. 1984. Melanoma of the skin. *British Medical Bulletin*, **40**, 346-350.

Armstrong, B.K. and Kricker, A. 1994. Cutaneous melanoma. *Cancer Surveys Trends Cancer Incidence*, **19**, 219-239.

Armstrong, B.K., Kricker, A. and English, D.R. 1997. Sun exposure and skin cancer. *Australian Journal of Dermatology*, **38**, S1-S6.

Armstrong, T.N., Reimschuessel, R. and Bradley, B.P. 2002. DNA damage, histological changes and DNA repair in larval Japanese medaka (*Oryzias latipes*) exposed to ultraviolet-B radiation. *Aquatic Toxicology*, **58**, 1-14.

ASCO. 2003. American Society of Clinical Oncology policy statement: oversight of clinical research. *Journal of Clinical Oncology*, **21**, 2377-2386.

Ateenyi-Agaba, C., Weiderpass, E., Smet, A., Dong, W., Dai, M., Kahwa, B., Wabinga, H., Katongole-Mbidde, E., Franceschi, S. and Tommasino, M. 2004. *Epidermodysplasia verruciformis* human papillomavirus types and carcinoma of the conjunctiva: a pilot study. *British Journal of Cancer*, **90**, 1777-1779.

ATSDR. 1995. *Toxicological profile for polycyclic aromatic hydrocarbons (PAHs)*. Department of Health and Human Services, Public Health Service. Atlanta, GA: U.S.

ATSDR. 2004. *Preliminary Health Assessment: Texarkana Wood Preserving Site, Texarkana, Bowie County, Texas*. Atlanta, GA: US.

Au, D.W., Chen, P. and Pollino, C.A. 2004. Cytological changes in association with ethoxyresorufin o-deethylase induction in fish upon dietary exposure to benzo(a)pyrene. *Environmental Toxicology and Chemistry*, **23**, 1043-1050.

Au, D.W.T., Chiang, M.W.L., Tang, J.Y.M., Yuen, B.B.H., Wang, Y.L. and Wu, R.S.S. 2002. Impairment of sea urchin sperm quality by UV-B radiation: predicting fertilization success from sperm motility. *Marine Pollution Bulletin*, **44**, 583-589.

Avogbe, P.H., Ayi-Fanou, L., Autrup, H., Loft, S., Fayomi, B., Sanni, A., Vinzents, P. and Møller, P. 2005. Ultrafine particulate matter and high-level benzene urban air pollution in relation to oxidative DNA damage. *Carcinogenesis*, **26**, 613-620.

Ayllon, F. and Garcia-Vazquez, E. 2000. Induction of micronuclei and other nuclear abnormalities in European minnow *Phoxinus phoxinus* and mollie *Poecilia latipinna*: an assessment of the fish micronucleus test. *Mutation Research*, **467**, 177-186.

Babich, H. and Borenfreund, E. 1987. Cultured fish cells for the ecotoxicity testing of aquatic pollutants. *Toxicity Assessment*, **2**, 119-133.

Babich, H. and Borenfreund, E. 1991. Cytotoxicity and genotoxicity assays with cultured fish cells: A review. *Toxicology in Vitro,* **5**, 91–100.

Babich, H. and Borenfreund, E. 1992. Neutral red assay for toxicology *in vitro*. Boca Raton, CRC Press. pp. 237-251.

Babich, H., Rosenberg, D.W. and Borenfreund, E. 1991. *In vitro* cytotoxicity studies with the fish hepatoma cell line, PLHC-1 (*Poeciliopsis lucida*). *Ecotoxicology and Environmental Safety*, **21**, 327–336.

Babich, H., Sardana, M.K. and Borenfreund, E. 1988. Acute cytotoxicities of polynuclear aromatic hydrocarbons determined *in vitro* with the human liver tumor cell line, HepG2. *Cell Biology and Toxicology*, **4,** 295-309.

Babin, M.M. and Tarazona, J.V. 2005. *In vitro* toxicity of selected pesticides on RTG-2 and RTL-W1 fish cell lines. *Environmental Pollution*, **135**, 267-274.

Bånrud, H., Stokke, T., Moan, J. and Berg, K. 1995. S phase arrest and induction of multinucleated cells after exposure to ultraviolet radiation. *Carcinogenesis*. **16**, 1087-1094.

Barnes, E.R. and Shurtz-Swirski, R. 1992. Modification of pulsatile human chorionic gonadotrophin secretion in first trimester placental explants induced by polycyclic aromatic hydrocarbons. *Human Reproduction*, **7**, 305-310.

Barron, M.G., Carls, M.G., Heintz, R. and Rice, S.D. 2004. Evaluation of fish early life-stage toxicity models of chronic embryonic exposures to complex polycyclic aromatic hydrocarbon mixtures. *Toxicological Sciences*, **78**, 60-67.

Barron, M.G., Carls, M.G., Short, J.W. and Rice, S.D. 2003. Photoenhanced toxicity of aqueous phase and chemically dispersed weathered Alaska North Slope crude oil to Pacific herring eggs and larvae. *Environmental Toxicology and Chemistry*, **22**, 650-660.

Barron, M. and Ka'aihue, L. 2001. Potential for photoenhanced toxicity of spilled oil in Prince William Sound and Gulf of Alaska waters. *Marine Pollution Bulletin*, **43**, 86-92.

Barron, M.G., Little, E.E., Calfee, R. and Diamond, D. 2000. Quantifying solar spectral irradiance in aquatic habitats for the assessment of photoenhanced toxicity. *Environmental Toxicology and Chemistry,* **19**, 920-925.

Battini, M., Rocco, V., Lozada, M., Tartarotti, B. and Zagarese, H.E. 2000. Effects of ultraviolet radiation on the eggs of landlocked *Galaxias maculatus* (Galaxidae, Pisces) in Northwestern Patagonia. *Freshwater Biology*, **44**, 547-552.

Bau, D., Gurr, J. and Jan, K. 2001. Nitric oxide is involved in arsenite inhibition of pyrimidine dimer excision. *Carcinogenesis*, **22**, 709-716.

Baudouin, C., Charveron, M., Tarroux, R. and Gall, Y. 2002. Environmental pollutants and skin cancer. *Cell Biology and Toxicology*, **18**, 341-348.

Baumann, P.C. 1998. Epizootics of cancer in fish associated with genotoxins in sediment and water. *Mutation Research*, **411**, 227–233.

Becker, S., Soukup, J. and Gallagher, J. 2002. Differential particulate air pollution induced oxidant stress in human granulocytes, monocytes and alveolar macrophages. *Toxicology in vitro*, **16**, 209-218.

Behrens, A., Schirmer, K., Bols, N.C. and Segner, H. 2001. Polycyclic aromatic hydrocarbons as inducers of cytochrome P4501A enzyme activity in the rainbow trout liver cell line, RTL-W1, and in primary cultures of rainbow trout hepatocytes. *Environmental Toxicology and Chemistry*, **20**, 632-643.

Beland, F., Browman, H.I., Rodriguez, C.A., and St. Pierre, J.F. 1999. Effect of solar ultraviolet radiation (280-400 nm) on the eggs and larvae of Atlantic cod (*Gadus morhua*). *Journal of Fisheries and Aquatic Sciences,* **56,** 1058-1067.

Bentham G. 1993. Depletion of the ozone layer: consequences for non-infectious human diseases. *Parasitology*, **106**, 39-46.

Besaratinia, A. and Pfeifer, G.P. 2003. Enhancement of the mutagenicity of benzo(a)pyrene diol epoxide by a non-mutagenic dose of ultraviolet A radiation. *Cancer Research*, **63**, 8708-8716.

Beyth, R., Hunnicutt, M. and Alguire, P.C. 1991. Tanning salons: an area survey of proprietors' knowledge of risks and precautions. *Journal of the American Academy of Dermatology,* **24**, 277-282.

Bickham, J.W., Sandhu, S., Herbert, P.D.N., Chikhi, L. and Athwal, R. 2000. Effects of chemical contaminants on genetic diversity in natural populations: implications for biomonitoring and ecotoxicology. *Mutation Research*, **463**, 33-51.

Binkova, B., Lewtas, J., Miskova, I., Lenicek, J. and Sram, R. 1995. DNA-adducts and personal air monitoring of carcinogenic polycyclic aromatic hydrocarbons in an environmentally exposed population. *Carcinogenesis*, **16**, 1037-1046.

Binkova, B., and Sram, R.J. 2004. The genotoxic effect of carcinogenic PAHs, their artificial and environmental mixtures (EOM) on human diploid lung fibroblasts. *Mutation Research,* **547**, 109-121.

Blumthaler, M., Ambach, W. and Ellinger R. 1997. Increase in solar UV radiation with altitude. *Journal of Photochemistry and Photobiology B: Biology*, **39**, 130-134.

Bock, C., Dittmar, H., Gemeinhardt, H., Bauer, E. and Greulich, K.O. 1998. Comet assay detects cold repair of UVA damages in a human B-lymphoblast cell line. *Mutation Research*, **408,** 111-120.

Boelsterli, U. 2003. *Mechanistic toxicology: The molecular basis of how chemicals disrupt biological targets.* Taylor & Francis, London.

Boese, B.L., Lamberson, J.O., Swartz, R.C. and Ozretich. R.J. 1997. Photoinduced toxicity of fluoranthene to seven marine benthic crustaceans. *Archives of Environmental Contamination and Toxicology*, **32**, 389-393.

Bojes, H.K. and Pope, P.G. 2007. Characterization of EPA's 16 priority pollutant polycyclic aromatic hydrocarbons (PAHs) in tank bottom solids and associated contaminated soils at oil exploration and production sites in Texas. *Regulatory Toxicology and Pharmacology,* **47**, 288-295.

Bols, N.C. and Lee, L.E.J. 1994. Cell line: availability, propagation and isolation. In: Hochachka PW & Mommsen TP (eds) *Biochemistry and molecular biology of fishes*. Vol III. Analytical techniques. Elsevier, Amsterdam, pp 145 - 159.

Bolton, J.L., Trush, M.A., Penning, T.M., Dryhurst, G. and Monks, T.J. 2000. Role of quinones in toxicology. *Chemical Research in Toxicology*, **13**, 135-160.

Bossi, O., Gartsbein, M., Leitges, M., Kuroki, T., Grossman, S. and Tennenbaum, T. 2008. UV irradiation increases ROS production via

PKCdelta signaling in primary murine fibroblasts. *Journal of Cellular Biochemistry*, **105**, 194-207.

Bracchini, L., Loiselle, S., Dattilo, A.M., Mazzuoli, S., Cózar, A. and Rossi, C. 2004. The spatial distribution of optical properties in the ultraviolet and visible in an aquatic ecosystem. *Photochemistry and Photobiology,* **80**, 139-149.

Brash, D., Ziegler, A., Jonason, A., Simon, J., Kunala, S. and Lefell, D. 1996. Sunlight and sunburn in human skin cancer: P53, apoptosis, and tumour production. *Journal of Investigative Dermatology Symposium Proceedings*, **1**, 136-142.

Bråthen, M., Bånrud, H., Berg, K. and Moan, J. 2000. Induction of multinucleated cells caused by UVA exposure in different stages of the cell cycle. *Photochemistry and Photobiology*, **71**, 620-626.

Braunbeck, T. and Neumuller, D. 1996. The Comet assay in permanent and primary fish cell cultures—a novel system to detect genotoxicity. *Cell and Developmental Biology*, **32**, 61A.

Brinkley, B.R., Tousson, A. and Valdivia, M. 1985. *The kinetochore of mammalian chromosomes: structure and function in normal mitosis and aneuploidy.* In: Dellarco VL, Voytek PE & Hollaender A (Eds) Aneuploidy and mechanisms. Plenum Press, New York, NY pp. 243-265.

Brown, R.A. and Weiss, F.T. 1978. *Fate and effects of polynuclear aromatic hydrocarbons in the aquatic environment.* Publication no. 4297. American Petroleum Institute, Washington, D.C., USA.

Buettner, G. R. 1987. Spin trapping: ESR parameters of spin adducts. *Free Radical Biology and Medicine*, **3**, 259-303.

Buettner, G.R. and Mason, R.P. 2003. Spin-trapping methods for detecting superoxide and hydroxyl free radicals *in vitro* and *in vivo*. In: *Critical Reviews of Oxidative Stress and Aging: Advances in Basic Science, Diagnostics and Intervention*. Eds: Cutler, RG and Rodriguez, H. World Scientific, New Jersey, London, Singapore, Hong Kong. **1**, 27-38.

Bullock, A.M. 1982. The pathological effects of ultraviolet radiation on the epidermis of teleost fish with reference to the solar radiation effect in higher animals. *Proceedings of the Royal Society of Edinburgh*, **81**, 199-210.

Bullock, A.M. 1985. The effect of ultraviolet-B radiation upon the skin of the plaice, *Pleuronectes platessa* L., infested with the bodonid

ectoparasite *Ichthyobodo necator* (Henneguy, 1883). *Journal of Fish Diseases,* **8**, 547-550.

Bullock, A.M. and Coutts, R.R. 1985. The impact of solar ultraviolet radiation upon the skin of rainbow trout, *Salmo gairdneri* Richardson, farmed at high altitude in Bolivia. *Journal of Fish Diseases,* **8**, 263-272.

Bullock, A.M., Marks, R. and Roberts, R.J. 1978. The cell kinetics of teleost fish epidermis: mitotic activity of the normal epidermis at varying temperatures in plaice (*Pleuronectes platessa*). *Journal of the Zoological Society of London*, **184**, 423-428.

Burlinson, B., Tice, R.R., Speit, G., Agurell, E., Brendler-Schwaab, S.Y., Collins, A.R., Escobar, P., Honma, M., Kumaravel, T.S., Nakajima, M., Sasaki, Y.F., Thybaud, V., Uno, Y., Vasquez, M., Hartmann, A. 2007. *In Vivo* Comet Assay Workgroup, part of the Fourth International Workgroup on Genotoxicity Testing. Fourth international workgroup on genotoxicity testing: results of the *in vivo* comet assay workgroup. *Mutation Research*, **627**, 31-35.

Burren, R., Scaletta, C., Frenk, E., Panizzon, R.G., Applegate L.E. 1998. Sunlight and carcinogenesis: expression of p53 and pyrimidine dimers in human skin following UVA I, UVA I + II and solar simulating radiations. *International Journal of Cancer*, **76**, 201-206.

Busch, D. B., White Ziffer, D., Coleman, D., Wills, L., Greg McDonough, H. and Jones, N. J. 2001. Phenotype of FAECB (Facility for automated experiments in cell biology) chinese hamster ovary mutants with minimal UV-sensitivity. *Mutation Research/DNA Repair*, **487**, 31-39.

Butterworth, B E., Smith-Oliver, T., Earle, L., Loury, DJ., White, R D., Doolittle, DJ., Working, PK, Cattley, RC., Jirtle, R., Michalopoulos, G. and Strom, S. 1989. Use of primary cultures of human hepatocytes in toxicology studies. *Cancer Research*, **49**, 1075-1084.

Call, D.J., Brooke, L.T., Harting, S.L., Poirier, S.H. and McCauley, D.J. 1986. Toxicity of phenanthrene to several freshwater species. Unpublished report, Center for Lake Superior Environmental Studies, University of Wisconsin-Superior, Superior, Wisconsin.

Calkins, J. and Thordardotter, T. 1980. The ecological significance of solar UV radiation on aquatic organisms. *Nature*, **283**, 563-566.

Canty, M.N., Hagger, J.A., Moore, R.T., Cooper, L. and Galloway, T.S. 2007. Sublethal impact of short term exposure to the organophosphate

pesticide azamethiphos in the marine mollusc *Mytilus edulis*. *Marine Pollution Bulletin*, **54**, 396-402.

Carlsten, C., Hunt, S.C. and Kaufman, J.D. 2005. Squamous cell carcinoma of the skin and coal tar creosote exposure in a railroad worker. *Environmental Health Perspectives*, **113**, 96-97.

Castaño, A. and Becerril, C. 2004. *In vitro* assessment of DNA damage after short- and long-term exposure to benzo(a)pyrene using RAPD and the RTG-2 fish cell line. *Mutation Research*, **552**, 141-151.

Castano, A., Bols, N.C., Braunbeck, T., Dierickx, P., Halder, M., Isomaa, B., Kawahara, K., Lee, L.E.J., Mothersill, C., Pärt, P., Repetto, G., Sintes, J.R., Rufli, H., Smith, R., Wood, C. and Segner, H. 2003. The use of fish cells in ecotoxicology. The report and recommendations of ECVAM workshop. *Alternatives To Laboratory Animals*, **31**, 317-351.

Castano, A., Cantario, M.J., Castillo, P. and Tarazona, J.V. 1996. Correlations between the RTG-2 cytotoxicity test and *in vivo* LC50 rainbow trout bioassay. *Chemosphere*, **32**, 2141-2157.

Castano, A. and Gomez-Lechon, M.J. 2005. Comparison of basal cytotoxicity data between mammalian and fish cell lines: A literature survey. *Toxicology in vitro*, **19**, 695-705.

Castaño, A., Sanchez, P., Llorente, M.T., Carballo, M., de la Torre, A. and Muñoz, M.J. 2000. The use of alternative systems for the ecotoxicological screening of complex mixtures on fish populations. *Science of the Total Environment*, **247**, 337-348.

Castano, A., Vega, M., Blazquez, T. and Tarazona, J.V. 1994. Biological alternatives to chemical identification for the toxicological assessment of industrial effluents: the RTG-2 *in vitro* cytotoxicity test. *Environmental Toxicology and Chemistry*, **13**, 1607-1611.

Cavaş, T. and Ergene-Gözükara, S. 2005. Micronucleus test in fish cells: a bioassay for *in situ* monitoring of genotoxic pollution in the marine environment. *Environmental and Molecular Mutagenesis*, **46**, 64-70.

Cayrol, C., Sarraute, J., Tarroux, R., Redoules, D., Charveron, M. and Gall, Y. 1999. A mineral sunscreen affords genomic protection against ultraviolet (UV) B and UVA radiation: *in vitro* and *in situ* assays. *British Journal of Dermatology*, **141**, 250-258.

Champion, A.R., Hanson, J.A., Court, J.B. and Venables, S.E. 1995. The micronucleus assay: an evaluation of its use in determining radiosensitivity *in vitro*. *Mutagenesis*, **10**, 203-208.

Chen, M., Chen, J. and Du, P. 2006a. An inventory analysis of rural pollution loads in China. *Water Science and Technology*, **54**, 65-74.

Chen, S.J., Luo, X.J., Mai, B.X., Sheng, G.Y., Fu, J.M. and Zeng, E.Y. 2006b. Distribution and mass inventories of polycyclic aromatic hydrocarbons and organochlorine pesticides in sediments of the Pearl River Estuary and the northern South China Sea. *Environmental Science and Technology*, **40**, 709-714.

Chen, S., Nguyen, N., Tamura, K., Karin, M. and Tukey, R.H. 2003. The role of the Ah receptor and p38 in benzo(a)pyrene-7,8-dihydrodiol and benzo(a)pyrene-7,8-dihydrodiol-9,10-epoxide-induced apoptosis. *Journal of Biological Chemistry*, **278**, 19526-19533.

Chen, H and Perdew, G.H. 1994. Subunit composition of the heteromeric cytosolic aryl hydrocarbon receptor complex. *Journal of Biological Chemistry*, **269**, 27554-27558.

Cheung, Y.L., Gray, T.J.B. and Ioannides, C. 1993. Mutagenicity of chrysene, its methyl and and benzo derivatives, and their interactions with cytochromes P-450 and the Ah-receptor; relevance to their carcinogenic potency. *Toxicology*, **81**, 69-86.

Chipman, J.K., Millburn, P. and Brooks, T.M. 1983. Mutagenicity and *in vivo* disposition of biliary metabolites of benzo(a)pyrene. *Toxicology Letters,* **17**, 233-240.

Choi, J. and Oris, J. 2000a. Evidence of oxidative stress in bluegill sunfish (*Lepomis macrochirus*) liver microsomes simultaneously exposed to solar ultraviolet radiation and anthracene. *Environmental Toxicology and Chemistry*, **19**, 1795-1799.

Choi, J. and Oris, J. 2000b. Anthracene photoinduced toxicity to PHLC-1 cell line (*Poeciliopsis lucida*) and the role of lipid peroxidation in toxicity. *Environmental Toxicology and Chemistry*, **19**, 2699-2706.

Choi, J. and Oris, J. 2003. Assessment of the toxicity of anthracene photo-modification products using the topminnow (*Poeciliopsis lucida*) hepatoma cell line (PLHC-1). *Aquatic Toxicology*, **65**, 243-251.

Chuang, T.Y., Popescu, A., Su, W.P. and Chute, C.G. 1990. Basal cell carcinoma. A population-based incidence study in Rochester, Minnesota. *Journal of the American Academy of Dermatology*, **22**, 413-417.

Cizmas, L., McDonald, T.J., Phillips, T.D., Gillespie, A.M., Lingenfelter, R.A., Kubena, L.F. and Donnelly, K.C. 2004. Toxicity characterization of complex mixtures using biological and chemical analysis in preparation for assessment of mixture similarity. *Environmental Science and Technology,* **38**, 5127-5133.

Clements, W.H. and P. M. Kiffney. 1994. An integrated approach for assessing the impact of heavy metals at the Arkansas River, CO. *Environmental Toxicology and Chemistry*, **13**, 397-404.

Clemons, E., Arkoosh, M.R. and Casillas, E. 1999. Enhanced superoxide anion production in activated peritoneal macrophages from English Sole (*Pleuronectes vetulas*) exposed to polycyclic aromatic hydrocarbons. *Marine Environmental Research*, **47**, 71-87.

Cole, R.H., Frederick, R.E., Nealy, R.P. and Rolan, R.G. 1984. Preliminary findings of the priority pollutant monitoring project of the nationwide urban runoff program journal. *Journal of Water Pollution Control Federation,* **56**, 898-908.

Cotelle, S. and Férard, J.F. 1999. Comet Assay in Genetic Ecotoxicology: a review. *Environmental and Molecular Mutagenesis*, **34**, 246-255.

Crallan, R.A., Ingham, E. and Routledge, M.N. 2005. Wavelength dependent responses of primary human keratinocytes to combined treatment with benzo(a)pyrene and UV light. *Mutagenesis*, **20**, 305-310.

Crespi, C.L., Altman, J.D. and Marletta, M.A. 1985. Xenobiotic metabolism and mutation in a human lymphoblastoid cell line. *Chemico-Biological Interactions*, **53**, 257-271.

Crews, D., Bergeron, JM. and McLachlan, JA. 1995. The role of estrogen in turtle sex determination and the effects of PCBs. *Environmental Health Perspectives*, **103**, 73-77.

Cridland, N. and Saunders, R. 1994. *Cellular and molecular effects of UVA and UVB.* National Radiological Protection Board, Didcot, Oxon.

Cullen, A.P., Monteith-McMaster, C.A. and Sivak, J.G. 1994. Lenticular changes in rainbow trout following chronic exposure to UV radiation. *Current Eye Research,* **13,** 731-737.

Czarnecki, D. and Meehan, C.J. 2000. Is the incidence of malignant melanoma decreasing in young Australians? *Journal of the American Academy of Dermatology,* **42**, 672-674.

Dagher, Z., Garcon, G., Gosset, P., Ledoux, F., Surpateanu, G., Courcot, D., Aboukais, A., Puskaric, E. and Shirali, P. 2005. Pro-inflammatory effects of Dunkerque city air pollution particulate matter 2.5 in human epithelial lung cells (L132) in culture. *Journal of Applied Toxicology*, **25**, 166-175.

Dahle, J., Brunborg, G., Svendsrud, D.H., Stokke, T. and Kvam, E. 2008. Overexpression of human OGG1 in mammalian cells decreases ultraviolet A induced mutagenesis. *Cancer Letters*, **267**, 18-25.

Dagher, Z., Garcon, G., Billet, S., Gosset, P., Ledoux, F., Courcot, D., Aboukais, A. and Shirali, P. 2006. Activation of different pathways of apoptosis by air pollution particulate matter (PM2.5) in human epithelial lung cells (L132) in culture. *Toxicology*, **225**, 12-24.

Danaee, H., Nelson, H., Liber, H., Little, J. and Kelsey, K. 2004. Low dose exposure to sodium arsenite synergistically interacts with UV radiation to induce mutations and alter DNA repair in human cells. *Mutagenesis*, **19**, 143-148.

Davoren, M., Ní Shúilleabháin, S., Hartl,, M.G., Sheehan, D., O'Brien, N.M., O'Halloran, J., Van Pelt, F.N. and Mothersill, C. 2005. Assessing the potential of fish cell lines as tools for the cytotoxicity testing of estuarine sediment aqueous elutriates. *Toxicology in Vitro*, **19**, 421-431.

Dean, R.G., Bynum, G., Jacobson-Kram, D. and Hadley, E. 1983. Activation of polycyclic hydrocarbons in Reuber H4-II-E hepatoma cells. An *in vitro* system for the induction of SCEs. *Mutation Research*, **111**, 419-427.

de Gruijl, F. R. and Forbes, P. D. 1995. UV-induced skin cancer in a hairless mouse model. *Bioessays*, **17**, 651-660.

de Gruijl, F.R., Longstreth, J., Norval, M., Cullen, A.P., Slaper, H., Kripke, M.L., Takizawa, Y. and van der Leun, J.C. 2003. Health effects from stratospheric ozone depletion and interactions with climate change. *Photochemical and Photobiological Sciences*, **2**, 16-28.

de Laat, A., van Tilburg, M., van der Leun, J.C., van Vloten, W.A. and de Gruijl, F.R. 1996. Cell cycle kinetics following UVA irradiation in

comparison to UVB and UVC irradiation. *Photochemistry and Photobiology,* **63**, 492-497.

Delfino, R.J., Zeiger, R.S., Seltzer, J.M., Street, D.H. and McLaren, C.E. 2002. Association of asthma symptoms with peak particulate air pollution and effect modification by anti-inflammatory medication use. *Environmental Health Perspectives*, **110**, 607-617.

DeMarini, D.M. 2004. Genotoxicity of tobacco smoke and tobacco smoke condensate: a review. *Mutation Research*, **567**, 447-474.

de Vries, E., Soerjomataram, I., Houterman, S., Louwman, M.W. and Coebergh, J.W. 2007. Decreased risk of prostate cancer after skin cancer diagnosis: a protective role of ultraviolet radiation? *American Journal of Epidemiology*, **165**, 966-972.

Diamond, S.A., Milroy, N.J., Mattson, V.R., Heinis, L.J. and Mount, D.R. 2003. Photoactivated toxicity in amphipods collected from polycyclic aromatic hydrocarbon-contaminated sites. *Environmental Toxicology and Chemistry,* **22**, 2752-2760.

Diamond, S.A., Mount, D.R., Mattson, V.R., Heinis, L.J., Highland, T.L., Adams, A.D. and Simcik, M.F. 2006. Photoactivated polycyclic aromatic hydrocarbon toxicity in medaka (*Oryzias latipes*) embryos: relevance to environmental risk in contaminated sites. *Environmental Toxicology and Chemistry,* **25**, 3015-3023.

Diamond, L., Kruszewski, F., Aden, D.P., Knowles, B.B. and Baird, W.M. 1980. Metabolic activation of benzo(a)pyrene by a human hepatoma cell line. *Carcinogenesis*, **1**, 871-875.

Diepgen, T.L. and Mahler, V. 2002. The epidemiology of skin cancer. *British Journal of Dermatology*, **146**, 1-6.

Diffey, B.L. 1999. Human exposure to ultraviolet radiation. In: Hawk JLM (ed) *Photodermatology*, Arnold, London, pp 5-25.

Ding, G., Nakahara, T. and Miyakoshi, J. 2003. Induction of kinetochore - positive and kinetochore - negative micronuclei in CHO cells by ELF magnetic fields and/or x-rays. *Mutagenesis*, **18**, 439-443.

Dixon, K.M., Deo, S.S., Norman, A.W., Bishop, J.E., Halliday, G.M., Reeve, V.E. and Mason, R.S. 2007. *In vivo* relevance for photoprotection by the vitamin D rapid response pathway. *Journal of Steroid Biochemistry and Molecular Biology*, **103**, 451-456.

Dixon, D.R., Pruski, A.M., Dixon, L.R.J. and Jha, A.N. 2002. Marine invertebrate eco-toxicology: a methodological overview. *Mutagenesis*, **17**, 495-507.

Dong, H., Bonala, R.R., Suzuki, N., Johnson, F., Grollman, A.P. and Shibutani, S. 2004. Mutagenic potential of benzo(a)pyrene-derived DNA adducts positioned in codon 273 of the human P53 gene. *Biochemistry*, **43**, 15922-15928.

Donkin, P., Smith, E.L. and Rowland, S.J. 2003. Toxic effects of unresolved complex mixtures of aromatic hydrocarbons accumulated by mussels, *Mytilus edulis*, from contaminated field sites. *Environmental Science and Technology*, **37**, 4825-4830.

Duesterloh, S., Short, J.W. and Barron, M.G. 2002. Photoenhanced toxicity of weathered Alaska North Slope crude oil to the calanoid copepods *Calanus marshallae* and *Metridia okhotensis*. *Environmental Science and Technology*, **36**, 3953-3959.

Durant, J.L., Busby, W.F. Jr., Lafleur, A.L., Penman, B.W. and Crespi, C.L. 1996. Human cell mutagenicity of oxygenated, nitrated and unsubstituted polycyclic aromatic hydrocarbons associated with urban aerosols. *Mutation Research*, **371**, 123-157.

Durant, J.L., Lafleur, A.L., Busby, W.F. Jr., Donhoffner, L.L., Penman, B.W. and Crespi, C.L. 1999. Mutagenicity of C24H14 PAH in human cells expressing CYP1A1. *Mutation Research*, **446**, 1-14.

Dybowski, J. A. 2000. Characterization of a period of vulnerability to the toxic effects of colchicine during regeneration of the goldfish optic nerve. *Dissertation Abstracts International Part B: Science and Engineering*, **60**, 3246.

Eichler, O., Sies, H. and Stahl, W. 2002. Divergent optimum levels of lycopene, beta-carotene and lutein protecting against UVB irradiation in human fibroblasts. *Photochemistry and Photobiology*, **75**, 503-506.

Ekunwe, S.I., Hunter, R.D. and Hwang, H.M. 2005. Ultraviolet radiation increases the toxicity of pyrene, 1-aminopyrene and 1-hydroxypyrene to human keratinocytes. *International Journal of Environmental Research and Public Health*, **2**, 58-62.

Elbekai, R.H., Korashy, H.M., Wills, K., Gharavi, N. and El-Kadi, A.O. 2004. Benzo(a)pyrene, 3-methylcholanthrene and beta-naphthoflavone induce oxidative stress in hepatoma hepa 1c1c7 cells by an AHR-dependent pathway. *Free Radical Research*, **38**, 1191-1200.

Elhajouji, A., Cunha, M. and Kirsch-Volders, M. 1998. Spindle poisons can induce polyploidy by mitotic slippage and micronucleate mononucleates in the cytokinesis-block assay. *Mutagenesis*, **13**, 193-198.

Ellard, S., Mohammed, Y., Dogra, S., Wolfel, C., Doehmer, J. and Parry, J.M. 1991. The use of genetically engineered V79 Chinese hamster cultures expressing rat liver CYP1A1, 1A2 and 2B1 cDNAs in micronucleus assays. *Mutagenesis*, **6**, 461-470.

Ellard, S. and Parry, J.M. 1993. A comparative study of the use of primary chinese hamster liver cultures and genetically engineered immortal V79 chinese hamster cell lines expressing rat liver CYP1A1, 1A2 and 2B1 cDNAs in micronucleus assays. *Toxicology*, **82**, 131-149.

Elliott, B.M., Dodd, N.J.F. and Elcombe, C.R. 1986. Increased hydroxyl radical production in liver peroxisomal fractions from rats treated with peroxisome proliferators. *Carcinogenesis*, **7**, 795-799.

Fabacher, D.L. and Little, E.E. 1985. Skin component may protect fishes from ultraviolet-B radiation. *Environmental Science and Pollution Research,* **2**, 30-32.

Fabacher, D.L., Little, E.E., Jones, S.B., DeFabo, E.C. and Webber, L.J. 1994. Ultraviolet-B radiation and the immune response of rainbow trout. In: *Modulators of fish immune responses: models for environmental toxicology, biomarkers, immunostimulators*, Vol 1 (JS Stolen & TC Fletcher, eds) SOS publications, Fair Haven, NJ, pp. 205-217.

Fears, T.R., Bird, C.C., Guerry, D., Sagebiel, R.W., Gail, M.H., Elder, D.E., Halpern, A., Holly, E.A., Hartge, P. and Tucker, M.A. 2002. Average Midrange Ultraviolet Radiation Flux and Time Outdoors Predict Melanoma Risk. *Cancer Research*, **62**, 3992-3996.

Feig, D.I., Reid, T.M. and Loeb, L.A. 1994. Reactive oxygen species in tumorigenesis. *Cancer Research*, **54**, 1890-1894.

Fenech, M. 2006. Cytokinesis-block micronucleus assay evolves into a "cytome" assay of chromosomal instability, mitotic dysfunction and cell death. *Mutation Research*, **600**, 58-66.

Fenech, M., Bonassi, S., Turner, J., Lando, C., Ceppi, M., Chang, W., Holland, N., Kirsch-Volders, M., Zeiger, E., Bigatti, M., Bolognesi, C., Cao, J., De Luca, G., Di Giorgio, M., Ferguson, L., Fucic, A., Lima, O., Hadjidekova, V., Hrelia, P., Jaworska, A., Joksic, G., Krishnaja, A., Lee,

T., Martelli, A., McKay, M., Migliore, L., Mirkova, E., Muller, W., Odagiri, Y., Orsiere, T., Scarfi, M., Silva, M., Sofuni, T., Surralles, J., Trenta, G., Vorobtsova, I., Vral, A. and Zijno, A. 2003a. Intra- and inter- laboratory variation in the scoring of micronuclei and nucleopasmic bridges in binucleated human lymphocytes. Results of an international slide-scoring exercise by the HUMN project. *Mutation Research,* **534**, 45-64.

Fenech, M., Chang, W., Kirsch-Volders, M., Holland, N., Bonassi, S. and Zeiger, E. 2003b. HUMN project: Detailed description of the scoring criteria for the cytokinesis-block micronucleus assay using isolated human lymphocyte cultures. *Mutation Research*, **534**, 65-75.

Fenech, M. and Crott, J.W. 2002. Micronuclei, nucleoplasmic bridges and nuclear buds induced in folic acid deficient human lymphocytes-evidence for breakage-fusion-bridge cycles in the cytokinesis-block micronucleus assay. *Mutation Research*, **504**, 131-136.

Fenech, M. and Morley, A.A. 1986. Cytokinesis-block micronucleus method in human lymphocytes: effect of *in vivo* ageing and low dose X-irradiation. *Mutation Research*, **161**, 193-198.

Fent, K. 2001. Fish cell lines as versatile tools in ecotoxicology: assessment of cytotoxicity, cytochrome P4501A induction potential and estrogenic activity of chemicals and environmental samples. *Toxicology in Vitro*, **15**, 477-488.

Fernandez, M. and l'Haridon, J. 1994. Effects of light on the cytotoxicity and genotoxicity of benzo(a)pyrene and an oil refinery effluent in the newt. *Environmental and Molecular Mutagenesis*, **24**, 124-136.

Finkelstein, E., Rosen, G.M. and Rauckman, E.J. 1982. Production of hydroxyl radical by decomposition of superoxide spin-trapped adducts. *Molecular Pharmacology*, **21**, 262-265.

Fourtanier, A., Moyal, D. and Seité, S. 2008. Sunscreens containing the broad-spectrum UVA absorber, Mexoryl SX, prevent the cutaneous detrimental effects of UV exposure: a review of clinical study results. *Photodermatology Photoimmunology and Photomedicine*, **24**, 164-174.

Frenkel, V., Kimmel, E. and Iger, Y. 2000. Ultrasound-induced intercellular space widening in fish epidermis. *Ultrasound in Medicine and Biology*, **26**, 473–480.

Freshney, R.I. 2000. *Culture of animal cells - a manual of basic techniques*. 4rd Edition. New York. Wiley-Liss.

Frieauff, W., Potter-Locher, F., Cordier, A. and Suter, W. 1998. Automatic analysis of the *in vitro* micronucleus test on V79 cells. *Mutation Research*, **413**, 57-68.

Gallagher, R.P., Bajdik, C.D., Fincham, S., Hill, G.B., Keefe, A.R., Coldman, A. and McLean, D.I. 1996. Chemical exposures, medical history, and risk of squamous and basal cell carcinoma of the skin. *Cancer Epidemiology, Biomarkers and Prevention*, **5**, 419-424.

Gao, D., Luo, Y., Guevara, D., Wang, Y., Rui, M., Goldwyn, B., Lu, Y., Smith, E.C.A., Lebwohl, M. and Wei, H. 2005. Benzo(a)pyrene and its metabolites combined with ultraviolet A synergistically induce 8-hydroxy-2'-deoxyguanosine via reactive oxygen species. *Free Radical Biology and Medicine*, **39**, 1177-1183.

Garcia-Pichel, F. and Bebout, B.M. 1996. Penetration of ultraviolet radiation into shallow water sediments: high exposure for photosynthetic communities. *Marine Ecology Progress Series,* **131**, 253-262.

Garcon, G., Dagher, Z., Zerimech, F., Ledoux, F., Courcot, D., Aboukais. A., Puskaric, E. and Shirali, P. 2006. Dunkerque City air pollution particulate matter-induced cytotoxicity, oxidative stress and inflammation in human epithelial lung cells (L132) in culture. *Toxicology in Vitro*, **20**, 519-528.

Garland, F.C., White, M.R., Garland, C.F., Shaw, E. and Gorham, E.D. 1990. Occupational sunlight exposure and melanoma in the U.S. Navy. *Archives of Environmental Health*, **45**, 261-267.

Garry, S., Nesslany, F., Aliouat, E., Haguenoer, J. and Marzin, D. 2003. Assessment of genotoxic effect of benzo(a)pyrene in endotracheally treated rat using the comet assay. *Mutation Research*, **534**, 33-43.

Gaspare, L., Machiwa, J.F., Mdachi, S.J., Streck, G. and Brack, W. 2009. Polycyclic aromatic hydrocarbon (PAH) contamination of surface sediments and oysters from the inter-tidal areas of Dar es Salaam, Tanzania. *Environmental Pollution*, **157**, 24-34.

Gehring, W. and Rosbash, M. 2003. The Coevolution of Blue-Light Photoreception and Circadian Rhythms. *Journal of Molecular Evolution,* **57**, 286-289.

George, S., Riley, C., McEvoy, J. and Wright, J. 2000. Development of a fish *in vitro* cell culture model to investigate oxidative stress and its

modulation by dietary vitamin E. *Marine Environmental Research*, **50**, 541-544.

Georgellis, A., Toppari, J., Veromaa, T., Rydstrom, J. and Parvinen, M. 1990. Inhibition of meiotic divisions of rat spermatocytes *in vitro* by polycyclic aromatic hydrocarbons. *Mutation Research*, **231**, 125-135.

Gmur, D.J. and Varanasi U. 1982. Characterization of benzo(a)pyrene metabolites isolated from muscle, liver, and bile of a juvenile flatfish. *Carcinogenesis,* **3**, 1397-1403.

Goldsmith, L.A. 1996. Skin effects of air pollution. *Otolaryngology - Head and Neck Surgery*, **114**, 217-219.

Grant, W.B. 2007. A meta-analysis of second cancers after a diagnosis of nonmelanoma skin cancer: additional evidence that solar ultraviolet-B irradiance reduces the risk of internal cancers. *Journal of Steroid Biochemistry and Molecular Biology,* **103**, 668-674.

Gravato, C. and Santos, M.A. 2002. Juvenile sea bass liver P450, EROD induction, and erythrocytic genotoxic responses to PAH and PAH-like compounds. *Ecotoxicology and Environmental Safety,* **51**, 115-127.

Grimmer, G. 1983. *Environmental Carcinogens: Polycyclic Aromatic Hydrocarbons*. CRC Press, Boca Raton, FL, USA.

Guerin, M.R., Jenkins, R.A. and Tomkins, B.A. 1992. In: Centre for indoor air research (Ed.). *The chemistry of environmental tobacco smoke: composition and measurement.* Chelsea, MI: Lewis Publishers.

Guieysse, B., Viklund, G., Toes, A. C. and Mattiasson, B. 2004. Combined UV-biological degradation of PAHs. *Chemosphere*, **55**, 1493-1499.

Gupta, P., Banerjee, D.K., Bhargava, S.K., Kaul, R. and Shankar, V.R. 1993. Prevalence of impared lung function in rubber manufacturing factory workers exposed to benzo(a)pyrene and respirable particulate matter. *Indoor and Built Environment*, **2**, 26-31.

Gupta, R., Dixon, K.M., Deo, S.S., Holliday, C.J., Slater, M., Halliday, G.M., Reeve, V.E. and Mason. R.S. 2007. Photoprotection by 1,25 dihydroxyvitamin D3 is associated with an increase in p53 and a decrease in nitric oxide products. *Journal of Investigative Dermatology,* **127**, 707-715.

Hader, D.P. and Sinha, R.P. 2005. Solar ultraviolet radiation-induced DNA damage in aquatic organisms: potential environmental impact. *Mutation Research,* **571**, 221-233.

Hader, D.P., Worrest, R.C., Kumar, H.D. and Smith, R.C. 1995. Effects of increased solar ultraviolet radiation on aquatic ecosystems. *Ambio,* **24**, 174-180.

Haenszel, W. 1963. Variations in skin cancer incidence within the United States. *NCI monographs: a publication of the National Cancer Institute,* **10**, 225-243.

Hagenhofer, M., Germaier, H., Hohenadl, C., Rohwer, P., Kalden, J.R. and Herrmann, M. 1998. UV-B irradiated cell lines execute programmed cell death in various forms. *Apoptosis*, **3**, 123-132.

Hakkinen, J., Vehniainen, E. and Oikari, A. 2004. High sensitivity of northern pike larvae to UV-B but no UV-photoinduced toxicity of retene. *Aquatic Toxicology*, **66**, 393-404.

Hamada, K., Suzaki, Y., Leme, A., Ito, T., Miyamoto, K., Kobzik, L. and Kimura, H. 2007. Exposure of pregnant mice to an air pollutant aerosol increases asthma susceptibility in offspring. *Journal of Toxicology and Environmental Health A,* **70**, 688-695.

Hara, K., Hanaoka, T., Yamano, Y. and Itani, T. 1997. Urinary 1-hydroxypyrene levels of garbage collectors with low-level exposure to polycyclic aromatic hydrocarbons. *Science of the Total Environment*, **199**, 159-164.

Hatch, A.C. and Blaustein, A.R. 2000. Combined effects of UV-B, nitrate, and low pH reduce the survival and activity level of larval cascades frogs (*Rana cascadae). Archives of Environmental Contamination and Toxicology,* **39**, 494–499.

Hattemer-Frey, H.A. and Travis, C.C. 1991. Benzo-a-pyrene: environmental partitioning and human exposure. *Toxicology and Industrial Health*, **7**, 141-157.

Hawkes, J.W. 1974. The structure of fish skin. *Cell and Tissue Research*, **149,** 147-158.

He, Y.Y., Huang, J.L. and Chignell, C.F. 2004. Delayed and sustained activation of extracellular signal-regulated kinase in human keratinocytes by UVA. *The Journal of Biological Chemistry*, **51**, 53867-53874.

Helleberg, H., Honglan, X., Ehrenberg, L., Hemminki, K., Rannug, U. and Tornqvist, M. 2001. Studies of dose distribution, premutagenic events and mutation frequencies for benzo(a)pyrene aiming at low dose cancer risk estimation. *Mutagenesis*, **16**, 333-337.

Hoeger, B., Koellner, B., Kotterba, G., van den Heuvel, M.R., Hitzfeld, B. and Dietrich, D.R. 2004. Influence of chronic exposure to treated sewage effluent on the distribution of white blood cell populations in rainbow trout (*Oncorhynchus mykiss*) spleen. *Toxicological Sciences*, **82**, 97-105.

Ho, K., Patton, L., Latimer, J., Pruell, R., Pelletier, M., Mckinney, R. and Jayaramen, S. 1999. The chemistry and toxicity of sediment affected by oil from the North Cape spilled into Rhode Island Sound. *Marine Pollution Bulletin*, **38**, 314-323.

Holst, L.L. and Giesy, J.P. 1989. Chronic effects of the photoenhanced toxicity of anthracene on *Daphnia magna* reproduction. *Environmental Toxicology and Chemistry*, **8**, 933-942.

Hooven, L.A., Mahadevan, B., Keshava, C., Johns, C., Pereira, C., Desai, D., Amin, S., Weston, A. and Baird, W.M. 2005. Effects of suberoylanilide hydroxamic acid and trichostatin A on induction of cytochrome P450 enzymes and benzo(a)pyrene DNA adduct formation in human cells. *Bioorganic and Medicinal Chemistry Letters*, **15**, 1283-1287.

Horáthová, E., Slameňová, D., Hlinčíková, L., Kumar Mandal, T., Gábelová, A. and Collins, A.R. 1998. The nature and origin of DNA single-strand breaks determined with the comet assay. *Mutation Research,* **409**, 163-171.

Horikawa-Miura, M., Matsuda, N., Yoshida, M., Okumura, Y., Mori, T. and Watanabe, M. 2007. The greater lethality of UVB radiation to cultured human cells is associated with the specific activation of a DNA damage-independent signalling pathway. *Radiation Research*, **167**, 655-662.

Huang, X.D., Dixon, D.G. and Greenberg, B.M. 1993. Impacts of UV radiation and photomodification on the toxicity of PAHs to the higher plant. *Lemna gibba* (duckweed). *Environmental Toxicology and Chemistry,* **12**, 1067-1077.

Hure, J. and Scotto di Carlo, B. 1974. New patterns of diurnal vertical migration of some deep-water copepods in the Tyrrhenian and Adriatis Seas. *Marine Biology*, **28**, 179-184.

Huynh-Delerme, C., Fessard, V., Kiefer-Biasizzo, H. and Puiseux-Dao, S. 2003. Characteristics of okadaic acid--induced cytotoxic effects in CHO-K1 cells. *Environmental Toxicology*, **18**, 383-394.

IARC, 1992. *Solar and ultraviolet radiation. Monographs on the evaluation of carcinogenic risks to humans.* Lyon, France. Vol 55 pp.

Ibuki, Y. and Goto, R. 2002. Phototoxicity of benzo(a)pyrene by ultraviolet A irradiation: induction of apoptosis in Jurkat cells. *Environmental Toxicology and Pharmacology*, **11**, 101-109.

Ibuki, Y., Warashina, T., Noro, T. and Goto, R. 2002. Coexposure to benzo(a)pyrene plus ultraviolet A induces 8-oxo-7,8-dihydro-2'-deoxyguanosine formation in human skin fibroblasts: preventive effects of anti-oxidant agents. *Environmental Toxicology and Pharmacology,* **12**, 37-42.

Ichihashi, M., Ueda, M., Budiyanto, A., Bito, T., Oka, M., Fukunaga, M., Tsuru, K. and Horikawa, T. 2003. UV-induced skin damage. *Toxicology*, **189**, 21-39.

Iger, Y., Hilge, V. and Abraham, M. 1992. The ultrastructure of fish-skin during stress in aquaculture, in: (1992). *Progress in aquaculture research: proceedings of the 4th German-Isreali Status Seminar held on October 30-31, 1990*. Special Publication (European Aquaculture Society) **17**, 205-214.

Ikehata, H., Kudo, H., Masuda, T. and Ono, T. 2003. UVA induces C-T transitions at methyl-CPG-associated dipyrimidine sites in mouse skin epidermis more frequently than UVB. *Mutagenesis*, **18**, 511-519.

Ilyas, M., Abdul Aziz, D. and Tajuddin, M.R. 1988. Medically important solar ultraviolet A radiation measurements. *International Journal of Dermatology*, **27**, 315-318.

Ingersoll, C.G., MacDonald, D.D., Brumbaugh, W.G., Johnson, B.T., Kemble, N.E., Kunz, J.L., May, T.W., Wang, N., Smith, J.R., Sparks, D.W. and Ireland, D.S. 2002. Toxicity assessment of sediments from the Grand Calumet River and Indiana Harbor Canal in Northwestern Indiana, USA. *Archives of Environmental Contamination and Toxicology*, **43**, 156–167.

Iordanov, M.S., Choi, R.J., Ryabinina, O.P., Dinh, T.H., Bright, R.K. and Magun, B.E. 2002. The UV (Ribotoxic) stress response of human keratinocytes involves the unexpected uncoupling of the Ras-extracellular signal-regulated kinase signaling cascade from the activated epidermal growth factor receptor. *Molecular and Cellular Biology*, **22**, 5380-5394.

Jedrychowski, W., Pac, A., Choi, H., Jacek, R., Sochacka-Tatara, E., Dumyahn, T.S., Spengler, J.D., Camann, D.E. and Perera, F.P. 2007. Personal exposure to fine particles and benzo(a)pyrene. Relation with indoor and outdoor concentrations of these pollutants in Kraków. *International Journal of Occupational Medicine and Environmental Health*, **20**, 339-348.

Jha, A. 1998. Editorial. *Mutation Research/Fundamental and Molecular Mechanisms of Mutagenesis*, **399**, 1-2.

Jiang, H., Vudathala, D.K., Blair, I.A. and Penning, T.M. 2006. Competing roles of aldo-keto reductase 1A1 and cytochrome P4501B1 in benzo(a)pyrene-7,8-diol activation in human bronchoalveolar H358 cells: role of AKRs in P4501B1 induction. *Chemical Research in Toxicology*, **19**, 68-78.

Jie, Y.M. and Jie, C. 2001. Chromosomal composition of micronuclei in mouse NIH 3T3 cells treated with acrylamide, extract of *Tripterygium hypoglaucum* (level) hutch, mitomycin C and colchicine, detected by multicolor FISH with centromeric and telomeric DNA probes. *Mutagenesis*, **16**, 145-149.

Johnson, T. E., Umbenhauer, D. R. and Galloway, S. M. 1996. Human liver S-9 metabolic activation: Proficiency in cytogenetic assays and comparison with phenobarbital/beta-naphthoflavone or aroclor 1254 induced rat S-9. *Environmental and Molecular Mutagenesis*, **28**, 51-59.

Jokinen, E.I., Salo, H.M., Markkula, S.E., Aaltonen, T.M., Immonen, A.K. 2000. Effects of ultraviolet light on immune parameters of the roach. *Toxicology Letters*, **112-113**, 303-310.

Kamiguchi, Y. and Tateno, H. 2002. Radiation and chemical induced structural chromosome aberrations in human spermatozoa. *Mutation Research*, **504**, 183-191.

Kammann, U., Bunke, M., Steinhart, H. and Theobald, N. 2001. A permanent fish cell line (EPC) for genotoxicity testing of marine sediments with the comet assay. *Mutation Research*, **498**, 67-77.

Karentz, D. and Lutze, L. 1990. Evaluation of biologically harmful ultraviolet radiation in Antarctica with a biological dosimeter designed for aquatic environments. *Limnology and Oceanography*, **35**, 549-561.

Karlehagen, S., Andersen, A. and Ohison, C. 1992. Cancer Incidence among Creosote-Exposed Workers. *Scandinavian Journal of Work, Environment & Health*, **18**, 26-29.

Kaslauskas, A., Poelinger, L. and Pongratz, I. 1999. Evidence that the co-chaperone p23 regulates ligand responsiveness of the dioxin (aryl hydrocarbon) receptor. *Journal of Biological Chemistry*, **274**, 13519-13524.

Kaufmann, W.K. and Paules, R.S. 1996. DNA damage and cell cycle checkpoints. *Federation of American Societies for Experimental Biology*, **10**, 238-247.

Kawanishi, S. Hiraku, Y. and Oikawa, S. 2001. Mechanism of guanine-specific DNA damage by oxidative stress and its role in carcinogenesis and aging. *Mutation Research*, **488**, 65-76.

Kaweewat, K. and Hofer, R. 1997. Effect of UV-B radiation on goblet cells in the skin of different fish species. *Journal of Photochemistry and Photobiology B: Biology*, **41**, 222-226.

Keller, A., Hargreaves, P., Jeon, H., Klein-Macphee, G., Klos, E., Oviatt, C. and Zhang, J. 1997. Ultraviolet-B radiation enhancement does not affect marine trophic levels during a winter-spring bloom. *Ecoscience,* **4**, 129-139.

Kennicutt, M.C. II., Wade, T.L., Presley, B.J., Requejo, A.G., Brooks, J.M. and Denoux, G.J. 1994. Sediment contaminants in Casco Bay, Maine: Inventories, sources, and potential for biological impact. *Environmental Science and Technology*, **28**, 1-15.

Keulers, R.A.C., de Roon, A.R., de Roode, S. and Tates, A.D. 1998. The induction and analysis of micronuclei and cell killing by ultraviolet-B radiation in human peripheral blood lymphocytes. *Photochemistry and Photobiology,* **67**, 426-432.

Kiefer, F., Cumpelik, O. and Wiebel, F. J. 1988. Metabolism and cytotoxicity of benzo(a)pyrene in the human lung tumour cell line NCI-H322. *Xenobiotica*, **18**, 747-55.

Kilemade, M., Hartl, M.G., Sheehan, D., Mothersill, C., van Pelt, F.N., O'Brien, N.M. and O'Halloran, J. 2004a. An assessment of the pollutant

status of surficial sediment in Cork Harbour in the South East of Ireland with particular reference to polycyclic aromatic hydrocarbons. *Marine Pollution Bulletin*, **49**, 1084-1096.

Kilemade, M.F., Hartl, M.G.J., Sheehan, D., Mothersill, C., van Pelt, F.N, O'Halloran, J. and O'Brian, N.M. 2004b. Genotoxicity of field-collected inter-tidal sediments from Cork Harbour, Ireland, to Juvenile Turbot (*Scophthalmus maximus* L.) as measured by the comet assay. *Environmental and Molecular Mutagenesis*, **44**, 56-64.

Kim, P.M., DeBoni, U. and Wells, P.G. 1997. Peroxidase-dependent bioactivation and oxidation of DNA and protein in benzo(a)pyrene initiated micronucleus formation. *Free Radicals in Biology and Medicine*, **23**, 579-596.

Kim, S.R., Kokubo, K., Matsui, K., Yamada, N., Kanke, Y., Fukuora, M., Yamada, M. and Nohmi, T. 2005. Light-dependent mutagenesis by benzo(a)pyrene is mediated via oxidative DNA damage. *Environmental and Molecular Mutagenesis*, **46**, 141-149.

Kime, D.E. 1999. Environmentally induced endocrine abnormalities in fish. In: *Issues in Environmental Science and Technology 12: Endocrine disrupting chemicals*. Hester RE & Harrison RM (eds) Royal Society of Chemistry. Pp: 27-48.

Kirsch-Volders, M., Elhajouji, A., Cundari, E. and Van Hummelen, P. 1997. The *in vitro* micronucleus test: A multi-endpoint assay to detect simultaneously mitotic delay, apoptosis, chromosome breakage, chromosome loss and non-disjunction. *Mutation Research*, **392**, 19-30.

Kirsch-Volders, M., Sofuni, T., Aardema, M., Albertini, S., Eastmond, D., Fenech, M., Ishidate, M., Kirchner, S., Lorge, E., Morita, T., Norppa, H., Surrallés, J., Vanhauwaert, A. and Wakata, A. 2003. Report from the *in vitro* micronucleus assay working group. *Mutation Research*, **540**, 153-163.

Koch-Paiz, C.A., Amundson, S.A., Bittner, M.L., Meltzer, P.S. and Fornace, A.J. Jr. 2004. Functional genomics of UV radiation responses in human cells. *Mutation Research*, **549**, 65-78.

Kolpoth, M., Rusche, B. and Nusse, M. 1999. Flow cytometric measurement of micronuclei induced in a permanent fish cell line as a possible screening test for the genotoxicity of industrial waste waters. *Mutagenesis*, **14**, 397-402.

Kouwenberg, J.H.M., Browman, H.I., Cullen, J.J., Davis, R.F., St-Pierre, J.F. and Runge, J.A. 1999a. Biological weighting of ultraviolet (280-400 nm) induced mortality in marine zooplankton and fish. I. Atlantic cod (*Gadus morhua*) eggs. *Marine Biology*, **134**, 269-284.

Kouwenberg, J.H.M., Browman, H.I., Runge, J.A., Cullen, J.J., Davis, R.F. and St-Pierre, J.F. 1999b. Biological weighting of ultraviolet (280-400 nm) induced mortality in marine zooplankton and fish. II. *Calanus finmarchicus* (Copepoda) eggs. *Marine Biology*, **134**, 285-293.

Kowalczuk, C.I., Priestner, M.C., Pearson, A.J., Saunders, R.D. and Bouffler, S.D. 2006. Wavelength dependence of cellular responses in human melanocytes and melanoma cells following exposure to ultraviolet radiation. *International Journal of Radiation Biology,* **82**, 781-792.

Kricker, A. and Armstrong, B. 2006. Does sunlight have a beneficial influence on certain cancers? *Progress in Biophysics and Molecular Biology*, **92**, 132-139.

Kuhn, P., Browman, H., McArthur, B. and St-Pierre, J.F. 1999. Penetration of ultraviolet radiation in the waters of the estuary and Gulf of St Lawrence. *Limnology and Oceanography*, **44**, 710-716.

Kuljukka-Rabb, T., Peltonen, K., Isotalo, S., Mikkonen, S., Rantanen, L. and Savela, K. 2001. Time and dose dependent DNA binding of PAHs derived from diesel particle extracts, benzo(a)pyrene and 5-methylchrysene in a human mammary carcinoma line (MCF-7). *Mutagenesis*, **16**, 353-358.

Kumar, S. and Joshi, P.C. 1992. Haemolysis by ultraviolet B of red blood cells from different animal species. *Toxicology in Vitro,* **6**, 345-347.

Kumaravel, T.S. and Jha, A.N. 2006. Reliable Comet assay measurements for detecting DNA damage induced by ionising radiation and chemicals. *Mutation Research*, **605**, 7-16.

Kushman, M.E., Kabler, S.L., Fleming, M.H., Ravoori, S., Gupta, R.C., Doehmer, J., Morrow, C.S. and Townsend, A.J. 2007. Expression of human glutathione S-transferase P1 confers resistance to benzo(a)pyrene or benzo(a)pyrene-7,8-dihydrodiol mutagenesis, macromolecular alkylation and formation of stable N2-Gua-BPDE adducts in stably transfected V79MZ cells co-expressing hCYP1A1. *Carcinogenesis*, **28**, 207-214.

Kwak, H.I., Bae, M.O., Lee, M.H., Lee, Y.S., Lee, B.J., Kang, K.S., Chae, C.H., Sung, H.J., Shin, J.S., Kim, J.H., Mar, W.C., Sheen, Y.Y. and Cho, M.H. 2001. Effects of nonylphenol, bisphenol A, and their mixture on the viviparous swordtail fish (*Xiphophorus helleri*). *Environmental Toxicology and Chemistry*, **20**, 787-795.

Lacour, S.A., de Monte, M., Diot, P., Brocca, J., Veron, N., Colin, P. and Leblond, V. 2006. Relationship between ozone and temperature during the 2003 heat wave in France: consequences for health data analysis. *BMC Public Health*, **6**, 261.

Landolt, M.L., and Kocan, R.M. 1983. Fish cell cytogenetics: a measure of the genotoxic effects of environmental pollutants. *Advances in Environmental Science and Technology*, **13**, 335-353.

Lannan, C.N. 1994. Fish cell culture: a protocol for quality control. *Journal of Tissue Culture Methodology*, **16**, 95-98.

Law, R.J., Dawes, V.J., Woodhead. R.J. and Matthiessen, P. 1997. Polycyclic aromatic hydrocarbons (PAH) in seawater around England and Wales. *Marine Pollution Bulletin*, **34**, 306-322.

Laycock, N., Schirmer, K., Bols, N. and Sivak, J. 2000. Optical properties of rainbow trout lenses after *in vitro* exposure to polycyclic aromatic hydrocarbons in the presence or absence of ultraviolet radiation. *Experimental Eye Research*, **70**, 205-214.

Lean, D.R.S. 1998. *Influence of ultraviolet radiation on aquatic ecosystems*. In: Little, E.E., Greenburg B.M. and A.J. DeLonay (eds) *Environmental Toxicology and Risk Assessment*: Vol 7 STP 1333. American Society for Testing and Materials. West Conshohocken, PA.

Lee, J., Kang, D., Lee, K., Ichiba, M., Zhang, J., Tomokuni, K., Hwang, E., Park, C., He, M., Kim, S., Han, S., Choi, J., Lee, E., Jang, J., Strickland, P., Hirvonen, A. and Cho, S. 2002. Influence of GSTM1 genotype on association between aromatic DNA adducts and urinary PAH metabolites in incineration workers. *Mutation Research-Genetic Toxicology and Environmental Mutagenesis*, **514**, 213-221.

Lee, J.A. and Strickland, D. 1980. Malignant melanoma: social status and outdoor work. *British Journal of Cancer*, **41**, 757-763.

Leech, D.M. and Williamson, C.E. 2000. Is tolerance to UV radiation in zooplankton related to body size, taxon, or lake transparency? *Ecological Applications*, **10**, 1530-1540.

Lehmann, J., Pollet, D., Peker, S., Steinkraus, V. and Hoppe, U. 1998. Kinetics of DNA strand breaks and protection by antioxidants in UVA- or UVB-irradiated HaCaT keratinocytes using the single cell gel electrophoresis assay. *Mutation Research*, **407**, 97-108.

Lehto, K, M., Puhakka, J.A. and Lemmetyinen, H. 2003. Biodegradation of selected UV-irradiated and non-irradiated polycyclic aromatic hydrocarbons (PAHs). *Biodegradation*, **14**, 249-263.

Lemiere, S., Cossu-Leguill, C., Bispo, A., Jourdain, M., Lanhers, M.C., Burnel, D. and Vasseur. P. 2004. Genotoxicity related to transfer of oil spill pollutants from mussels to mammals via food. *Environmental Toxicology,* **19**, 387-395.

Li, J., Tang, M.S., Liu, B., Shi, X. and Huang, C. 2004. A critical role of PI-3K/Akt/JNKs pathway in benzo(a)pyrene diol-epoxide (B(a)PDE)-induced AP-1 transactivation in mouse epidermal Cl41 cells. *Oncogene*, **23**, 3932-3944.

Li, H. and Zhang, S. 2002. *In vitro* cytotoxicity of the organophosphorus insecticide methylparathion to FG-9307, the gill cell line of flounder (*Paralichthys olivaceus*). *Cell Biology and Toxicology*, **18**, 235-241.

Lim, J.L. and Stern, R.S. 2005. High levels of ultraviolet B exposure increase the risk of non-melanoma skin cancer in psoralen and ultraviolet A-treated patients. *Journal of Investigative Dermatology*, **124**, 505-513.

Linet, M.S., Malker, H.S.R., Chow, W., McLaughlin, J.K., Weiner, J.A., Stone, B.J., Ericsson, J.L.E. and Fraumeni, F. 1995. Occupational risk for cutaneous melanoma among men in Sweden. *Journal of Occupational and Environmental Medicine*, **37**, 1127-1133.

Lion, Y., Gandin, E. and Van de Vorst, A. 1980. On the production of nitroxide radicals by singlet oxygen reaction: an EPR study. *Photochemistry and Photobiology*, **31**, 305-309.

Little. E.E., Cleveland, L., Calfee, R. and Barron, M.G., 2000. Assessment of the photoenhanced toxicity of weathered oil to the tidewater silverside. *Environmental Toxicology & Chemistry*, **19**, 926-932.

Little, E.E. and Fabacher, D.L. 1994. Comparative sensitivity of rainbow trout and two threatened salmonids, Apache trout and Lahontan

cutthroat trout, to ultraviolet B radiation. *Archiv fur Hydobiologie*, **43**, 217-226.

Liu, Y., Che, W., Li, J. 2005. Monitor-based evaluation of pollutant load from urban stormwater runoff in Beijing. *Water Science and Technology*, **52**, 191-197.

Liu, Y., Chen, L., Jianfu, Z., Qinghui, H., Zhiliang, Z. and Hongwen, G. 2008. Distribution and sources of polycyclic aromatic hydrocarbons in surface sediments of rivers and an estuary in Shanghai, China. *Environmental Pollution*, **154**, 298-305.

Liu, Y-Q., Keane, M., Ensell, M., Miller, W., Kashon, M., Ong, T., Mauderly, J., Lawson, D., Gautam, M., Zielinska, B., Whitney, K., Eberhardt, J. and Wallace, W. 2005. *In vitro* genotoxicity of exhaust emissions of diesel and gasoline engine vehicles operated ona unified driving cycle. *Journal of Environmental Monitoring*, **7**, 60-66.

Liu, Z.S., Lu, Y.H., Rosenstein, B., Lebwohl, M. and Wei, H.C. 1998. Benzo(a)pyrene enhances the formation of 8-hydroxy-2'-deoxyguanosine by ultraviolet A radiation in calf thymus DNA and human epidermal carcinoma cells. *Biochemistry,* **37**, 10307-10312.

Lowe, D.M., Moore, M.N. and Evans, B.M. 1992. Contaminant impact on interactions of molecular probes with lysosomes in living hepatocytes from dab *Limanda limanda*. *Marine Ecology Progress Series*, **91**, 135-140.

Luckenbach, T., Ferling, H., Gernhofer, M., Kohler, H-R., Negele, R-D., Pfefferle, E. and Triebskorn, R. 2003. Developmental and subcellular effects of chronic exposure to sub-lethal concentrations of ammonia, PAH and PCP mixtures in brown trout (*Salmo trutta* f. *fario* L.) early life stages. *Aquatic Toxicology*, **65**, 39-54.

Luo, X.J., Chen, S.J., Mai, B.X., Yang, Q.S., Sheng, G.Y. and Fu, J.M. 2006. Polycyclic aromatic hydrocarbons in suspended particulate matter and sediments from the Pearl River Estuary and adjacent coastal areas, China. *Environmental Pollution*, **139**, 9-20.

Lyons, B.P., Pascoe, C.K. and McFadzen, I.R. 2002. Phototoxicity of pyrene and benzo(a)pyrene to embryo-larval stages of the Pacific oyster *Crassostrea gigas*. *Marine Environmental Research*, **54**, 627-631.

Ma, W., Wlaschek, M., Tantcheva-Poór, I., Schneider, L.A., Naderi, L., Razi-Wolf, Z., Schüller, J. and Scharffetter-Kochanek, K. 2001.

Chronological ageing and photoageing of the fibroblasts and the dermal connective tissue. *Clinical and Experimental Dermatology,* **26**, 592-599.

Mabey, W.R., Smith, J.H., Podoll, R.T., Johnson, H.L., Mill, T., Chou, T.W., Cates, J., Waight-Partridge, I., Jaber, H. and Vandenberg, D. 1982. Aquatic fate process data for organic priority pollutants. EPA 440/4-81-014. US Environmental Protection Agency, Office of Water Regulations and Standards. Washington, D.C.

Machala, M., Vondracek, J., Blaha, L., Ciganek, M. and Neca, J.V. 2001. Aryl hydrocarbon receptor-mediated activity of mutagenic polycyclic aromatic hydrocarbons determined using *in vitro* reporter gene assay. *Mutation Research*, **497**, 49-62.

Mackay, J. 1995. Dose selection in *in vivo* genetic toxicology assays. *Ecotoxicology and Environmental Safety*, **25**, 323-327.

Mackay, D., Shiu, W.Y. and Ma, K. 1992. *Illustrated handbook of physical-chemical properties and environmental fate for organic chemicals(2).* Lewis Publishers, Chelsea, MI.

Madronich, S., McKenzie, R.E., Björn, L.O., and Caldwell, M.M. 1998. Changes in biologically active ultraviolet radiation reaching the Earth's surface. *Journal of Photochemistry and Photobiology B: Biology,* **46**, 5–19.

Madronich, S., McKenzie, R.L., Björn, L. and Caldwell, M. 1995. Changes in ultraviolet radiation reaching the Earth's surface, *Ambio*, **24**, 143-152.

Mahadevan, B., Luch, A., Atkin, J., Nguyen, T., Sharma, A.K., Amin, S. and Baird, W.M. 2006. Investigation of the genotoxicity of dibenzo(c,p)chrysene in human carcinoma MCF-7 cells in culture. *Chemico Biological Interactions*, **164**, 181-191.

Mahadevan, B., Luch, A., Bravo, C.F., Atkin, J., Steppan, L.B., Pereira, C., Kerkvliet, N.I. and Baird, W.M. 2005. Dibenzo(a,l)pyrene induced DNA adduct formation in lung tissue *in vivo*. *Cancer Letters*, **227**, 25-32.

Mallakin, A., McConkey, B.J., Miao, G., McKibben, B., Snieckus, V., Dixon, D.G. and Greenberg, B.M. 1999. Impacts of structural photomodification on the toxicity of environmental contaminants: anthracene photooxidation products. *Ecotoxicology and Environmental Safety*, **43**, 204-212.

Malloy, K.D., Holman, M.A., Mitchell, D. and Detrich III, H.W. 1997. Solar UVB-induced DNA damage and photoenzymatic DNA repair in Antarctic zooplankton. *Proceedings of the National Academy of Science USA*, **94**, 1258-1263.

Mann, K.K., Matulka, R.A., Hahn, M.E., Trombino, A.F., Lawrence, B.P., Kerkvliet, N.I. and Sherr, D.H. 1999. The role of polycyclic aromatic hydrocarbon metabolism in dimethylbenz(a)anthracene-induced pre-B lymphocyte apoptosis. *Toxicology and Applied Pharmacology,* **161**, 10-22.

Manning, W.J. and Van Tiedemann, A. 1995. Climate change: potential effects of increased atmospheric carbon dioxide (CO_2), ozone (O_3), and ultraviolet-B (UV-B) radiation on plant diseases. *Environmental Pollution*, **88**, 219-245.

Marrot, L., Belaidi, J.P., Lejeune, F., Meunier, J.R., Asselineau, D. and Bernerd, F. 2004. Photostability of sunscreen products influences the efficiency of protection with regard to UV-induced genotoxic or photoageing-related endpoints. *British Journal of Dermatology,* **151**, 1234-1244.

Marshall, R.R., Murphy, M., Kirkland, D.J. and Bentley, K.S. 1996. Fluorescence *in situ* hybridisation with chromosome-specific centromeric probes: a sensitive method to detect aneuploidy. *Mutation Research*, **372**, 233-245.

Martin-Alguacil, N., Babich, H., Rosenberg, D.W. and Borenfreund, E. 1991. *In vitro* response of the brown bullhead catfish cell line BB to aquatic pollutants. *Archives of Environmental Contamination and Toxicology,* **20**, 113-117.

Marty, G. C., Short, J. W., Dambach, D. M., Willits, N. H., Heintz, R. A., Rice, S. D., Stegeman, J. J. and Hinton, D. E. 1997. Ascites, premature emergence, increased gonadal cell apoptosis, and cytochrome P4501A induction in pink salmon larvae continuously exposed to oil-contaminated gravel during development. *Canadian Journal of Zoology*, **75**, 989-1007.

Matsuzawa, S., Nasser-Ali, L. and Garrigues, P. 2001. Photolytic behavior of polycyclic aromatic hydrocarbons in diesel particulate matter deposited on the ground. *Environmental Science and Technology*, **35**, 3139-3143.

Mayer, S.J. 1992. Stratospheric ozone depletion and animal health. *The Veterinary Record*, **131**, 120-122.

McCloskey, J.T. and Oris, J.T., 1993. Effect of anthracene and solar ultraviolet radiation exposure on gill ATPase and selected hematologic measurements in the bluegill sunfish (*Leptomis macrochirus*). *Aquatic Toxicology*, **24**, 207–218.

McCord, M.W., Mendenhall, W.M., Parsons, J.T., Amdur, R.J., Stringer, S.P., Cassisi, N.J. and Million, R.R. 2000. Skin cancer of the head and neck with clinical perineural invasion. *International Journal of Radiation Oncology Biology Physics*, **47**, 89-93.

McKenzie, R.L., Aucamp, P.J., Bais, A.F., Björn LO and Ilyas M. 2007. Changes in biologically-active ultraviolet radiation reaching the Earth's surface. *Photochemical and Photobiological Sciences*, **6**, 218-231.

McKenzie, R., Connor, B. and Bodeker, G. 1999. Increased summertime UV radiation in New Zealand in response to ozone loss. *Science*, **285**, 1709–1711.

McLuckie, K. I., Gaskell, M., Farmer, P. B., Martin, E. A., Jones, G. D. and Routledge, M. N. 2004. Effects of the order of exposure to a binary mixture of mutagens on the induced mutation spectra in the *supF* gene. *Mutagenesis*, **19**, 137-141.

McMillan, T.J., Leatherman, E., Ridley, A., Shorrocks, J., Tobi, S.E. and Whiteside, J.R. 2008. Cellular effects of long wavelength UV light (UVA) in mammalian cells. *Journal of Pharmacy and Pharmacology*, **60**, 969-976.

McRae, D.G., Baker, J.E. and Thompson, J.E. 1982. Evidence for the involvement of the superoxide radical in the conversion of 1 aminocyclopropane-1-carboxylic acid to ethylene by pea microsomal membranes. *Plant and Cell Physiology*, **23**, 375–383.

Meador, J.A., Walter, R.B. and Mitchell, D.L. 2000. Induction, distribution and repair of UV photodamage in the platyfish, *Xiphophorus signum*. *Photochemisty and Photobiology*, **72**, 260-266.

Mendelshon, M.L., Moore, D.H. and Lohman, P.H.M. 1992. A method for comparing and combining short-term genotoxicity test data: results and interpretation. *Mutation Research*, **266**, 43-60.

Menichini, E., Iacovella, N., Monfredini, F. and Turrio-Baldassarri, L. 2007. Atmospheric pollution by PAHs, PCDD/Fs and PCBs simultaneously collected at a regional background site in central Italy and at an urban site in Rome. *Chemosphere*, **69**, 422-434.

Merlo, F., Andreassen, A., Weston, A., Pan, C.F., Haugen, A., Valerio, F., Reggiardo, G., Fontana, V., Garte, S., Puntoni, R. and Abbondandolo, A. 1998. Urinary excretion of 1-hydroxypyrene as a marker for exposure to urban air levels of polycyclic aromatic hydrocarbons. *Cancer Epidemiology Biomarkers and Prevention*, **7**, 147-155.

Mitchell, D.L., Greinert, R., de Gruijl, F.R., Guikers, K.L., Breitbart, E.W., Byrom, M., Gallmeier, M.M., Lowery, M.G. and Volkmer, B. 1999. Effects of chronic low-dose ultraviolet B radiation on DNA damage and repair in mouse skin. *Cancer Research*, **59**, 2875-2884.

Mitchelmore, C.L. and Chipman, J.K. 1998. DNA strand breakage in aquatic organisms and the potential value of the comet assay in environmental monitoring. *Mutation Research*, **399**, 135-147.

Moermond, C.T., Roessink, I., Jonker, M.T., Meijer, T. and Koelmans, A.A. 2007. Impact of polychlorinated biphenyl and polycyclic aromatic hydrocarbon sequestration in sediment on bioaccumulation in aquatic food webs. *Environmental Toxicology and Chemistry,* **26**, 607-615.

Møller, P. 2006. Assessment of reference values for DNA damage detected by the comet assay in human blood cell DNA. *Mutation Research,* **612**, 84–104.

Monteiro, P.R., Reis-Henriques, M.A. and Coimbra, J. 2000. Plasma steroid levels in female flounder (*Platichthys flesus*) after chronic dietary exposure to single polycyclic aromatic hydrocarbons. *Marine Environmental Research*, **49**, 453-467.

Moore, M.N., Depledge, M.H., Readman, J.W. and Paul Leonard, D.R. 2004. An integrated biomarker-based strategy for ecotoxicological evaluation of risk in environmental management. *Mutation Research*, **552**, 247-268.

Morales, J., Snow, E. and Miurnane, J. 2003. Environmental factors affecting transcription of the human l1 retrotransposon. Ii. Stressors. *Mutagenesis*, **18**, 151-158.

Mori, M. and Wakabayashi, M. 2000. Cytotoxicity evaluation of chemicals using cultured fish cells. *Water Science and Technology*, **42**, 277-282.

Morley, N., Clifford, T., Salter, L., Campbell, S., Gould, D. and Curnow, A. 2005. The green tea polyphenol (-)-epigallocatechin gallate and green tea can protect human cellular DNA from ultraviolet and visible

radiation-induced damage. *Photodermatology, Photoimmunology and Photomedicine*, **21,** 15-22.

Mosser, D.D., Heikkila, J.J. and Bols, N.C. 1986. Temperature ranges over which rainbow trout fibroblasts survive and synthesize heat-shock proteins. *Journal of Cell Physiology*, **128**, 432-440.

Mouret, S., Baudouin, C., Charveron, M., Favier, A., Cadet, J. and Douki, T. 2006. Cyclobutane pyrimidine dimers are predominant DNA lesions in whole human skin exposed to UVA radiation. *Proceedings of the National Academy of Science of the U.S.A*, **103**, 13765-13770.

Mouron, S.A., Grillo, C.A., Dulout, F.N. and Golijow, C.D. 2006. Genotoxic effects of benzo(a)pyrene and dibenzo(a,l)pyrene in a human lung cell line. *International Journal of Toxicology*, **25**, 49-55.

Moyal, D.D. and Fourtanier, A.M. 2002. Effects of UVA radiation on an established immune response in humans and sunscreen efficacy. *Experimental Dermatology*, **11**, 28-32.

Moyal, D.D. and Fourtanier, A.M. 2008. Broad-spectrum sunscreens provide better protection from solar ultraviolet-simulated radiation and natural sunlight-induced immunosuppression in human beings. *Journal of the American Academy of Dermatology*, **58**, S149-154.

Myllynen, P., Kurttila, T., Vaskivuo, L. and Vähäkangas, K. 2007. DNA damage caused by benzo(a)pyrene in MCF-7 cells is increased by verapamil, probenecid and PSC833. *Toxicology Letters*, **169**, 3-12.

Myllyperkiö, M.H., Koski, T.R.A., Vilpo, L.M. and Vilpo, J.A. 2000. Kinetics of excision repair of UV-induced DNA damage, measured using the comet assay. *Mutation Research*, **448**, 1-9.

Naumova, Y.Y., Eisenreich, S.J., Turpin, B.J., Weisel, C.P., Morandi, M.T., Colome, S.D., Totten, L.A., Stock, T.H., Winer, A.M., Alimokhtari, S., Kwon, J., Shendell, D., Jones, J., Maberti, S. and Wall, S.J. 2002. Polycyclic aromatic hydrocarbons in the indoor and outdoor air of three cities in the U.S. *Environmental Science and Technology*, **36**, 2552-2559.

Neff, J. 1979. *Polycyclic aromatic hydrocarbons in the aquatic environment*. Applied Science, London, UK.

Nehls, S. and Segner, H. 2005. Comet assay with the fish cell line rainbow trout gonad-2 for *in vitro* genotoxicity testing of xenobiotics and

surface waters. *Environmental Toxicology and Chemistry*, **24**, 2078-2087.

Nehls, S. and Segner, H. 2001. Detection of DNA damage in two cell lines from rainbow trout, RTG-2 and RTL-W1, using the comet assay. *Environmental Toxicology*, **16**, 321-329.

Newsted, J.L. and Giesy, J.P. 1987. Predictive models for photo-induced acute toxicity of polycyclic aromatic hydrocarbons to *Daphnia-magna*, Strauss (Cladocera, Crustacea). *Environmental Toxicology and Chemistry*, **6**, 445-461.

Nghiem, D.X., Kazimi, N., Clydesdale, G., Ananthaswamy, H.N., Kripke, M.L. and Ullrich, S.E. 2001. Ultraviolet A radiation suppresses an established immune response: Implications for sunscreen design. *Journal of Investigatory Dermatology*, **117**, 1193-1199.

Nicholson, B.L. 1971. Macromolecule Synthesis in RTG-2 Cells Following Infection with Infectious Pancreatic Necrosis (IPN) Virus. *Journal of General Virology*, **13**, 369-372.

Nigro, M., Falleni, A., Barga, I.D., Scarcelli, V., Lucchesi, P., Regoli, F. and Frenzilli, G. 2006. Cellular biomarkers for monitoring estuarine environments: transplanted versus native mussels. *Aquatic Toxicology*, **77**, 339-347.

Nigro, M., Frenzilli, G., Scarcelli, V., Gorbi, S. and Regoli, F. 2002. Induction of DNA strand breakage and apoptosis in the eel *Anguilla anguilla*. *Marine Environmental Research*, **54**, 517-520.

Nishigaki, R., Mitani, H., Tsuchida, N. and Shima, A. 1999. Effect of cyclobutane pyrimidine dimers on apoptosis induced by different wavelengths of UV. *Photochemistry and Photobiology*, **70**, 228-235.

Nohynek, G.J., Lademann, J., Ribaud, C. and Roberts, M.S. 2007. Grey goo on the skin? Nanotechnology, cosmetic and sunscreen safety. *Critical Reviews in Toxicology*, **37**, 251-277.

Norval, M., Cullen, A.P., de Gruijl, F.R., Longstreth, J., Takizawa, Y., Lucas, R.M., Noonan, F.P. and van der Leun, J.C. 2007. The effects on human health from stratospheric ozone depletion and its interactions with climate change. *Photochemical and Photobiological Sciences*, **6**, 232-251.

NRC, 1983. *Polycyclic aromatic hydrocarbons: evaluation of sources and effects*. Washington D.C., National Research Council, National Academy Press, ES/1-ES/7.

NRCC, 1983. *Polycyclic aromatic hydrocarbons in the aquatic environment: formation, sources, fate and effects on aquatic biota*. NRC associate committee on Scientific Criteria for Environmental Quality, National Research Council of Canada, NRCC Publication No. 18981, Ottawa, 209 pp.

Nwagbara, O., Darling-Reed, S.F., Tucker, A., Harris, C., Abazinge, M., Thomas, R.D. and Gragg, R.D. 2007. Induction of Cell Death, DNA Strand Breaks, and Cell Cycle Arrest in DU145 Human Prostate Carcinoma Cell Line by Benzo(a)pyrene and Benzo(a)pyrene-7,8-diol-9,10-epoxide. *International Journal of Environmental Research and Public Health*, **4**, 10-14.

Odagiri, Y., Zhang, J.X., Uchida, H., Kawamura, K., Adachi, S. and Takemoto, K. 1994. Predominant induction of kinetochore-containing micronuclei by extracts of diesel exhaust particulates in cultured human lymphocytes. *Environmental and Molecular Mutagenesis*, **23**, 45-50.

Okay, O.S. and Karacik, B. 2007. Photoinduced toxicity of selected PAHs to the marine microalga *Phaeodactylum tricornutum*. *Journal of Environmental Science and Health, Part A, Toxic/Hazardous Substances and Environmental Engineering*, **42**, 707-714.

Olive, P.L., Banath, J.P. and Durand, R.E. 1990. Heterogeneity in radiation – induced DNA damage and repair in tumour and normal cells measured using the 'comet' assay. *Radiation Research,* **122**, 86-94.

Onuska, F.I. 1989. Analysis of polycyclic aromatic hydrocarbons in environmental samples. In: "*Analysis of trace organics in the aquatic environment*". Ed: Afghan, B.K. and Chan, A.S.Y. CRC Press Inc. pp. 205-241.

O'Reilly, J.P. and Mothersill, C. 1997. Comparative effects of UVA and UVB on clonogenic survival and delayed cell death in skin cell lines from humans and fish. *International Journal of Radiation Biology,* **72**, 111-119.

Ortiz-Delgado, J.B., Segner, H., Arellano, J.M. and Sarasquete, C. 2007. Histopathological alterations, EROD activity, CYP1A protein and biliary metabolites in gilthead seabream *Sparus aurata* exposed to benzo(a)pyrene. *Histology and Histopathology*, **22**, 417-432.

OSPARCOM, 1994. *Ecotoxicological assessment criteria for trace metals and organic microcontaminants in the north-east Atlantic*. Oslo and Paris commissions, London, 39 pp.

Ostling, O. and Johanson, K.J. 1984. Microelectrophoretic study of radiation-induced DNA damages in individual mammalian cells. *Biochemical and Biophysical Research Communication*, **123**, 291-298.

Palli, D., Krogh, V., Tumino, R., Panico, S., Bueno-De-Mesquita, H.B., Peeters, P.H., Kumle, M., Gonzalez, C.A., Martinez, C., Dorronsoro, M., Barricarte, A., Navarro, C., Quiros, J.R., Berglund, G., Janzon, L., Jarvholm, B., Day, N.E., Key, T.J., Saracci, R., Kaaks, R., Riboli, E. and Vineis, P. 2005. DNA adducts and lung cancer risk: a prospective study. *Cancer Research*, **65**, 8042-8048.

Panin, L.E., Chasovskikh, M.I. and Poliakov, L.M. 1991. Characteristics of binding and transport of benzo(a)pyrene by blood serum lipoproteins. *Biulleten' Eksperimental'noi Biologii i Meditsiny*, **111**, 31-33.

Papadopoulos, N.G., Dedoussis, G.V., Spanakos, G., Gritzapis, A.D., Baxevanis, C.N. and Papamichail, M. 1994. An improved fluorescence assay for the determination of lymphocyte-mediated cytotoxicity using flow cytometry. *Journal of Immunological Methods*, **177**, 101-111.

Parry, E., Parry, J., Corso, C., Doherty, A., Haddad, F., Hermine, T., Johnson, G., Kayani, M., Quick, E., Warr, T. and Williamson, J. 2002. Detection and characterisation of mechanisms of action of aneugenic chemicals. *Mutagenesis*, **17**, 509-521.

Patton, W.P., Routledge, M.N., Jones, G.D., Lewis, S.E., Archer, D.B., Davies, R.J. and Chakravarthy, U. 2002. Retinal pigment epithelial cell DNA is damaged by exposure to benzo(a)pyrene, a constituent of cigarette smoke. *Experimental Eye Research*, **74**, 513-522.

Pekey, B., Karakas, D. and Ayberk, S. 2007. Atmospheric deposition of polycyclic aromatic hydrocarbons to Izmit Bay, Turkey. *Chemosphere*, **67**, 537-547.

Pelletier, M., Burgess, R., Ho, K., Kuhn, A., McKinney, R. and Ryba, S. 1997. Phototoxicity of individual polycyclic aromatic hydrocarbons and petroleum to marine invertebrate larvae and juveniles. *Environmental Toxicology and Chemistry*, **16**, 2190-2199.

Peluso, M., Munnia, A., Hoek, G., Krzyzanowski, M., Veglia, F., Airoldi, L., Autrup, H., Dunning, A., Garte, S., Hainaut, P., Malaveille, C., Gormally, E., Matullo, G., Overvad, K., Raaschou-Nielsen, O., Clavel-Chapelon, F.,

Linseisen, J., Boeing, H., Trichopoulou, A., Trichopoulos, D., Kaladidi, A., Palli, D., Krogh, V., Tumino, R., Panico, S., Bueno-De-Mesquita, H.B., Peeters, P.H., Kumle, M., Gonzalez, C.A., Martinez, C., Dorronsoro, M., Barricarte, A., Navarro, C., Quiros, J.R., Berglund, G., Janzon, L., Jarvholm, B., Day, N.E., Key, T.J., Saracci, R., Kaaks, R., Riboli, E. and Vineis, P. 2005. DNA adducts and lung cancer risk: a prospective study. *Cancer Research*, **65**, 8042-8048.

Peluso, M., Munnia, A., Hoek, G., Krzyzanowski, M., Veglia, F., Airoldi, L., Autrup, H., Dunning, A., Garte, S., Hainaut, P., Malaveille, C., Gormally, E., Matullo, G., Overvad, K., Raaschou-Nielsen, O., Clavel-Chapelon, F., Linseisen, J., Boeing, H., Trichopoulou, A., Trichopoulos, D., Kaladidi, A., Pelletier, M., Burgess, R., Ho, K., Kuhn, A., McKinney, R. and Ryba, S. 1997. Phototoxicity of individual polycyclic aromatic hydrocarbons and petroleum to marine invertebrate larvae and juveniles. *Environmental Toxicology and Chemistry*, **16**, 2190-2199.

Pennington, J.T. and Emlet, R.B. 1986. Ontogenetic and diel vertical migration of a planktonic echinoid larva, *Dendraster excentricus* (Eschscholtz): occurrence, causes, and probable consequences. *Journal of Experimental Marine Biology and Ecology*, **104**, 69-95.

Perdew, G.H. 1988. Association of the Ah receptor with the 90-kDa heat shock protein. *Journal of Biological Chemistry*, **263**, 13802-13805.

Perico, A., Gottardi, M., Boddi, V., Bavazzano, P., Lanciotti, E. 2001. Assessment of exposure to polycyclic aromatic hydrocarbons in police in Florence, Italy, through personal air sampling and biological monitoring of the urinary metabolite 1-hydroxypyrene. *Archives of Environmental Health*, **56**, 506-512.

Petroeschevsky, A., Simpson, R.W., Thalib, L. and Rutherford, S. 2001. Associations between outdoor air pollution and hospital admissions in Brisbane, Australia. *Archives of Environmental Health*, **56**, 37-52.

Phillipson, R.P, Tobi, S.E., Morris, J.A. and McMillan, T.J. 2002. UV-A induces persistent genomic stability in human keratinocytes through an oxidative stress mechanism. *Free Radical Biology and Medicine*, **32**, 474-480.

Ping, L.F., Luo, Y.M., Zhang, H.B., Li, Q.B. and Wu, L.H. 2007. Distribution of polycyclic aromatic hydrocarbons in thirty typical soil profiles in the Yangtze River Delta region, east China. *Environmental Pollution*, **147**, 358-365.

Pion, I.A., Koenig, K.L. and Lim, H.W. 1995. Is dermatologic usage of coal tar carcinogenic? A review of the literature. *Dermatologic Surgery,* **21**, 227-231.

Plant, A.L., Benson, D.M. and Smith, L.C. 1985. Cellular uptake and intracellular localization of benzo(a)pyrene by digital fluorescence imaging microscopy. *Journal of Cell Biology,* **100**, 1295-1308.

Polyakov, L.M., Chasovskikh, M.I. and Panin, L.E. 1996. Binding and transport of benzo(a)pyrene by blood plasma lipoproteins: the possible role of apolipoprotein B in this process. *Bioconjugate Chemistry*, **7**, 396-400.

Poma, A., Arrizza, L., Picozzi, P. and Spano, L. 2002. Monitoring urban air particulate matter (fractions pm 2.5 and pm 10) genotoxicity by plant systems and human cells *in vitro*: A comparative analysis. *Teratogenesis, Carcinogenesis and Mutagenesis*, **22**, 271-284.

Pou, S., Ramos, C.L., Gladwell, T., Renks, E., Centra, M., Young, D., Cohen, M.S. and Rosen, G.M. 1994. A kinetic approach to the selection of a sensitive spin-trapping system for the detection of hydroxyl radical. *Analytical Biochemistry*, **217**, 76–83.

Pouget, J.P., Douki, T., Richard, M.J. and Cadet, J. 2000. DNA damage induced in cells by and UVA radiation as measured by HPLC/GC-MS and HPLC-EC and comet assay. *Chemical Research in Toxicology*, **13**, 541-549.

Poulos, T.L. and Raag, R. 1992. Cytochrome P450cam: crystallography, oxygen activation, and electron transfer. *The FASEB Journal: Official Publication of the Federation of American Societies for Experimental Biology,* **6**, 674-679.

Qian, Z., He, Q., Kong, L., Xu, F., Wei, F., Chapman, R.S., Chen, W., Edwards, R.D. and Bascom, R. 2007. Respiratory responses to diverse indoor combustion air pollution sources. *Indoor Air*, **17**, 135-142.

Rafnsson, V., Hrafnkelsson, J. and Tulinius, H. 2000. Incidence of cancer among commercial airline pilots. *Occupational and Environmental Medicine*, **57**, 175-179.

Raisuddin, S. and Jha, A. N. 2004. Relative sensitivity of fish and mammalian cells to sodium arsenate and arsenite as determined by alkaline single-cell gel electrophoresis and cytokinesis-block micronucleus assay. *Environmental and Molecular Mutagenesis*, **44**, 83-89.

Readman, J.W., Mantoura, R.F.C., Rhead, M.M. and Brown, L. 1982. Aquatic distribution and heterotrophic degradation of polycyclic aromatic hydrocarbons (PAH) in the Tamar Estuary. *Estuarine, Coastal and Shelf Science*, **14**, 369-389.

Reeves, J.F., Davies, S.J., Dodd, N.J. and Jha, A.N. 2008. Hydroxyl radicals ($^{\cdot}OH$) are associated with titanium dioxide (TiO_2) nanoparticle-induced cytotoxicity and oxidative DNA damage in fish cells. *Mutation Research*, **640**, 113-122.

Reichert, W.L., Myers, M.S., Peck-Miller, K., French, B., Anulacion, B.F., Collier, T.K., Stein, J.E. and Varanasi. U. 1998. Molecular epizootiology of genotoxic events in marine fish: linking contaminant exposure, DNA damage, and tissue-level alterations. *Mutation Research*, **411**, 215-225.

Roberts, R.J. and Bullock, A.M. 1981. Recent observations on the pathological effects of ultraviolet light on fish skin. *Fish Pathology*, **15**, 237-239.

Rosefort, C., Fauth, E. and Zankl, H. 2004. Micronuclei induced by aneugens and clastogens in mononucleate and binucleate cells using the cytokinesis block assay. *Mutagenesis*, **19**, 277-284.

Routledge, M. N., McLuckie, K. I., Jones, G. D., Farmer, P. B. and Martin, E. A. 2001. Presence of benzo(a)pyrene diol epoxide adducts in target DNA leads to an increase in UV-induced DNA single strand breaks and *supF* gene mutations. *Carcinogenesis*, **22**, 1231-1238.

Roy, C.R., Gies, H.P. and Toomey, S. 1995. The Solar UV radiation environment: measurement techniques and results. *Journal of Photochemistry and Photobiology B: Biology,* **31**, 21-27.

Ruchirawat, M., Navasumrit, P., Settachan, D. and Autrup, H. 2006. Environmental impacts on children's health in Southeast Asia: genotoxic compounds in urban air. *Annals of the New York Academy of Science*, **1076**, 678-690.

Ruiz-Leal, M. and George, S. 2004. An *in vitro* procedure for evaluation of early stage oxidative stress in an established fish cell line applied to investigation of PAH and pesticide toxicity. *Marine Environmental Research*, **58**, 631-635.

Russo, P.A. and Halliday, G.M. 2006. Inhibition of nitric oxide and reactive oxygen species production improves the ability of a sunscreen

to protect from sunburn, immunosuppression and photocarcinogenesis. *British Journal of Dermatology*, **155**, 408-415.

Sadovy, Y., Randall, J.E. and Rasotto, M.B. 2005. Skin structure in six dragonet species (Gobiesociformes; Callionymidae): interspecific differences in glandular cell types and mucus secretion. *Journal of Fish Biology*, **66**, 1411–1418.

Said, T.O. and El Agroudy, N.A. 2006. Assessment of PAHs in water and fish tissues from Great Bitter and El Temsah lakes, Suez Canal, as chemical markers of pollution sources. *Chemistry in Ecology*, **22**, 159-173.

Saladi, R., Austin, L., Gao, D., Yuhun, L., Phelps, R. and Lebwohl, M. 2003. The combination of benzo(a)pyrene and ultraviolet A causes an *in vivo* time-related accumulation of DNA damage in mouse skin. *Photochemistry and Photobiology*, **77**, 413-419.

Salo, H.M., Jokinen, E.I., Markkula, S.E., Aaltonen, T.M. and Penttilä, H.T. 2000. Comparative effects of UVA and UVB irradiation on the immune system of fish. *Journal of Photochemistry and Photobiology B*, **56**, 154-162.

Salo, P.M., Xia, J., Johnson, C.A., Li, Y., Kissling, G.E., Avol, E.L., Liu, C. and London, S.J. 2004. Respiratory symptoms in relation to residential coal burning and environmental tobacco smoke among early adolescents in Wuhan, China: a cross-sectional study. *Environmental Health*, **3**, 14.

Sanchez, P., Llorente, M. and Castano, A. 2000. Flow cytometric detection of micronuclei and cell cycle alterations in fish-derived cells after exposure to three model genotoxic agents: Mitomycin C, vincristine sulfate and benzo(a)pyrene. *Mutation Research*, **465**, 113-122.

Sánchez-Fortún, S., Llorente, M.T. and Castano, A. 2005. Genotoxic effects of selected biocides on RTG-2 fish cells by means of a modified Fast Micromethod Assay. *Aquatic Toxicology*, **73**, 55-64.

Santodonato, J. 1981. Polycyclic organic matter. *Journal of Environmental Pathology and Toxicology*, **5**, 1-364.

Sargaonkar, A. 2006. Estimation of land use specific runoff and pollutant concentration for Tapi River basin in India. *Environmental Monitoring and Assessment*, **117**, 491-503.

Savabieasfahani, M., Lochmiller, R.L. and Janz, D.M. 1999.

Elevated ovarian and thymic cell apoptosis in wild cotton rats inhabiting petrochemical-contaminated terrestrial ecosystems. *Journal of Toxicology and Environmental Health. Part A*, **57**, 521-527.

Schirmer, K., Chan, A.G.J. and Bols, N. C. 2000. Transitory metabolic disruption and cytotoxicity elicited by benzo(a)pyrene in two cell lines from rainbow trout liver. *Journal of Biochemical and Molecular Toxicology*, **14**, 262-276.

Schirmer, K., Chan, A. G. J., Greenberg, B. M., Dixon, D. G., and Bols, N. C. 1997. Methodology for demonstrating and measuring the photocytotoxicity of fluoranthene to fish cells in culture. *Toxicology in Vitro,* **11**, 107-119.

Schirmer, K., Dixon, D., Greenberg, B. and Bols, N. 1998. Ability of 16 priority PAHs to be directly cytotoxic to a cell line from the rainbow trout gill. *Toxicology*, **127**, 129-141.

Schirmer, K., Herbrick, J.S., Greenberg, B.M., Dixon, D.G. and Bols, N.C. 1999. Use of fish cells in culture to evaluate the cytotoxicity and photocytotoxicity of intact and photomodified creosote. *Environmental Toxicology and Chemistry*, **18**, 1277-1288.

Schlezinger, J.J., White, R.D. and Stegeman, J.J. 1999. Oxidative inactivation of cytochrome P-450 1A (CYP1A) stimulated by 3,3',4,4'-tetrachlorobiphenyl: production of reactive oxygen by vertebrate CYP1As. *Molecular Pharmacology*, **56**, 588-597.

Schmid, T. E., Xu, W. and Adler, I. D. 1999. Detection of aneuploidy by multicolor fish in mouse sperm after *in vivo* treatment with acrylamide, colchicine, diazepam or thiabendazole. *Mutagenesis*, **14**, 173-179.

Scholz, S. and Segner, H. 1999. Induction of CYP1A in primary cultures of rainbow trout (*Oncorhynchus mykiss*) liver cells: concentration-response relationships of four model substances. *Ecotoxicology and Environmental Safety*, **43**, 252-260.

Schriever-Schwemmer, G., Kliesch, U. and Adler, I. D. 1997. Extruded micronuclei induced by colchicine or acrylamide contain mostly lagging chromosomes identified in paintbrush smears by minor and major mouse DNA probes. *Mutagenesis*, **12**, 201-207.

Secco, T., Pellizzato, F., Sfriso, A. and Pavoni, B. 2005. The changing state of contamination in the Lagoon of Venice. Part 1: organic pollutants. *Chemosphere*, **58**, 279-290.

Sega, G.A. 1984. A review of the genetic effects of ethyl methanesulphonate. *Mutation Research*, **134**, 113–142.

Segner, H. 1998. *Fish cell lines as a tool in aquatic toxicology*. In: *Fish Ecotoxicology*. Braunbeck T, Hinton DE, & Streit B (Eds.) Birkhäuser Verlag pp. 1-38.

Seité, S., Medaisko, C., Christiaens, F., Bredoux, C., Compan, D., Zucchi, H., Lombard, D. and Fourtanier, A. 2006a. Biological effects of simulated ultraviolet daylight: a new approach to investigate daily photoprotection. *Photodermatology, Photoimmunology and Photomedicine*, **22**, 67-77.

Seité, S., Zucchi, H., Septier, D., Igondjo-Tchen, S., Senni, K. and Godeau, G. 2006b. Elastin changes during chronological and photo-ageing: the important role of lysozyme. *Journal of the European Academy of Dermatology and Venereology*, **20**, 980-987.

Seo, S.J., Choi, H.G., Chung, H.J. and Hong, C.K. 2002. Time course of expression of mRNA of inducible nitric oxide synthase and generation of nitric oxide by ultraviolet B in keratinocyte cell lines. *British Journal of Dermatology*, **147**, 655-662.

Sexton, K.G., Jeffries, H.E., Jang, M., Kamens, R.M., Doyle, M., Voicu, I. and Jaspers, I. 2004. Photochemical products in urban mixtures enhance inflammatory responses in lung cells. *Inhalation Toxicology,* **16**, 107-114.

Sharma, J. G., Masuda, R., and Tanaka, M. 2005. Ultrastructural study of skin and eye of UV-B irradiated *Plecoglossus altivelis*. *Journal of Fish Biology*, **67**, 1646–1652.

Shemer, H. and Linden, K.G. 2007. Aqueous photodegradation and toxicity of the polycyclic aromatic hydrocarbons fluorene, dibenzofuran, and dibenzothiophene. *Water Research*, **41**, 853-861.

Shiaris, M.P. 1989. Seasonal Biotransformation of Naphthalene, Phenanthrene, and Benzo(a)pyrene in Surficial Estuarine Sediments. *Applied and Environmental Microbiology*, **55**, 1391-1399.

Shorrocks, J., Tobi, S.E., Latham, H., Peacock, J.H., Eels, R., Eccles, D. and McMillan, T.J. 2004. Primary fibroblasts from BRCA1 heterozygotes display an abnormal G1/S cell cycle checkpoint following UVA irradiation but show normal levels of micronuclei following oxidative stress or mitomycin C treatment. *International Journal of Radiation Oncology, Biology, Physics*, **58**, 470-478.

Shyong, E.Q., Lu, Y., Goldstein, A., Lebwohl, M. and Wei, H. 2003. Synergistic enhancement of H_2O_2 production in human epidermoid carcinoma cells by benzo(a)pyrene and ultraviolet A radiation. *Toxicology and Applied Pharmacology*, **188**, 104-109.

Singer, B. and Grűnberger, D. 1983. *Molecular biology of mutagens and carcinogens.* Plenum, New York.

Singh, N., McCoy, M., Tice, R. and Schneider, E. 1988. A simple technique for quantitation of low levels of DNA damage in individual cells. *Experimental Cell Research*, **175**, 184-191.

Smith, T.L., Merry, S.T., Harris, D.L., Joe Ford, J., Ike, J., Archibong, A.E. and Ramesh, A. 2007. Species-specific testicular and hepatic microsomal metabolism of benzo(a)pyrene, an ubiquitous toxicant and endocrine disruptor. *Toxicology In Vitro*, **21**, 753-758.

Smolarek, T., Morgan, S. and Baird, W. 1988. Temperature-induced alterations in the metabolic activation of benzo(a)pyrene to DNA-binding metabolites in the bluegill fry cell line BF-2. *Aquatic Toxicology*, **13**, 89-98.

Sorensen, M., Autrup, H., Moller, P., Hertel, O., Jensen, S.S., Vinzents, P., Knudsen, L.E. and Loft, S. 2003. Linking exposure to environmental pollutants with biological effects. *Mutation Research*, **544**, 255-271.

Spielmann, H., Balls, M., Dupuis, J., Pape, W. J., Pechovitch, G., de Silva, O., Holzhutter, H.G., Clothier, R., Desolle, P., Gerberick, F., Liebsch, M., Lovell, W. W., Maurer, T., Pfannenbecker, U., Potthast, J. M., Csato, M., Sladowski, D., Steiling, W. and Brantom, P. 1998. The international EU/COLIPA *in vitro* phototoxicity validation study: Results of phase II (blind trial). Part 1: The 3T3 NRU phototoxicity test. *Toxicology in Vitro*, **12**, 305-327.

Sram, R.J., Benes, I., Binkova, B., Dejmek, J., Horstman, D., Kotesovec, F., Otto, D., Perreault, S.D., Rubes, J., Selevan, S.G., Skalik, I., Stevens, R.K. and Lewtas, J. 1996. Teplice program--the impact of air pollution on human health. *Environmental Health Perspectives*, **104**, 699-714.

Steeger, H. U., Freitag, J. F., Michl, S., Wiemer, M. and Paul, R. J. 2001. Effects of UV-B radiation on embryonic, larval and juvenile stages of northern sea plaice (*Pleuronectes platessa*) under simulated ozone-hole conditions. *Helgoland Marine Research,* **55**, 56-66.

Steevens, J.A., Slattery, M., Schlenk, D., Aryl, A. and Benson, W.H. 1999. Effects of ultraviolet-B light and polyaromatic hydrocarbon exposure on sea urchin development and bacterial luminescence. *Marine Environmental Research*, **48**, 439-457.

Stracquadanio, M., Dinelli, E. and Trombini, C. 2003. Role of volcanic dust in the atmospheric transport and deposition of polycyclic aromatic hydrocarbons and mercury. *Journal of Environmental Monitoring*, **5**, 984–988.

Strniste, G., Martinez, E., Martinez, A. and Brake, R. 1980. Photo-induced reactions of benzo(a)pyrene with DNA *in vitro*. *Cancer Research*, **40**, 245-252.

Surrales, J., Antoccia, A., Creus, A., Degrassi, F., Peris, F., Tanzarella, C., Xamena, N. and Marcos, R. 1994. The effect of cytochalasin B concentration on the frequency of micronuclei induced by four standard mutagens. Results from two laboratories. *Mutagenesis*, **9**, 347-353.

Swartz, R.C., Ferraro, S.P., Lamberson, J.O., Cole, F.A., Ozretich, R.J., Boese, B.L., Schults, D.W., Behrenfeld, M. and Ankley, G.T. 1997. Photoactivation and toxicity of mixtures of polycyclic aromatic hydrocarbon compounds in marine sediment. *Environmental Toxicology and Chemistry,* **16**, 2151-2157.

Swerdlow, A.J., English, J.S., MacKie, R.M., O'Doherty, C.J., Hunter, J.A., Clark, J. and Hole, D.J. 1988. Fluorescent lights, ultraviolet lamps, and risk of cutaneous melanoma. *British Medical Journal*, **297**, 647-650.

Taalas, P., Damski, J., Kyrö, E., Ginzburg, M. and Talamoni, G. 1997. Effect of stratospheric ozone variations on UV radiation and on tropospheric ozone at high latitudes. *Journal of Geophysical Research*, **102**, 1533-1540.

Tampio, M., Loikkanen, J., Myllynen, P., Mertanen, A. and Vähäkangas, K.H. 2008. Benzo(a)pyrene increases phosphorylation of p53 at serine 392 in relation to p53 induction and cell death in MCF-7 cells. *Toxicology Letters*, **178**, 152-159.

Tarazona, J.V., Cebrian, M. and Castano, A. 1993. Development of *in vitro* cytotoxicity tests using fish cell lines. In: *Progress in standardisation of aquatic toxicology tests*. Soares & Calow (eds) Lewis, Boca Raton pp.119 – 128.

Tasdemir, Y. and Esena, F. 2007. Urban air PAHs: concentrations, temporal changes and gas/particle partitioning at a traffic site in Turkey. *Atmospheric Research*, **84**, 1-12.

Taylor, M.R. and Harrison, P.T.C. 1999. Ecological effects of endocrine disruption: current evidence and research priorities. *Chemosphere*, **39**, 1237-1248.

Thieden, E., Philipsen, P.A., Heydenreich, J. and Wulf, H.C. 2004. UV radiation exposure related to age, sex, occupation, and sun behaviour based on time-stamped personal dosimeter readings. *Archives of Dermatology*, **140**, 197-203.

Thieden, E., Philipsen, P.A., Sandby-Møller, J. and Wulf, H.C. 2005. Sunscreen use related to UV exposure, age, sex, and occupation based on personal dosimeter readings and sun-exposure behavior diaries. *Archives of Dermatology*, **141**, 967-73.

Thomas, P., Umegaki, K. and Fenech, M. 2003. Nucleoplasmic bridges are a sensitive measure of chromosome rearrangement in the cytokinesis-block micronucleus assay. *Mutagenesis*, **18**, 187-194.

Thomas-Ahner, J.M., Wulff, B.C., Tober, K.L., Kusewitt, D.F., Riggenbach, J.A. and Oberyszyn, T.M. 2007. Gender differences in UVB-induced skin carcinogenesis, inflammation, and DNA damage. *Cancer Research,* **67**, 3468-3474.

Thompson, A.J., Shields, M.D. and Patterson, C.C. 2001. Acute asthma exacerbations and air pollutants in children living in Belfast, Northern Ireland. *Archives of Environmental Health*, **56**, 234-241.

Thornalley, P.J. and Dodd, N.J.F. 1985. Free radical production from normal and adriamycin-treated rat cardiacsarcasomes. *Biochemical Pharmacology*, **34**, 669-674.

Thyssen, J., Althoff, J.K.G. and Mohr, U. 1981. Inhalation studies with benzo(a)pyrene in Syrian golden hamsters. *Journal of the National Cancer Institute*, **66**, 575-577.

Tice, R., Agurell, E., Anderson, D., Burlinson, B., Hartmann, A., Kobayashi, H., Miyamae, Y., Rojas, E., Ryu, J. and Sasaki, Y. 2000. Single cell gel/comet assay: Guidelines for *in vitro* and *in vivo* genetic toxicology testing. *Environmental and Molecular Mutagenesis*, **35**, 206-221.

Tilghman Hall, A. and Oris, J. 1991. Anthracene reduces reproductive potential and is maternally transferred during long-term exposure in fathead minnows. *Aquatic Toxicology*, **19**, 249-264.

Ting, W.W., Vest, C.D. and Sontheimer, R. 2003. Practical and experimental consideration of sun protection in dermatology. *International Journal of Dermatology*, **42**, 505-513.

Toyooka, T., Ibuki, Y., Koike, M., Ohashi, N., Takahashi, S. and Goto, R. 2004. Coexposure to benzo(a)pyrene plus UVA induced DNA double strand breaks: visualization of Ku assembly in the nucleus having DNA lesions. *Biochemical and Biophysical Research Communications,* **322**, 631-636.

Toyooka, T., Ibuki, Y., Takabayashi, F. and Goto, R. 2006. Coexposure to benzo(a)pyrene and UVA induces DNA damage: first proof of double-strand breaks in a cell-free system. *Environmental and Molecular Mutagenesis*, **47**, 38-47.

Tsapakis, M., Apostolaki, M., Eisenreich, S. and Stephanou, E.G. 2006. Atmospheric deposition and marine sedimentation fluxes of polycyclic aromatic hydrocarbons in the Eastern Mediterranean Basin. *Environmental Science and Technology,* **40**, 4922-4927.

Tsilimigaki, S., Messini-Nikolaki, N., Kanariou, M. and Piperakis, S. 2003. A study on the effects of seasonal solar radiation on exposed populations. *Mutagenesis*, **18**, 139-143.

Tucker, M.A., Halpern, A., Holly, E.A., Hartge, P., Elder, D.E., Sagebiel, R.W., Guerry, D. and Clark, W. 1997. Clinically recognised dysplastic nevi, a central risk factor for cutaneous melanoma. *JAMA: the Journal of the American Medical Association,* **277**, 1439-1444.

Tucker, J. and Preston, R. 1996. Chromosome Aberrations, Micronuclei, Aneuploidy, Sister Chromatid Exchanges and cancer risk assessment. *Mutation Research*, **365**, 147-159.

Uhl, M., Helma, C. and Knasmuller, S. 1999. Single-cell gel electrophoresis assays with human-derived hepatoma (Hep G2) cells. *Mutation Research*, **441**, 215-224.

Urbach, F. 1997. Ultraviolet radiation and skin cancer of humans. Journal *of Photochemistry and Photobiology B,* **40**, 3-7.

Vainio, H., Miller, A.B. and Bianchini, F. 2000. An international evaluation of the cancer-preventive potential of sunscreens. *International Journal of Cancer*, **88,** 838-842.

Vainio, H., Sorsa, M. and McMichael, A. 1990. *Complex mixtures and cancer risk*. IARC Scientific Publications, Lyon. 104 pp.

Valencia, A. and Kochevar, I.E. 2006. Ultraviolet A induces apoptosis via reactive oxygen species in a model for Smith-Lemli-Opitz syndrome. *Free Radical Biology and Medicine,* **40**, 641-650.

Van den Brule, F., Califice, S., Garnier, F., Fernandez, P.L., Berchuck, A. and Castronovo, V. 2003. Galectin-1 accumulation in the ovary carcinoma peritumoral stroma is induced by ovary carcinoma cells and affects both cancer cell proliferation and adhesion to laminin-1 and fibronectin. *Laboratory Investigations,* **83**, 377-386.

Vander, S.M., Carrasco, D., Paterson, M.S., McCrary, M.L., Meyer, D.J. and Tyring, S.K. 2001. Tobacco use and skin disease. *Southern Medical Journal,* **94**, 621-634.

Van Dolah, R.F., Riekerk, G.H., Levisen, M.V., Scott, G.I., Fulton, M.H., Bearden, D., Sivertsen, S., Chung, K.W. and Sanger, D.M. 2005. An evaluation of polycyclic aromatic hydrocarbon (PAH) runoff from highways into estuarine wetlands of South Carolina. *Archives of Environmental Contamination and Toxicology,* **49**, 362-370.

Varga, D., Johannes, T., Jainta, S., Schuster, S., Schwarz-Boeger, U., Kiechle, M., Patino Garcia, B. and Vogel, W. 2004. An automated scoring procedure for the micronucleus test by image analysis. *Mutagenesis*, **19**, 391-397.

Verweij, F., Booij, K., Satumalay, K., van der Molen, N. and van der Oost, R. 2004. Assessment of bioavailable PAH, PCB and OCP concentrations in water, using semipermeable membrane devices (SPMDs), sediments and caged carp. *Chemosphere*, **54**, 1675-1689.

Vidal-Martinez, V.M., Aguirre-Macedo, M.L., Del Rio-Rodriguez, R., Gold-Bouchot, G., Rendon-von Osten, J. and Miranda-Rosas, G.A. 2006. The pink shrimp *Farfantepenaeus duorarum*, its symbionts and helminths as bioindicators of chemical pollution in Campeche Sound, Mexico. *Journal of Helminthology*, **80**, 159-174.

Vienneau, D.S., DeBoni, U. and Wells, P.G. 1995. Initiation of micronuclei by benzo(a)pyrene and benzo(e)pyrene in UDP-

glucuronosyltransferase-deficient cultured rat skin fibroblasts. *Cancer Research,* **55**, 1045-1051.

Villarini, M., Moretti, M., Damiani, E., Greci, L., Santroni, A.M., Fedeli, D. and Falcioni, G. 1998. Detection of DNA damage in stressed trout nucleated erythrocytes using the comet assay: protection by nitroxide radicals. *Free Radical Biology and Medicine,* **24**, 1310-1315.

Villena, A., 2003. Applications and needs of fish and shellfish cell cultures for disease control in aquaculture. *Reviews in Fish Biology and Fisheries*, **13**, 111-140.

Vimercati, L., Carrus, A., Bisceglia, L., Tato, I., Bellotta, M.R., Russo, A., Martina, G., Daprile, C., Di Leo, E., Nettis, E. and Assennato, G. 2006. Biological monitoring and allergic sensitization in traffic police officers exposed to urban air pollution. *International Journal of Immunopathology and Pharmacology,* **4**, 57-60.

Vineis, P., Hoek, G., Krzyzanowski, M., Vigna-Taglianti, F., Veglia, F., Airoldi, L., Overvad, K., Raaschou-Nielsen, O., Clavel-Chapelon, F., Linseisen, J., Boeing, H., Trichopoulou, A., Palli, D., Krogh, V., Tumino, R., Panico, S., Bueno-De-Mesquita, H.B., Peeters, P.H., Lund, E.E., Agudo, A., Martinez, C., Dorronsoro, M., Barricarte, A., Cirera, L., Quiros, J.R., Berglund, G., Manjer, J., Forsberg, B., Day, N.E., Key, T.J., Kaaks, R., Saracci, R. and Riboli, E. 2007. Lung cancers attributable to environmental tobacco smoke and air pollution in non-smokers in different European countries: a prospective study. *Environmental Health,* **6**, 7.

Vitaliano, P.P. 1978. The use of logistic regression for modelling risk factors: with application to non-melanoma skin cancer. *American Journal of Epidemiology*, **108**,402-414.

Walker, C.H. 2001. *Organic Pollutants: An ecotoxicological perspective*. London, Taylor & Francis Ltd 282 pp.

Walters, C. and Ward, B. 1998. Is solar radiation responsible for declines in marine survival rates of anadromous salmonids that rear in small streams? *Canadian Journal of Fisheries and Aquatic Sciences,* **55**, 2533-2538.

Walton, D.G., Acton, A.B. and Stich, H.F. 1987. DNA repair synthesis in cultured fish and human cells exposed to fish S9-activated aromatic hydrocarbons. *Comparative Biochemistry and Physiology C*, **86**, 399-404.

Walton, D.G., Acton, A.B. and Stich, H.F. 1988. Chromosome aberrations in cultured central mudminnow heart cells and chinese hamster ovary cells exposed to polycyclic aromatic hydrocarbons and sediment extracts. *Comparative Biochemistry and Physiology C*, **89**, 395-402.

Walum, E., Stenberg, K. and Jenssen, D. 1990. *Understanding Cell Toxicology*. Ellis Horwood, New York, 206 pp.

Wang, Q., Gu, G. and Higano, Y. 2006. Toward integrated environmental management for challenges in water environmental protection of Lake Taihu basin in China. *Environmental Management*, **37**, 579-588.

Wang, X.M., Terasaki, P.I., Rankin, G.W. Jr., Chia, D., Zhong, H.P. and Hardy, S. 1993. A new microcellular cytotoxicity test based on calcein AM release. *Human Immunology*, **37**, 264-270.

Weglarz, A. and Skrok, R. 2000. Application of GC-FID and GC-MS for assessing PAHs in suspended dust. *Central European Journal of Public Health*, **8**, 86-88.

Weindling, P. 2001. "The Origins of Informed Consent: The International Scientific Commission on Medical War Crimes, and the Nuremberg Code". *Bulletin of the History of Medicine,* **75**, 37-71.

Weinstein, J E. and Diamond, S.A. 2006. Relating daily solar ultraviolet radiation dose in salt marsh-associated estuarine systems to laboratory assessments of photoactivated polycyclic aromatic hydrocarbon toxicity. *Environmental Toxicology and Chemistry,* **25**, 2860-2868.

Weinstein, J.E., Oris, J.T. and Taylor, D.H. 1997. An ultrastructural examination of the mode of UV-induced toxic action of fluoranthene in the fathead minnow *Pimephales promelas. Aquatic Toxicology,* **39**, 1-22.

Whitear, M., Mittal, A.K. and Lane, E.B. 1980. Endothelial layers in fish skin. *Journal of Fish Biology,* **17**, 43–65.

Whiteman, D.C. and Green, A.C. 1999. Melanoma and sun exposure: where are we now? *International Journal of Dermatology,* **38**, 481-489.

Whiteman, D.C., Whiteman, C.A. and Green, A.C. 2001. Childhood sun exposure as a risk factor for melanoma: a systematic review of epidemiologic studies. *Cancer Causes Control*, **12**, 69-82.

Whitlock, J.P. Jr. 1990. Genetic and molecular aspects of 2,3,7,8-tetrachlorodibenzo-p-dioxin action. *Annual Review of Pharmacology and Toxicology,* **30**, 251.

WHO. 2003. Polynuclear aromatic hydrocarbons in drinking-water. Background document for preparation of WHO Guidelines for drinking water quality. Geneva, World Health Organization.

Wiklund, S. and Agurell, E. 2003. Aspects of design and statistical analysis in the comet assay. *Mutagenesis*, **18**, 167-175.

Wilcke, W., Krauss, M., Safronov, G., Fokin, A.D. and Kaupenjohann, M. 2005. Polycyclic aromatic hydrocarbons (PAHs) in soils of the Moscow region: concentrations, temporal trends, and small-scale distribution. *Journal of Environmental Quality*, **34**, 1581-1590.

Wilkins, R.C., Kutzner, B.C., Truong, M., Sanchez-Dardon, J. and McLean, J.R. 2002. Analysis of radiation-induced apoptosis in human lymphocytes: flow cytometry using Annexin V and propidium iodide versus the neutral comet assay. *Cytometry,* **48**, 14-19.

Willett, K.L., Gardinali, P.R., Lienesch, L.A. and Di Giulio, R.T. 2000. Comparative metabolism and excretion of benzo(a)pyrene in 2 species of ictalurid catfish. *Toxicological Sciences*, **58**, 68-76.

Willett, K.L., Lienesch, L.A. and Di Giulio, R.T. 2001. No detectable DNA excision repair in UV exposed hepatocytes from two catfish species. *Comparative Biochemistry and Physiology — C Pharmacology Toxicology and Endocrinology*, **128**, 349–358.

Wlaschek, M., Tantcheva-Poór, I., Naderi, L., Ma, W., Schneider, L.A., Razi-Wolf, Z., Schüller, J. and Scharffetter-Kochanek, K. 2001. Solar UV irradiation and dermal photoaging. *Journal of Photochemistry and Photobiology B,* **63**, 41-51.

Wolf, K. and Ahne, W. 1982. Fish cell culture. *Advances in Cell Culture*, **2**, 305-328.

Wolf, K. and Mann, J. A. 1980. Poikilotherm vertebrate cell lines and viruses: A current listing for fishes. *In Vitro*, **16**, 168-179.

Wolf, K. and Quimby, M.C. 1962. Established eurythermic line of fish cells *in vitro*. *Science,* **135**, 1065-1066.

Wolfe, M., Schwartz, G., Singaram, S., Mielbrecht, E., Tjeerdema, R. and Sowby, M. 2000. Influence of dispersants on the bioavailability and

trophic transfer of phenanthrene to algae and rotifers. *Aquatic Toxicology*, **48**, 13-24.

Wulff, A., Nilsson, C., Sundback, K., Wangberg, S.A. and Odmark, S. 1999. UV radiation effects on microbenthos–a four month field experiment. *Aquatic Microbial Ecology*, **19**, 269-278.

Würgler, F.E. and Kramers, P.G. 1992. Environmental effects of genotoxins (eco-genotoxicology). *Mutagenesis*, **7**, 321-327.

Wright, J., George, S., Martinez-Lara, E., Carpene, E. and Kindt, M. 2000. Levels of cellular glutathione and metallothionein affect the toxicity of oxidative stressors in an established carp cell line. *Marine Environmental Research*, **50**, 503-508.

Yamada, M., Takada, H., Toyoda, K., Yoshida, A., Shibata, A., Nomura, H., Wada, M., Nishimura, M., Okamoto, K. and Ohwada, K. 2003. Study on the fate of petroleum-derived polycyclic aromatic hydrocarbons (PAHs) and the effect of chemical dispersant using an enclosed ecosystem, mesocosm. *Marine Pollution Bulletin,* **47**, 105-113.

Yan, J., Wang, L., Fu, P.P. and Yu, H. 2004. Photomutagenicity of 16 polycyclic aromatic hydrocarbons from the US EPA priority pollutant list. *Mutation Research*, **557**, 99-108.

Yanase, H., Ando, H., Horikawa, M., Watanabe, M., Mori, T. and Matsuda, N. 2001. Possible involvement of ERK 1/2 in UVA-induced melanogenesis in cultured normal human epidermal melanocytes. *Pigment Cell Research*, **14**, 103-109.

Yang, M. and Cao, J. 2000. Studies on micronuclei induced by colchicine and cyclophosphamide using multicolor fluorescence *in situ* hybridization. *Zhonghua Yu Fang Yi Xue Za Zhi*, **34**, 101-103.

Ye, M., Liu, B.C., Shi, X.L., You, B.R., Du, H.J., Jia, X.W. and Shen, F.H. 2008. Different patterns of cyclin D1/CDK4-E2F-1/4 pathways in human embryo lung fibroblasts treated by benzo(a)pyrene at different doses. *Biomedical and Environmental Sciences*, **21**, 30-36.

Yendle, J.E., Tinwell, H., Elliott, B.M. and Ashby, J. 1997. The genetic toxicity of time: importance of DNA-unwinding time to the outcome of single-cell gel electrophoresis assays. *Mutation Research*, **375**, 125-136.

Yin, J.J., Xia, Q., Cherng, S.H., Tang, I.W., Fu, P.P., Lin, G., Yu, H. and Sáenz, D.H. 2008. UVA photoirradiation of oxygenated benz(a)anthracene and 3-methylcholanthene--generation of singlet

oxygen and induction of lipid peroxidation. *International Journal of Environmental Research and Public Health*, **5**, 26-31.

Young, A. 1987. The sunburn cell. *Photodermatology*, **4**, 127-134.

Young, A.R., Walker, S.L., Kinley, J.S., Plastow, S.R., Averbeck, D., Morlière, P. and Dubertret, L. 1990. Phototumorigenesis studies of 5-methoxypsoralen in bergamot oil: evaluation and modification of risk of human use in an albino mouse skin model. *Journal of Photochemistry and Photobiology B*, **7**, 231-250.

Yu, R.M., Ng, P.K., Tan, T., Chu, D.L., Wu, R.S. and Kong, R.Y. 2008. Enhancement of hypoxia-induced gene expression in fish liver by the aryl hydrocarbon receptor (AhR) ligand, benzo(a)pyrene (BaP). *Aquatic Toxicology*, **90**, 235-242.

Yuen, B.B. and Au, D.W. 2006. Temporal changes of ethoxyresorufin-o-deethylase (EROD) activities and lysosome accumulation in intestine of fish on chronic exposure to dietary benzo(a)pyrene: linking EROD induction to cytological effects. *Environmental Toxicology and Chemistry*, **25**, 2593-2600.

Zagarese, H.E. and Williamson, C.E. 2001. The implications of solar UV radiation exposure for fish and fisheries. *Fish and Fisheries*, **2**, 250–260.

Zhang, A., Feng, H., Yang, G., Pan, X., Jiang, X., Huang, X., Dong, X., Yang, D., Xie, Y., Peng, L., Jun, L., Hu, C., Jian, L. and Wang, X. 2007. Unventilated indoor coal-fired stoves in Guizhou province, China: cellular and genetic damage in villagers exposed to arsenic in food and air. *Environmental Health Perspectives*, **115**, 653-658.

Zhang, X., Wu, R. S., Fu, W., Xu, L. and Lam, P. K. 2004. Production of reactive oxygen species and 8-hydroxy-2'deoxyguanosine in KB cells co-exposed to benzo(a)pyrene and UV-A radiation. *Chemosphere*, **55**, 1303-1308.

Zheng, B., Hwang, H-M., Yu, H. and Ekunwe, S. 2004. DNA damage produced in HaCaT cells by combined fluoranthene exposure and ultraviolet A irradiation. *Environmental and Molecular Mutagenesis*, **44**, 151-155.

Zhou, J., Wanga, T., Huanga, Y., Maoa, T. and Zhong, N. 2005. Size distribution of polycyclic aromatic hydrocarbons in urban and suburban sites of Beijing, China. *Chemosphere*, **61**, 792-799.

Zijno, A., Marcon, F., Leopardi, P.and Crebelli, R. 1996. Analysis of chromosome segregation in cytokinesis-blocked human lymphocytes: non-disjunction is the prevalent damage resulting from low dose exposure to spindle poisons. *Mutagenesis*, **11**, 335-340.